# Studies on the Mode of Action of the Pyrithione Biocides

**Anthony Joseph Dinning, BSc(Hons)**

A Thesis submitted in partial fulfilment of the requirements of the

**University of Abertay Dundee**

for the degree of

**Doctor of Philosophy**

The research programme was carried out in collaboration with

**Zeneca Specialties, Blackley, Manchester**

**December 1995**

**I certify that this thesis is the true and accurate version of the thesis approved by the examiners.**

**Signed.** [redacted] **Date**.....9/2/96

**Director of Studies**

# Abstract

Sodium and zinc pyrithiones (NaPT and ZnPT respectively) are inhibitors of both pathogenic fungi and bacteria and are widely used in the cosmetics industry as preservatives. However, little is known of their mode of action. Growth inhibitory data exhibited NaPT to be a poorer growth inhibitor of *Escherichia coli* and *Pseudomonas aeruginosa* than ZnPT. A *Pseudomonas*-gap was observed between *E. coli* and *P. aeruginosa* upon their exposure to ZnPT. The antimicrobial action of these compounds was neutralised by the presence of EDTA and extracellular phosphatidylethanolamine. ZnPT was also neutralised by the presence of cysteine. Molecular modelling studies indicated direct chemical interactions between the pyrithiones and cysteine and the pyrithiones and phosphatidylethanolamine. Oxygen electrode studies exhibited low levels of pyrithione induced inhibition of substrate metabolism for several substrates in both *E. coli* and *P. aeruginosa*. The most sensitive metabolism towards the pyrithiones was that for thymidine, which exhibited inhibition to about 30% of the rate of metabolism in the control. At pyrithione concentrations approaching the MIC, the exposure of *E. coli* and *P. aeruginosa* to both biocides was shown to increase inhibited substrate metabolism for acetate, thymidine and uracil. ATP metabolism indicated extreme sensitivity to both NaPT and ZnPT in both *E. coli* and *P. aeruginosa.* The membrane effect of the pyrithiones were investigated by observing leakage of potassium ions and $E_{260nm}$ absorbing material from exposed cells of *E. coli* and *P. aeruginosa.* Although NaPT and ZnPT did not induce observable leakage of potassium ions from *E. coli* or *P. aeruginosa* it was found that leakage of 260nm material occurs and suggests that the leakage of potassium ions is being masked by some other event. Transmission electron microscopy indicated a disrupted bacterial envelope after exposure of *P. aeruginosa* to NaPT. Coagulation of the cytosol in proximity to the envelope was also observed. Both NaPT and ZnPT were observed to be present in the bacterial cytosol after assaying and ZnPT was observed in the envelope of *P. aeruginosa.* These results suggest that the pyrithione antimicrobial agents are mainly membrane active agents which enter the cytosol *via* membrane disruption where they may chelate intracellular metal cations and metalloenzymes.

# Acknowledgements

I would like to thank the following people, without whom the completion of this project and thesis would not have been possible. Dr Phillip J Collier, for his expert supervision, guidance and support throughout the last three years (not to mention the occasional pint in times of stress). Drs Alex Cornish, Peter Austin and Ian Eastwood from Zeneca Specialities in Blackley Manchester for their industrial support, academic input and the utilisation of various facilities. Dr Michael Charlton for his guidance in the molecular modelling studies at Zeneca Specialities, Blackley, Manchester. Thanks are due to the University of Perugia, Italy for the provision of electron microscope techniques and facilities. The technical and academic staff from the Divisions of Biological Sciences and Applied Chemistry at the University of Abertay Dundee for their help and advice during the project. The other research students and research associates involved with the Microbial Physiology Research Group (you know who you are), thank you for the good times. My mother and father for an excess of encouragement. And, last but not least, Miss Alison Mackie for her support, care and concern.

# Contents

# List of Figures

Figure 80: Suggested mode of action for ZnPT. 215

# List of Tables

Table 16: Distribution of NaPT and ZnPT in subcellular fractions of *E. coli* and *P. aeruginosa.* 195

# INTRODUCTION

Antimicrobial agents are extensively used worldwide to control the growth of unwanted microbial populations. On a daily basis the majority of the planet's population come into direct contact with antimicrobial agents in various forms. They may include antibiotics to treat systemic infections, antiseptics for topical application, the utilisation of disinfectants for household cleaning chores and contact with antimicrobial preservatives used in many applications at work and at home.

Many people have little understanding of the history and science of these compounds and the events which lead to their development despite their widespread utilisation. Even less is understood of the detrimental effects which may occur if such compounds had not been observed.

## HISTORY OF ANTIMICROBIALS

Although the onset of modern antimicrobial agents (such as antibiotics and preservatives) is thought to be relatively recent, dating from the discovery of penicillin by Flemming in the late 20's (Neu 1993, Aharonowitz & Cohen 1981) and the later discovery of streptomycin by Waksman in the early 1940's, the causes of putrefaction and the chemicals which disable these degradative processes have been studied since the mid 18th century. Pringle, in the 1750's, defined as antiseptics the substances which prevent the process of putrefaction. In 1825, Labarraque observed the antiseptic effects of the chlorine releasing agent hypochlorite. In 1846, the standard medical practice of hand-washing was brought into daily use, when Semmelweiss suggested that medical students under his supervision in a maternity ward should wash their hands in a chlorine solution (probably hypochlorite) after handling cadavers and before examining expectant mothers and new-born babies. This suggestion resulted in a 90% decrease in the cases of puerpural or childbed fever (caused by *Streptococcus pyogenes*) (Boyce *et al* 1990, Salyers & Whit 1994). The discovery of phenol by Lemaire in 1860 was one of the major steps in the development of antimicrobial technology. This antiseptic was used in the 1870's, by Lister to clean wounds, sterilise

surgical implements prior to use and as an aerosol to give the operating room an antiseptic environment. The widespread utilisation of phenol lead to studies into it's mode of action, and the observation of the phenolic coagulation of proteins by Ritthausen in 1872 (Denyer & Hugo 1991a).

At about this time, the separate works of Pasteur and Koch were beginning to identify and isolate forms of microbial life as the potential sources of infection and disease. In 1881, Koch began to isolate bacteria in pure culture and the ability to study the effects of antimicrobial agents upon single strains of bacteria was enabled.

**Table 1**: Various antimicrobial agents and their sites of action

| Antimicrobial Agent | Cellular Target |
|---|---|
| Beta-lactam antibiotics | Peptidoglycan structure |
| Quaternary ammonium biocides | Membrane integrity |
| 4-Quinolone antibiotics | DNA Replication |
| Isothiazolone biocides | Protein integrity/Thiol interactions |
| Phenolic biocides | Membrane integrity /Protein structure |
| Rifampicin | RNA Replication |

While working on the effect of the dye trypan red on trypanosomiasis in horses, Paul Ehrlich in 1902, began to develop the principles for the future study of antimicrobials and chemotherapy. It was Paul Ehrlich who observed that antimicrobial agents are essentially toxic chemicals which have in their design a structure which predisposes them towards a chemical reaction at a specific target in the bacterial cell (Table 1). There are sufficient evolutionary, biochemical and metabolic differences between bacteria and their hosts to largely preclude the action of antibiotics upon the host metabolism. This means that most antibiotics are capable of acting against the target microorganism whilst having little effect upon the host (Cohen 1979, Aharonowitz & Cohen 1981, Salyers & Whit 1994).

## CLASSIFICATION OF ANTIMICROBIAL COMPOUNDS

Antimicrobial agents comprise a wide array of compounds which target various components of the bacterial cell as sites for their action. The classification of these agents can at times be confusing due to the fine line which exists between the classification of antibiotics, antiseptics, disinfectants, preservatives and biocides. An antibiotic is a chemotherapeutic agent which may be administered systemically in order to combat microbial infection. The majority possess low toxicity towards the host and high specificity towards the causative agent (Salyers & Whit 1994), having the subsequent ability to combat infection with minimal damage to the host organism. The target mechanisms of antibiotic action may include inhibition of both cell wall synthesis and DNA and protein synthesis as major targets (Table 1). Antiseptics and disinfectants tend to be grouped together when classifying antimicrobial agents, but they are antimicrobials which have separate functions. Antiseptics are compounds which are used as topical agents in the cleansing of wounds (ie, cuts and abrasions to the skin) and are generally too toxic for systemic application. Disinfectants are cleansing agents used for the attempted erradication of microorganisms from inanimate objects (ie, instruments, toilets, drains and kitchen and laboratory workbenches). Disinfectants are too toxic for application against systemic infection, either topically or otherwise. Preservatives and biocides (although 'biocide' is a general term which may be used to describe all antimicrobial agents) are antimicrobials which are used to prevent colonisation of microorganisms on or within a product (ie, foodstuffs and cosmetics) or an industrial or environmental situation which may support microbial growth (eg, heating /cooling appliances, fuel lines, water cooling towers and central heating systems).

An understanding of the classification of antimicrobial agents and therefore their modes of action enables the future study of other novel antimicrobial agents, whether they are biocides, disinfectants, preservatives or antibiotics. This understanding also illustrates how the bacterial cell serves as a series of potential sites of action for antimicrobial agents.

# THE MICROBIAL CELL AS A SERIES OF POTENTIAL ANTIMICROBIAL TARGETS

In the study of antimicrobial agents, it is imperative that the differences in biological and biochemical make-up of both the target microbial cells and the cells of potential host organisms are fully understood. It is these differences which allow the development of new synthetic antimicrobial agents which are designed specifically for particular microbial targets. In order to achieve this it is also important to understand the structure and function of the microbial cell. This understanding facilitates the observation of the mode of action of different antimicrobials, helping to discern between general cellular toxins (ie radical formers which act both against the membranes of organisms and the cytosol) and antimicrobials which target specific sites in the microbial cell (Table 1). This study concerns the mode of action of the pyrithione antimicrobials upon bacteria. The pyrithiones are non-systemic agents which may be applied topically in order to combat the onset of dandruff. Subsequently, much of the work concerning their mode of action has been carried out on fungi. It is due to this that a short comparison of the differences between fungal eukaryotic cells and bacteria will be considered before discussing the make up and envelope structure of the bacterial cell.

**Fungi and Bacteria: The Basic Differences**

Fungi possess a true nucleus which contains a major part of the genome as a set of chromosomes. The chromosomes of fungi replicate by mitosis and the chromosomal DNA is associated with proteins termed histones. Bacteria are not compartmentalised and possess only one chromosome which is termed the nucleoid or genome. Bacteria also contain small DNA duplex molecules (plasmids) which encode non-essential genes and are therefore not essential to bacterial life. However, the plasmids may give the bacteria an evolutionary advantage as a result of their ability to code for antibiotic resistance genes. The fungal cell possesses other compartmentalised intracellular organelles; ie, mitochondria, endoplasmic reticula, vacuoles and golgi apparatus. Bacteria do not possess any intracellular compartmentalised organelles and have free-floating ribosomes. The ribosomes of eukaryotes are situated on the endoplasmic reticulum and are larger (80S) than those in prokaryotic organisms (70S). Some bacteria also possess an outer membrane and most possess a two-dimensional protein layer (S-layer) on the cellular periphery. Fungal organisms do not possess an outer membrane or an S-layer. However, they do possess a cell wall and a cytoplasmic membrane. The fungal cell wall is unlike bacterial cell walls which are made up of peptidoglycan. Fungal cell walls consist of several carbohydrates (cellulose, chitin, mannan or glucan) as well as proteins and lipids (including steroids such as sterol). Their cytoplasmic membranes are made up of lipids, containing many steroids. Traces of carbohydrate (glucan and mannan) are also found in the fungal cytoplasmic membrane, unlike the bacterial cytoplasmic membrane which consists solely of phospholipid units and proteins.

**The Bacterial Cell**

Bacteria may be broadly classified into two groups, Gram-positive and Gram-negative (Fig 1). This classification was devised by Christian Gram, who observed a difference in the ability of both classes of bacteria to retain the dye crystal violet after carrying out and characterising the staining process which bares his name (Beveridge 1988). The staining sequence and classification process is dependent upon the differences between the Gram-positive and Gram-negative envelopes (Fig 1). The main differences between the two groups of organisms is the presence of an outer membrane possessed by Gram-negative bacteria and not found in Gram-positive cells. The peptidoglycan layers (cell walls) of the Gram-positive

**Figure 1:** Diagram of the bacterial cell. A, The generalised structure of the bacterial cell; B, Gram-positive structure; C, Gram-negative structure (Russell & Chopra 1990).

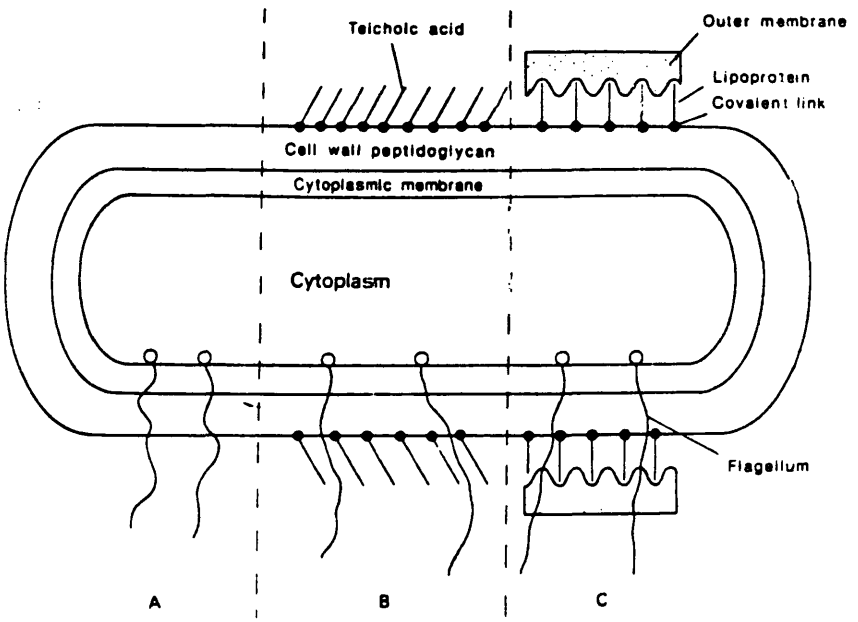
Teichoic acid
Outer membrane
Lipoprotein
Covalent link
Cell wall peptidoglycan
Cytoplasmic membrane
Cytoplasm
Flagellum
A
B
C

bacteria are also much thicker than those found in Gram-negative cells, with the Gram-positive cell wall representing 25-40% of the total dry cell weight and the Gram-negative peptidoglycan layer being of only 5-7% of the total dry cell weight (Ingraham *et al* 1983, Poxton 1993). This reflects a need for the Gram-positive cells to have a physically stronger envelope than Gram-negative bacteria, showing elementary differences in the cytosolic make-up of the two bacterial groups. The cytosol of Gram-positive bacteria has a much higher osmolarity than that of the Gram-negative bacteria. It also exhibits differences in the evolution of Gram-positive and Gram-negative cell types. Work carried out upon bacterial phylogeny, using the comparison of rRNA from several bacterial genera, suggests that Gram-positive bacteria are evolved from species which were exposed to extremes of pH and osmolarity (Woese 1987). Subsequently, they are shown to be closely related to many of the archaebacteria. The possession of increased cytoplasmic osmolarity and thicker peptidoglycan structure by the Gram-positive bacteria suggests that they once existed at extremes of osmotic pressure. This existence would have been depleted if the cells were not able to resist death from turgor pressure. However, the possession of the Gram-positive attributes decreased the possibilities of bacterial destruction from increased pH and osmolarity. Subsequently, these phylogenic observations increase the understanding of the diversity between Gram-positive and Gram-negative species.

**The Bacterial Cytoplasmic Membrane**

Both Gram-negative and Gram-positive bacteria possess a cytoplasmic (or plasma) membrane. The cytoplasmic membrane is a natural biological phospholipid bilayer which surrounds the bacterial cytoplasm. This is illustrated by the fluid mosaic model (Cronan *et al* 1987, Poxton 1993) (Fig 2). The bacterial plasma membrane is generally made up of three separate phospholipids, (phosphatidylethanolamine, phosphatidylcholine and diphosphatidylglycerol). However, the most abundant phospholipids in Gram-positive bacteria are phosphatidyl glycerol and diphosphatidyl glycerol (Poxton 1993). In Gram-negative bacteria the most abundant membrane lipid is phosphatidyl ethanolamine (Nikaido & Vaara 1987, Waigh & Gilbert 1991, Poxton 1993). The plasma membrane also contains many proteins which act as electron transport systems, ATPase subunits and various transport enzymes (Cronan *et al* 1987). Subsequently, the cytoplasmic membrane is implicated in oxidative phosphorylation, carbohydrate metabolism and transport of nutrients

**Figure 2:** The fluid mosaic model of the cytosolic membrane structure (Woodcock 1988).

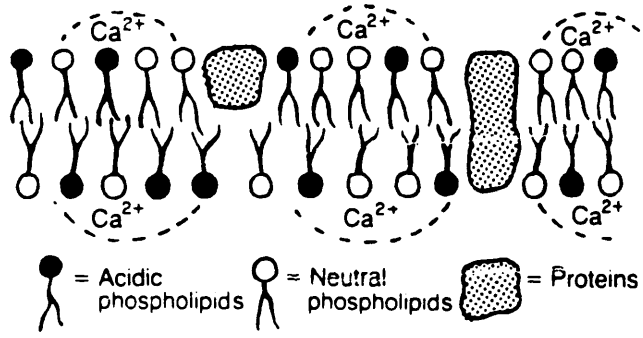
Ca2+
Ca2+
Ca2+
Ca2+
Ca2+
Ca2+
= Acidic phospholipids
= Neutral phospholipids
= Proteins

both in and out of the cell. It should also be noted that because the phospholipid bilayer is a membrane, it is also a physical barrier and subsequently provides the first array of protection for the bacterial cytoplasm from various factors (eg, antimicrobial agents, extremes of pH, osmolarity, etc). In doing so it helps to maintain osmotic and pH gradients (involved in driving many metabolic processes, ie, ATP production and sugar transport) (Harold 1972, Stryer 1988) and also helps to maintain bacterial shape. The bacterial cytoplasmic membrane is one of the major sites of action for antimicrobial agents and once the integrity of the membrane is ruptured the leakage of cytoplasmic constituents into the environment may be observed (ie, $K^+$ ions, free nucleotides, 260nm absorbing material) (Wiseman 1964, Rye & Wiseman 1964, Bernheim 1976, Denyer & Hugo 1991b).

**The Bacterial Cell Wall**

The bacterial cell wall (murein layer or peptidoglycan layer, Park 1987) is present in nearly all forms of bacterial life (Poxton 1993). In Gram-negative bacteria the murein cell wall structure exists as a bilayer of peptidoglycan (Cooper 1991). In Gram-positive bacteria the peptidoglycan may be as much as forty layers thick (Park 1987, Poxton 1993) and is readily visualised using electron microscopy (Poxton 1993). The chemical constitution of peptidoglycan consists of two aminosugars, N-acetyl glucosamine (NAG) and it's corresponding lactic acid ether N-acetyl muramic acid (NAM) (Schlegel 1988, Park 1987, Poxton 1993) (Fig 3). These sugars exist together as alternating units in the cell wall which are bonded by beta-1,4-glycosidic links and are synthesised in the bacterial cytosol from an intracellular pool of UDP-N-acetylglucosamine residues. Some of the residues remain as the precursors to NAG, while others are reduced to give rise to NAM precursors (Park 1987). During biosynthesis of peptidoglycan a pentapeptide tail is added onto the NAM residue of the muramic acid precursor (Park 1987, Poxton 1993) (Fig 3). This involves the sequential addition of three amino-acids and a subsequent addition of a D-alanyl-D-alanine dimer, which together make up the pentapeptide tail. The enzymes involved are specific for the addition of each amino acid residue and the system is dependent upon utilisation of ATP and divalent metal cations (ie, $Mn^{2+}$ or $Mg^{2+}$) (Park 1987). The pentapeptide tail consists of L-alanine, D-glutamic acid, meso-diaminopimelic acid (or L-lysine) and a D-alanyl-D-alanine residue. Although generally highly conserved, the amino acids constituting the pentapeptide

**Figure 3:** Diagrammatic representation of the peptidoglycan of *E. coli.* A, The arrangement of N-acetylglucosamine (NAG and N-acetylmuramic acid (NAM) residues linked by ß-1,4 glycoside bonds (diagonal lines). B, the portion of A enclosed within the dotted line is enlarged to show the cross linkage between tetrapeptides attached to NAM residues of adjacent chains. The peptidoglycan of other species may differ in nature of the amino acids at positions 2 and 3 of the tetrapeptide and in the nature and frequency of cross link (noted by asterisks in the figure (Ingraham *et al* 1983).

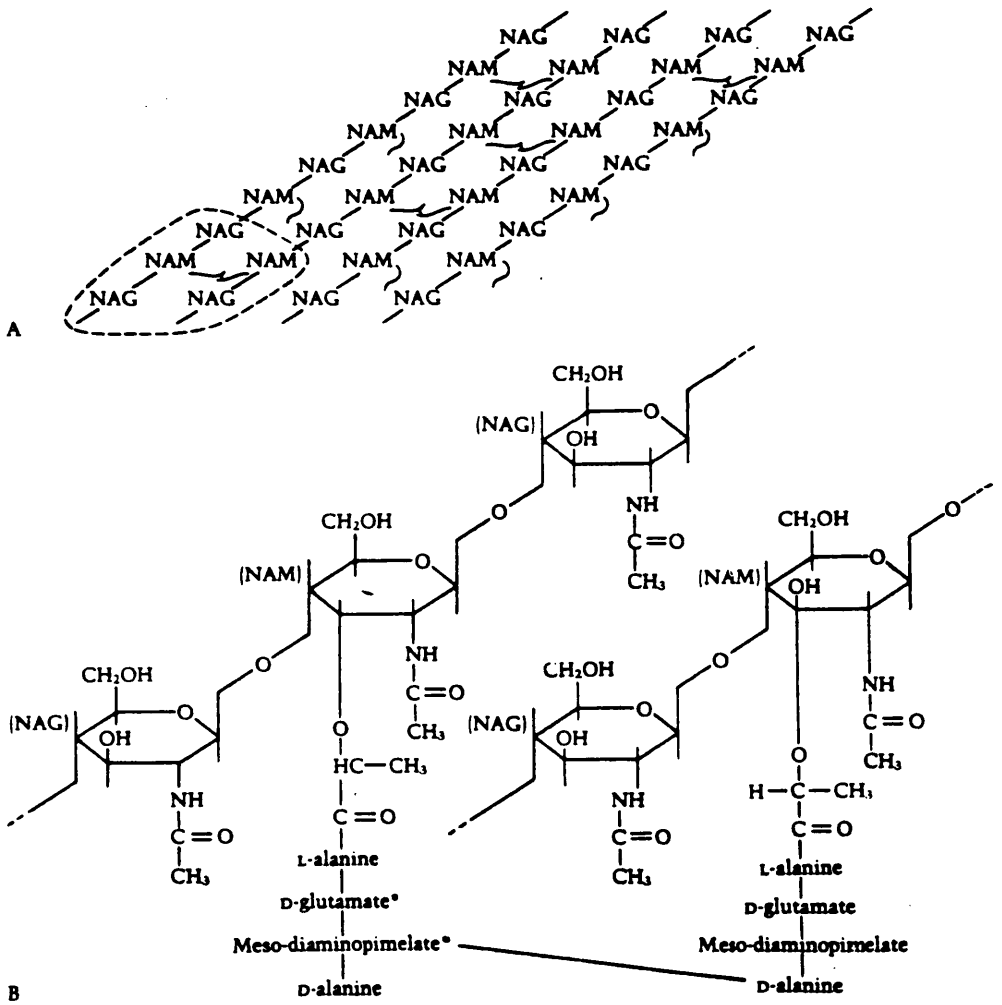
A
NAG
NAM
B
(NAG)
(NAM)
CH₂OH
OH
NH
C=O
CH₃
HC—CH₃
L-alanine
D-glutamate*
Meso-diaminopimelate*
D-alanine
H—C—CH₃
L-alanine
D-glutamate
Meso-diaminopimelate
D-alanine

tail may vary between bacterial species. The repeating unit of the two aminosugars and the peptide chain are known as muropeptide (Park 1987). In the biosynthesis of the cell wall, the crosslinking or transpeptidation of the pentapeptide tails of the muropeptide subunits forms the peptidoglycan layer (Park 1987). Transpeptidation occurs as a condensation reaction between the meso-diaminopimelic acid residue of one subunit and the sub-terminal D-alanine residue of another with the concurrent loss of the terminal D-alanine residue. Subsequently, the rigidity of the peptidoglycan polymer is maintained due to the transpeptidation between the pentapeptide tails of the peptidoglycan subunits, giving rise to tetrapeptide-tetrapeptide bridges in the final peptidoglycan polymer (Park 1987) (Fig 3).

**The Periplasm**

The area which lies between the outer face of the plasma membrane and the cell wall (in Gram-positive bacteria) and the inner face of the outer membrane (in Gram-negative bacteria) is termed the periplasm (Graham *et al* 1991a, Poxton 1993) (Fig 1). The periplasm contains various enzymes and precursors as a result of diffusion and transport through the cell wall and outer membrane. The proteins contained within the periplasm are mainly concerned with nutrient metabolism and binding of essential nutrients (eg, sugars and amino acids) (Oliver 1987). The periplasm also contains some of the enzymes responsible for the biosynthesis and transpeptidation reactions of the murein layer, the penicillin binding proteins or PBPs. The PBPs are involved in the various processes of cell wall formation and maintenance of structure and as a result are mainly transpeptidases (Park 1987). The PBPs are the site of action of the ß-lactam antibiotics. Electrophilic and thiol-interactive antimicrobial agents are also known to have activity within the periplasm where they disrupt various aspects of metabolism and both outer and inner membrane integrity.

**The Gram-Negative Outer Membrane**

The Gram-negative outer membrane differs dramatically from the cytoplasmic membrane. It consists of a bilayer of two amphipathic moieties. However, only the inner layer of the outer membrane consists solely of phospholipids and proteins (Nikaido & Vaara 1987) (Fig 4). The outer-most phase of the bilayer mainly consists of a molecule called lipopolysaccharide (LPS) with some phospholipids and proteins (Fig 6). LPS consists of three regions, lipid A , the core region and the O side chain (or O antigen). Lipid A is the section of LPS which

maintains the hydrophobic bonds with the outer membrane phospholipid. Lipid A consists of two phosphorylated glucosamine units which possess fatty acid tails (Fig 5). Lipid A is covalently attached to the core region *via* one of the glucosamine residues. The core region consists of two units of 2-keto-3-deoxyoctonic acid (KDO). Each unit of KDO has one phosphorylethanolamine (Pet) group, two units of L-glycero-D-mannoheptose (hep) and one monosaccharide attached (Ferris & Beveridge 1986b, Nikaido & Vaara 1987) (Fig 5). The distal region of the LPS is an oligopeptide tail called the O side chain (or O antigen) (Nikaido & Vaara 1987, Wainwright 1988, Poxton 1993) (Fig 5). Different Gram-negative bacterial species exhibit high levels of O antigen variability and it is this variability which allows the classification of Gram-negative bacteria *via* serotyping (Jann *et al* 1982, Poxton 1993).

The Gram-negative outer membrane also contains three major types of protein. These are; (a) Braun's lipoprotein which is covalently linked to the peptidoglycan layer and anchors the outer membrane to the cell wall; (b) porins, which are nonspecific trimeric protein channels which allow entry of low molecular weight hydrophilic molecules into the cell (Nikaido & Vaara 1987, Russell & Chopra 1990) and (c) specific diffusion proteins, which are involved in the transport of specific molecules into the cell; ie, maltose, nucleosides and vitamins (Nikaido & Vaara 1987).

It should be noted that particular sections of the Gram-negative outer membrane have a requirement for divalent metal cations ($Mg^{2+}$ and $Ca^{2+}$). The divalent cations are required for the stabilisation of the murein lipoprotein at the peptidoglycan layer and the stability of phosphorylethanolamine residues present at the LPS core (Ferris & Beveridge 1986a, 1986b, Wainwright 1988). If Gram-negative bacteria are treated with the ion sequestering agent EDTA (ethylenediaminetetraacetic acid) a loss of divalent metal cations and LPS is observed (Russell & Chopra 1990). Nonetheless, the outer membrane is still an effective barrier to many hydrophobic and hydrophilic molecules (eg, rifamycin, macrolides and bile salts) (Nikaido & Vaara 1987).

**Figure 4:** The structure of the Gram-negative outer membrane (Russell & Chopra 1990).

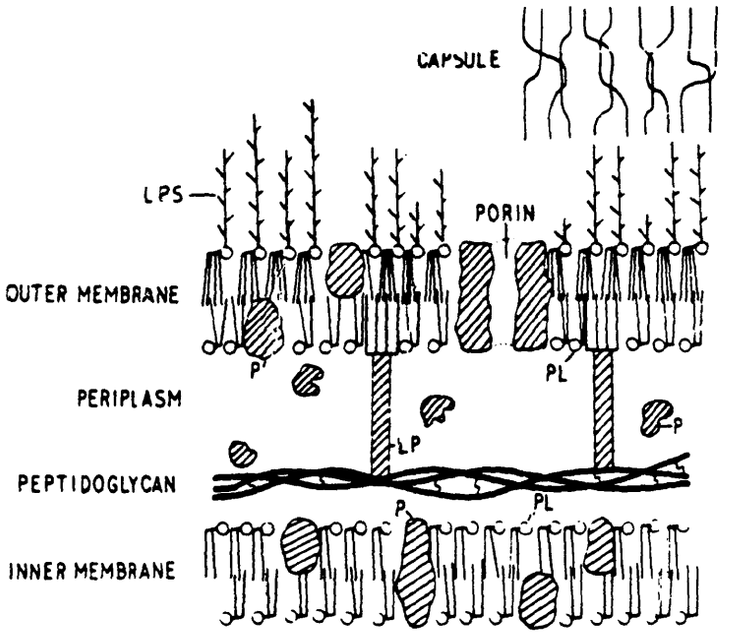
CAPSULE
LPS
PORIN
OUTER MEMBRANE
P
PL
PERIPLASM
LP
P
PEPTIDOGLYCAN
P
PL
INNER MEMBRANE

**Figure 5:** The structure of lipopolysaccharide (LPS). The structure of lipid A region is highly conserved amongst a wide range of Gram-negative bacteria. Considerable variation is present in the monosaccharides that constitute the outer core and O side chain regions.Therefore, they have been left as empty blocks. (Russell & Chopra 1990).

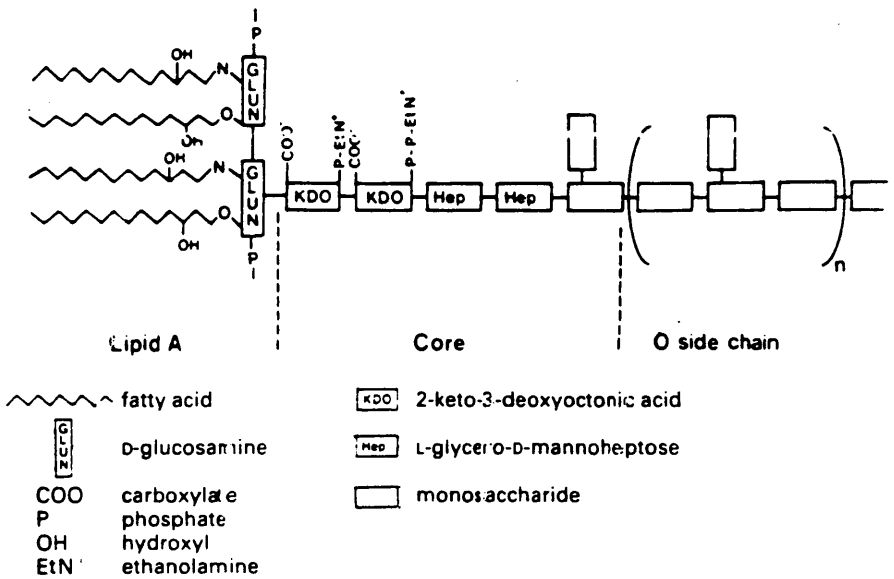
OH
N
O
OH
OH
N
O
OH
P
COO
P-EtN
COO
P-P-EtN
KDO
KDO
Hep
Hep
n
Lipid A
Core
O side chain
fatty acid
D-glucosamine
COO carboxylate
P phosphate
OH hydroxyl
EtN ethanolamine
2-keto-3-deoxyoctonic acid
L-glycero-D-mannoheptose
monosaccharide

**Figure 6:** Schematic representation of the process of strand separation at the replication fork. The action of DNA gyrase in allowing free rotation within the double helix is illustrated by the circular arrow. A helix inwinding protein (HUP) is shown at the point of separation; it's direction of movement is indicated by the arrow. Molecules of helix-destabilising proteins (HDP) are shown attached to the single-stranded regions. As indicated, the action of DNA gyrase and inwinding protein involve ATP hydrolysis. (Ingraham *et al* 1983).

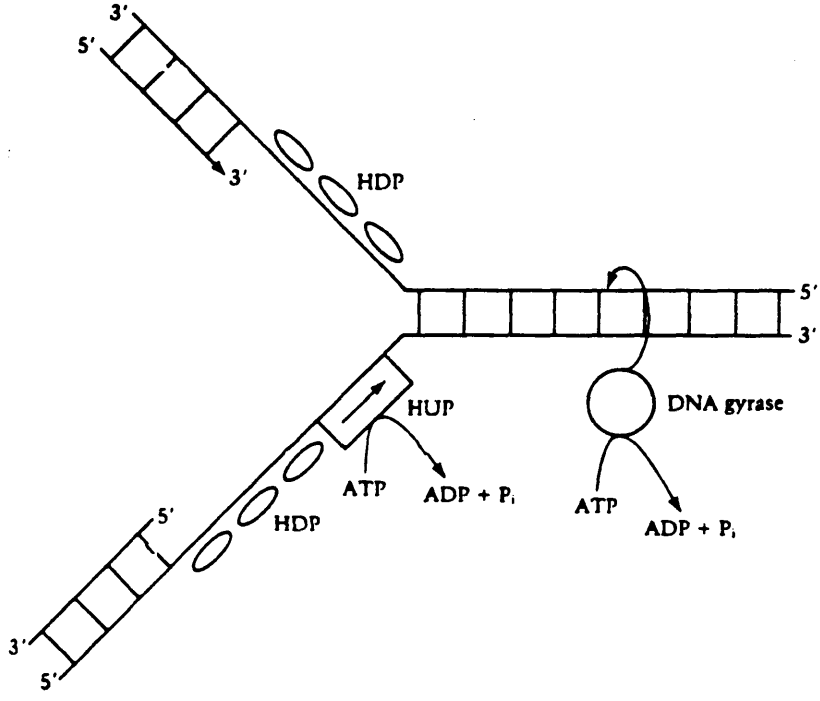
3'
5'
3'
HDP
5'
3'
HUP
DNA gyrase
ATP
ADP + Pi
ATP
ADP + Pi
5'
HDP
3'
5'

**The Bacterial Cell Surface Layer (S-Layer)**

The S-layer is a 2-D proteinatious or glycoproteinatious layer which is non-covalently attached to the bacterial cell wall (in Gram-positive bacteria) or the Gram-negative outer membrane (Sleytr & Messner 1988, Sleytr *et al* 1993) (Fig 1). S-layers are made up from protein or glycoprotein subunits which have a molecular weight of between 40 and 200 KDa. In the S-layer, the subunits are generally made up of hydrophobic and acidic amino acids, they possess few sulphur containing amino acids. The S-layer subunits are held together by non-covalent bonds (Sleytr *et al* 1993). S-layers possess pores situated between each protein subunit. The pores are of identical shape and size and possess low absorption properties, allowing nutrient exchange to occur without affecting pore size and S-layer structure (Sleytr & Messner 1988, Sara *et al* 1992, Sleytr *et al* 1993). Due to the pore size, the S-layer functions partly as a molecular sieve for the individual bacterial cell, allowing molecules of up to 45000 daltons to freely pass into contact with either the cell wall (in Gram-positive) or the outer membrane of the Gram-negative cell (Sleytr *et al* 1993, Beveridge 1993). The S-layer is also thought to be a protective coat for the bacterium, it has been shown to play an important part in bacterial adhesion and host infection (Kay & Trust 1991, Sleytr *et al* 1994a, 1994b) and may also play an important role in the maintenance of bacterial morphology (Sleytr *et al* 1993).

**Bacterial DNA, RNA and Protein Synthesis**

The bacterial genome, unlike that of the eukaryotes, is not compartmentalised. The bacterial genome consists of single looped chromosome which forms a negatively supercoiled DNA duplex. The genome exists in close proximity to the inner periphery of the cytoplasmic membrane. This proximity is thought to involve a chemical bond between DNA structure and the inner leaflet of the cytoplasmic membrane, resulting in the formation of the mesosome (Ingraham *et al* 1983).

The bacterial chromosome replicates in a semi-conservative manner (Schlegel 1988, Ingraham *et al* 1983). The mechanism by which the duplication of the bacterial genome is replicated is known as the rolling circle mechanism and it occurs in a 5' to 3' direction for both strands (Stryer 1988, Ingraham *et al* 1983).

Duplication of the bacterial chromosome begins at the origin of replication, where helix unwinding proteins (*hup*) begin to relax the negatively supercoiled DNA (Fig 6). At this point, the enzyme DNA gyrase begins to act on the relaxed single stranded DNA and stops the unwound DNA from supercoiling on itself (McMacken *et al* 1987, Drlica 1987) (Fig 6). The bacterial DNA is then replicated in a 5' to 3' direction. (Stryer 1988). However, in the genome, the single strands of DNA are orientated in antiparallel directions. As a result one strand is replicated continuously (the 5' to 3' strand) and the other strand is replicated semi-continuously, by the formation of short fragments (Okazaki fragments) which contain small RNA primers (Ingraham *et al* 1983, McMacken *et al* 1987) by the DNA polymerase enzymes. The RNA primers of the Okazaki fragments are removed after they reach about 200 base pairs in length (McMacken *et al* 1987) and replication of the genome continues until the site of the termination of replication is reached. At this point, the enzyme DNA ligase seals the duplicated chromosome which is then supercoiled by the action of DNA gyrase (Stryer 1988, McMacken *et al* 1987).

The formation of messenger RNA (mRNA) from the bacterial chromosome (mRNA transcription) is the first step in the transfer of genetic information from the genome in order to yield newly synthesised proteins. The newly transcribed mRNA is single stranded and is in fact a complementary base pair sequence of the 5' to 3' DNA strand which is being transcribed. The formation of mRNA occurs as a result of the action of the RNA polymerase enzymes which are responsible for the transcription of DNA to mRNA. Once the newly transcribed mRNA is formed, the process of protein formation by active 70S ribosomes (the process of translation) may begin (Hershey 1987).

The mRNA is translated into protein by an active ribosome and utilises transfer RNA molecules (tRNA), amino acids and is dependent upon GTP hydrolysis (Hershey 1987). On the mRNA sequence, each triplet of ribonucleotides encodes the genetic information to give rise to the addition of a specific amino acid to a growing polypeptide chain.

The mRNA molecule to be translated at the active ribosome forms a 30S initiation complex by adjoining with a 30S ribosomal subunit. This then binds with a 50S subunit to form the 70S initiation complex. At this point the process of translation and protein formation begins

(Fig 7). For each amino acid residue encoded in the mRNA sequence, a separate amino-acyl tRNA molecule is required at the donor site of the ribosome. The ribosome then moves along the mRNA sequence and recognises the different amino acid codes, each time incorporating a new corresponding tRNA molecule. The bacterial ribosome contains two sites for tRNA molecules involved in the translation process. The first site encodes the formation of the amino acid. The second site carries out the addition of the previously translated amino acid onto the growing polypeptide chain via peptide bond formation. In this way the ribosome-mRNA-tRNA complex translates an entire protein in a 5' to 3' direction.

**The Bacterial Cytosol**

The bacterial cytoplasm (cytosol) contains the majority of metabolic pathways which drive the replicative and metabolic processes of the cell. The cytoplasm is rich in proteins (80% by dry weight which carry out most of the metabolic processes, it utilises water as it's solvent (about 80% of the cytosol is water) and in this solvent exists the basic building blocks for life; amino acids, free sugars, free nucleotides, ribosomes, plasmids and several tRNA molecules (Ingraham *et al* 1983). With important metabolic functions being carried out within the cytoplasm, and the flow of nutrients between the bacterial environment and the cytosol, high intracellular osmolarity is important. It is this process which drives many of the metabolic processes between the cytosol, and the cytosolic membrane. It is therefore important that proton-gradients and osmotic gradients are maintained between the cytosol and the cell's environment. It is in the cytosol that many antimicrobial agents work, by disrupting protein integrity and function and uncoupling redox reactions which can also debilitate microbial metabolism.

The following section illustrates some of the antimicrobial agents which act upon the various parameters of bacterial physiology discussed previously. It indicates how a wide array of natural, synthetic and semi-synthetic compounds target various sites inside and outside the bacterial cell.

**Figure 7:** Pathway for the intracellular biosynthesis of an active ribosome complex.

mRNA

30s Subunit Pool

30S Initiation Complex

50S Subunit Pool

70S Initiation Complex

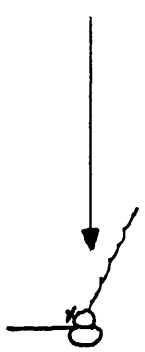

t-RNA Pool

Active Ribosome

## Inhibitors of Cell Wall Synthesis

### Beta-Lactam Antibiotics

The action of the ß-lactam group antibiotics (Fig 8) were first observed in 1928 by Alexander Flemming (Flemming 1929, Neu 1993). Flemming noticed the inhibition of *Staphylococcus* spp by a contaminant fungus, *Penicillium notatum* (Boyd 1988). The fungus was later cultured and the active compound named and purified (Schlegel 1988). The observed antibiotic was benzyl penicillin (also called penicillin G). The ß-lactam antibiotics include the penicillins, cephalosporins, monobactams and carbapenems, all containing a ß-lactam ring (Fig 8) (Aharonowitz & Cohen 1981, Neu 1993, Salyers & Whit 1994).

The ß-lactam antibiotics inhibit the final stage of cell wall biosynthesis and transpeptidation. The three stages of cell wall synthesis are;

i) synthesis of peptidoglycan precursors in the cytoplasm;

ii) transport of these precursors to the cell membrane *via* an undecaprenylphosphate carrier lipid through the cytoplasmic membrane;

iii) subsequent transpeptidation, transacylation and crosslinking of the subunits to form the new cell wall (Gabriel 1987, Park 1987, Schlegel 1988).

Prevention of the cross linking mechanism by the ß-lactam antibiotics occurs due to the binding of penicillin binding proteins or penicillin sensitive proteins (PBP's) to the ß-lactam molecule, partly as a result of the chemical analogy of the ß-lactam compounds to the D-alanyl-D-alanine segment of the muramic acid oligopeptide (Park 1987). PBP's are enzymes which carry out transpeptidation and transcarboxylation of peptidoglycan (Salyers & Whit 1994, Park 1987). The ß-lactam affinity for these proteins inhibits the replication of the peptidoglycan and results in a cell which is too small to accommodate it's replicating interior.

### Glycopeptides

The glycopeptide antibiotics (eg, vancomycin, Fig 9) inhibit the biosynthesis of the murein layer after the muramyl pentapeptide subunit has been transferred from the cytoplasm to the

**Figure 8:** Basic chemical structures for the ß-lactam group of antibiotics.

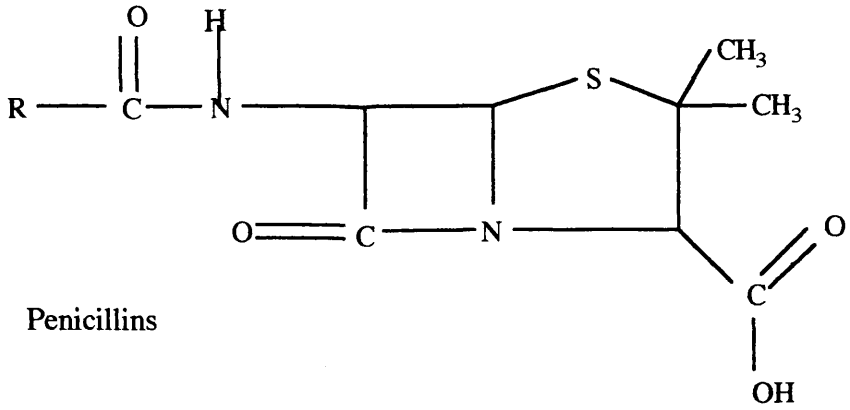

Penicillins

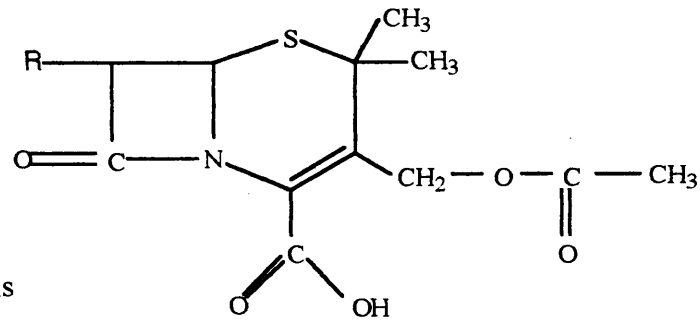

Cephalosporins

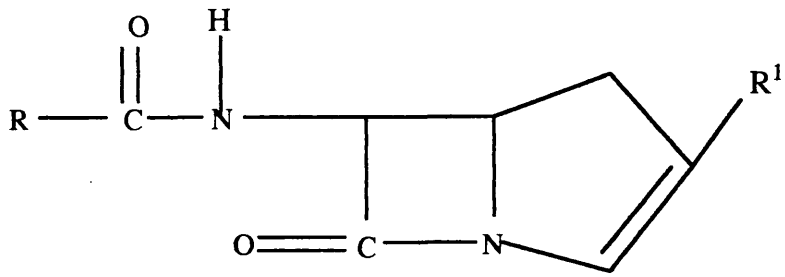

Carbapenems

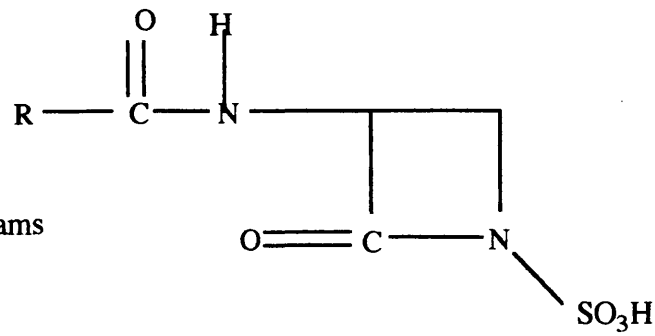

Monobactams

**Figure 9:** Chemical structure of the glycopeptide antibiotic vancomycin. (Franklin & Snow 1991).

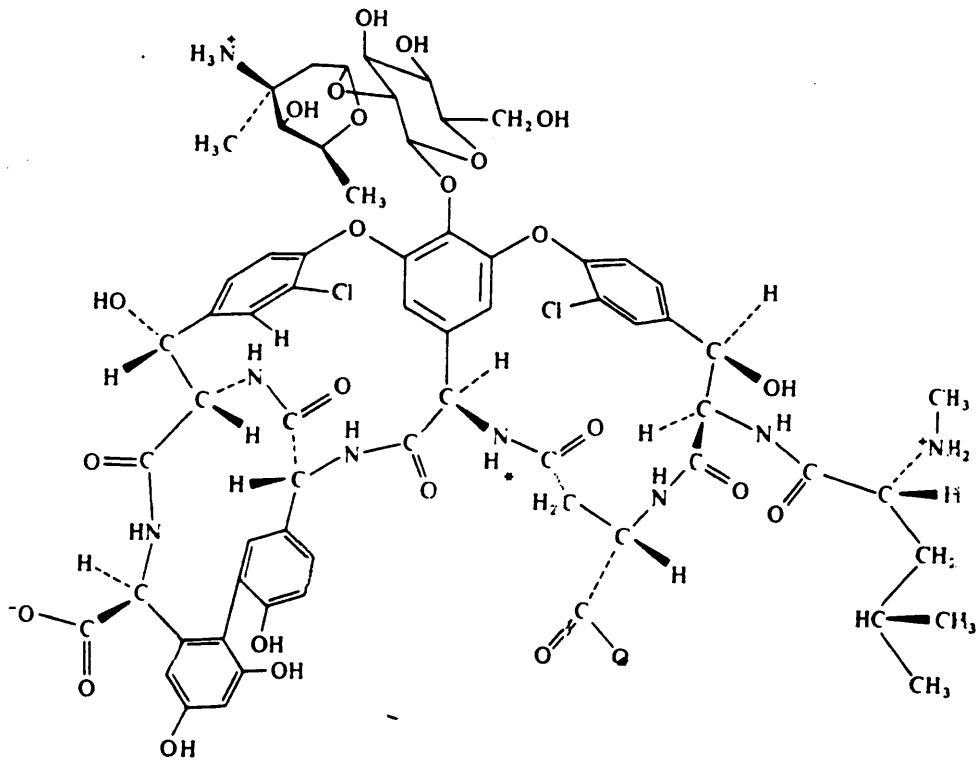

periplasm (Salyers & Whit 1994, Schlegel 1988). The glycopeptides bind to the D-alanyl-D-alanine group of the UDP-muramyl pentapeptide. This results in the inhibition of transpeptidation (similar to the beta-lactams) and also the inhibition of transglycosylation of the peptidoglycan monomers (Franklin & Snow 1991, Russell & Chopra 1990).

**D-Cycloserine**

D-cycloserine (Fig 10) inhibits the first stage of cell wall biosynthesis. It is structurally analogous to D-alanine and it's action is due to competitive inhibition of the two enzymes (alanine racemase and D-alanyl-D-alanine synthetase) which catalyse the formation of the D-alanine dipeptide portion of the pentapeptide muramic acid tail (Park 1987). This results in the inhibition of the attachment of peptidoglycan subunits *via* transpeptidation and therefore no subsequent cell wall polymerisation occurs.

**Bacitracin**

Bacitracin (Fig 11) is a polypeptide antibiotic which inhibits the second stage of cell wall synthesis by forming complexes with the lipid carrier in it's pyrophosphate form. (Franklin & Snow 1991). This may be due to the action of bacitracin upon the pyrophosphatase essential for the synthesis of the undecaprenylpyrophosphate carrier lipid (Rick 1987, Siewart & Strominger 1967). Bacitracin has also been shown to inhibit O antigen biosynthesis (Osborn 1969, Jann *et al* 1982) in the outer membrane of *Salmonella typhimurium.* This may also be due to the action of bacitracin on the carrier lipid pyrophosphatase (Rick 1987, Siewart & Strominger 1967). Bacitracin also disables the transportation and polymerisation of the murein monomers into the polymerised cell wall.

**Figure 10:** Comparison of the antibiotic D-cycloserine (a) and the peptidoglycan peptide subunit D-alanine (b).
(Russell & Chopra 1990).

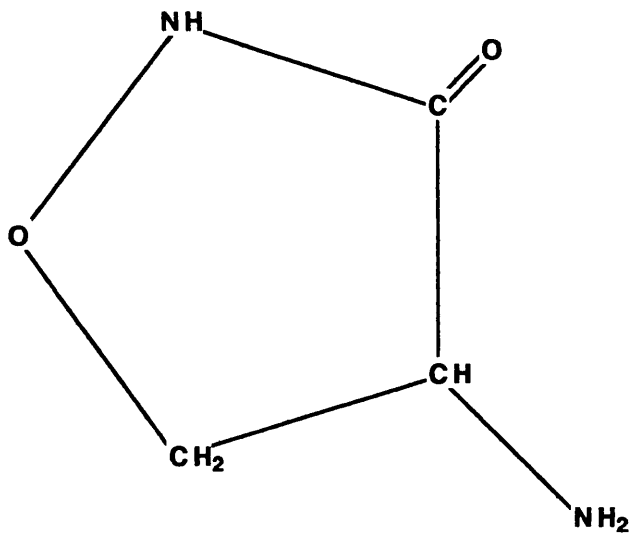


(a)

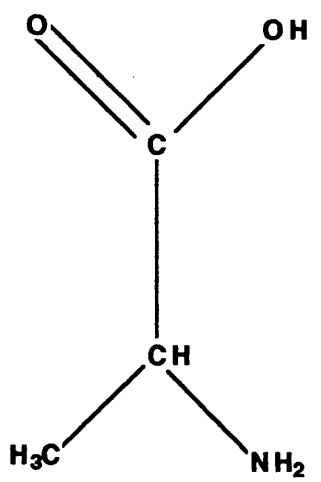


(b)

**Figure 11:** Chemical structure of the polypeptide antibiotic bacitracin A. (Franklin & Snow 1991).

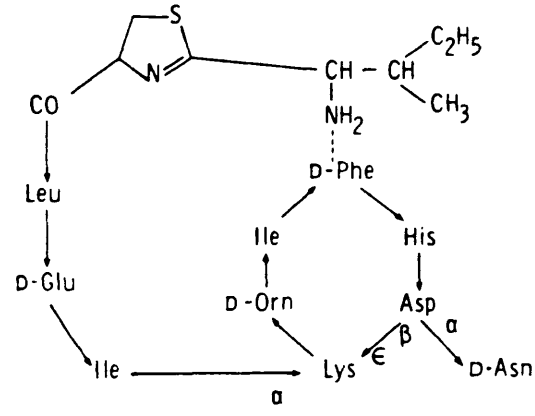
S
N
CO
CH – CH
$C_2H_5$
$CH_3$
$NH_2$
D-Phe
Leu
Ile
His
D-Glu
D-Orn
Asp
α
β
ϵ
Ile
Lys
D-Asn
α

## Inhibitors of Membrane Integrity

### Polymixins

The polymixin antibiotics (eg, polymixin B1, Fig 12) are cyclic peptides comprising of seven, nine or ten amino acids with a fatty acid tail adjoined to the peptide ring *via* a peptide bond (Schlegel 1988). These compounds usually have five positively charged amine groups associated with the 2-aminobutyric acid components of the cyclic peptide. However, they possess no overall charge due to the presence of the oxyanions from the intra-cyclic peptide bonds between the amino acids making up the cyclic peptide (Nikaido & Vaara 1987, Schlegel 1988). The mode of action of these antibiotics is against the cell membrane but the exact mechanism is not yet fully understood. The cyclic peptides are generally disruptive of the lipopolysaccharide of the outer membrane (Nikaido & Vaara 1987) and as a result cause deformation of the bacterial envelope structure. These compounds are more active towards membranes which possess phosphatidylethanolamine as the most abundant phospholipid (Waigh & Gilbert 1991). Therefore Gram-negative bacteria are more sensitive to exposure to the polymixins than Gram-positives, the most abundant phospholipid within Gram-positives being phosphatidylglycerol (Poxton 1993).

### Biguanides and Bisbiguanides

Biguanides and bisbiguanides (Fig 13) are membrane active agents which are readily absorbed by bacterial cells (Hugo & Longworth 1964). They have been widely used as disinfectants for the cleaning of machinery and packaging in the food and drinks industry (Woodcock 1988) and have also been highly recommended for use as antiseptic oral mouthwashes (Woodcock 1988). The biguanides and bisbiguanides include the compounds polyhexamethylene bisbiguanide (PHMB, which normally exists as a polymer of five monomeric units shown in Fig 13) (Broxton *et al* 1983b) and the biguanides chlorhexidine and alexidine (Hugo & Longworth 1964, Hugo & Longworth 1965, Broxton *et al* 1983a, Chawner & Gilbert 1989a, Chawner & Gilbert 1989b) (Fig 13). They are known to cause leakage of intracellular constituents (eg, $K^+$ ions, nucleotides, amino acids, etc) (Hugo & Longworth 1964, Broxton *et al* 1983a, Broxton *et al* 1983b, Chawner & Gilbert 1989a) and PHMB and alexidine have been shown to cause lysis of whole cells, but this is not the case for chlorhexidine. The ability of alexidine

**Figure 12:** Structure of the membrane active antibiotic polymixin B1. (Franklin & Snow 1991).

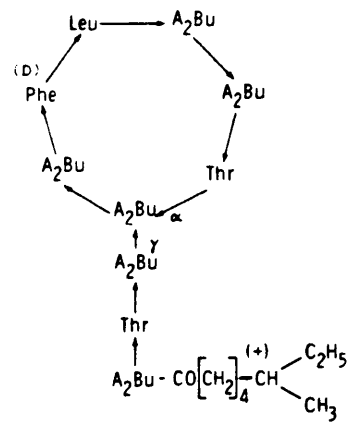
Leu
$A_2Bu$
$A_2Bu$
Thr
$A_2Bu$ α
γ $A_2Bu$
Thr
$A_2Bu$ - CO[$CH_2$]$_4$ (+) CH
$C_2H_5$
$CH_3$
$A_2Bu$
(D) Phe

**Figure 13:** General chemical formula for PHMB and the chemical structures of alexidine and chlorhexidine.

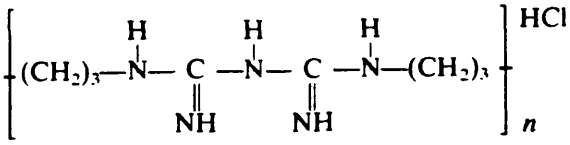

The general chemical formula for the polyhexamethyl biguanide (PHMB) biocides.

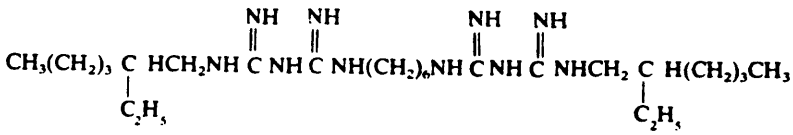

The chemical structure for alexidine.

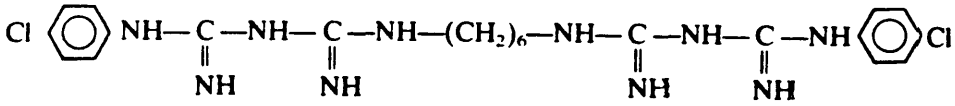

The chemical structure for chlorhexidine.

to cause cell lysis is thought to be due to the difference between the tail groups of the two compounds alexidine and chlorhexidine (Chawner & Gilbert 1989a, Chawner & Gilbert 1989b) (Fig 13). It is thought that in solution (due to the chemical make up of it's tail group) alexidine may increase it's chain length by adjoining to other alexidine molecules (Chawner & Gilbert 1989b). This factor may increase it's bactericidal activity in a similar manner to that of PHMB, where increases of polymer chain length have been shown to effectively increase bactericidal ability (Broxton *et al* 1983a, Broxton *et al* 1983b, Gilbert *et al* 1990c, Gilbert *et al* 1991). The exact mode of action of the biguanides has not been observed. However, the mode of action of the bisbiguanide PHMB has been shown to be due to the chemical interaction of the antimicrobial agent with the acidic head-group of the membrane lipid phosphatidylethanolamine (Gilbert *et al* 1991, Woodcock 1988). The binding of PHMB to the bacterial membrane causes chemical instability of the fluid mosaic lipid bilayer structure (Fig 14). This PHMB lipid complex stabilises *via* bonds made with proteins present in the membrane. As a result of this action membrane integrity is lost and the leakage of vital cytoplasmic constituents may result in cell death (Woodcock 1988).

**Quaternary Ammonium Compounds (QAC's)**

The quaternary ammonium compounds (QAC's) consist of a nitrogen which has a valency of five with four of the five groups surrounding it being covalently linked alkyl and heterocyclic radicals and the fifth having a cationic structure (Fig 15). Compounds classed as QAC's include cetrimide and benzalkonium chloride (Chapman 1987). The QAC's are membrane active agents which on exposure to bacteria rapidly induce the leakage of cytoplasmic constituents. This is due to the cationic QAC's interaction with the phospholipid head-groups in the bacterial membrane (Chapman 1987, Russell & Chopra 1990). This interaction is somewhat similar to that of PHMB and as a result disintegrates membrane integrity and membrane related metabolism. The QAC's are sometimes used as cosmetic preservatives (Moore & Stretton 1981) and are widely used as biocides in the water treatment industry (Skaliy *et al* 1980).

**Figure 14:** Proposed mechanism of action by PHMB (represented by ∧∧∧) (Woodcock 1988).

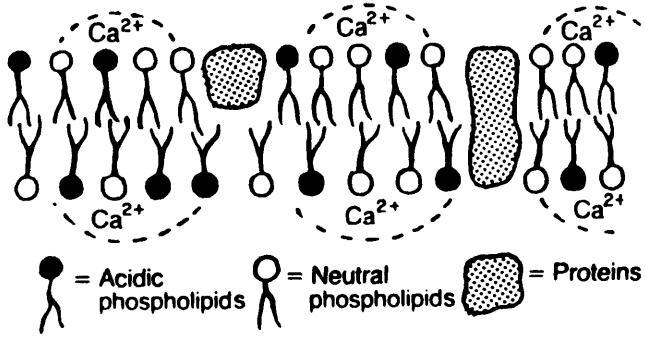


(A) Bacterial cytoplasmic membrane conforming to "fluid mosaic" model; stabilised by $Ca^{++}$ and phospholipid mixture and distribution

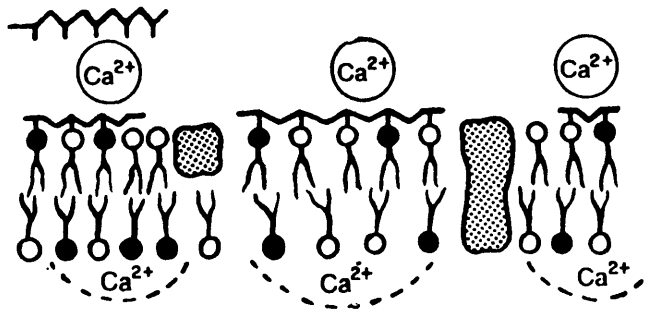


(B) Initial wave of phmb displaces surface cations, binds to phospholipids, causes change in packing

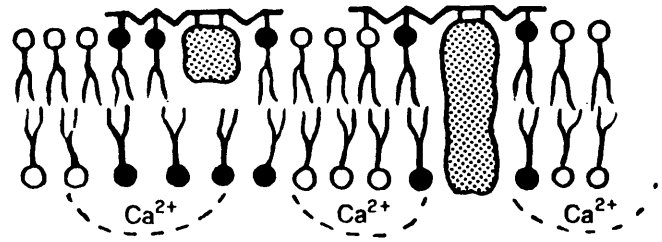


(C) Phmb induces a phospholipid phase separation, effects concentrate in the area of integral proteins; causes increase in membrane permeability, $K^{+}$ efflux, loss of enzyme function, *i.e.* bacteriostatic level

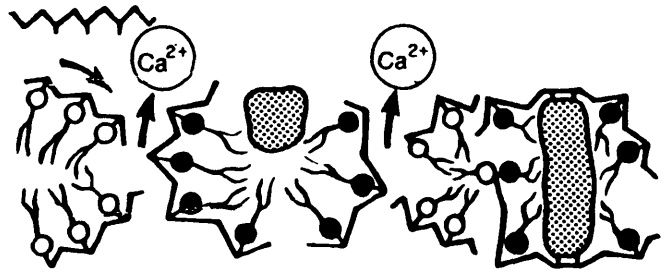


(D) De-stabilised zones aggregate into favourable hexagonal phase, further stabilised by binding of excess phmb (electrostatic and hydrophobic); complete loss of membrane function, *i.e.* bactericidal level

**Figure 15:** The general chemical formula for quaternary ammonium compounds, ie, cetrimide. (Russell & Chopra 1990).

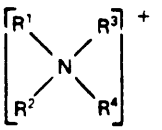


$X^-$ General structure

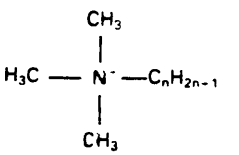


(n=12, 14 or 16)
Cetrimide
(a mixture of dodecyl-, tetradecyl- and hexadecyl-trimethylammonium bromide)

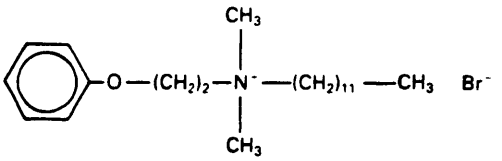


Domiphen bromide
(dodecyldimethyl-2-phenoxyethyl-ammonium bromide)

### Phenolic Compounds

Phenols, phenol containing compounds and phenolic derivatives (eg, xylenol, lysol, dichlorophen and fentichlor) have been shown to be active at the bacterial cytoplasmic membrane (Kroll & Patchett 1991) (Fig 16). They are used widely as disinfectants (ie, 'Dettol') and derivatives such as fentichlor and dichlorophen are used in the treatment of water cooling towers (Dept of Health 1989). Studies with fentichlor (Bloomfield 1974) show the mode of action of the phenolics as the uncoupling of the pH gradient which exists between the bacterial cell and it's bathing solution, thereby inducing subsequent uncoupling of the $F_1/F_0$ membrane-bound ATPase (Bloomfield 1974, Kroll & Patchett 1991). Although membrane active agents, the phenolics have also been shown to induce intracellular protein coagulation and precipitation (Wainwright 1988).

## Inhibitors of DNA and RNA Synthesis

### 4-Quinolone Antibiotics

The 4-quinolone antibiotics (Fig 17) are powerful antibacterial agents exhibiting a 3 log cycle reduction in bacterial numbers only two hours after addition of the antibiotic to a bacterial culture (Russell & Chopra 1990). Although the exact mechanism is not fully understood it is thought that they inhibit the bacterial DNA gyrase enzymes (Howard *et al* 1994). DNA gyrases are involved in the separation and relaxation of supercoiled DNA double helixes (Stryer 1988). DNA gyrases are composed of four protein subunits, two A subunits and two B subunits (Howard *et al* 1994). The A subunits are involved in breakage and sealing of DNA strands and the B subunits carry out the hydrolysis of ATP resulting in supercoil formation (Fig 6).

The 4-quinolones are thought to form complexes with the A subunits, directly inhibiting the function of the A subunit and partially inhibiting that of the B subunit. This results in direct inhibition of DNA replication within the target cell. The cell responds by activating an SOS process (Walker 1987, Donachie & Robinson 1987). Subsequent cell division does not occur due to the inhibited bacterial cell's inability to complete DNA replication, which in turn disrupts the controlling mechanisms for septum formation (Donachie & Robinson 1987).

**Figure 16:** The chemical structures of the phenolic biocides dichlorophen and fentichlor.

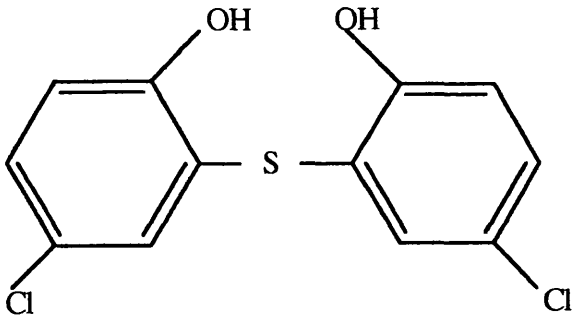


Fentichlor

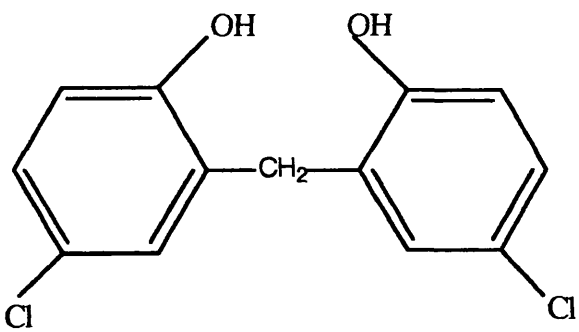


Dichlorophen

**Figure 17:** Quinoline and antibacterial 4-quinolones (Russell & Chopra 1990).

*Quinoline*

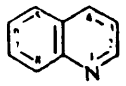

*4-Quinolone*

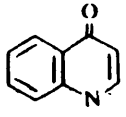

*Example:* Ciprofloxacin

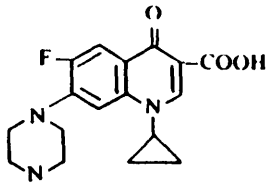

*Other examples:*
Norfloxacin
Oxolinic acid
Ofloxacin
Acrosoxacin
Flumequine
Enoxacin

*8-Aza-4-Quinolone*

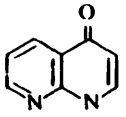

*Example:* Nalidixic acid

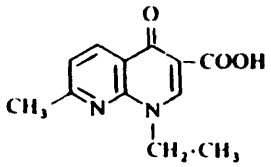

*2-Aza-4-Quinolone*

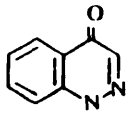

*Example:* Cinoxacin

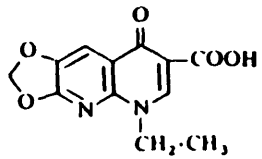

*6,8-Diaza-4-Quinolone*

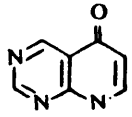

*Examples:* Pipemidic and Piromidic acids

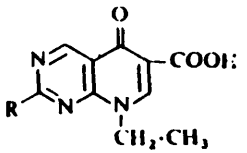

R(Pipemidic):

R(Piromidic):

When the cells are exposed to nalidixic acid they are unable to repair the subsequent cellular damage and cell death rapidly ensues. However, sufficient experimental evidence exists to show that other 4-quinolone antibacterial agents (eg, ciprofloxacin, ofloxacin and norfloxacin) work *via* a different mechanism to that of nalidixic acid (Howard *et al* 1993, 1994). The work carried out by Howard *et al* (1994) has shown that cells treated with ciprofloxacin and ofloxacin were capable of DNA replication after exposure to these antibiotics. The mode of action of these 4-quinolone antimicrobials is still thought to be targeted towards DNA replication (Howard *et al* 1994), but the subsequent course of cell death is not yet fully understood.

**Ansamycin**

The ansamycin group of antibiotics consist of the rifamycins (eg, rifampicin or rifampin) and the streptovaricins (eg, streptovaricin D, Fig 18). Both groups inhibit the action of the RNA polymerases directly at the beta-subunit of the core enzyme (Ingraham *et al* 1983, Drlica 1987, Salyers & Whit 1994). The action of these antibiotics affects the initiation process of RNA transcription (Drlica 1987). The inhibition of the initiation process can be observed both *in vivo* (using the whole enzyme) and *in vitro* (using only the beta-subunit) (Salyers & Whit 1994). The inability of the bacterial cell to complete transcription after the disruption of primer initiation results in the bacterial cell becoming deficient in vital proteins. This will result in metabolic disruption and subsequent cell death.

## Inhibitors of Protein Synthesis

**Aminoglycosides**

The aminoglycoside antibiotics (ie, gentamicin and kanamycin, Fig 19) target the bacterial ribosome by binding to the 30S subunit of the ribosome (Russell & Chopra 1990, Salyers & Whit 1994). This does not stop the binding of mRNA to the subunit, but disables the binding of the 50S subunit and the formation of a 70S initiation complex (Russell & Chopra 1990, Salyers & Whit 1994). It is thought that the build up of 30S ribosomal subunits inside the bacterial cell is toxic and it is this factor that causes cell death (Salyers & Whit 1994). It has also been shown that some aminoglycosides (eg, gentamicin) may also have an

inhibitive effect on the cell membrane (Martin & Beveridge 1986), where the outer membranes of exposed cells exhibit a subsequent blistering.

### The Macrolides

The macrolide antibiotics (eg, erythromycin, Fig 20) consist of a macro cyclic lactone ring which has two aromatic ring structures joined *via* oxide bridges (Nikaido & Vaara 1987, Schlegel 1988, Salyers & Whit 1994). They have been shown to inhibit protein synthesis by binding to the 50S subunit of bacterial ribosomes (unlike the aminoglycosides which bind the 30S subunit) (Schlegel 1988, Salyers & Whit 1994). This subsequently inhibits the elongation of new protein production by peptidyl transferase and may also inhibit ribosomal translocation (Salyers & Whit 1994).

## Inhibitors of Metabolic Intermediates

### Sulphonamides

Although the 4-quinolones inhibit DNA synthesis at the formation of a new double helix, the sulphonamides (Fig 21) inhibit the synthesis of DNA and RNA by inhibition of nucleotide formation *via* tetrahydrofolic acid (THFA) metabolism (Neuhard & Nygaard 1987, Brown & Williamson 1987) (Fig 22).

The sulphonamides are structurally analogous to p-aminobenzoic acid (PABA) (Fig 21) a major substrate in the synthesis of THFA . In turn THFA acts as a coenzyme in the metabolism of inosine (the first purine base to be synthesised and subsequent precursor of all other purines), whereby THFA donates carbon atoms to the purine base precursors (Neuhard & Nygaard 1987, Brown & Williamson 1987). The structural analogy of the sulphonamides to PABA allows them to act as alternative substrates for dihydropteroate synthase (DHPS). DHPS converts PABA into dihydropteroic acid, the first step in the pathway for the production of THFA from PABA (Brown & Williamson 1987, Neuhard & Nygaard 1987) (Fig 22).

As a result THFA analogues are produced at the end of the pathway which are inactive and

**Figure 18:** Chemical structure of streptovaricin D. (Franklin & Snow 1991).

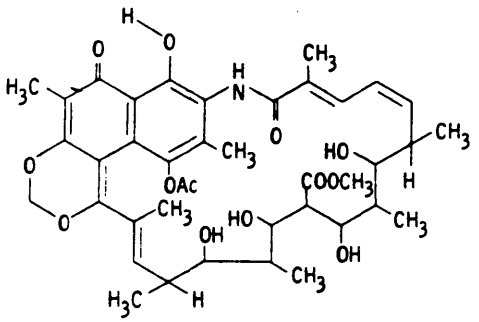

Streptovaricin D

**Figure 19:** The aminoglycoside antibiotics gentamycin and kanamycin. (Franklin & Snow 1991).

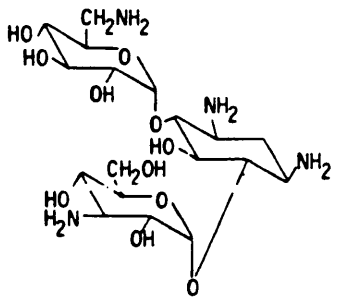

Kanamycin A

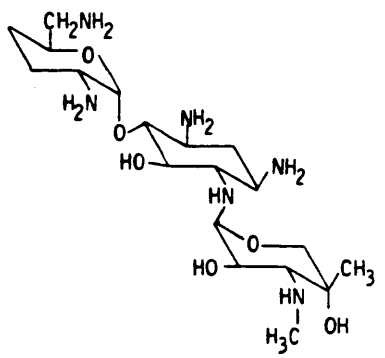

Gentamicin $C_{1a}$

**Figure 20:** The chemical structure of the macrolide antibiotic erythromycin. (Franklin & Snow 1991).

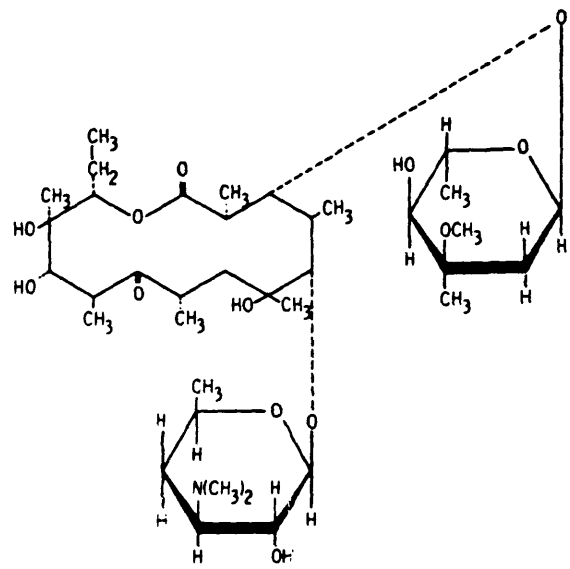

**Figure 21:** Comparison of the structure of the sulphonamide antibiotics with the tetrahydrofolic acid (THFA) precursor para-aminobenzoic acid (PABA).

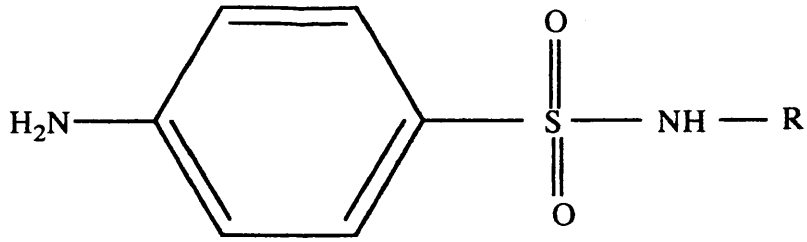


Sulphonamide Antibiotic Group

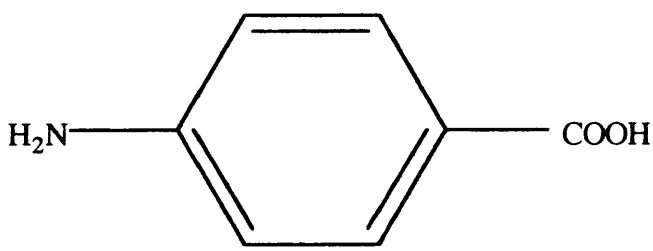


Chemical Structure of Para-aminobenzoic Acid

**Figure 22:** The sites of action (⊗) of the sulphonamide antibiotics in the production pathway of THFA.

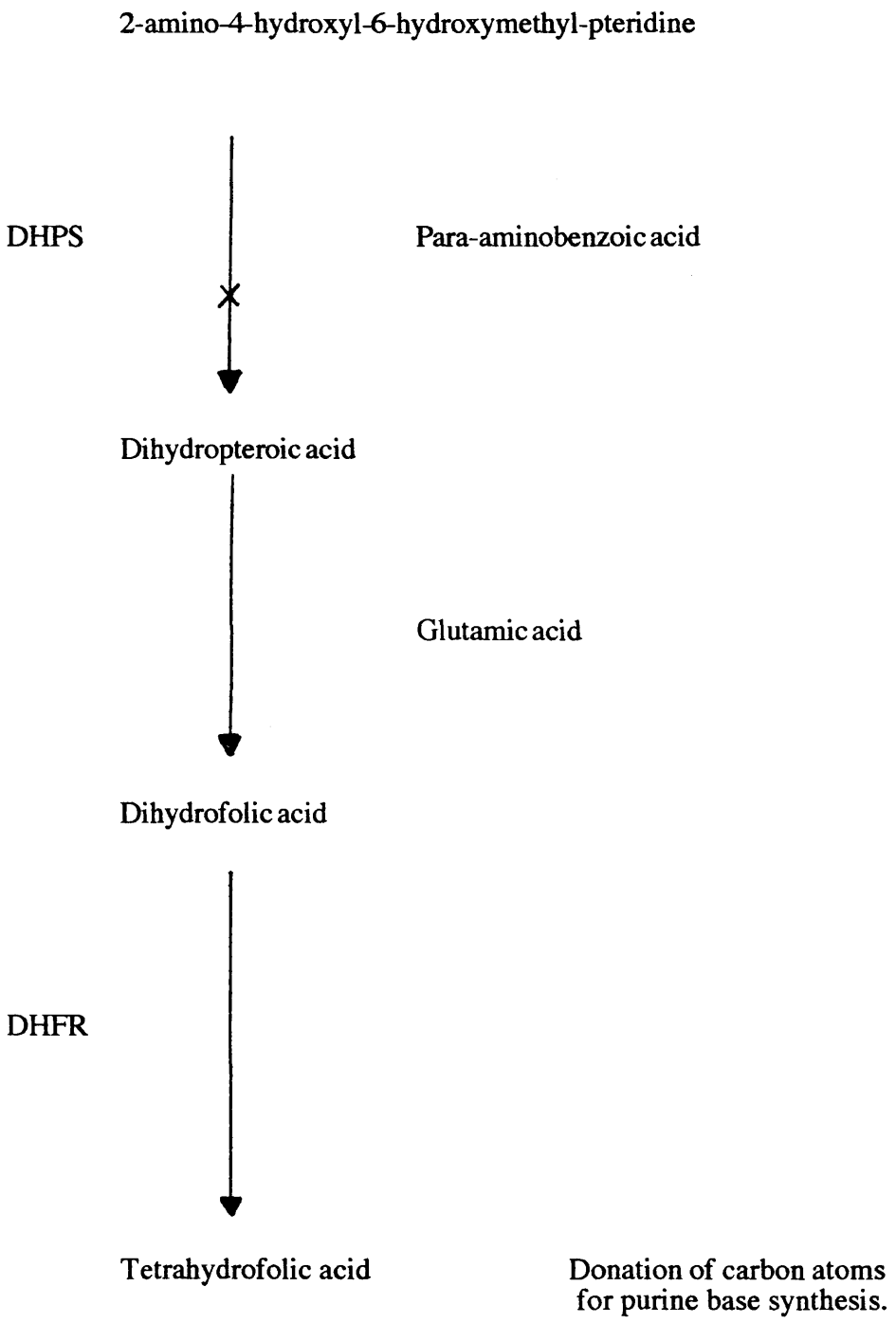
2-amino-4-hydroxyl-6-hydroxymethyl-pteridine
DHPS
Para-aminobenzoic acid
Dihydropteroic acid
Glutamic acid
Dihydrofolic acid
DHFR
Tetrahydrofolic acid
Donation of carbon atoms
for purine base synthesis.

inadequate for the donation of carbon atoms to the formation of inositol and subsequent purine base formation. (Brown & Williamson 1987, Neuhardt & Nygaard 1987, Russell & Chopra 1990). This in turn inhibits the formation of new DNA and RNA precursors, inhibiting DNA and RNA synthesis and further cell division.

## Thiol Interactive Agents

### Bronopol

Bronopol (Fig 23) is widely used in the treatment of water cooling towers for the elimination or preservation of cooling water from *Legionella* spp and is included in various toiletries and cosmetics as a preservative (Dept of Health 1987, Waigh & Gilbert 1991). The mode of action of Bronopol has been reported as being thiol interactive, oxidatively catalysing thiol groups present in the bacterial cell to their corresponding disulphides in the presence of oxygen (Waigh & Gilbert 1991, Shepherd 1987). The addition of Bronopol to cells which are readily utilising cysteine has been shown to stimulate oxygen uptake. The increased oxygen uptake was later shown to be accompanied by free radical generation (both thiyl and hydroxy radicals) (Shepherd 1987). This oxidatively corrupts the tertiary and secondary structure of vital proteins and other thiol containing compounds (eg, glutathione and cysteine) . Subsequently, this exposes the cell to the detrimental consequences of oxidative stress (eg. membrane disruption, oxidation of non-thiol biochemical precursors etc). Consequently, the cell dies due to disruption of intracellular metabolic processes which results in the disability of the cell to utilise nutrients and synthesise essential metabolic precursors.

### The Isothiazolones

The isothiazolone biocides (eg, 5-chloro-N-methyl-isothiazolone (CMIT), N-Methyl-isothiazolone (MIT) and benzisothiazolone (BIT), Fig 24) are thiol interactive agents (Collier *et al* 1990a, Collier *et al* 1990b, Collier *et al* 1990c, Collier *et al* 1991, Waigh & Gilbert 1991) which affect cysteine interactions in proteins and upset the tertiary and secondary structure of proteins rendering them useless (Fig 25). Exposure of the fission yeast *Schizosaccharomyces pombe* to CMIT results in the increased elongation and aggregation of

cells at cell division with septum formation but without complete division (Collier *et al* 1990b). This may be indicative of interruption of DNA replication by CMIT. CMIT has also been shown to react with labile nitrogen groups in the form of amines (Collier *et al* 1990b), this means that CMIT can also interrupt protein structure and function by binding with free amine groups as well as being thiol interactive. CMIT, MIT and BIT are used widely as biocides in the water industry and fuel systems. MIT and CMIT are used as preservatives in cosmetic and pharmaceutical products (Collier *et al* 1990c).

**Hydrogen Peroxide and Generators of Radical Formation**

Although compounds which induce bacterial cell death due to radical formation are known to be active on the bacterial envelope, it is usually understood that these compounds work by disruption of protein structure and function (Baldry & Fraser 1988). Many compounds induce cell death due to radical formation eg, hydrogen peroxide, peracetic acid, ozone, hypochlorous acid and many aliphatic peracids (Baldry & Fraser 1988, Halliwell 1993). Once inside the cell, the hydrogen peroxide breaks down to give rise to two hydroxy radicals. These are then extremely chemically reactive and readily break protein-thiol interactions, the result of which is the generation of a thiyl radical (Halliwell 1993) (Equation 1). This not only causes the breakdown of metabolism *via* disruption of protein integrity but generates a greater number of active radicals due to the thiyl radical reacting with oxygen subsequently producing thiyl peroxil radicals (Halliwell 1993, Asmus 1990) ( Equation 2).

(1) $OH\cdot + SH \longrightarrow S\cdot + H_2O$

(2) $S\cdot + O_2 \longrightarrow SO_2\cdot$

Radical formers are also active against membrane structure and function due to radical oxidation of lipid head groups and interactions with lipid bound proteins eg, Braun's Lipoprotein, transportases and ATPase complexes. This, together with the breakdown of protein integrity, renders the cellular barriers dysfunctional. Furthermore, the internal and external mediators of microbial metabolism are disabled, resulting in cell death. Generators of oxygen-free radicals are widely used to disinfect and sterilise packaging for the food and

drinks industry, to treat waste sewage sludge and in the leisure industry to clean bathing water (Baldry & Fraser 1988).

**Figure 23:** The chemical structure of Bronopol.

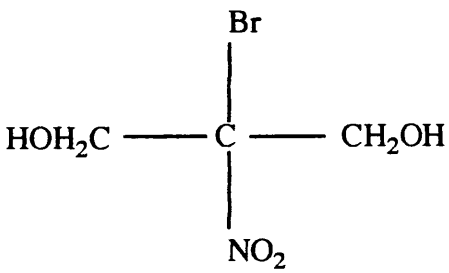


Chemical structure of bronopol

**Figure 24:** Chemical structures of some isothiazolone biocides.

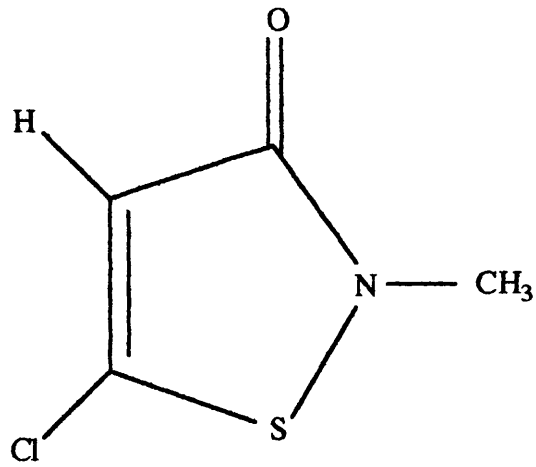


CMIT (5-chloro-N-methyl-isothiazolone)

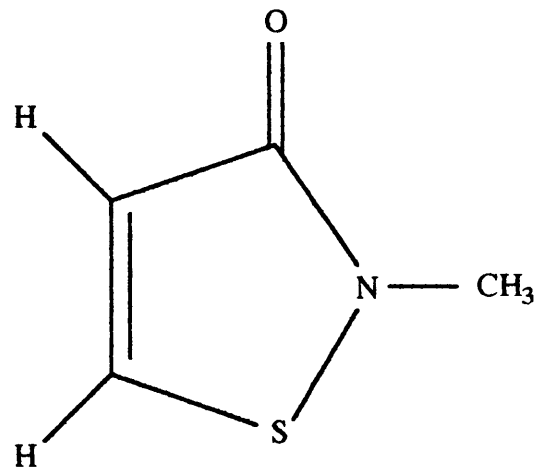


MIT (N-methyl-isothiazolone)

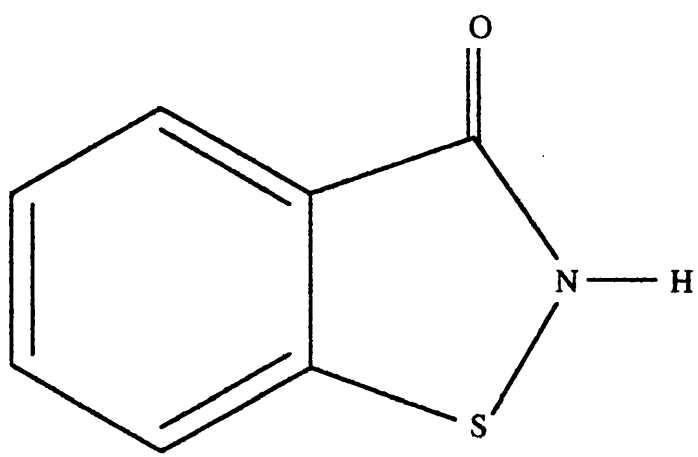


BIT (Benzisothiazolone)

**Figure 25:** The generally accepted mode of thiol (RSH) interaction for the isothiazolone biocide BIT. (Collier *et al* 1990c).

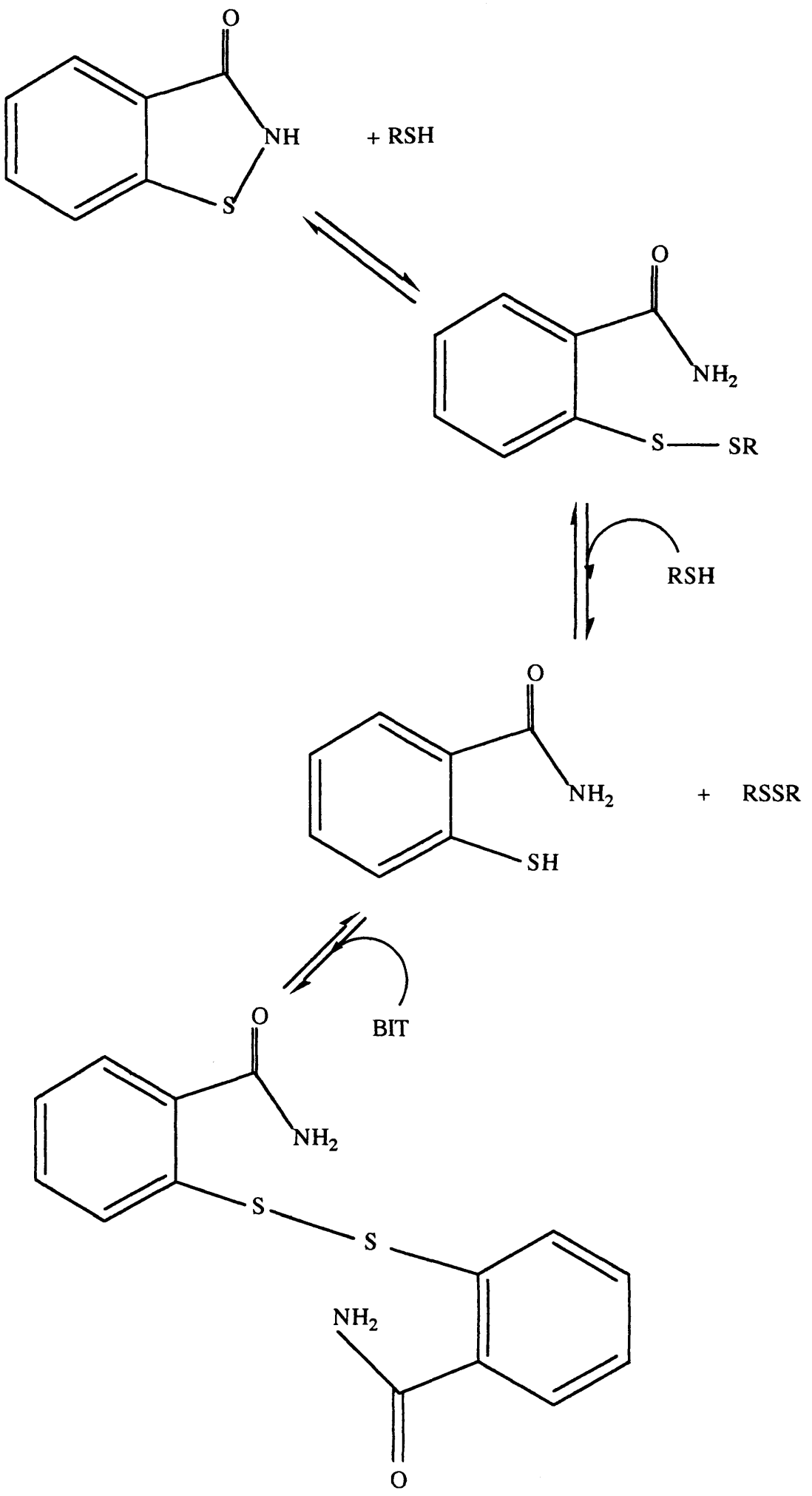
O
NH
S
+ RSH
O
NH2
S
SR
RSH
O
NH2
SH
+ RSSR
BIT
O
NH2
S
S
NH2
O

# THE PYRITHIONE ANTIMICROBIALS

## DISCOVERY OF THE PYRITHIONE ANTIMICROBIALS

1-Hydroxypyridine-2-thione (2-mercaptopyridine-N-oxide, Hydroxypyrithione, omadine or HPT) (Fig 26) was first synthesised by Shaw *et al* (1950) at the Squibb Institute for Medical Research, New Jersey, USA. Shaw and coworkers synthesised HPT as a sulphur analogue of aspergillic acid (Shaw *et al* 1949, 1950) (Fig 26). This led to the screening and subsequent observation of the pyrithione group compounds as antimicrobial agents, especially the sodium salt of hydroxypyrithione, sodium pyrithione (NaPT, Fig 26) and the zinc chelate, zinc pyrithione (ZnPT) (Albert *et al* 1956) (Fig 26). The Squibb Institute later merged with the Olin Corporation, Connecticut, USA (Hyde & Nelson 1984) and they are currently the largest producers of pyrithiones in the world.

## PATENTED APPLICATIONS OF THE PYRITHIONE BIOCIDES

The first US patent (Shaw *et al* 1954) was granted in 1954 to the Olin Corporation for the production of HPT and NaPT. Three years later another patent (Bernstein & Losee 1957) was granted for the production of heavy metal chelates (Nelson & Hyde 1981). With the patenting of the production of ZnPT in 1957 (Bernstein & Losee 1957), Procter and Gamble (a subsidiary of Olin) launched the ZnPT containing anti-dandruff shampoo 'Head and Shoulders' (Hyde & Auerbach 1979, Nelson & Hyde 1981, Hyde & Nelson 1984). In 1966, Procter and Gamble together with R T Vanberbilt Co were granted joint patents for the use and incorporation of pyrithiones into detergent and cosmetic formulations (Karsten *et al* 1966, 1968). Most recently, the incorporation of chitosan pyrithione (Fig 27) as an antimicrobial in personal care products was granted to Olin Corporation in 1990 (Nelson 1990).

**Figure 26:** The chemical structures for aspergillic acid, the pyrithione biocides and the metal-chelating biocide 8-hydroxyquinoline. The highlighted area denotes the pseudo-QAC area proposed by Hyde & Nelson (1984).

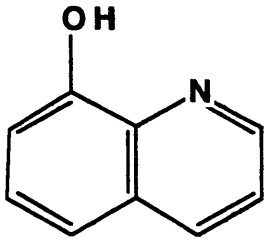


8-Hydroxyquinoline

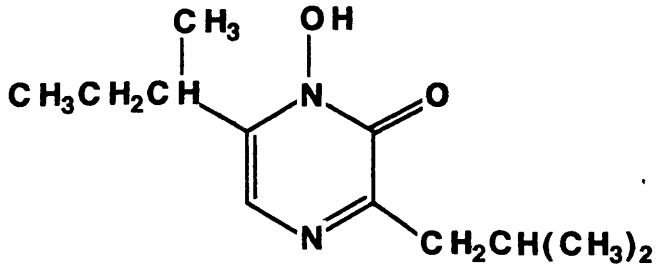


Aspergillic Acid

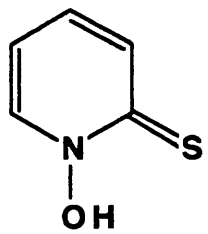


Hydroxypyrithione (HPT)

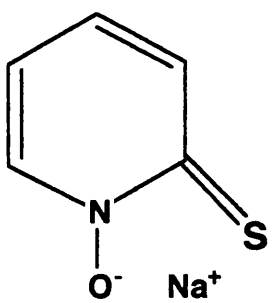


Sodium Pyrithione (NaPT)

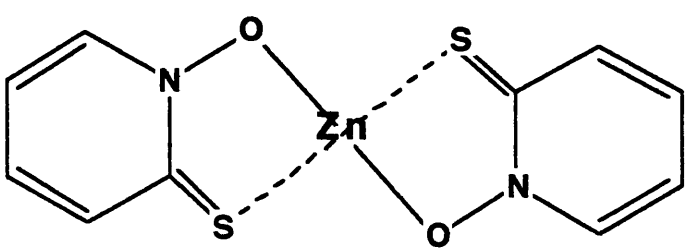


Zinc Pyrithione (ZnPT)

**Figure 27:** The chemical structure of chitosan pyrithione.

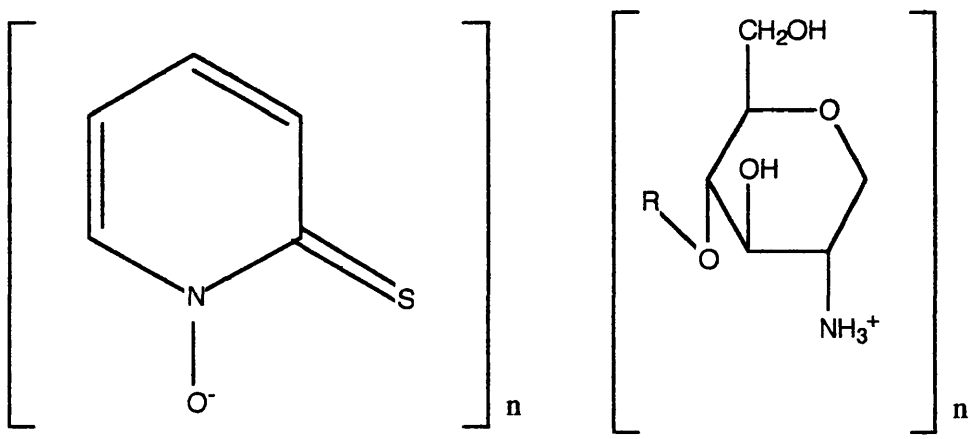


Chitosan Pyrithione

## PYRITHIONE CHEMISTRY

### Chemical Synthesis of Hydroxypyrithione

The chemical synthesis of hydroxypyrithione is readily achieved by the reaction of a 2-halopyridine with a peracid (ie, peracetic acid). This reaction yields a 2-halopyridine-N-oxide. The halogen can then be replaced by reacting the 2-halopyridine-N-oxide with an alkali metal hydrosulphide (Hyde & Nelson 1984) (Equations 3 & 4).

(3) 2-Chloropyridine + Peracetic acid ⟶ 2-Chloropyridine-N-oxide

(4) 2-Chloropyridine-N-oxide + Sodium hydrosulphide ⟶ 2-Mercaptopyridine-N-oxide(hydroxypyrithione) + Sodium Chloride

### Chemical Properties of the Pyrithione Biocides

HPT exists as both thiol and thione tautomers when in solution and may form disulphides between monomers of itself in solution (Nelson & Hyde 1981, Hyde & Nelson 1984) (Fig 28). Below pH 3, the thione form of HPT is most abundant, at pH 7.6 both the thiol and thione are in equal concentrations and from pH 7.6 to pH 10 the thiol is most prevalent. In solution at a pH greater than 10 oxidation occurs and the pyrithione molecule breaks down to produce a sulphinic acid anion (Hyde & Nelson 1984, Fenn & Csejka 1982) (Fig 29). The pyrithione group compounds are easily oxidised by many oxidising agents, particularly organic peroxides which may be found in cosmetics as a result of impurities from the addition of glycols and polyglycols incorporated into cosmetic base formulations (Nelson & Hyde 1981, Hyde & Nelson 1984).

Sodium pyrithione has a molecular weight of 149.2 Daltons and exhibits good solubility in water (53% w/w at 25°C) and is relatively soluble in ethanol (19% w/w at 25°C) (Nelson & Hyde 1981). Zinc pyrithione has a molecular weight of 317.7 Daltons and with a solubility in water of 0.0015% w/w at 25°C and a solubility in ethanol of 0.01% w/w at 25°C,

demonstrates a greatly decreased solubility than it's sodium counterpart (Nelson & Hyde 1981). Both compounds are relatively heat stable, exhibiting activity after 24 hours at 100°C (Nelson & Hyde 1981).

In solution NaPT dissociates to give a separate sodium ion and pyrithiolate ion (Fig 30). ZnPT exists in the polar phase as a pyrithione dimer around a central zinc ion *via* two sulphur-oxygen bridges (Fig 26). In the solid phase, gaseous phase, and when solubilised in organic solvents, ZnPT exists as a ZnPT dimer (Barnett *et al* 1977, Fig 31). The two ZnPT monomers within the dimer are held together by bonds between the zinc atom of one ZnPT monomer, and the oxygen atom of the other, producing the two zinc-oxygen bridges which maintain the dimer structure (Fig 31) (Barnett *et al* 1977).

**Photolysis of the Pyrithione Biocides**

The pyrithiones can be photolysed by day light (wavelength = 320 to 355nm, Neihof *et al* 1979) with a consequential reduction in bactericidal qualities (Neihof *et al* 1979, Seymour & Bailey 1981, Nelson & Hyde 1981, Hyde & Nelson 1984). Exposure of hydroxypyrithione to visible light (within 320 to 355nm, or with a standard 500 watt light bulb) will yield pyrithione radicals and hydroxy radicals (Boivin *et al* 1992), which are of interest in the chemical industry (Equation 5).

(5) Pyrithione —(Photon)→ Pyrithione + OH

**Metal Chelating Properties of the Pyrithiones**

The pyrithiones have excellent metal chelating properties. The most utilised pyrithione metal chelate being zinc pyrithione (Hyde & Nelson 1984, Davies 1985, Fenn & Alexander 1988, Seymour & Bailey 1981, Nakajima *et al* 1993, Marks *et al* 1985, Imokawa & Okamoto 1982, Hyde & Auerbach 1979) (Fig 26). Transchelation is also observable when ZnPT and NaPT are in the presence of strong Lewis bases, ie, $Cu^{2+}$ and $Fe^{3+}$ (Edrissi *et al* 1971). The chelating properties of the pyrithione biocides, including the sodium salt, enable the utilisation of more simplistic methodologies for the assay of pyrithiones by thin layer chromatography (TLC) (Seymour & Bailey 1981) and high performance liquid

**Figure 28:** The chemical structures of the thiol and thione tautomers of hydroxypyrithione.

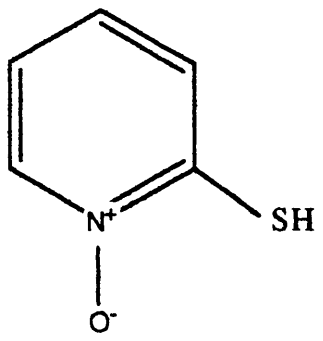


Thiol tautomer of pyrithione

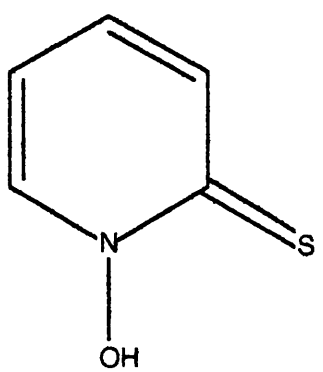


Thione tautomer of pyrithione

**Figure 29:** The reaction sequence for the oxidation of hydroxypyrithione.

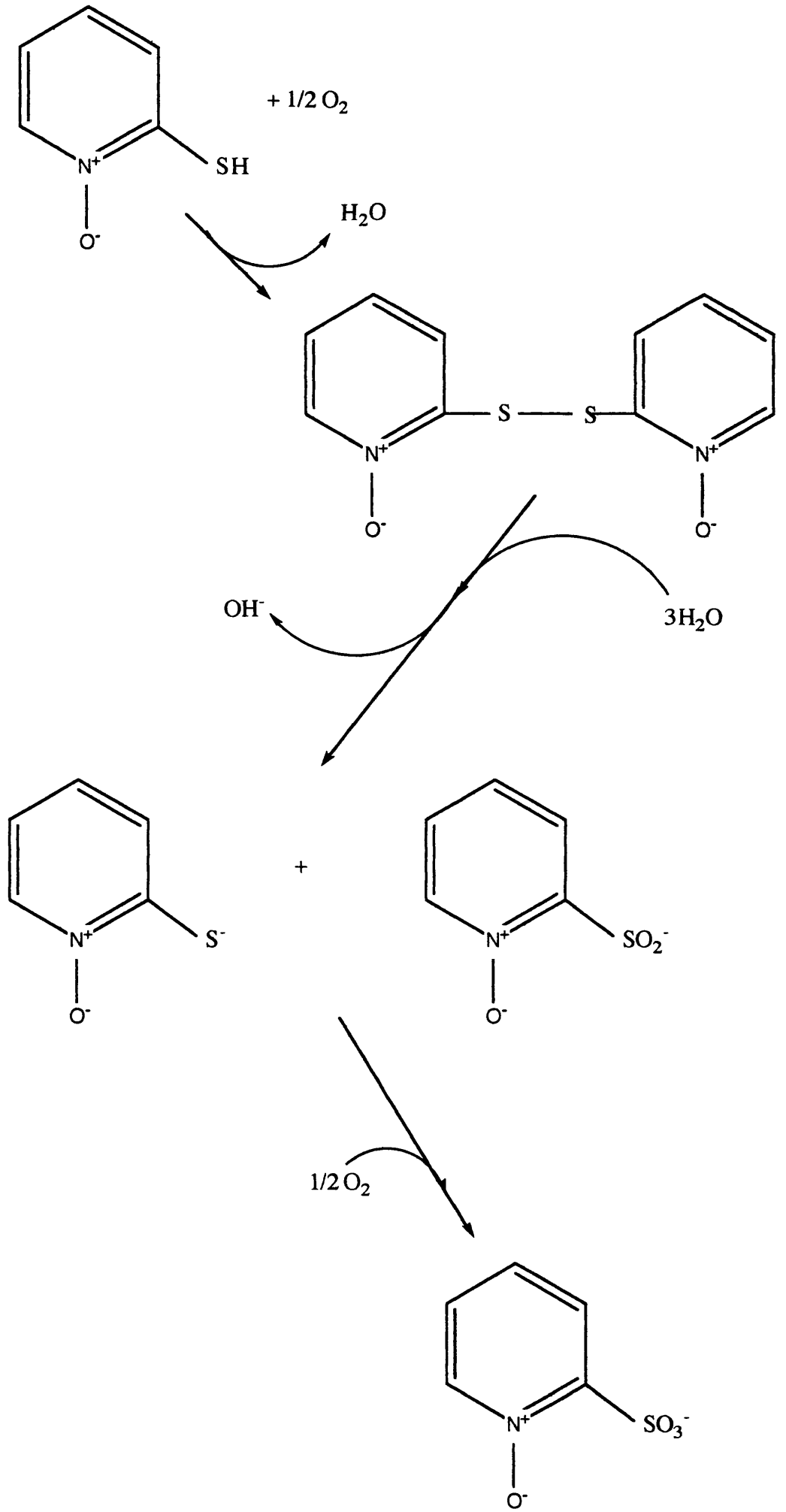
+ 1/2 O2
SH
N+
O-
H2O
S
S
OH-
3H2O
S-
SO2-
1/2 O2
SO3-

**Figure 30:** The chemical structure of the pyrithiolate anion of sodium pyrithione.

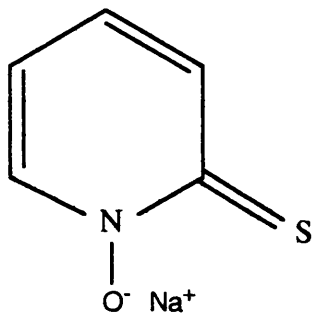


Sodium pyrithione

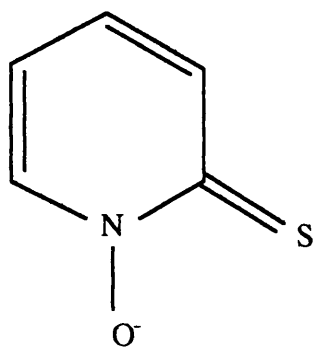


+ $Na^+$

Pyrithiolate anion

**Figure 31:** Filled orbital and capped stick chemical structure for the zinc pyrithione monomer and dimer: yellow = sulphur, grey = carbon, blue = hydrogen, dark blue = nitrogen, red = oxygen and green = zinc.

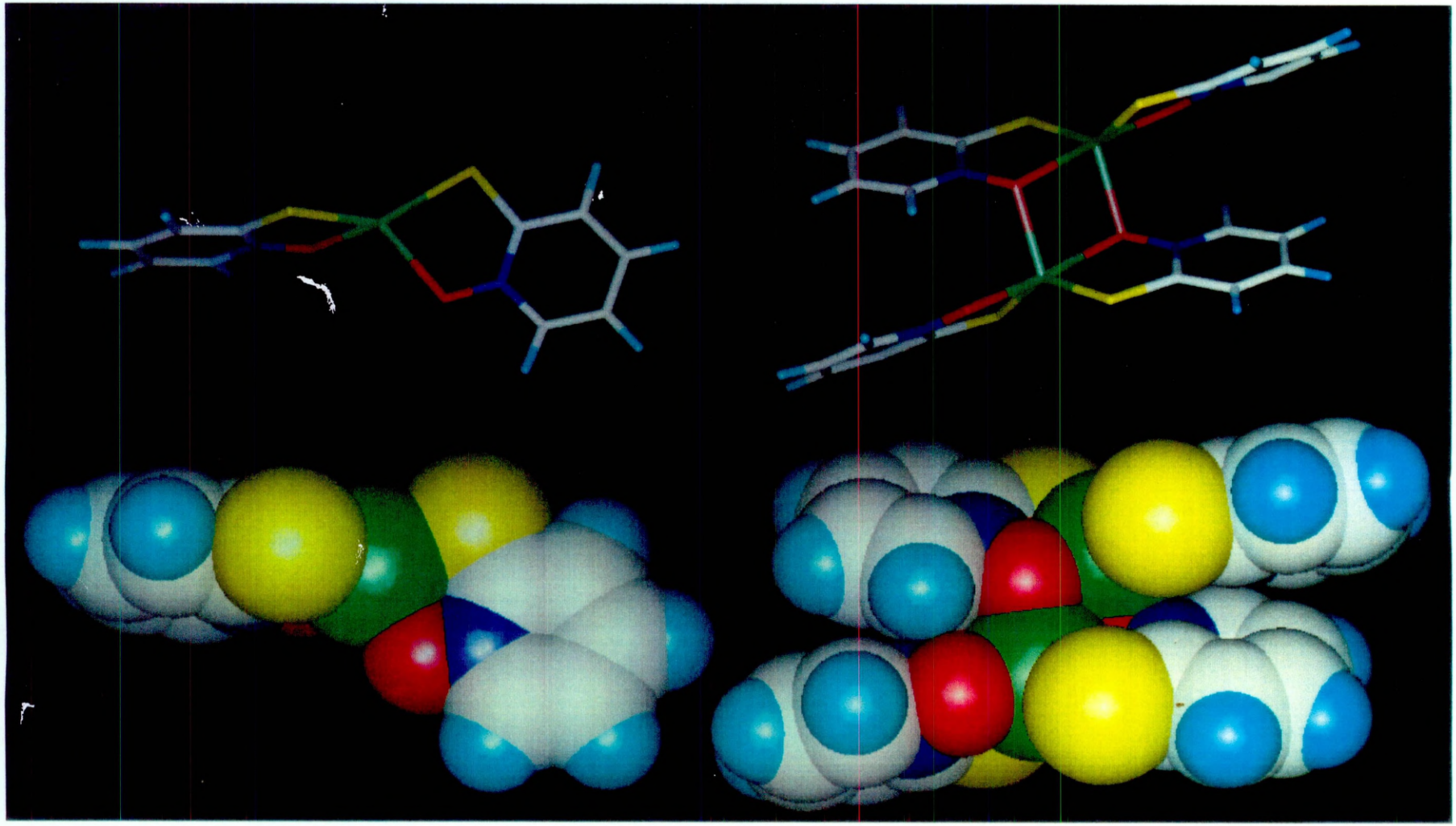

chromatography (HPLC) (Fenn & Alexander 1988, Nakajima *et al* 1993). These chelating properties have proved problematic in the incorporation of these compounds into cosmetic formulations where colourless and clear products may develop an unsightly blue or green colouration in the presence of pyrithiones (Nelson & Hyde 1981). The metal chelating properties of the pyrithiones have also been utilised to estimate metal content of ores in the metal purification industry (eg, Hg, Ag, Cu and Fe, Edrissi *et al* 1971).

## APPLICATIONS OF THE PYRITHIONE BIOCIDES

Sodium and zinc pyrithione are the most abundantly used pyrithione compounds (Hyde & Nelson 1984). Both sodium and zinc pyrithione have extensive antimicrobial properties (Khattar *et al* 1989, Khattar *et al* 1988, Vancutsem *et al* 1990, Hyde & Nelson 1984, Nelson & Hyde 1981, Pansy *et al* 1953). They have been widely used as cosmetic preservatives (Khattar & Salt 1993, Khattar *et al* 1988, Hyde & Nelson 1984, Nelson & Hyde 1981, Hyde & Auerbach 1979) and are incorporated as antidandruff agents into various shampoo formulations (Fredrikson & Faergemann 1983, Hyde & Nelson 1984, Khattar *et al* 1988). They have been widely utilised as preservatives in various industrial applications, ie, as preservatives in fuel lines and fuel tanks (Neihof *et al* 1979, Cooney 1969) and as antimicrobial finishing agents in the production of cotton (Morris & Welch 1983).

## TOXICOLOGICAL PROPERTIES OF THE PYRITHIONE BIOCIDES

ZnPT has been shown to possess greater toxic properties than HPT and in turn HPT is reported to be more toxic than NaPT (Black & Howes 1978). Oral $LD_{50}$ values (the dose at which 50% of a treated population die) have been reported in mice as 1172mg/Kg body weight for NaPT, 533mg/Kg body weight for HPT and 300mg/Kg body weight for ZnPT (Black & Howes 1978). These $LD_{50}$ values reflect the acute toxicological order of the pyrithione biocides. The differences in acute toxicity of HPT and NaPT have also been observed in mice for several routes of biocide administration (Moe *et al* 1960, Table 2). The $LD_{50}$ values from table 2 exhibit the increased strength of HPT toxicity over NaPT for

intraperitoneal and oral biocide administration in mice.

**Table 2:** Table of $LD_{50}$ values for HPT and NaPT in mice

| Route of Administration | $LD_{50}$ (mg/Kg body weight) | |
|---|---|---|
| | HPT | NaPT |
| Intravenous | 340 | 335 |
| Intraperitoneal | 165 | 265 |
| Subcutaneous | 490 | 450 |
| Oral | 535 | 1000 |

Pyrithione induced vomiting has been observed in subacute toxicity tests using dogs as the target population (Moe *et al* 1960). Upon administering dogs with HPT at concentrations of 10, 20 and 40mg/Kg body weight *via* an intraperitoneal tube, all of the dogs exposed to HPT exhibited an emetic effect. A decrease in vomiting was observed by decreasing the biocide dose to between 0.1 and 0.6mg/Kg body weight showing the degree of emesis to be dose dependent (Moe *et al* 1960). A repeated increased oral dose of HPT at concentrations of 40, 85 and 105mg/Kg body weight was given to a population of 8 mongrel dogs (Moe *et al* 1960). Seven out of the eight dogs that received the increased oral dose exhibited lacrimation (Moe *et al* 1960). The onset of lacrimation was observed up to a period of 1 hour after dose administration. From the pool of 7 dogs exhibiting lacrimation, 6 showed visual difficulties such as pupil dilation and loss of the light reflex. The visual difficulties occurred between 72 and 250 hours after administration of the initial dose. Ocular toxicological effects similar to those observed by Moe *et al* (1960) have also been reported upon oral administration of 25mg/Kg body weight of HPT to dogs for periods of 2, 4 and 10 days (Delahunt *et al* 1962). Sacrificial autopsy of the dogs exposed to HPT in these studies exhibited increased leucocyte content in the spinal cord and cellular congestion of underlying brain structure (Moe *et al* 1960, Delahunt *et al* 1962). The effects upon light reflexes, spinal cord and brain physiology have led to suggestions that HPT effects the neural physiology of animals exposed to high HPT concentrations (40 to 105 mg/Kg body weight, Moe *et al* 1960).

Observation of the decrease of neural stimulation of rats exposed to ZnPT also exhibited neurotoxic effects of the pyrithiones (Snyder *et al* 1976). On comparison with an unexposed control group of rats, the ZnPT exposed population required a neural stimulation of 5 to 7 times greater than the control stimulation with the result of a weaker muscular response than the control group. However, the velocity of neural conduction was uninhibited and was shown to be the same as the control group (Snyder *et al* 1977).

Observations of ZnPT induced muscular fatigue have been reported (Snyder et al 1977, Black & Howes 1978). Weaknesses in rear limb movements were observable upon feeding a repeated dose of 250ppm ZnPT to male rats over a period of 10 days (Snyder *et al* 1977). The weakness was observable in the exposed population on the 8th day of the study. After 10 days (the last day of dose administration) complete loss of movement from the hind limbs of exposed rats was reported. Both control and ZnPT exposed rat populations showed a decrease in body weight during the study. However, the loss of weight in the treated rats (falling from 280g to 220g) was significantly more than that of the control group (280g to 250g) (Snyder *et al* 1977). This suggests that the pyrithione biocides have a detrimental effect upon mammalian nervous tissue function. However, it is not a permanent effect as rats fed with ZnPT were shown to regain lost weight within two weeks of final ZnPT administration (Snyder *et al* 1977).

ZnPT has been shown to have little effect as a subcutaneous irritant in animal studies. Snyder *et al* (1965) reported the observation of primary skin irritancy after application of 2.5, 5.0 and 10g/Kg body weight of a 2% ZnPT preparation to rabbit skin for 24 hours. No deaths or other systemic effects were reported as a result of topical ZnPT application (Black & Howes 1978). Mortalities have been observed upon the topical application of pure, dry ZnPT powder to clipped rabbit skin (Snyder *et al* 1965). The application of 125, 250 and 1000mg/Kg body weight of dry ZnPT to a rabbit population of 7 resulted in an 85.2% mortality rate within 2 days of dose application. The cause of death upon examination by *post mortem* was found to be pulmonary congestion and haemhorrage (Snyder *et al* 1965). No skin irritancy was observed in the test population. Although no epidermal irritancy was observed, the cause of pulmonary congestion and haemhorrage must have been in part due to pyrithione induced haematic irritation.

Despite reported cases of the pyrithiones causing subject death at high concentrations (125 to 1000mg/Kg body weight, Snyder *et al* 1965, Moe *et al* 1960) the overall toxicological and irritation properties are low. They have been shown to be Ames Test negative (Skoulis *et al* 1993) and are subsequently non-mutagenic and are thought to be non-carcinogenic. There has been no reported evidence to suggest that the pyrithiones are teratogenic compounds. The pyrithiones therefore possess good toxicological properties and because they are used at low concentrations (0.5% w/v and less) are regarded as pharmacologically safe for topical application *via* the utilisation of cosmetics.

## OBSERVED MODE OF ACTION OF THE PYRITHIONE BIOCIDES

Suggestions regarding the antimicrobial activity of the pyrithione biocides have been made since the compounds were first synthesised in 1950 (Shaw *et al* 1950, Albert *et al* 1956, Pansy *et al* 1953, Cooney 1969, Chandler & Segel 1978, Imokawa *et al* 1982, Tomsikova *et al* 1982, Marks *et al* 1985, Vancutsem *et al* 1990, Khattar *et al* 1988, Khattar *et al* 1989, Khattar & Salt 1993). Much of this research addressed the activity of the pyrithiones against fungi and their killing mechanisms towards mammalian cell lines *in vitro* and *in vivo*. This latter work was carried out due to the incorporation of the pyrithione biocides into cosmetics as preservatives and an increased interest in the causative agent in dandruff, *Pityrosporum ovale* (Leyden *et al* 1976, Priestly & Savin 1976, Imokawa *et al* 1982, Tomsikova *et al* 1982). As a result of the widespread utilisation of the pyrithiones as general antimicrobial agents and as topical antidandruff agents, the pyrithione mode of action may be reviewed in three sections: observed antifungal effects of the pyrithiones, the observed effects of the pyrithiones upon mammalian cell lines and the antibacterial mode of action of the pyrithione biocides.

### The Antifungal Action of the Pyrithione Antimicrobials

The antimycotic effects of the pyrithiones have been well documented, both in general (Chandler & Segel 1978, Pansy 1953, Khattar *et al* 1988, Ermolayeva *et al* 1995) and in the

specific considerations of the activity of ZnPT against *P. ovale* in the formation of dandruff (Leyden & Kligman 1979, Imokawa *et al* 1982, Tomsikova *et al* 1982, Marks *et al* 1985, Vancutsem *et al* 1990). Literature survey has revealed few publications concerning the antimycotic mode of action of the pyrithiones. However, work has been published in the following areas; the effect of the pyrithiones upon fungal metabolism (Chandler & Segel 1978), membrane integrity (Ermolayeva *et al* 1995) and the effect of the pyrithiones upon the growth kinetics of the target organism (Khattar *et al* 1988).

Data exhibiting the effectiveness of ZnPT upon the erradication of *P. ovale* from infected scalps has been published (Imokawa *et al* 1982, Marks *et al* 1985, Vancutsem *et al* 1990). ZnPT has been shown to inhibit *P. ovale* infections at a concentration of 0.1% w/v or greater (Imokawa *et al* 1982). A minimum inhibitory concentration (MIC) of 0.01$\mu$gml$^{-1}$ for ZnPT against the target organism *Emmonsia crescens*, a fungal dimorphic opportunistic lung pathogen, has also been reported (Tomsikova *et al* 1982). However, these studies compared the antimicrobial efficiency of ZnPT with other antifungal agents such as ketoconazole and coal tars and did not consider the antimicrobial nature of the pyrithiones *per se* (Imokawa *et al* 1982, Tomsikova *et al* 1982, Marks *et al* 1985, Vancutsem *et al* 1990). None of the studies investigating the general antifungal activity of ZnPT proposed a mode of action for this agent. Each of the publications did, however, report the effectiveness of ZnPT erradication of *P. ovale in vivo* and *in vitro* ie, a three log cycle decrease was observed by treating an infected scalp with a ZnPT (1% w/v) containing shampoo. This result compares favourably with that observed where an infected scalp was treated with Irgasan DP-300 (0.2%w/v) medicated shampoo (incorporated antimicrobial agent not reported) (Imokawa *et al* 1982).

Studies concerning the effect of the pyrithiones upon nutrient uptake and membrane integrity in fungi (Ermolayeva *et al* 1995, Chandler & Segel 1978) have shown an effect upon the transmembrane transportases for sulphate and phenylalanine in *Penicillium* species by HPT (Chandler & Segel 1978). Observations of $^{35}S$ sulphate and $^{14}C$ phenylalanine uptake in *Penicillium chrysogenum* and *Penicillium notatum*, respectively, revealed a 50% decrease over the control on exposure to $10^{-3}$M HPT. The transport of phenylalanine has been shown

to decrease by 80% by increasing the time of incubation of $10^{-3}$M HPT with the fungi from 5 minutes to ten minutes (Chandler & Segel 1978). A 45% decrease in cellular ATP levels was also observed after the fungi were exposed to $10^{-3}$M HPT for five minutes. Increasing the incubation time to ten minutes resulted in a 65% decrease in ATP levels with exposure to the same concentrations of HPT (Chandler & Segel 1978). It has been suggested that these effects are due to the depolarisation of the membrane potential by the action of pyrithione (Chandler & Segel 1978, Ermolayeva *et al* 1995). Depolarisation of the membrane has been shown to occur in *Neurospora crassa* on exposure to $6x10^{-4}$M ZnPT and $10^{-3}$M HPT (Ermolayeva *et al* 1995). However, although this phenomenon has been observed, no conclusive proof of the direct action of the biocides has been reported. Decreases in membrane potential may have been due to secondary effects of pyrithione action, ie, pyrithione chelation of membrane-bound metal cations causing a change in membrane integrity and function. This would upset transmembrane pH and osmolarity gradients and depolarisation of the membrane potential may occur as a result.

Khattar and coworkers (1988) observed the effect of 0 to 0.02 $\mu$g $ml^{-1}$ NaPT upon the growth kinetics of the dimorphic opportunistic pathogen *Candida albicans*. A correlation between the decrease of growth rate and increasing drug concentration was observed. This drug dependent growth rate was observed by addition of biocide to the culture before the cells entered exponential growth phase. The effect of rechallenging *C. albicans* cells, in the exponential phase of growth, with NaPT (0 to 0.1 $\mu$g $ml^{-1}$ NaPT) was marked. The growth rate of *C. albicans* decreased less dramatically after further aliquots of pyrithione were added during exponential phase of growth than was the case when the same concentrations of NaPT were applied prior to the onset of exponential phase. This may be indicative of a biocide induced resistance mechanism, wherein, previously exposed cells are less susceptible to the antimycotic action of the biocide than cells which have not been previously exposed to NaPT.

More general studies on the antimycotic activity of the pyrithiones have reported several MIC values against an array of fungal species (Hyde & Nelson 1981, Table 3).

From the published data concerning the antimycotic action of the pyrithiones, it appears that ZnPT is more effective at causing inhibition of fungal growth than NaPT. ZnPT also exhibits increased fungistatic action in comparison with NaPT, with low MIC values of 0.25 and 0.5 $\mu g$ $ml^{-1}$ against *Trychophyton mentagrophytes* (Table 3). Both compounds have been shown to exhibit good antifungal activity.

**Table 3:** Published MIC values for some target fungi against ZnPT and NaPT

| | MIC ($\mu g$ $ml^{-1}$) | |
|---|---|---|
| Target Fungi | ZnPT | NaPT |
| *Aspergillus niger* | 2.0 | 2.0 |
| *Penicillium vermiculatum* | 1.0 | 2.0 |
| *Trychophyton mentagrophytes* | 0.25 | 0.5 |

## Action of the Pyrithione Antimicrobials against Mammalian Cell Lines

The pyrithione antimicrobial agents possess low toxicological properties, thus facilitating their widespread application into cosmetics and other preparations which may result in direct host-pyrithione contact. It is because of these properties, and the studies on pyrithione toxicology, that work has been carried out upon the action of these biocides against animal cell lines *in vitro* and *in vivo*. Studies concerning this work have debated the nature of the antimicrobial action of the pyrithione agents, their action against mammalian cells and their mode of action in antidandruff erradication.

The pyrithione biocides possess good antifungal activity and have subsequently been incorporated into antidandruff preparations and cosmetics. However, disputes as to the

mode of action of dandruff depletion by the pyrithione biocides have occurred (Imokawa & Okamoto 1982, Imokawa & Okamoto 1983, Priestly & Brown 1980, Gibson *et al* 1985, Pearse *et al* 1985, Cotton 1963). Work carried out upon the mode of action of the pyrithione compounds against eukaryotic cell lines has shown that the antidandruff action may be due to the pyrithione ability to inhibit host cell proliferation as well as acting at an antimycotic level (Imokawa & Okamoto 1982, Imokawa & Okamoto 1983).

The stimulated blood flow to epidermal cells of the scalp caused by an infection of *P. ovale* results in an increase in the sloughing of dead skin cells and hence, supports further fungal growth (Pearse *et al* 1985, Gibson *et al* 1985). It has been demonstrated, using tritiated thymidine, that exposure of epidermal layers *in vivo* to ZnPT and NaPT (at concentrations of 1% w/v) results in the inhibition of DNA synthesis and subsequent mitotic inhibition (Imokawa & Okamoto 1982, Imokawa & Okamoto 1983). This biocide exposure was later shown not to affect protein synthesis or RNA synthesis, as demonstrated in studies observing the uptake of tritiated uridine and tritiated leucine in guinea pigs (Imokawa & Okamoto 1983). Imokawa and Okamoto (1983) suggested that the antidandruff action of the pyrithiones was not solely an antimicrobial one, but was also due to the animal-cytotoxic effects of the pyrithiones. The observation of decreased epidermal proliferation was suggested to be due to pyrithione inhibition of DNA synthesis and mitosis, resulting in the subsequent reduction of *P. ovale* activity (Imokawa & Okamoto 1982, Imokawa & Okamoto 1983).

Observations on the effects of ZnPT upon epidermal proliferation of the arms of human males *in vivo* have been published (Pearse *et al* 1985). The application of 2 to 20 $\mu$g ml$^{-1}$ ZnPT to epidermal layers of the right forearms of volunteers exhibited no cytotoxic effects. The *in vitro* cytotoxic effects of the pyrithiones were also described by Priestly & Brown (1980). They observed complete inhibition of cultured epithelial growth at low concentrations of HPT (0.1 to 0.5 $\mu$g ml$^{-1}$). However, no mitotic inhibition was reported with the epithelial cell line used (Priestly & Brown 1980). Gibson *et al* (1985) observed the effect of HPT (1% w/v) upon thymidine incorporation into non-dividing mast cells *in vitro*. Changes in morphology and membrane integrity of non-dividing mast cells in tissue culture

were observed, but no inhibition of incorporation of tritiated thymidine into host cells was demonstrated (Gibson *et al* 1985).

It is apparent from the above studies that the pyrithiones have cytotoxic effects upon mammalian cells. However, these studies have yielded little information regarding the potential mode of action of these compounds (Imokawa & Okamoto 1982, 1983, Priestly & Brown 1980). Cotton (1963) observed the stasis of mouse mast tumour cells upon exposure to HPT *in vitro* (concentrations not reported). The inhibition of proliferation of mitochondria in cells which had been exposed to HPT at sub-inhibitory concentrations was observed (Cotton 1963). Together with this data, the inhibition of alcohol dehydrogenase and succinoxidase by the action of HPT upon mouse mast cells *in vitro* has been exhibited (Cotton 1963). This, together with the evidence of membrane disruption by Gibson *et al* (1985), may be indicative of membrane action by the pyrithiones. The pyrithiones may act upon the cristae membrane complexes of mitochondria and subsequently inhibit the ability of the cell to complete membrane-bound metabolic steps (ie, Krebs Cycle, and ATPase function) (Cotton 1963, Stryer 1988).

Previous studies on the pyrithiones and their mode of action on eukaryotic cells *in vitro*, have given an insight into the effect of these antimicrobial agents upon prokaryotic cells despite their biological diversity. However, upon reviewing the work concerning the action of the pyrithiones upon bacteria, it is evident that the conclusions from the eukaryotic studies have not been fully considered. A deeper understanding of the pyrithione effect upon eukaryotic membranes and more particularly mitochondria would have perhaps increased the knowledge or eased the design of experiments upon the mode of action of the pyrithiones upon bacteria. Work observing the effects of the pyrithione biocides upon bacteria has been published (Shaw *et al* 1950, Pansy *et al* 1953, Albert *et al* 1956, Hyde & Nelson 1981, Khattar *et al* 1988, 1989, Khattar & Salt 1993), however, literature surveys have shown that the published papers do not consider an antibacterial pyrithione effect at the level of the bacterial envelope. Action of the pyrithiones at a membrane level cannot be ignored, especially from the effects observed by Chandler & Segel (1978) and Ermolayeva & coworkers (1995) upon membrane depolarisation and nutrient uptake by fungi.

**The Action of the Pyrithione Antimicrobials against Bacteria**

Low MIC values for the pyrithiones have been reported in both Gram-negative and Gram-positive bacteria (Shaw *et al* 1950, Pansy *et al* 1953, Hyde & Nelson 1981, Khattar *et al* 1988, Khattar & Salt 1993, Table 4). Although the data from Table 4 shows the pyrithiones to be effective bacteristatic agents, the observed MIC values show the Gram-positive bacteria to be more susceptible to growth inhibition by the pyrithiones than Gram-negative bacteria (Albert *et al* 1956, Pansy *et al* 1953, Khattar *et al* 1988). This is exhibited when comparing the NaPT MICs for *Bacillus subtilis* and *Staphylococcus aureus*, both Gram-positive bacteria, with the MICs for the Gram-negative bacteria *Escherichia coli* and *Pseudomonas aeruginosa* (Table 4). The data from Table 4 also exhibits the existence of a *Pseudomonas*-gap (Dept of Health). This is observed by differences in MIC values for *E.coli* and *S. aureus* against ZnPT (8.0 $\mu$g ml$^{-1}$ and 0.6 $\mu$g ml$^{-1}$ respectively) in comparison with those for *P. aeruginosa* (512 $\mu$g ml$^{-1}$). This comparison is also observed with the values reported for NaPT (Hyde & Nelson 1981, Khattar *et al* 1988, Table 4).

The effects of varying concentrations of NaPT (0.0 to 6.0 $\mu$g ml$^{-1}$) upon the growth kinetics of actively growing *Klebsiella pneumoniae* and *Bacillus licheniformis* have been observed (Khattar *et al* 1988, 1989). The cells were inoculated into 100ml aliquots of CDM already prepared to contain NaPT. The cultures were then grown in a shaking incubator (90rpm, 37°C) and growth was monitored each hour by observing $OD_{650nm}$ (Khattar *et al* 1988, 1989). The microorganisms in these studies exhibited lag phases which increased with increasing NaPT concentration. The lag phase varied from 60 minutes for 1.0 $\mu$g ml$^{-1}$ NaPT to greater than 700 minutes for 6.0 $\mu$g ml$^{-1}$ NaPT against *K. pneumoniae* (Khattar *et al* 1988). Once the cells had reached an $OD_{650nm}$ greater than 0.4, the growing cells were rechallenged with a further aliquot of NaPT at the same concentration. No additional effect of the extra addition of biocide was observed on the cells already growing in pyrithione-containing CDM (Khattar *et al* 1988). This work suggests that the pyrithiones may be more active against cells which are not in the exponential phase of growth. This is indicated by pyrithione rechallenged exponential-phase cells exhibiting no observable growth rate effects. Cells which are exposed to the pyrithiones a second time exhibit a form of drug-induced

biocide resistance. This may be similar to that observed with the isothiazolone biocides (Brozel & Cloete 1994) and may be indicative of phenotypic drug-resistance towards the pyrithiones. This observation of decreased sensitivity of exponentially growing microorganisms to the pyrithiones may also suggest that the pyrithiones are more active against slow growing or non-growing cells. If this is true, then the pyrithione biocides may be regarded as breaking one of the paradigms of antimicrobial chemotherapy. The reason that cells which are growing exponentially are more susceptible to antimicrobial action is because of their increased biochemical activity in comparison with slow or non-growing cells. Actively growing cells are constantly carrying out *de novo* synthesis of biochemical precursors and utilise increased membrane transport processes than comparable non-growing cells. This increased metabolic activity facilitates the targeting of many antimicrobials towards their respective biochemical targets, ie, new cell wall synthesis, increased protein content in the cytosol and bacterial membranes. Non-growing cells have reduced synthetic activity and energy utilisation. Non-growing or slow growing cells are affected by antimicrobial agents, but in general these agents are more effective against actively growing cells than slow or non-growing ones. If the pyrithiones are more active against slow and non-growing cells, then the work of Khattar *et al* (1988) exhibits this group of antimicrobials as a singular set of compounds which break one of the steadfast rules of antimicrobial chemotherapy.

Inhibition of the uptake of $^{14}C$ radiolabelled uracil has been observed in *E. coli* exposed to MIC levels (50$\mu$M) of HPT (Friedman 1981). Inhibition of the uptake of tritiated thymidine has also been shown to occur in the presence of HPT, but to a lesser extent than the inhibition of uracil uptake (Friedman 1981). Cells of *E. coli* exposed to levels of HPT greater than the MIC exhibited a shiftdown effect, which may trigger the stringent response. This leads to subsequent increases in intracellular levels of polyphosphorylated guanosine (ppGpp, or magic spot) (Gilbert *et al* 1990a, Friedman 1981). Decreases in intracellular levels of ATP were also observed. Khattar and coworkers (1989, 1993) observed inhibition of $^{14}C$ thymidine and $^{14}C$ uridine uptake in *K. pneumoniae* by MIC levels of NaPT (2.5 $\mu$g $ml^{-1}$). Inhibition of radiolabelled nucleotide and nucleoside uptake in *E. coli* exposed to NaPT was similar to that observed by Friedman (1981), with the inhibition of uridine uptake

shown to be more greatly inhibited than thymidine uptake in *K. pneumoniae* exposed to NaPT (Khattar *et al* 1989, Khattar & Salt 1993). Inhibition of thymidine uptake in *K. pneumoniae* was shown to recover quickly with the onset of the exponential phase of growth (Khattar & Salt 1993).

**Table 4:** MIC values for various species of Gram-positive and Gram-negative bacteria against HPT, NaPT and ZnPT.

| | MIC ($\mu$g ml$^{-1}$) | | |
|---|---|---|---|
| Microorganism | HPT | NaPT | ZnPT |
| *Bacillus subtilis* | * | 0.06 | * |
| *Staphylococcus aureus* | 0.06 | 0.6 | 4.0 |
| *Klebsiella pneumoniae* | 1.5 | 5.0 | * |
| *Micrococcus tuberculosis* | * | 0.06 | * |
| *Pseudomonas aeruginosa* | * | 512.0 | 512.0 |
| *Escherichia coli* | * | 8.0 | 16.0 |

* = No data available

Neutralisation of the antimicrobial properties of NaPT has been observed by the addition of EDTA, serum and saliva (Pansy *et al* 1953, Khattar *et al* 1988). The neutralisation of the antimicrobial action of NaPT by bodily fluids (Pansy *et al* 1953) may be indicative of potential thiol or amine interactions. However, as the pyrithiones have been shown to be effective metal ion-chelating agents (Hyde & Nelson1984) and bodily fluids are known to contain free metal cations (eg, $Ca^{2+}$ and $Mg^{2+}$, Vander *et al* 1986) then perhaps the neutralisation of NaPT by saliva and serum is due to metal cation chelation.

EDTA is a chelating agent as are the pyrithiones. Both compounds chelate metal cations due to their behaviour as Lewis Bases (Holum 1986). The action of Lewis Bases in solution

requires the donation of free electrons. With both the pyrithiones and EDTA, this means the donation of electrons to metal cations. The result of which is a stable pyrithione or EDTA metal chelate. However, EDTA and pyrithione cannot chelate each other as both are anionic. Therefore, any quenching effect observed by the presence of EDTA with pyrithione cannot be due to a direct interaction of the two compounds. It may be the chelation of ions present in the bacterial environment and on the bacterial cell by EDTA which neutralises the pyrithione antimicrobial effect. The presence of EDTA together with the pyrithiones would bring about competitive chelation of metal cations between the two compounds. This would lead to a lack of metal cations at the bacterial envelope, which may reduce the capacity of pyrithione entry into the cell. This mode of action has been suggested by Albert and coworkers (1956) who likened the mode of action of the pyrithiones to that of oxine (8-hydroxyquinoline, Albert *et al* 1956, Fig 26). Comparative studies between oxine and HPT as bacteristatic agents on the two Gram-positive bacteria *Staphylococcus aureus* and *Streptococcus pyogenes* demonstrated that the action of HPT was four times greater than that of oxine concentration for concentration (Albert *et al* 1956). Oxine is thought to act by forming metal chelates outside of the bacterial cell and subsequently entering the cell. Once inside the cell dissociation occurs due to the decrease in pH between the cytosol and the extracellular environment. This yields free unchelated oxine which acts intracellularly, binding metalloenzymes and metalloenzyme-cofactors rendering them inactive and disabling bacterial metabolism (Albert *et al* 1953, Rubbo *et al* 1950) (Fig 32). If the pyrithiones act in this way, then it may indicate that competitive chelation between the pyrithiones and EDTA causes the neutralisation of the antimicrobial effects of the pyrithiones. However, no experimental evidence has been reported which details the similarity of the modes of action of the pyrithiones towards oxine. It has also been reported that the pyrithiones may act as nicotinic acid antimetabolites (Cooney 1969, Fig 33). Again, no experimental evidence was given for this hypothesis and it seems that this was based purely upon the structural similarities between the two compounds.

In summary, the reported information upon the observed mode of action of the pyrithiones to date suggests that they act at a series of sites on the microbial cell. Studies of the mode of action on both fungi and mammalian cells suggest that the pyrithiones are membrane active agents (Chandler & Segel 1978, Cotton 1963, Gibson *et al* 1985). However, an intracellular

mode of action cannot be ruled out, particularly if inhibition of RNA and DNA synthesis is considered (Imokawa & Okamoto 1982, Imokawa & Okamoto 1983, Friedman 1981, Khattar *et al* 1989, Khattar & Salt 1993). Such studies suggest that the pyrithiones may be active in the bacterial cytosol. Pyrithione activity in the cytosol is also suggested by the neutralisation of NaPT by protein containing fluids (saliva and serum, Pansy *et al* 1953) This together with the knowledge that pyrithione disulphides may be formed between HPT monomers, also implicates the pyrithiones as being active in the cytosol due to potential thiol interactions (Hyde & Nelson 1984). These suggestions are valid, but due to a lack of conclusive experimental evidence, the mode of action of the pyrithione biocides remains elusive.

## OBJECTIVES OF THIS STUDY

The objective of this study was to attempt to elucidate the mode or modes of action of the two pyrithione biocides NaPT and ZnPT upon the target organisms *Escherichia coli* NCIMB 10000 and *Pseudomonas aeruginosa* PAO1 NCIMB 10548. An understanding of the physiology and metabolism of the Gram-negative bacterial cell was used to underpin these studies and to direct the development of experimentation.

**Figure 32:** A diagrammatic representation of the mode of action of the antimicrobial agent oxine (8-hydroxyquinoline).

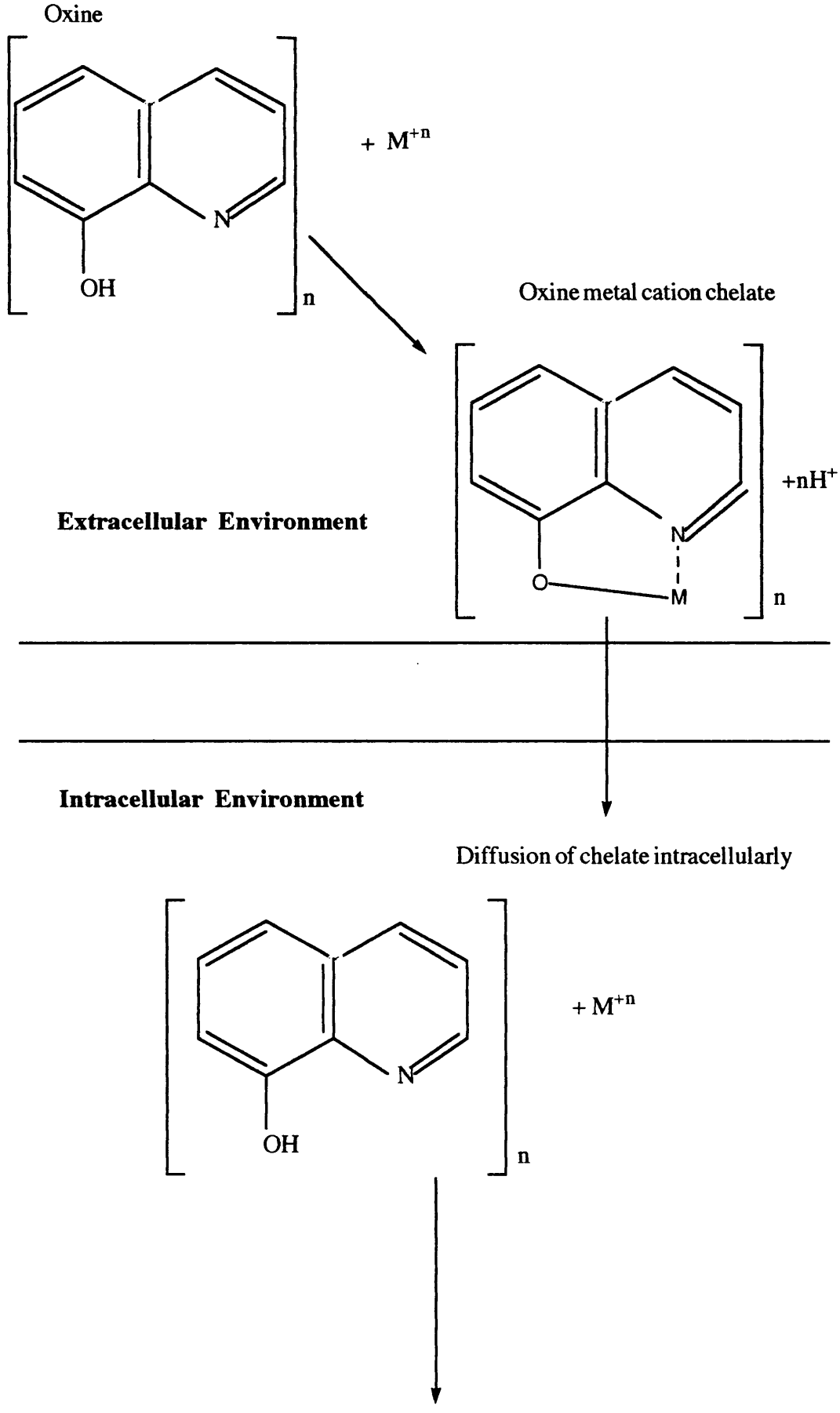
Oxine
+ $M^{+n}$
OH
N
n
Oxine metal cation chelate
+$nH^+$
O
M
Extracellular Environment
Intracellular Environment
Diffusion of chelate intracellularly
+ $M^{+n}$
Chelation of metallic enzyme cofactors
by the dissociated oxine molecule

**Figure 33:** Comparison of the chemical structures of nicotinic acid and hydroxypyrithione.

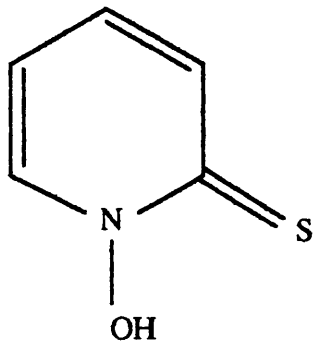


Hydroxypyrithione

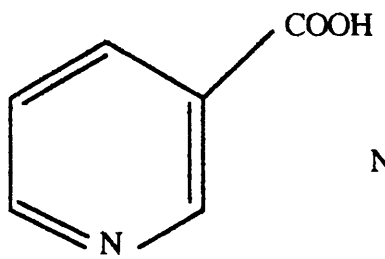


Nicotinic acid

# GENERAL EXPERIMENTAL METHODS

## Organisms and Culture Maintenance

*Escherichia coli* NCIMB 10000 and *Pseudomonas aeruginosa* PAO1 NCIMB 10548 were both obtained from the National Collections of Industrial and Marine Bacteria (NCIMB), Aberdeen, UK. Both organisms were maintained on nutrient agar slopes (Oxoid CM3) in quadruplicate. The four slopes were numbered from 1 to 4. Slope number 1 was used to inoculate overnight cultures for experimental purposes and slope number two was the backup slope in case of contamination. Slope number three was used for further subculturing and slope number four was kept as part of a refrigerated stock culture collection. The maintenance of cultures in quadruplicate ensured that the stock bacterial cultures were not ruined by a single occurrence of contamination. Inoculated agar slopes were incubated overnight at 37°C. After the incubation period, stock cultures were maintained at room temperature in a darkened cupboard. Culture maintenance was observed by subculturing onto fresh nutrient agar slopes at fortnightly intervals.

## Reagents

Sigma, Poole, Dorset: Dimethylformamide; thymidine; uracil; trizma hydrochloride; ethylenediaminetetraacetic acid; ß-Nicotinamide adenine dinucleotide (ß-NAD); 18-crown-6-ether; pyruvic acid; L-glucose; thymidine phosphorylase; alcohol dehydrogenase; glutathione-S-transferase; glutathione; D-cysteine; D-alanine; phosphatidylcholine; linoleic acid; L-proline; luciferin-luciferase firefly lantern extract; adenosine triphosphate (ATP); tetraethylammoniumchloride; 1-chloro-2,4-dinitrobenzene; phosphatidylethanolamine; gluteraldehyde; cacodylic acid; osmium tetraoxide ($OsO_4$); propylene oxide; araldite CY212; Araldite HY964; 2, 4, 6-dimethylaminomethylphenol.

BDH Chemicals, Poole, Dorset: Disodium hydrogen phosphate ($Na_2HPO_4$); potassium dihydrogen phosphate ($KH_2PO_4$); dipotassium orthophosphate ($K_2HPO_4$); ferric ammonium citrate; ammonium chloride ($NH_4Cl$); glycerol; ethanol; sodium chloride (NaCl); D-glucose; sodium dithionite; tetrasodium decahydrate pyrophosphate; calcium chloride

($CaCl_2$); magnesium sulphate heptahydrate ($MgSO_4.7H_2O$); hydrochloric acid (HCl); sodium hydroxide (NaOH); sodium nitrate ($NaNO_3$).

Sodium pyrithione, zinc pyrithione, cetrimide and BIT were kind gifts from Zeneca Specialties Plc, Biocides Research, Blackley, Manchester M9 3DA.

**Culture Media**

Nutrient broth (Oxoid CM1) and Nutrient agar (Oxoid CM3) were obtained from Oxoid, Basingstoke, Hants. Preparation was by the manufacturers instructions and sterilisation was carried out by autoclaving at 121°C, 15psi for 15 minutes.

Both organisms were routinely grown on chemically defined media (medium number 149, *Pseudomonas* media, 1994 NCIMB Catalogue, replacing 0.5% succinic acid with glycerol).

Solution A was prepared by dissolving $K_2HPO_4$ (2.56g), $KH_2PO_4$ (2.08g) and $NH_4Cl$ (1.00g) in that order in 900ml of deionised water. The pH of this solution was adjusted to pH6.8 with the addition of either 0.1M HCl or 0.1M NaOH and the total volume was made up to 1l with deionised water and sterilised by autoclaving at 121°C, 15psi for 15 minutes. Solution B was prepared by dissolving ferric ammonium citrate (1.0g) and $CaCl_2$ (0.1g) in 100ml of deionised water and this was sterilised by filtration through a 0.22$\mu$m pore size cellulose acetate filter under vacuum. Solution C, 1M glycerol (46.45g glycerol made up to 500ml with deionised water) was prepared and the pH was adjusted to pH 6.0 by the addition of either 0.1M NaOH or 0.1M HCl. The glycerol solution was sterilised by autoclaving at 121°C, 15psi for 15 minutes. Solution D was prepared by dissolving $MgSO_4.7H_2O$ (0.5g) in 900ml deionised water. The $MgSO_4.7H_2O$ was made up to a volume of 1l using deionised water and sterilised by autoclaving at 121°C, 15psi for 15minutes. The aseptic addition of 5ml of solution B, 15ml of solution C and 10ml of solution D to 1l of solution A completed the preparation of the CDM (1994 NCIMB Catalogue).

## Preparation of Washed Cell Suspensions

*E. coli* and *P. aeruginosa* were both grown in 25ml of sterile liquid media (CDM or nutrient broth, Oxoid CM1) in 100ml Ehrlenmeyer flasks in a Gallenkamp orbital incubator (200 oscillations per minute, 37°C) overnight. The cells were then harvested by centrifugation at 3000rpm in either a Sanyo MSE Microcentaur (Sanyo UK) or in an IEC Centra-4R Centrifuge (International Equipment, Dunstable) at room temperature. The supernatants were decanted and the cell pellets were resuspended in sterile saline (0.9% w/v NaCl), or sterile buffer solution (0.067M phosphate buffer or 0.2M Tris HCl buffer, pH7.0). After resuspending the pellets in the appropriate cellular bathing solution, the cells were washed by centrifugation (3000rpm, 15 minutes) and resuspended in the same bathing solution as was used previously. This step was repeated a second time. The cells were then resuspended to a desired optical density, OD 1.36 ($E_{470nm}$), using a Cecil Series 2 Spectrophotometer (Cecil Instruments, Cambridge).

## Assessment of Cell Density by Optical Absorption

Washed cell suspensions were prepared from overnight cultures of *E. coli* and *P. aeruginosa*. Serial dilutions were made in sterile saline and optical densities were measured at $E_{470nm}$ using a Cecil Series 2 Spectrophotometer. Expected optical densities were calculated for each sample by multiplication of the observed $E_{470nm}$ for the most dilute sample by the appropriate dilution factors. These were plotted against the measured $E_{470nm}$ (Fig 34). Beer-Lambert Law was observed for $E_{470nm}$ values below OD 0.5 (Lawrence & Maier 1977). Above this value, deviations from linearity in optical density were observed. In subsequent experiments samples with an $E_{470nm}$ greater than 0.5 were diluted ten fold, and the true $E_{470nm}$ values were calculated (Lawrence & Maier 1977).

## Determination of Viable Count

An aliquot (0.1ml) of bacterial cell suspension was aseptically removed from the test culture and placed in 9.9ml of sterile normal saline. The diluted suspension was mixed thoroughly using a rotary vortex and further 0.1ml aliquots were removed. Removed aliquots of diluted cell suspension were spread onto the surfaces of sterile nutrient agar plates (Oxoid CM3), using a sterile glass spreader which had been flamed in alcohol and

**Figure 34:** Calibration curve of optical density ($E_{470nm}$) (○) against cell density per ml (△) as a function of time, facilitating the direct enumeration of cell number from optical density. Error bars are calculated from and plotted as the Standard Error of the data set.

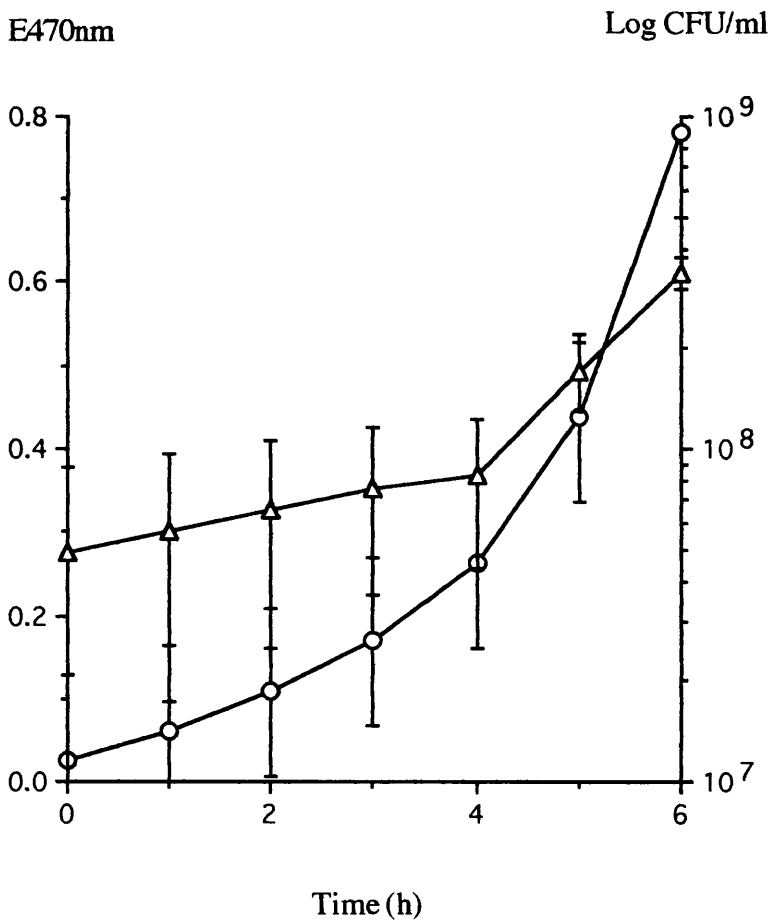
E470nm
Log CFU/ml
0.8
0.6
0.4
0.2
0.0
$10^9$
$10^8$
$10^7$
0
2
4
6
Time (h)

allowed to cool. This was carried out in triplicate for a number of dilutions of the cell suspension (the dilutions ranging from a $10^{-3}$ to $10^{-9}$ dilution of the original suspension). The inoculated nutrient agar plates were then incubated for 24 hours at 37°C. After incubation, colonies on the agar plates were counted by hand. The number of colonies observed was multiplied by the reciprocal of the dilution factor and the number of colony forming units (CFU) per ml of original suspension was calculated. This is represented by a mathematical formula (Equation 6), where CFU/ml is the number of colony forming units per ml of the original suspension, 1/DF is the reciprocal of the dilution factor and N is the number of colonies counted on the incubated agar plates.

$$\text{CFU/ml} = N\,(1/DF) \tag{6}$$

The numbers of bacterial cells present in the sample were also observed using spectrophotometry. Subsequently, a calibration curve was constructed (Fig 34) showing $E_{470nm}$ of a cell suspension and viable count against time. This was used in future experiments to determine cell concentrations at a specific $E_{470nm}$. This experiment was repeated for both *E. coli* and *P. aeruginosa*.

## Observation of Microbial Growth

Ehrlenmeyer flasks (100ml) containing 25ml aliquots of sterile media (either CDM or nutrient broth Oxoid CM1) were inoculated with 0.1ml of overnight bacterial culture which had been grown up in the same test medium prior to inoculation. Flasks were incubated in a rotary incubator (200 osc/min, 37°C) and growth was monitored for a period of 7 hours by observing increase in $E_{470nm}$.

## Operation of Oxygen Electrode

Oxygen uptake by metabolising cell suspensions was monitored using an oxygen electrode and metabolic chamber (Rank Bros, Cambridge. Fig 35). The oxygen electrode measures oxygen tension in suspension of cells contained within the metabolic chamber. The oxygen electrode consists of a platinum/silver-silver chloride electrode and is separated from the metabolic chamber during experimental by a piece of teflon membrane. An aliquot (1ml) of a

saturated solution of potassium chloride was placed on the electrode and covered by a piece of teflon membrane ($1cm^2$). The metabolic chamber was then screwed into place, taking care not to disrupt the teflon membrane. Cell suspensions were then added to the metabolic chamber and stirred *via* a magnetic flea. The suspensions were then allowed to equilibrate until a steady oxygen tension was observed.

The oxygen electrode and metabolic chamber assembly were connected to a potentiometric chart recorder (Servogor 120, BBC Goerz Metrawatt, Austria). This enabled the observation of a trace which is proportional to oxygen tension. Oxygen within the suspension diffuses across the teflon membrane and is subsequently reduced at the platinum electrode (Equations 7 & 8).

(7) $$O_2 + 2e^- + 2H^+ \longrightarrow H_2O_2$$

(8) $$H_2O_2 + 2e^- + 2H^+ \longrightarrow 2H_2O$$

Upon sealing the metabolic chamber of the electrode assembly (ensuring the exclusion of bubbles), the amount of oxygen present in the chamber and therefore the oxygen uptake of the cell suspension can be directly observed. An injection port present in the sealing piston allows the addition of solutions of substrates and biocides to be added. Therefore inhibition or stimulation of substrate metabolism by biocide addition can be observed as a function of oxygen uptake by the cell suspension.

**Figure 35:** Diagrammatic representation of a closed chamber oxygen electrode (Rank Brothers, Cambridge, UK).

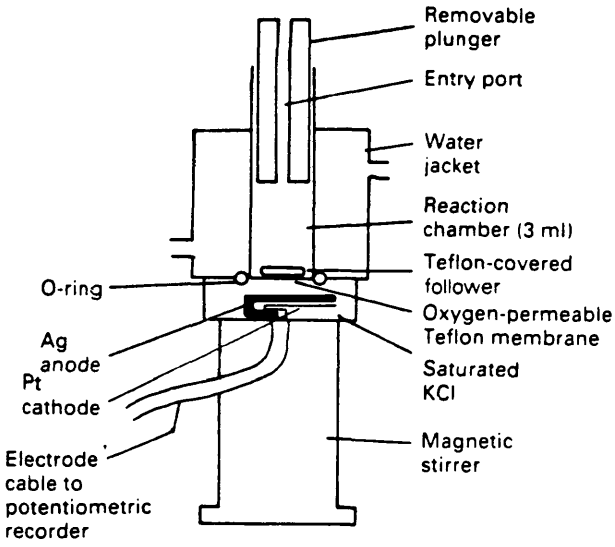
Removable plunger
Entry port
Water jacket
Reaction chamber (3 ml)
Teflon-covered follower
Oxygen-permeable Teflon membrane
Saturated KCl
Magnetic stirrer
O-ring
Ag anode
Pt cathode
Electrode cable to potentiometric recorder

## Operation of the Potassium Electrode

Potassium ion contents of bacterial cell bathing solutions were monitored using a potassium ion sensing electrode (Qualiprobe QSE 314, EDT Instruments Dover) and it's reference electrode (Qualiprobe Double Junction Reference Electrode E8092, EDT Instruments, Dover). Two hours prior to the use of the electrodes, the sensing electrode was placed in a $10^{-1}$M solution of potassium chloride. The cover on the reference electrode and it's tip were removed immediately prior to use. The reference electrode was then topped up with electrolyte (0.1M $NaNO_3$) and the tip carefully screwed back in place. Before placing the electrodes into the standard solutions or cell suspensions, 5ml of ionic strength adjustment buffer (18.37g/100ml of tetraethylammoniumchloride) was added to the test solution. This ensured that the background ionic strength of all test solutions was kept constant. Both electrodes were placed into a stirred cell suspension and the potential derived by the electrodes was measured using a Whatman PHA 220 pH/mV meter (Whatman, Maidstone, Kent) set to read mV. Readings were recorded for cell suspensions at various intervals up to 20 minutes after addition of biocide. The electrodes were placed in the standard solution for 5 minutes, or until the reading in mV remained stable. A calibration graph (Fig 44) was constructed of potassium ion concentration against mV using standard solutions of potassium chloride ($10^{-1}$ to $10^{-6}$M).

**Figure 36:** Calibration curve of the concentration of potassium chloride (M) against mV.

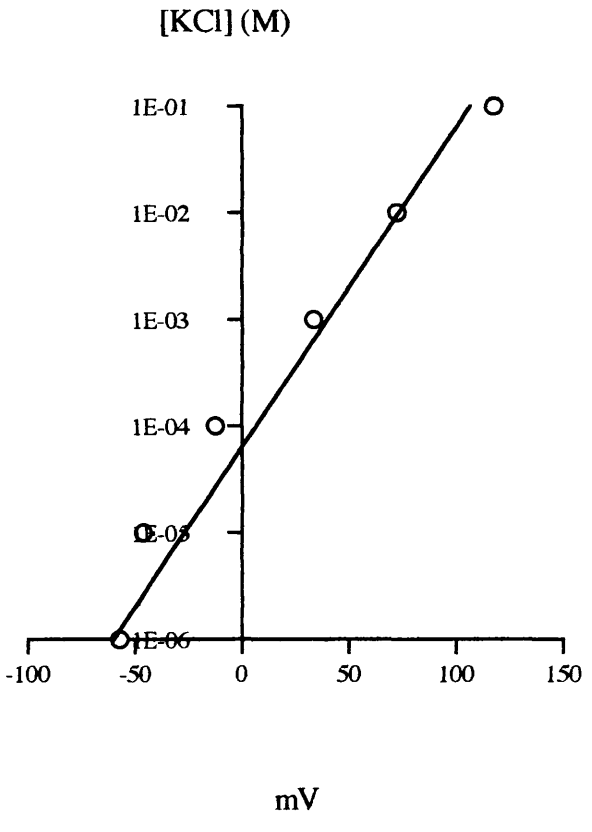
[KCl] (M)
1E-01
1E-02
1E-03
1E-04
1E-05
1E-06
-100
-50
0
50
100
150
mV

## Assay of ATP

Intracellular ATP levels were assayed *via* the luciferin/luciferase firefly extract system which emits light upon the breakdown of ATP to produce ADP and inorganic phosphate (Wishart 1984, Equation 9). Light production was monitored using a luminometer which was linked to a potentiometric chart recorder (Servogor 120 Chart Recorder, BBC Goerz Metrawatt, Austria). This enabled the observation and quantification of ATP present in the sample as a function of light released on reaction with luciferin/luciferase firefly extract. The intensity of light emission in this system is proportional to the concentration of ATP present.

(9) $$ATP \xrightarrow{\text{Luciferin/luciferase}} ADP + Pi$$

Photon

### Firefly Extract Preparation

An aliquot (5ml) of deionised water was added to a vial of luciferin/luciferase firefly extract. This was then diluted by adding 0.3ml of stock firefly extract to 4.7ml of deionised water. An aliquot (0.8ml) of diluted extract was then drawn up into a 1ml capacity syringe and this was placed securely into the rubber septum on top of the luminometer turret in preparation for application to luminometer tubes by depressing the syringe.

### Standard Preparation

An aliquot (10$\mu$l) of 10$\mu$M ATP was added to 190$\mu$l of deionised water in a perspex luminometer tube. This was then placed inside the luminometer. The chart recorder was switched on and a base line was observed. An aliquot of diluted firefly extract (0.8ml) was subsequently added to the ATP standard inside the luminometer chamber.

**Sample Preparation**

An aliquot (200$\mu$l) of deionised water was boiled at 100°C for 2 minutes in a preheated pyrex tube in a Gallenkamp water bath. An aliquot (200$\mu$l) of bacterial cell suspension was lysed by addition to the pyrex tube in the water bath. The tube containing the lysed bacterial suspension was removed from the water bath after three minutes and cooled on ice. Cell debris was then removed from the bacterial sample by centrifugation for 1 minute at 13000rpm in a Sanyo MSE Microcentaur Microfuge (Sanyo, UK). An aliquot (200$\mu$l) of cell-free extract (supernatant) was placed in a perspex luminometer tube and the luminometer turret was moved to the 'sample in' position. The sample was then assayed for ATP by the addition of 0.8ml of dilute firefly extract into the luminometer turret.

## Preparation of Cell Free Extracts

**Determination of Homogenisation Time (Ht)**

Cell free extracts were prepared using a hand-held homogeniser (Ultra Turrax T8, S8N-5G, IKA Labortechnik, Staufer, Germany). Determination of the time required to homogenise cells into a cell free extract (homogenisation time or Ht) was observed by plotting $E_{260nm}$ against homogenisation time. Observation of increase in absorbance ($E_{260nm}$) from a cell suspension is indicative of the leakage of cytosolic constituents (free bases, inorganic phosphate etc) into the bacterial bathing solution. In turn, this is indicative of cellular disruption. By plotting the increase of absorbance ($E_{260nm}$) against the time of homogenisation (Ht) can be observed by recording the minimum time of homogenisation which yields the maximum absorbance ($E_{260nm}$).

Ht was determined by homogenising washed cell suspensions for 5 minutes (flow rate = 25000l/min) after which the cell debris suspension was centrifuged at 13000rpm for 1 min in order to remove the cell debris from the supernatant (cytosol). The optical density ($E_{260nm}$) of the supernatant was observed using a Cecil Series 2 spectrophotometer (Cecil Instruments, Cambridge). This process was repeated every 5 minutes until the optical density readings ceased increasing. The recorded increase of $E_{260nm}$ absorbing material

leaking from the cell suspension against time gave an L-shaped curve (Fig 37 & 38). Ht for both *E. coli* and *P. aeruginosa* was determined as five minutes after the onset of the $E_{260nm}$ plateau. In future experiments, Ht for *E. coli* was 10 minutes at a flow rate of 250001/min and for *P. aeruginosa* the Ht was 45 minutes at a flow rate of 250001/min.

## Statistical Methods

All experiments in this project were designed to allow for statistical analysis and were performed in triplicate. Experimental data presented in this thesis represent the mean of those triplicate data sets. Where Standard Error bars are shown these were calculated *via* the methods of Hoel (1971).

**Figure 37:** Determination of the homogenisation time (Ht) of *E. coli* NCIMB 10000 as an observable increase in $E_{260nm}$ from homogenised cells with increasing time of homogenisation. Error bars are calculated from and plotted as the Standard Error of the data set.

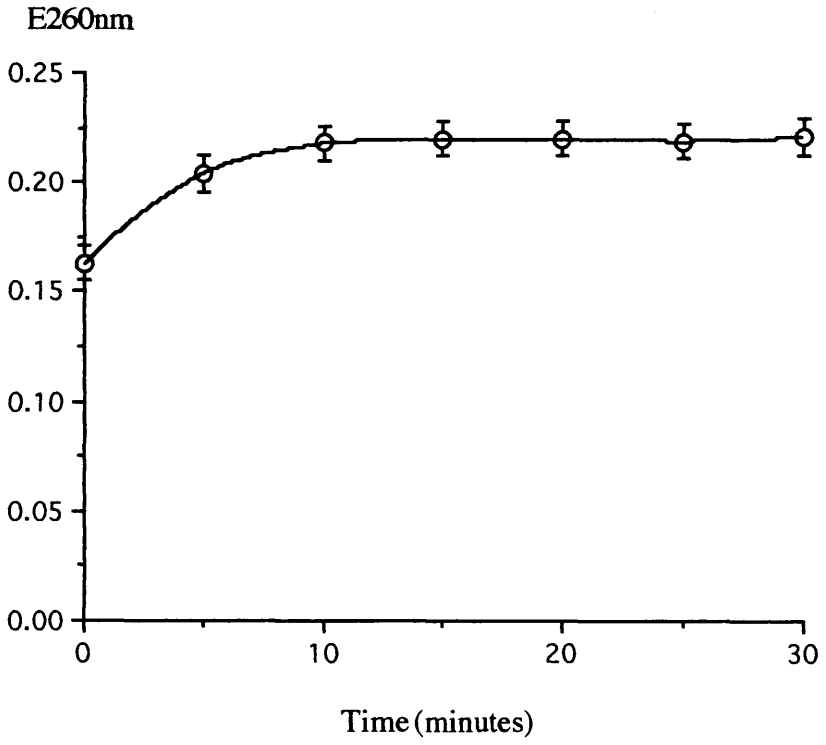
E260nm
0.25
0.20
0.15
0.10
0.05
0.00
0
10
20
30
Time (minutes)

**Figure 38:** Determination of the homogenisation time (Ht) of *P. aeruginosa* NCIMB 10548 as an observable increase in $E_{260nm}$ from homogenised cells with increasing time of homogenisation. Error bars are calculated from and plotted as the Standard Error of the data set.

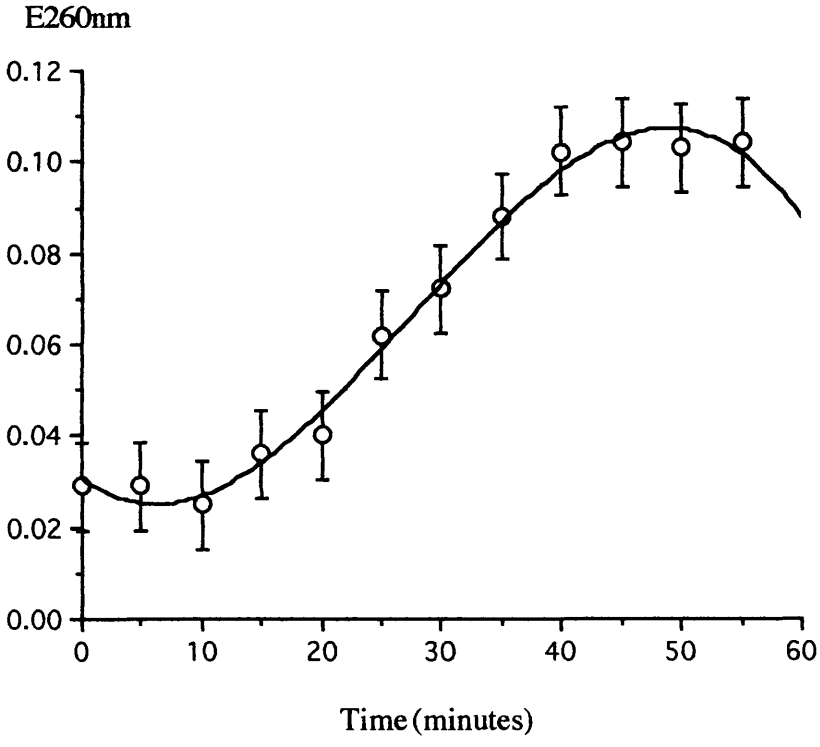
E260nm
0.12
0.10
0.08
0.06
0.04
0.02
0.00
0
10
20
30
40
50
60
Time (minutes)

# THE GROWTH INHIBITORY AND BIOCIDAL ACTIVITY OF THE PYRITHIONE BIOCIDES

## GROWTH INHIBITORY STUDIES

When beginning a study on the mode of action of novel biocides, it is important to know or ascertain the lowest concentration of the biocide at which growth of the microorganisms becomes inhibited (minimal inhibitory concentration or MIC). It is also important to understand the effects of the biocide upon growth kinetics of the test organisms and the stages in the growth cycle, if any, which are affected by the biocide action. A deeper understanding of the effect of a biocide upon specific phases of the growth cycle may give indications of the mode of action of the biocide.

There are two methods by which the MIC of a biocide can be estimated, the tube dilution method (Bloomfield 1991) and the estimation of MIC by growth inhibition (Collier *et al* 1990b). The tube dilution method is well documented and gives a simple method for MIC estimation. Estimation of the MIC by this method utilises the addition of a biocide, in increasing concentrations, to sterile media which is then inoculated with a known cell density of test microorganism. This series of tubes is then statically incubated for a known period of time (usually 48 hours). After incubation, the MIC is determined by recording the lowest biocide concentration exhibiting no visible signs of growth. It has been suggested that when applied *in vivo* the test biocide targets cells which are actively growing. The utilisation of static incubation in this method limits aeration of the incubating cultures and effectively prevents rapid aerobic growth. Although this is a limiting process, it is suggested that this is a more accurate reflection of a natural microbial niche in which cells will be nutrient limited and not exhibiting maximal growth rates.

The estimation of MIC by the growth inhibition method determines the MIC by comparing the effect of various concentrations of biocide upon the growth rates of test microorganisms growing in well aerated conditions in an orbital incubator. Subsequently, unlike the tube dilution method, the growth rate inhibition method determines the effect of biocides upon

cells which are growing in predetermined conditions that are conducive to maximum microbial growth. The growth rates of the growing cultures are then calculated as a percentage of the control (where 100% is the rate of growth with no biocide present in the culture). The 'percentage of control' values are then plotted against biocide concentration. The point of intersection of a curve of best fit through the x-axis indicates the biocide MIC against the test microorganism. Comparison of the two methods suggests that the growth inhibitory method may yield more information about the action of the biocide upon actively growing cells than the tube dilution method.

In this study, the estimation of MIC for ZnPT against both *E. coli* and *P. aeruginosa* was carried out using both techniques. MICs for NaPT, however, were observed only by the tube dilution method. This was due to the formation of particulate iron in the media after NaPT addition as a result of chelation of iron by the biocide. This precipitation affected the optical densities within the cultures and hence, prevented the use of this technique for MIC determination.

## Estimation of MIC Values

### Determination of ZnPT and NaPT MICs against *E. coli* and *P. aeruginosa* Using the Tube Dilution Method

Screw-cap tubes, each containing 9.0ml of sterile CDM had aliquots of NaPT (0.75ml) added to give the following final biocide concentrations in a total volume of 10ml: 0, 30, 60, 70, 80, 90, 100, 110, 120 and 130 $\mu g\ ml^{-1}$. An aliquot (0.25ml) of a 25ml bacterial culture grown overnight in CDM in an orbital incubator (200osc/min, 37°C) was aseptically added to the previously prepared tubes. These tubes were then incubated statically at 37°C for 48 hours. During this period the tubes were examined for visible growth at 19 hours and 48 hours. The MIC was determined as the lowest concentration of NaPT showing no visible growth after 19 hours (Table 5). This experiment was repeated for both *E. coli* NCIMB 10000 and *P. aeruginosa* PAO1 NCIMB 10548 for both NaPT and ZnPT. The determination of the ZnPT MIC values using the same concentration range as the NaPT MIC experiments gave no visible growth. Subsequently, ZnPT was applied at a much lower

concentration range of 0 to 20 $\mu$g ml$^{-1}$ in 2 $\mu$g ml$^{-1}$ intervals.

**Determination of ZnPT MIC Values Against *E. coli* and *P. aeruginosa* Using the Growth Inhibition Method**

Sterile 100ml Ehrlenmeyer flasks containing 24.0ml of sterile CDM were inoculated with 0.25ml of bacterial overnight culture. The optical densities ($E_{470nm}$) of the flask contents were recorded and the flasks were incubated in an orbital incubator (37°C, 200osc/min). Growth was monitored by measuring the optical density ($E_{470nm}$) at hourly intervals. Aliquots of ZnPT (0.75ml) were added after the third optical density reading was taken. This time was chosen for the biocide addition as previous experiments had shown the cells to be in the exponential phase of growth. The concentrations of biocide in 25ml were; 0, 1, 2, 4, 16, 32, and 64 $\mu$g ml$^{-1}$. Growth was observed for up to 7 hours after inoculation and optical density ($E_{470nm}$) was plotted against time for each biocide concentration (Figs 39 & 40). This experiment was repeated for both *E. coli* and *P. aeruginosa* against ZnPT. Growth rates were calculated as the gradient of the exponential phase. The growth rates were then calculated as a percentage of the control growth rate (0 $\mu$g ml$^{-1}$ ZnPT) and then plotted against biocide concentration (Figs 41 & 42). A computer generated curve of best fit was placed through the points. The point of intersection of the curve through the x-axis yielded an estimate of the MIC.

Table 5 shows the MIC data for NaPT and ZnPT as determined by the tube dilution method and for ZnPT as estimated by the growth inhibition method against *E. coli* and *P. aeruginosa*. The MIC data obtained from both methods of MIC estimation shows a significant difference between the levels determined by the tube dilution method and those observed by growth inhibition method (6.0 $\mu$g ml$^{-1}$ for *E. coli* as opposed to 4.5 $\mu$g ml$^{-1}$ from the growth inhibition method and 16.0 $\mu$g ml$^{-1}$ for *P. aeruginosa* as opposed to 13.0 $\mu$g ml$^{-1}$ for the growth inhibition method). This difference is particularly noticeable if the MIC values are expressed as a percentage of the tube dilution method. This gives a 25% difference for *E. coli* and an 18.8% difference for *P. aeruginosa* between the two methods.

**Table 5**: MIC values for NaPT and ZnPT against *E. coli* NCIMB 10000 and *P.aeruginosa* NCIMB 10548 for both tube dilution and growth inhibition methods.

| | | MIC ($\mu$g ml$^{-1}$) | |
|---|---|---|---|
| Microorganism | Method | NaPT | ZnPT |
| *E. coli* | Tube Dilution | 120 | 6.0 |
| *E. coli* | Growth Inhibition | * | 4.5 |
| *P. aeruginosa* | Tube Dilution | 100 | 16.0 |
| *P. aeruginosa* | Growth Inhibition | * | 13.0 |

*=Not Done

From the data presented in table 5, a distinct difference can be observed between the inhibitory activities of NaPT and ZnPT. Much lower MIC values are exhibited by ZnPT against both organisms than is the case for NaPT. This is particularly evident for the results of both biocides against *E. coli* where more than a twenty-fold difference is observed. The MIC values obtained for NaPT exhibit a 16.6% difference between the values for *E. coli* (120 $\mu$g ml$^{-1}$) and *P. aeruginosa* (100 $\mu$g ml$^{-1}$). This difference may be due to experimental error (eg, in biocide addition to flasks or variation in the addition of inocula cell density). Nonetheless, it is a sizeable difference and as such, the increased susceptibility of *P. aeruginosa* to NaPT in comparison to *E. coli* must be taken into consideration in the analysis of further experimental data.

The growth inhibitory data exhibits a 280% increase in MIC levels for ZnPT between *P. aeruginosa* (4.5 $\mu$g ml$^{-1}$) and *E. coli* (13.0 $\mu$g ml$^{-1}$). Such a large difference in the ZnPT MIC values between these organisms indicates a greater bacteristatic activity of ZnPT towards *E. coli* than is the case for *P. aeruginosa*. This difference may also signify the

presence of a *Pseudomonas*-gap with ZnPT.

The effect of ZnPT upon the growth kinetics of *E. coli* and *P. aeruginosa* are shown in figures 39 and 40. From these figures, it is evident that exposure of both *P. aeruginosa* and *E. coli* to ZnPT causes both a drug-dependant exponential phase change and the premature onset of stationary phase. The appearance of a drug-dependent lag phase is not observable in this experiment. The onset of a premature stationary phase may indicate the induction of the stringent response in *E. coli* (Gilbert *et al* 1990a). However, the stringent response is not observed in *P. aeruginosa* and does not fully explain the premature stationary phase onset observed here.

**Figure 39:** Effect of ZnPT upon the growth kinetics of *Escherichia coli* NCIMB 10000, showing the onset of a premature stationary phase after biocide addition (○), 0 $\mu$g ml$^{-1}$; (△), 1 $\mu$g ml$^{-1}$; (□), 2 $\mu$g ml$^{-1}$; (●), 4 $\mu$g ml$^{-1}$; (▲), 8 $\mu$g ml$^{-1}$; (■),16 $\mu$g ml$^{-1}$; (+), 32 $\mu$g ml$^{-1}$ and (×), 64 $\mu$g ml$^{-1}$. All data shown here was normalised on the zero time control value. Error bars are calculated from and plotted as the Standard Error of the data set.

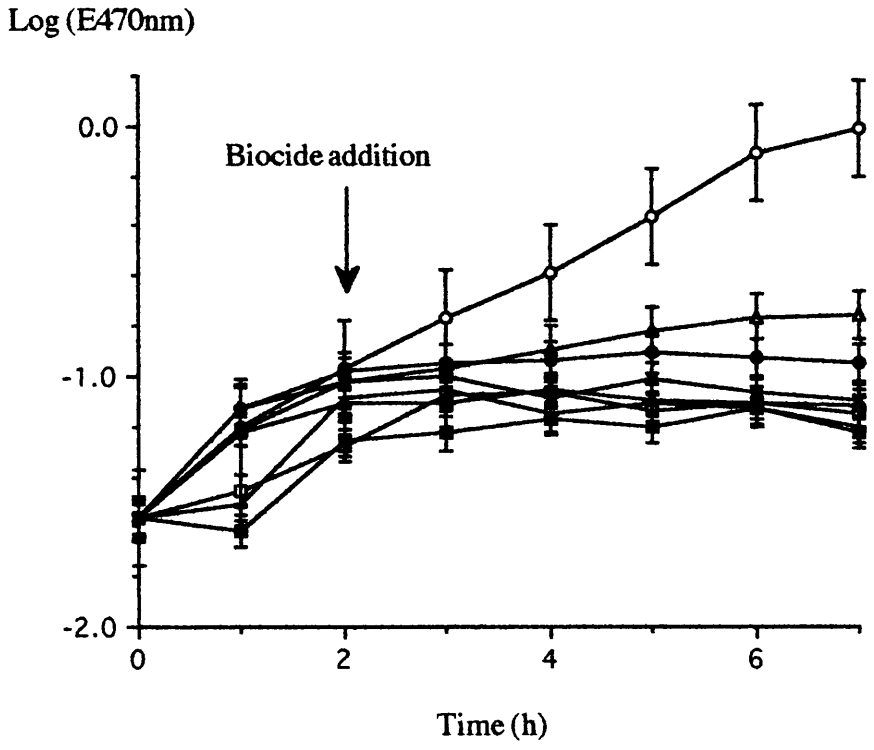
Log (E470nm)
0.0
-1.0
-2.0
Biocide addition
0
2
4
6
Time (h)

**Figure 40:** Effect of ZnPT upon the growth kinetics of *Pseudomonas aeruginosa* PAO1 NCIMB 10548, showing the onset of a premature stationary phase after biocide addition (○), 0 $\mu$g ml$^{-1}$; (△), 1 $\mu$g ml$^{-1}$; (□), 2 $\mu$g ml$^{-1}$; (●), 8 $\mu$g ml$^{-1}$; (▲)16 $\mu$g ml$^{-1}$; (■), 32 $\mu$g ml$^{-1}$ and (+), 64 $\mu$g ml$^{-1}$. All data shown here was normalised on the zero time control value. Error bars are calculated from and plotted as the Standard Error of the data set.

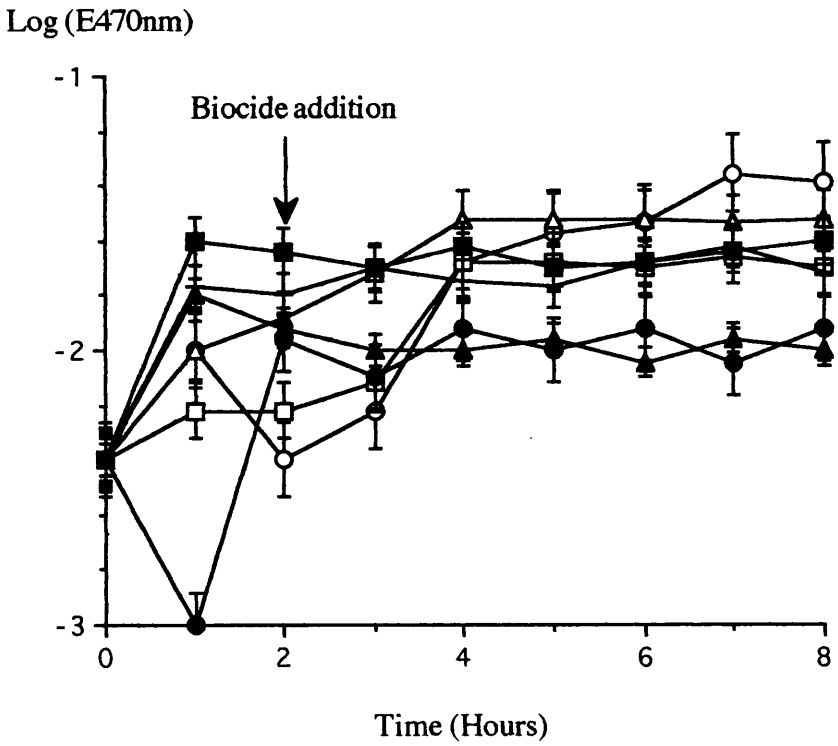
Log (E470nm)
-1
-2
-3
Biocide addition
0
2
4
6
8
Time (Hours)

**Figure 41:** MIC determination of ZnPT against *Escherichia coli* NCIMB 10000 as a percentage of control growth rate against biocide concentration. The intersection of the x-axis indicates the MIC (4.5$\mu$gml$^{-1}$). Error bars are calculated from and plotted as the Standard Error of the data set.

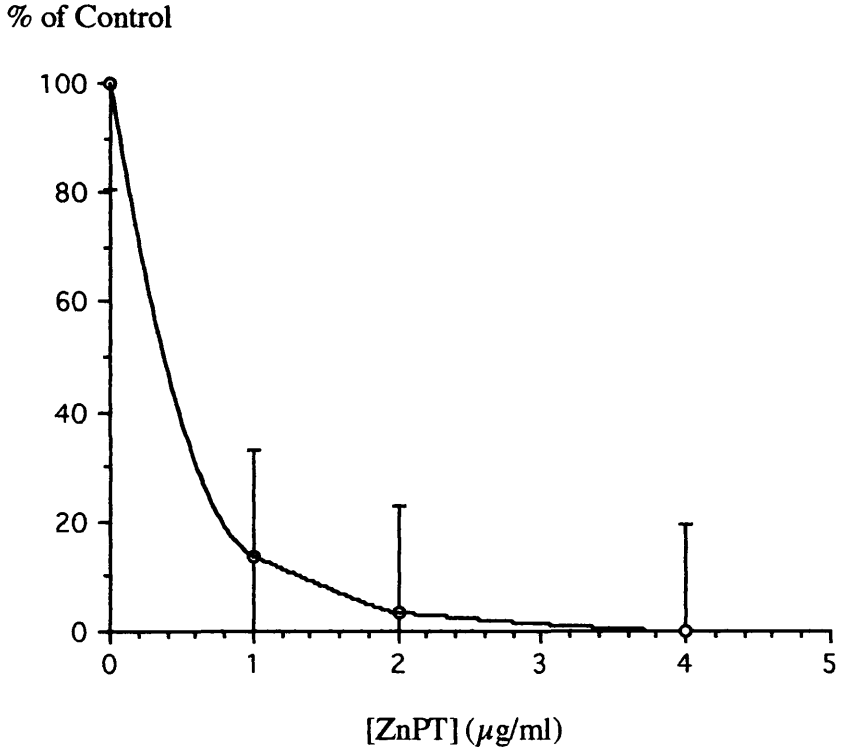
% of Control
100
80
60
40
20
0
0
1
2
3
4
5
[ZnPT] (μg/ml)

**Figure 42:** MIC determination of ZnPT against *Pseudomonas aeruginosa* NCIMB 10548 as a percentage of control growth rate against biocide concentration. The intersection of the x-axis indicates the MIC ($13.0\mu gml^{-1}$). Error bars are calculated from and plotted as the Standard Error of the data set.

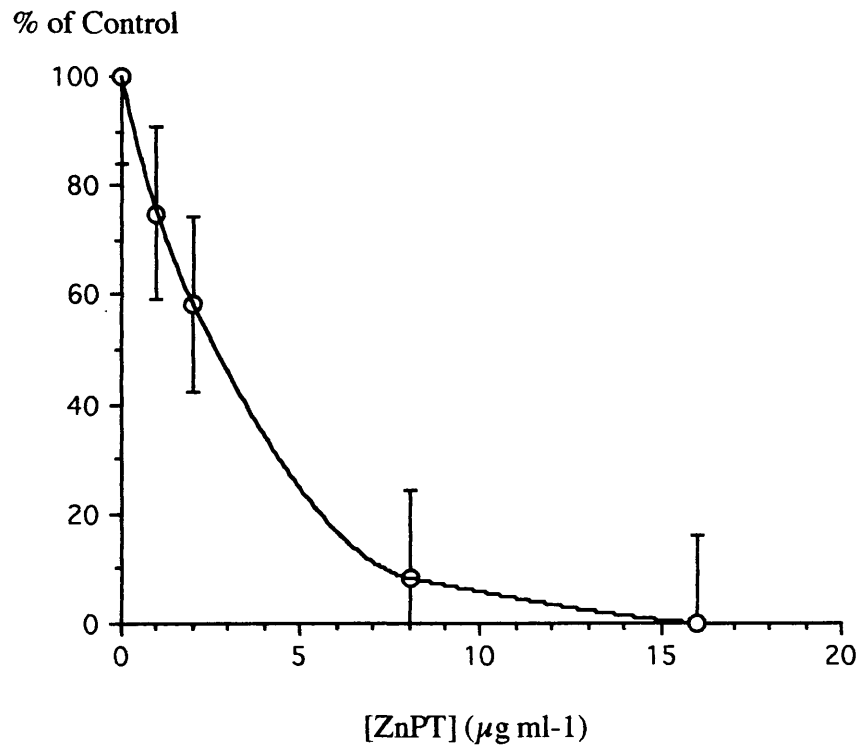
% of Control
100
80
60
40
20
0
0
5
10
15
20
[ZnPT] (μg ml-1)

## BIOCIDAL STUDIES

The growth inhibition studies which have detailed the activity of NaPT and ZnPT as bacteriostatic agents do not elucidate the killing or bactericidal activity of the pyrithiones. Although the application of the biocides at MIC causes growth to become static, no observations have been made to indicate the relationship between the MIC and the killing properties of the pyrithiones at their respective MICs.

The bactericidal properties of a biocide and the relationship between biocide concentrations which cause cell death and the MIC is readily observed by the construction of a time-survivor or death curve (Bloomfield 1991, Collier *et al* 1990b). The construction of time-survivor curves allows the elucidation of the microbicidal effects of a known agent at specific concentrations. This is achieved by plotting the log number of viable cells exposed to the biocide as a function of time. The plot facilitates the observation of the ability of a biocide at MIC levels to cause cell death and subsequently, estimates the biocidal efficacy of any antimicrobial agent. Subsequently, the bactericidal efficiency of the MIC may be expressed as two statistics, the $LT_{90}$ value and the MIC:[$LT_{90}$] ratio. The $LT_{90}$ is the time at which 90% (one $\log_{10}$ cycle) of a microbial population dies on exposure to a given concentration of biocide and is an indication of the rapidity of biocidal activity. The MIC:[$LT_{90}$] ratio expresses the relationship between the rapidity of biocidal action and concentration as a ratio to the MIC. It is generally accepted that a 'good' biocide has an $LT_{90}$ of 4 hours or less and an MIC:[$LT_{90}$] ratio of 1:4 or less. $LT_{90}$ values greater than 4 hours and MIC:[$LT_{90}$] ratios of greater than 1:4 indicate bacteristatic agents and subsequently ineffective bactericidal agents. However, it is not always possible to either calculate or rely upon $LT_{90\%}$ values from such experiments. In these cases it is possible to express the killing effect of the antimicrobial agents as either $LT_{90\%}$ values of greater than some predetermined experimental time value or to calculate the percentage survival of populations at the end of the experimentation.

The classification of an antimicrobial agent as a static or bactericidal agent may be indicative of the action of the biocide. Bacteristatic agents generally cause growth inhibition by

targeting a single important but non-vital metabolic pathway, ie, glycolysis or ß-oxidation. The inactivation of these pathways would be detrimental to cell division, but not to the production of sufficient energy for cell stasis. Subsequently, the exposed microorganism can still exist via the generation of energy from other less active pathways such as breakdown of DNA or RNA precursors. However, the exposed microorganisms are not fully metabolically active and cannot generate sufficient biochemical precursors in order to replicate and grow. Therefore, bactericidal agents may be seen as destructive agents which physically impair the bacterial cell. The exposed microorganism may be targeted at the cell envelope which would result in leakage of cytoplasmic constituents. If the antimicrobial agent does not act by causing physical damage, it may target a vital metabolic site, ie, DNA replication or ribosome formation. Exposure of microorganisms to such agents results in cell death. These general observations upon the activity of an antimicrobial agent facilitate the classification and experimental design for the study of the mode of action of a biocide.

## Determination of Killing Efficiency for both NaPT and ZnPT against *E. coli* NCIMB 10000 and *P. aeruginosa* PAO1 NCIMB 10548

In this study percentage survival values were determined using the time exposure method (Collier *et al* 1990b). Five sterile 100ml Ehrlenmeyer flasks were prepared to contain 23.0 ml of sterile CDM. The flasks were then made up to 24.0ml by the addition of biocide and deionised water in order to obtain biocide concentrations equivalent to 0xMIC, 1xMIC, 2xMIC, 3xMIC, and 4xMIC. Each of the flasks were pre-warmed to 37°C by orbital incubation (200 osc/min) for 10 minutes. The flasks were inoculated with 1.0ml of overnight culture of the respective microorganism. They were then incubated in an orbital incubator for 24 hours (37°C, 200osc/min). The time of inoculation was recorded. At times 0, 2, 4, 6, 8, and 24 hours 0.1ml of culture was aseptically removed from the flasks and CFU/ml were determined using viable count. The antimicrobial activity of the pyrithiones in solution was neutralised by dilution during the viable count methodology. $Log_{10}$ CFU/ml cells was plotted as $log_{10}$ survivors/ml against time (Figs 43, 44, 45 & 46). This experiment was repeated for both *E. coli* NCIMB 10000 and *P. aeruginosa* PAO1 NCIMB 10548 against both biocides.

**Figure 43:** The killing effect of NaPT against *Escherichia coli* NCIMB 10000 at various multiples of the MIC; ( ○ ), 0xMIC; ( △ ), 1xMIC; ( □ ), 2xMIC; ( ● ), 3xMIC and ( ▲ ), 4xMIC.
Error bars are calculated from and plotted as the Standard Error of the data set.

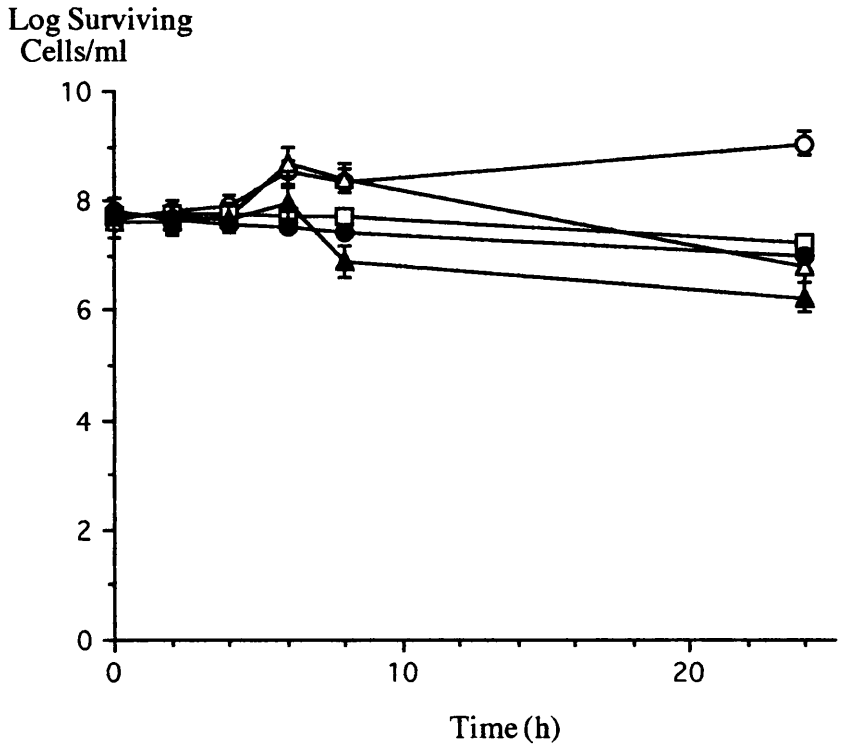
Log Surviving
Cells/ml
10
8
6
4
2
0
0
10
20
Time (h)

**Figure 44:** The killing effect of NaPT against *Pseudomonas aeruginosa* PAO1 NCIMB 10548 at various multiples of the MIC; ( ○ ), 0xMIC; ( △ ), 1xMIC; ( □ ), 2xMIC; ( ● ), 3xMIC and ( ▲ ), 4xMIC. Error bars are calculated from and plotted as the Standard Error of the data set.

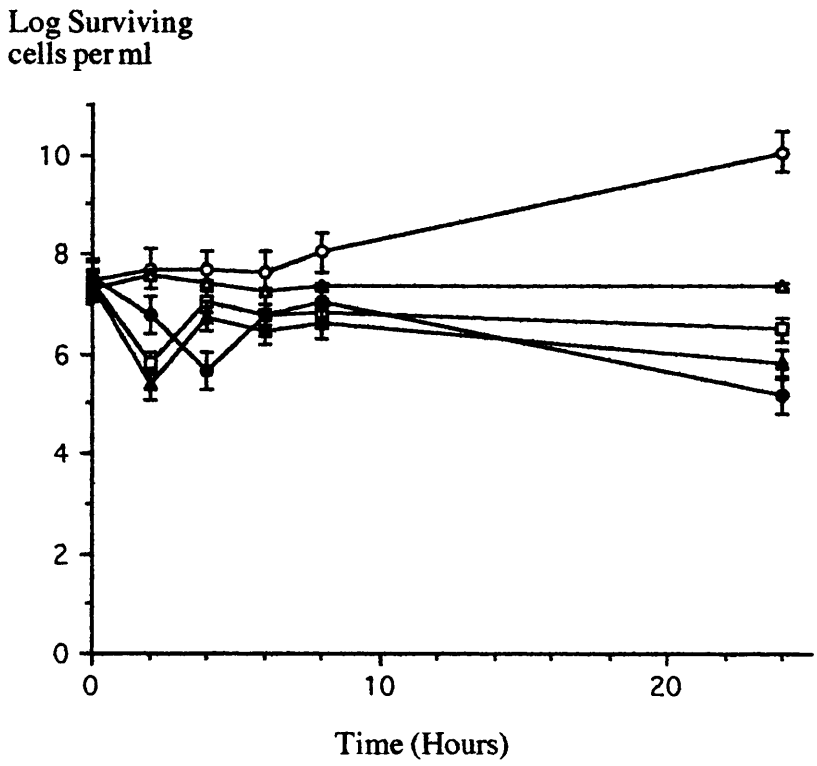
Log Surviving
cells per ml
10
8
6
4
2
0
0
10
20
Time (Hours)

**Figure 45:** The killing effect of ZnPT against *Escherichia coli* NCIMB 10000 at various multiples of the MIC; ( ○ ), 0xMIC; ( △ ), 1xMIC; ( □ ), 2xMIC; ( ● ), 3xMIC and ( ▲ ), 4xMIC. Error bars are calculated from and plotted as the Standard Error of the data set.

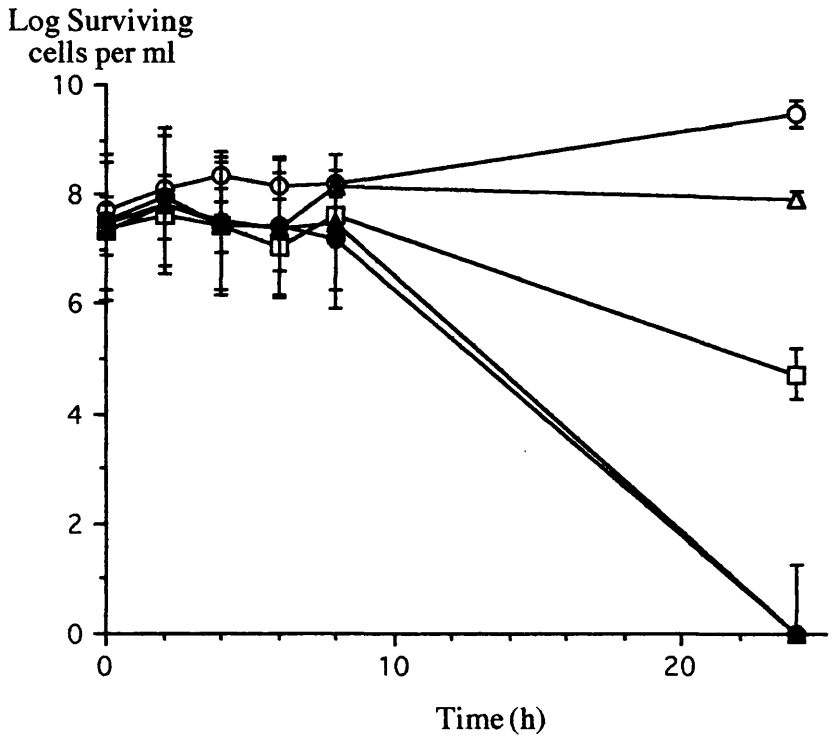
Log Surviving
cells per ml
10
8
6
4
2
0
0
10
20
Time (h)

**Figure 46:** The killing effect of ZnPT against *Pseudomonas aeruginosa* NCIMB 10548 at various multiples of the MIC; ( ○ ), 0xMIC; ( △ ), 1xMIC; ( □ ), 2xMIC; ( ● ), 3xMIC and ( ▲ ), 4xMIC. Error bars are calculated from and plotted as the Standard Error of the data set.

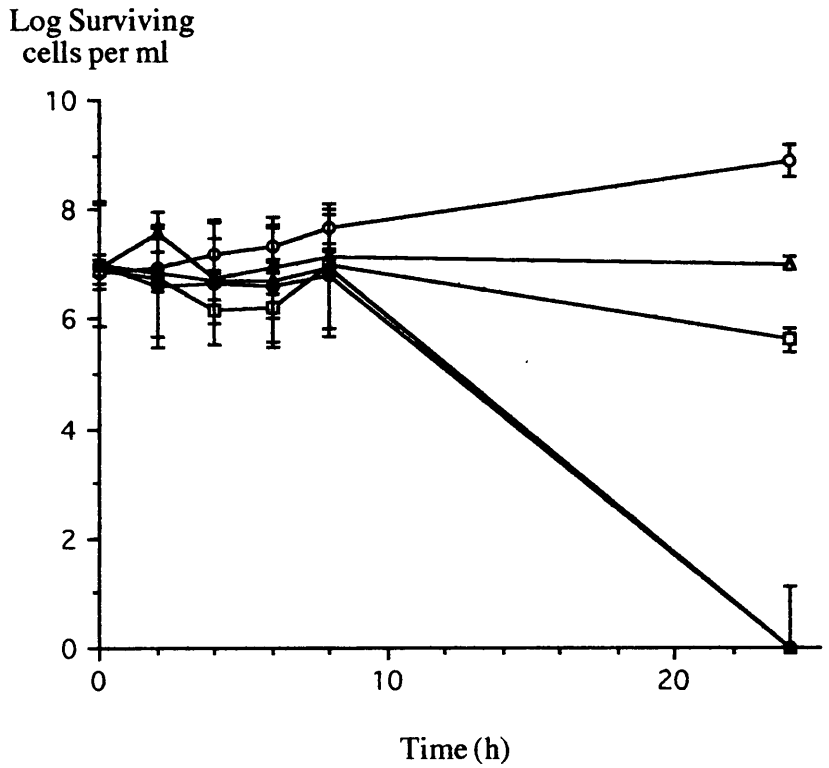
Log Surviving
cells per ml
10
8
6
4
2
0
0
10
20
Time (h)

**Table 6:** 24 hour survival values obtained for NaPT and ZnPT against *E. coli* and *P. aeruginosa* at varying multiples of MIC.

| Biocide | Organism | MIC Multiple | 24 Hour Survival Values (as a % of zero time value) |
|---|---|---|---|
| NaPT | *E. coli* | 1 x MIC | 14.50% |
| | | 2 x MIC | 36.00% |
| | | 3 x MIC | 15.60% |
| | | 4 x MIC | **2.80%** |
| NaPT | *P. aeruginosa* | 1 x MIC | 119.40% |
| | | 2 x MIC | 11.90% |
| | | 3 x MIC | **0.45%** |
| | | 4 x MIC | **2.59%** |
| ZnPT | *E. coli* | 1 x MIC | 215.00% |
| | | 2 x MIC | **0.22%** |
| | | 3 x MIC | **0.00%** |
| | | 4 x MIC | **0.00%** |
| ZnPT | *P. aeruginosa* | 1 x MIC | 109.80% |
| | | 2 x MIC | **5.47%** |
| | | 3 x MIC | **0.00%** |
| | | 4 x MIC | **0.00%** |

Emboldened values correspond to those treatments which gave an $LT_{90\%}$ or greater in 24 hours.

The data above (Table 6) indicates that neither NaPT or ZnPT is an effective, rapid killing agent. This is shown by the failure of either compound to exhibit $LT_{90\%}$ values of less than 4 hours in any treatment. Indeed, the data shows that $LT_{90\%}$ values, where achieved, were all in excess of 8 hours. However, both compounds exhibited achievement of 90% kill rates against both bacteria at at least one multiple of the MIC. In the case of NaPT against *E. coli*, a concentration of biocide equal to four times the MIC achieved a 24 hour survival value of 2.8%. The same compound against *P. aeruginosa* achieved two 24 hour killing values of greater than 90% at three and four times the MIC. ZnPT proved a better killing agent than NaPT, achieving greater than 90% killing at all multiples of the MIC of two times or greater against both bacterial species. It would seem that, from this data, both NaPT and ZnPT may best be described as biostatic agents with bactericidal potential. This data suggests, however, that ZnPT has a greater bactericidal activity than NaPT and subsequently reflects the activity observed in the MIC data (Table 5). The *Pseudomonas*-gap which is observable in the MIC data for ZnPT is not exhibited by the killing data (Table 6, Figs 43, 44, 45 &46).

## NEUTRALISER STUDIES

Various biologically active compounds can undergo chemical reactions with antimicrobial agents and subsequently neutralise their microbicidal effect. This is not unusual as biocides are chemically active and may react with many biologically active substances, ie, the isothiazolone biocides and thiol-containing compounds (Collier *et al* 1990c). Such substances which quench the effect of an antimicrobial agent are termed neutralisers. The effect of a potential neutraliser upon the action of a biocide can be seen as an increase in MIC levels in the presence of the neutraliser. At a biological level the effect of potential neutralisers are observed by repeating the tube dilution MIC experiment. Except for the presence of the potential neutraliser in the dilution tubes with the biocide, the method is carried out using identical conditions for MIC determination. At a chemical level, in order to observe direct chemical interactions between neutraliser and biocide, various methods may be used, ie, NMR, scanning spectrophotometry, isoelectric point studies, melting point studies and computer generated molecular modelling. The results obtained from these studies may give indications as to the target area of the biocide within the microbial cell. For

instance, neutralisation by phospholipids may be indicative of a membrane active agent. If the biocide is shown to be neutralised by proteinaceous agents, then the antimicrobial may work *via* disruption of protein integrity as a result of amine or thiol interactions.

Literature survey has shown reports of pyrithione neutralisation by bodily fluids (serum and saliva, Pansy *et al* 1953) and also by the metal chelating agent EDTA in Gram-negative bacteria (Khattar *et al* 1988). However, as reported in the introduction, no direct chemical evidence was given for the neutralisation effect observed. It is logical, therefore, to investigate the chemical activity of the pyrithione biocides, both at a biological and chemical level.

## Observation of the effects of Potential Neutralisers upon the MIC Values of NaPT and ZnPT against *E. coli* NCIMB 10000 and *P. aeruginosa* NCIMB 10548

The tube dilution method was used to investigate the effect of potential neutralisers upon the MIC values of NaPT and ZnPT against *E. coli* and *P. aeruginosa*. The following seven potential neutralisers were chosen: D-Cysteine, D-Alanine, ethylenediaminetetraacetic acid (EDTA), phosphatidylcholine, phosphatidylethanolamine, linoleic acid and L-glucose.

The D-forms of the amino acids and the L-form of glucose were used as they are not metabolically active in those orientations. The use of the non-metabolically active forms ensured that they would not be metabolised by either *P. aeruginosa* or *E. coli* during the course of the experiment and hence, induce better growth. This array of compounds was chosen to represent the major groups of biologically active chemicals. D-cysteine was chosen as it represents thiol containing biochemicals (eg; glutathione, dithiothreitol, CoASH, proteins etc). If neutralisation of the pyrithiones was observed with the presence of D-cysteine, then it would be indicative of potential neutralisation by other thiol-containing agents. D-alanine, unlike D-cysteine, does not possess any thiol groups. Therefore, any neutralisation in the presence of D-alanine would be indicative of amine interactions by the biocides. Phosphatidylcholine and phosphatidylethanolamine were used to investigate the

potential neutralisation of the pyrithiones by phospholipid groups. Both phosphatidylcholine and phosphatidylethanolamine are phospholipid components of bacterial membranes. The investigation of the effects of these phospholipids upon the antimicrobial activity of the pyrithiones would suggest pyrithione activity at the bacterial cell membranes. Linoleic acid is a long chain fatty acid which does not possess a polar head group (unlike the phospholipids), but is extremely similar to the fatty acid tails of the phospholipids. Any observed effect of the phospholipids upon the activity of NaPT and ZnPT may be clarified by observing the effects of linoleic acid upon the biocides. If an interaction does occur with linoleic acid alone, then this may suggest that the pyrithione biocides interact with the phospholipid tails as well as long-chain fatty acids. If no interaction is observed with linoleic acid, but an effect is observed with phosphatidylcholine and phosphatidylethanolamine, then this would suggest that the pyrithiones are interactive with the polar phospholipid head groups. L-glucose was used to observe the effect of carbohydrate groups upon the antimicrobial activity of NaPT and ZnPT. The metal chelating agent EDTA was chosen as a potential neutraliser as a result of it's representation in published literature which has recorded the neutralisation of the pyrithiones by this chemical (Khattar *et al* 1988).

Sterile dilution tubes were prepared to contain 9.0ml of sterile CDM. NaPT and sterile deionised water were added (0.125ml) in triplicate to give the following biocide concentration range: 0, 80, 90, 100, 110, 120, 130, 140, 150 and 160 $\mu$g ml$^{-1}$. One of each of the three sets of tubes were prepared to contain neutraliser concentrations which were equivalent to equimolar, semi-equimolar and quarter-equimolar concentrations of biocide present. However, as a result of their irregular formula weights, the two phospholipid compounds, phosphatidylethanolamine and phosphatidylcholine, were added at equal, semi-equal and quarter-equal $\mu$g ml$^{-1}$ concentrations of biocide. The total volume of potential neutraliser and deionised water was 0.625ml, but the exact relationship between the volumes of both components was altered to give the final required potential neutraliser concentration. The tubes containing the potential neutralisers were then inoculated with an aliquot (0.25ml) of overnight culture which had been grown in CDM. The tubes were then statically incubated for 19 hours (37°C). After this time, they were removed and the MIC values for the biocide were determined in the presence of potential neutralisers. This experiment was carried out for both bacteria against both biocides. The concentration ranges used for ZnPT

were; 0, 8, 12, 16, 20 and 24 $\mu$g ml$^{-1}$ for *P. aeruginosa* and 0, 2, 4, 6, 8 and 10 $\mu$g ml$^{-1}$ for *E. coli*.

**Table 7:** Observed neutralisation of NaPT and ZnPT by various potential neutralisers.

| Biocide | Organism | Neutraliser | Observed MIC ($\mu$g ml$^{-1}$) | |
|---|---|---|---|---|
| | | | With PN | Without PN |
| NaPT | *E. coli* | EDTA | 160 | 120 |
| | *P. aeruginosa* | EDTA | 150 | 100 |
| | | PE | 120 | 100 |
| ZnPT | *E. coli* | EDTA | 10 | 4.5 |
| | | Cysteine | 10 | 4.5 |
| | | PE | 10 | 4.5 |
| | *P. aeruginosa* | EDTA | 24 | 13 |
| | | Cysteine | 16 | 13 |
| | | PE | 24 | 13 |

PN = potential neutraliser, PC = phosphatidylcholine,
PE = phosphatidylethanolamine.

**Figure 47:** Comparison of the chelating properties of the structures of EDTA and NaPT. The parts of the molecules which are involved in metal cation chelation are emboldened. The structure of EDTA possesses six regions which are involved in cationic chelation, NaPT possesses only two. This indicates that EDTA is a more powerful chelating agent than NaPT.

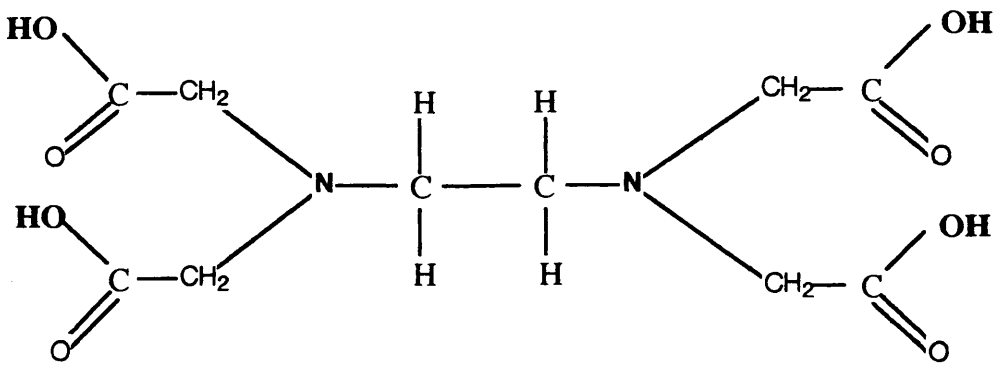


EDTA

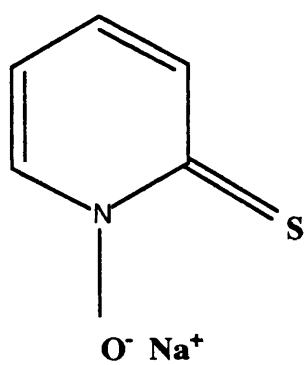


Sodium Pyrithione (NaPT)

No observed neutralisation of the pyrithione biocides was observed for D-alanine, L-glucose, phosphatidylcholine or linoleic acid. However, effective increases in MIC were observed for EDTA and phosphatidylethanolamine against both biocides and for cysteine against ZnPT (Table 7). The neutralisation of NaPT by EDTA was shown to be effective when EDTA was present at quarter-equimolar concentrations of the biocide. It should be noted that upon carrying out this experiment with EDTA, the chelation of iron from the media by both EDTA and NaPT was limiting and no growth was observable. This was overcome by doubling the amount of iron present in the CDM by addition of 10ml of solution B (instead of 5ml) to 1l of Solution A (Page ). After the addition of extra iron, growth was shown not to be limited. The presence of EDTA at quarter-equimolar concentrations increased the MIC for NaPT against *E. coli* from 120 to 160 $\mu g\ ml^{-1}$ and the MIC for NaPT against *P. aeruginosa* from 100 to 150 $\mu g\ ml^{-1}$. No observed neutralisation of pyrithione activity occurred with the presence of EDTA at equimolar or semi-equimolar concentrations of the biocide. This result, and the observed limitation of growth, as a result of iron chelation from the media, suggested that neutralisation of NaPT by EDTA was occurring due to competitive chelation between the two compounds. However, EDTA is a more effective chelating agent being a tetradentate ligand, as opposed to the bidentate characteristic of NaPT, and as a result has stronger metal chelating properties (Fig 47). This indicates that EDTA is chelating more of the metal cations present in solution and on the cell surface than NaPT. If the theory of Albert *et al* (1956) is correct and if the pyrithione biocides enter the cell by metal cation chelation, then the lack of metal cations may subsequently inhibit the activity of NaPT. However, this does not explain the occurrence of EDTA neutralisation of NaPT at only quarter-equimolar concentrations. With ZnPT, EDTA is shown to inhibit the antimicrobial action at all three neutraliser concentrations. In this case, the competitive chelation would seem to be a more credible argument. Another possible reason for EDTA neutralisation of ZnPT may be the chelation of the central zinc atom from both the monomer and dimer forms of ZnPT. This would result in the formation of free pyrithiolate ions which resemble the form of NaPT in solution. Subsequently, the MIC would be increased as a result of the different levels of activity exhibited by ZnPT and NaPT in solution.

The MIC values for *E. coli* and *P. aeruginosa* exposed to ZnPT and for *P. aeruginosa*

exposed to NaPT were shown to increase with the presence of the phospholipid phosphatidylethanolamine (Table 7). The MIC for NaPT against *P. aeruginosa* increased by 20 $\mu$g ml$^{-1}$ from 100 $\mu$g ml$^{-1}$ to 120 $\mu$g ml$^{-1}$, showing effective neutralisation of this biocide by phosphatidylethanolamine. The MIC for *E. coli* exposed to ZnPT was shown to increase from 4.5 $\mu$g ml$^{-1}$ to 10 $\mu$g ml$^{-1}$ at all concentrations of applied phosphatidylethanolamine and the MIC for ZnPT against *P. aeruginosa* was shown to increase from 100 $\mu$g ml$^{-1}$ to 150 $\mu$g ml$^{-1}$ in the presence of the same compound. These results indicate that phosphatidylethanolamine neutralises the growth inhibitory action of ZnPT when applied to *E. coli* and *P. aeruginosa* and the action of NaPT in the presence of *P. aeruginosa*. The observed neutralisation of the action of these biocides in the presence of phosphatidylethanolamine may suggest that these antimicrobial agents act towards bacterial membranes. Phosphatidylethanolamine is one of the most abundant phospholipids in the bacterial envelope and the head group structure of this compound (phosphorylethanolamine) is present in the lipopolysaccharide layer of Gram-negative bacteria (Fig 5). Therefore, an observed effect upon the activity of NaPT and ZnPT by this neutraliser is indicative of chemical activity at the level of the bacterial membranes.

There were observed increases in MIC for ZnPT against both *E. coli* and *P. aeruginosa* upon addition of cysteine to the system. This observation indicates potential neutralisation. In *E. coli*, the effective neutralisation of the inhibitory action of ZnPT was observed at all three concentrations of neutraliser present. The neutralising effect of cysteine with *E. coli* increased the MIC for ZnPT from 4.5 $\mu$g ml$^{-1}$ to 10.0 $\mu$g ml$^{-1}$ for all three concentrations of neutraliser. This result is not indicative of amine interactions as no increase in MIC was observed for ZnPT against D-alanine. However, as cysteine is a thiol-containing amino acid, this result may indicate that ZnPT is thiol-interactive. Observations of neutralisation of ZnPT against *P. aeruginosa* showed an increase in MIC when the neutraliser was present at semi-equimolar and quarter-equimolar concentrations of the biocide present. The increase in MIC for ZnPT against cysteine in *P. aeruginosa* was from 13.0 $\mu$g ml$^{-1}$ to 16.0 $\mu$g ml$^{-1}$ and this increase of 3.0 $\mu$g ml$^{-1}$ may be indicative of thiol-interactions between ZnPT and *P. aeruginosa*. However, no increase in MIC was observed with biocide concentrations greater

than 16.0 $\mu$g ml$^{-1}$ and this may suggest that the observed neutralisation could have been as a result of experimental error; ie, too many cells in the inoculum or errors of judgment in the estimation of visible growth. The presence of too many cells in the inoculum would have been concurrent in all three neutraliser concentrations. This would have resulted in the observation of increased MIC values at equimolar concentrations of cysteine as well as semi- and quarter-equimolar concentrations of biocide present. However, the same volume of the same inoculum was added to each tube and any inherent errors should have been observable at all three cysteine concentrations. Nonetheless, the increases in MIC for ZnPT against *P. aeruginosa* in the presence of semi- and quarter-equimolar concentrations of cysteine are observable and do indicate the neutralisation of antimicrobial activity of ZnPT by thiol-containing agents.

The observations of increased MICs of both compounds in the presence of EDTA, phosphatidylethanolamine and the MICs for ZnPT in the presence of cysteine were indicative of neutralisation of the pyrithiones at a biological level. The neutralisation may have been caused by the biological activity of the neutraliser in or on the cell and may not have been as a direct result of chemical interactions between the biocides and the neutralisers. Therefore, observations of the presence of possible direct chemical interactions between the biocides and the two neutralisers EDTA and cysteine were carried out using scanning spectrophotometry. Subsequent to this, computer generated molecular interactions were projected between these biocides, cysteine and the phosphatidylethanolamine head group.

## Determination of Direct Pyrithione-Neutraliser Chemical Interactions using Scanning Spectrophotometry

Scanning spectrophotometry utilises the observation of changes in the spectrophotometric profile of a particular compound to any potential chemical reactions with a reactant. The UV/Vis spectrophotometric profiles of individual compounds of interest are obtained and the presence of peaks and the wavelengths at which they occur are recorded. The peaks and troughs observed in such spectra may indicate the different bonding and electrical states of orbitals associated with the structures involved in the potential reaction. The emission of a

proton at a specific wavelength excites different conjugate and non-conjugate electrons in different ways. A conjugate system of electrons, eg; a benzene ring, is commonly denoted by two peaks in such spectra. A non-conjugate system, however, is denoted by a single peak which lies further towards the visible end of the spectrum (Crooks 1978; Williams & Fleming 1980). Therefore, the recorded profile exhibits the spectrophotometric signature of an individual compound at a known concentration. After individual profiles of the two potential reactants have been analysed, the compounds are mixed at known concentration ratios and the mixture is scanned in the same range of wavelengths as that used for individual chemicals. The spectrophotometric profile of the mixture is then obtained. Observation of peaks which fall at the same wavelengths as those of the individual compounds corresponds to the presence of the original compounds within the reaction mixture and to the presence of unreacted compound. The occurrence of peaks which are not present in the individual profiles signifies either the presence of new chemical bonds, which absorb light at different wavelengths than the bonds present in the individual compounds, or the formation of ions of the original compound. The formation of these new peaks may therefore, signify the formation of a reaction product between the two compounds of interest and subsequently, indicates the nature of any chemical interactions between a set of compounds.

In this study, the effects of EDTA and cysteine were observed upon the UV/vis spectrophotometric profiles of both NaPT and ZnPT. These compounds were used in this experiment as they had been shown to neutralise the antibacterial activities of the pyrithiones *in vitro* by increasing biocide MIC values against *P. aeruginosa* and *E. coli*. The UV/vis spectra (250nm to 450nm) of NaPT and ZnPT (0.335mM in the organic solvent dimethyl formamide (DMF)) were individually obtained using a Shimadzu UV/vis scanning spectrophotometer UV-160 (Shimadzu Corporation, Kyoto, Japan). The observation of peaks and their corresponding wavelengths were recorded (Table 8, Figs 48, 49, 50 & 51). The biocides were then mixed with the neutralisers at equimolar concentrations (0.335mM in DMF) and the UV/vis spectra of the respective reaction mixtures were obtained as printed traces of absorbance against wavelength. Peaks and their corresponding wavelengths were recorded (Table 9, Fig 48 & 49). The traces for biocide, neutraliser and biocide plus neutraliser were then overlayed for ease of comparison and changes in peak wavelengths were recorded and tabulated.

**Table 8:** Wavelengths (nm) of peaks obtained from Scanning spectrophotometric traces for NaPT, ZnPT, EDTA and Cysteine.

| NaPT | ZnPT | EDTA | Cysteine |
|---|---|---|---|
| 269 | 275 | 272 | 332 |
| 304 | 287 | 305 | |
| 373 | 323 | 333 | |

**Table 9:** Wavelengths (nm) of peaks obtained for various reaction mixtures of ZnPT and NaPT and their potential neutralisers.

| NaPT + EDTA | ZnPT + EDTA | NaPT + Cysteine | ZnPT + Cysteine |
|---|---|---|---|
| 269 | 275 | 269 | 269* |
| [272] | 283* | 304 | 280* |
| 300* | [287] | [332] | [287] |
| [304] | 300* | 358* | 323 |
| [305] | [305] | [373] | [332] |
| [333] | 312* | | |
| 367* | [323] | | |
| [373] | 331* | | |
| | [333] | | |
| | 358* | | |

* = New peaks which appeared in the reaction mixture UV/vis spectra,

[] = peaks which disappeared from the reaction mixture UV/vis spectra.

**Figure 48:** Traces obtained from the scanning spectrophotometry studies which investigated the interactions between EDTA and NaPT. (·····) represents the trace for 0.335mM NaPT; (·–··) the trace for 0.335mM EDTA and (——), the trace for 0.335mM NaPT + 0.335mM EDTA.

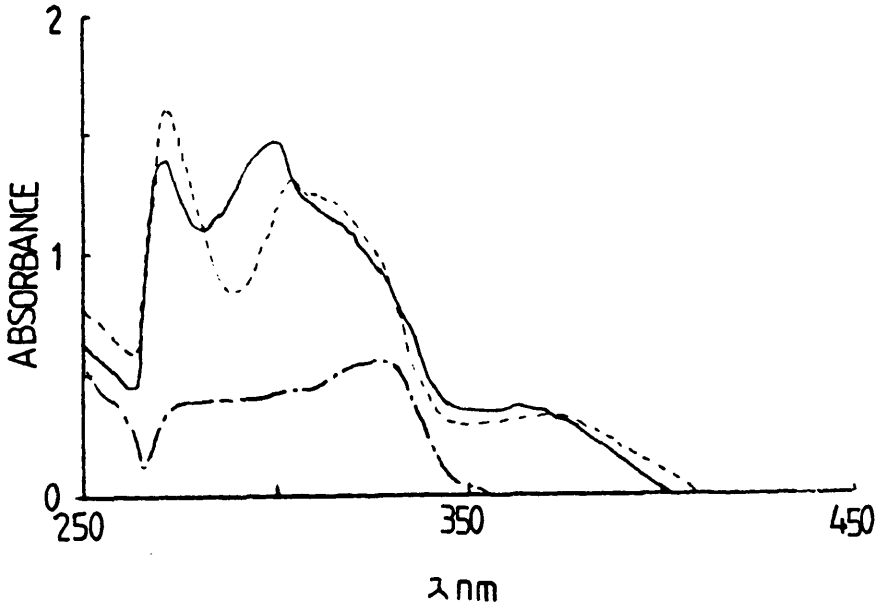
2
1
0
ABSORBANCE
250
350
450
λ nm

**Figure 49:** Traces obtained from the scanning spectrophotometry studies which investigated the interactions between cysteine and NaPT; (·····) represents the trace for 0.335mM NaPT; (—·—) the trace for 0.335mM cysteine and ( — ) the trace for 0.335mM NaPT + 0.335mM cysteine.

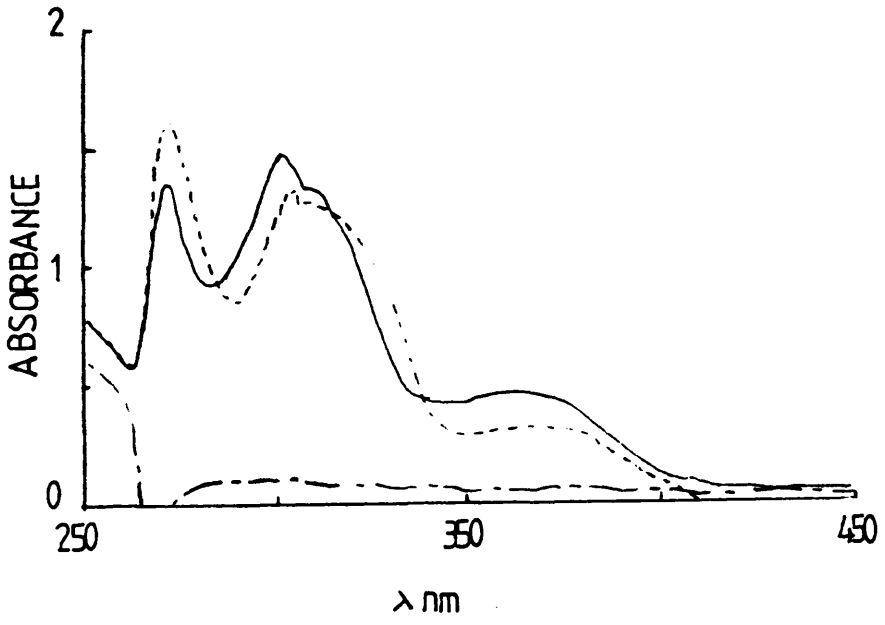
2
1
0
ABSORBANCE
250
350
450
λ nm

**Figure 50:** Traces obtained from the scanning spectrophotometry studies which investigated the interactions between EDTA and ZnPT; (----) represents the trace for 0.335mM ZnPT; (._._) the trace for 0.335mM EDTA and ( ___ ) the trace for 0.335mM ZnPT + 0.335mM EDTA.

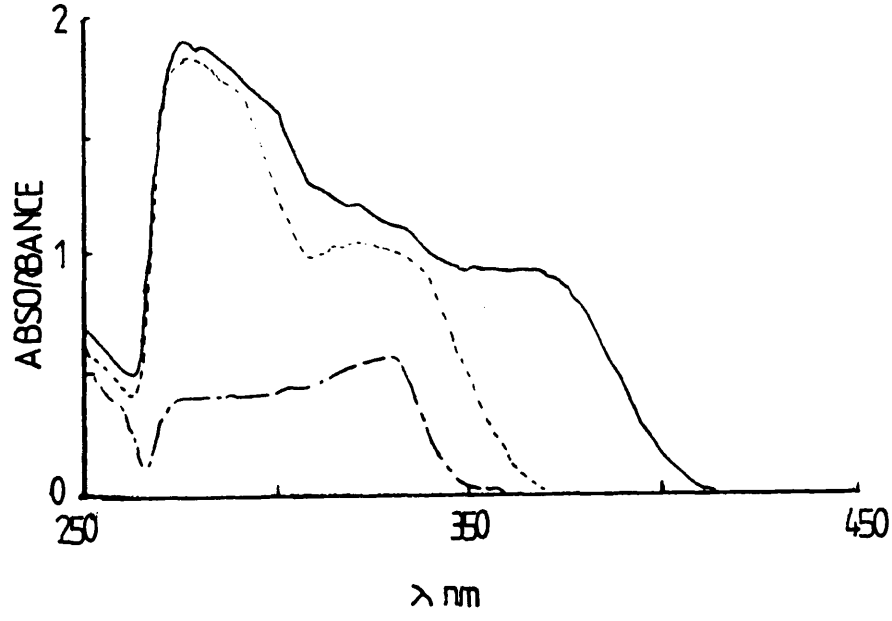
2
1
0
ABSORBANCE
250
350
450
λ nm

**Figure 51:** Scanning spectrophotometry traces for ZnPT and cysteine; (- - -) represents the trace for 0.335mM ZnPT; (- - -) the trace for 0.335mM cysteine and ( — ) the trace for 0.335mM ZnPT + 0.335mM cysteine.

ABSORBANCE
0
1
2
250
350
450
λ nm

From the scanning spectrophotometric traces (Figs 48 to 51) and the results from tables 8 and 9 it can be seen that NaPT and ZnPT both exhibit three peaks. For NaPT (Figs 48 & 49, Table 8) the peaks appearing at 269nm and 304nm are due to the excitation of shared electrons in the conjugate pyridine ring structure (Crooks 1978). These shared electrons have moved from a stable $\pi$-orbital to an excited $\pi^*$-orbital upon exposure to light in the region of 270 to 300nm (Crooks 1978; Williams & Fleming 1980). The third peak of 373nm is due to excitation of the electrons on the sulphur atom of the pyridine ring structure. Towards this region of the visible spectrum the electrons of non-conjugate heterologous atoms become excited and move from a ground state $\pi$-orbital to a p-orbital (Crooks 1978; Williams & Fleming 1980).

The peaks exhibited by ZnPT (Figs 50 & 51, Table 8) account for the excitation of shared conjugate electrons from the $\pi$-orbital to the $\pi^*$-orbital. This is understandable as ZnPT exists as a complex of either two or four conjugate pyridine rings around a central zinc atom which is hidden from the light by these rings.

The changes observed in the spectrum for NaPT upon the addition of equimolar EDTA were due to an additive effect of the two spectra (Fig 56, table 9). No change was observed which indicated the movement of conjugate electrons to a non-conjugate state. Consequently, this suggests that no reaction occurred between NaPT and EDTA.

Figure 49 indicates that a reaction occurred between NaPT and cysteine. The first two peaks observed at 269 and 304nm (Table 9) in the equimolar mixture of cysteine and NaPT account for the conjugate pyridine ring system. However, the appearance of a peak which turns into a shoulder at 358nm signifies the movement of electrons from a conjugate state to a non-conjugate state. This may be indicative of hydrogen bonding between NaPT and cysteine, drawing electrons away from the conjugate system. This removes electrons from an excitation state where they move from $\pi$ to $\pi^*$-orbitals and to an excitation state where they move between $\pi$ and p-orbitals (Williams & Fleming 1980).

The traces for the reaction of ZnPT with EDTA (Fig 50) indicate that a reaction has occurred between these two compounds. The observed peaks at 275 and 283nm (Table 9) denote the

presence of conjugate electrons in the pyridine ring system of ZnPT. The presence of new peaks at 300, 312 and 331nm suggest that electrons have been moved from a conjugate system to a non-conjugate system (similar to the change in spectrum observed for NaPT with cysteine). The movement of these electrons to a non-conjugate state suggests that EDTA has had an effect upon ZnPT; namely the chelation of the zinc atom from the centre of the molecule. Further proof to suggest that EDTA has chelated the central ZnPT zinc atom is the appearance of a peak and shoulder at 358nm which correlates to the sulphur atom in the NaPT spectrum (Figs 48, 49 & 50, Tables 8 & 9). Consequently, this indicates the release of sodium pyrithione after chelation of the zinc by EDTA. It should be noted that EDTA is solubilised in NaOH, which produces a solution of sodium-EDTA. Therefore, the chelation of zinc by EDTA would displace the sodium ions which would then be accepted by the free pyrithiolate rings to yield NaPT.

No noticeable effect was observed upon reacting ZnPT with equimolar concentrations of cysteine (Fig 51, Table 9). No observed increase or decrease in peak wavelengths would indicate that no changes have occurred to the electron orbital excitation states. This suggests that any observed changes in the spectrum for ZnPT in the presence of cysteine were due to an additive effect of the two spectra.

The use of scanning spectrophotometry did not fully elucidate the mode of neutralisation between the EDTA and NaPT or cysteine and ZnPT. However, it did give some information as to the mode of neutralisation of ZnPT and EDTA. This suggests that ZnPT is neutralised by chelation and subsequent removal of the central zinc atom by EDTA. Further work investigating the chemical reactivity of the pyrithione biocides was carried out using computer generated molecular modelling.

## Investigations into the Chemical Reactivity of the Pyrithione Biocides using Computer Generated Molecular Modelling

The utilisation of computer generated molecular modelling enables the projection of stable chemical reaction product formation between two compounds using quantum mechanical analysis. The programs used in computer generated modelling calculate the energy required for stable bond formation between two compounds in a solvent free system and subsequently, enable the visualisation of the projected stable complex formation between the reactants.

A complex is formed between the linkage or bonding of two monomers (Equation 10 where, $M^1$ and $M^2$ are the reactants, and C is the complex).

(10) $$M^1 + M^2 \longrightarrow C$$

The enthalpy or binding energy required in the formation of the complex is calculated by subtracting the sum of the heat of formation of the monomers in the reaction from the heat of formation of the complex (Equation 11, where $\Delta E$ is the enthalpy of the reaction, $\Delta Hf^c$ is the heat of formation of the complex and $\Delta Hf^m$ is the heat of formation of the monomers), the heat of formation is the amount of energy required in the chemical formation of a compound.

(11) $$\Delta E = \Delta Hf^c - (\Delta Hf^{m1} + \Delta Hf^{m2})$$

A negative energy of formation, enthalpy, indicates the formation of a stable product and therefore a stable chemical structure (Holum 1986).

This study utilised computer generated molecular modelling to project interactions between the pyrithiolate anion (the diffused pyrithione anion from NaPT in solution) and cysteine (Fig 52a); the pyrithiolate anion and a glycine dimer (Fig 52b); the pyrithiolate anion and the phosphatidyl ethanolamine head group (Fig 52c). Interactions were also projected between the zinc pyrithione dimer and cysteine (Fig 53); the ZnPT dimer and a glycine dimer (Fig

54); the ZnPT dimer and phosphatidylethanolamine head group (Figs 55 & 56); the ZnPT monomer and the phosphatidyl ethanolamine head group (Fig 57). Compound structures used were in their free energy states. ZnPT structures were obtained from x-ray crystallography data (Barnett *et al* 1977). The structures of cysteine and the glycine dimer were based on zwitterion forms of the amino acids (Stryer 1988). The phosphatidyl ethanolamine head group structure was obtained from Stryer (1988). All of the structures were refined using AM1 Hamiltonian calculations (Dewar *et al* 1985) applied through the program MOPAC 93 (QCPE Program 455, Dept of Chemistry, Indiana University, Bloomington, Indiana, USA).

The experimental manipulations were carried out using the program MOPAC 93 to calculate the quantum mechanic equations and enthalpies of complex formation (Table 10). The display manipulation package SYBYL 6.1 (Tripos Associates Inc, St Louis, Missouri, USA) was used for the visual display and onscreen manipulation of the compounds. All of the procedures were carried out using a Silicon Indigo computer (Silicon Graphics Computer Systems, Calgary, Alberta, Canada).
The experimental protocol observed was that defined by Dewar *et al* 1985. Onscreen, the compounds were placed in a proposed stable complex formation using the approximate geometrical docking procedure from the program SYBIL 6.1. The docking procedure involved the placement of the test compounds in a proposed stable complex formation by the use of initial operator judgement of polar and hydrophobic interactions. The MOPAC 93 program was then utilised to refine the interactions observed using SYBIL 6.1 by quantum mechanical analysis. The data from the MOPAC 93 program was then read back into SYBIL 6.1 and the original proposed complex structures were adjusted to fit the results of the quantum mechanical calculations. This procedure also defined the heats of formation of the reactants and complexes formed which were retrieved from MOPAC 93 and the enthalpy for the reaction complex was calculated using equation 11.

Negative binding energies were calculated for the complexes formed between the pyrithione structures used in the projection and the reactants (Table 10), showing the formation of stable complexes between the pyrithiones and their potential reactants. These results indicate that the neutralisation of the pyrithiones by amines (glycine dimer), thiols (cysteine) and the

phosphatidylethanolamine head group occurs at a chemical level as well as a proposed biochemical or biological level.

Figure 60 exhibits the computer generated complex formation between the pyrithiolate anion and a cysteine monomer. The enthalpy required for the chemical production of this complex is -21.0 Kcal $mole^{-1}$ (Table 10) and subsequently signifies stable complex formation. Hydrogen bonding is observed between the oxygen molecule on the pyrithiolate ion and the amine tail of the cysteine monomer (Figure 52a). The application of NaPT *in vitro* or *in vivo* together with cysteine would be affected by the presence of other cations which would bind more strongly to the free pyrithiolate anions in solution. The presence of these ions would disturb and prevent hydrogen bond formation between the pyrithiolate ion and the neutralisers as a result of their increased electrostatic interactions. This explains why no neutralisation was observed with cysteine in the tube dilution neutraliser studies with NaPT.

**Table 10:** Heats of formation of biocide/reactant complexes.

| | Enthalpy (Kcal $Mole^{-1}$) | | |
|---|---|---|---|
| Potential Reactants | NaPT (Pyrithiolate ion) | ZnPT Monomer | Dimer |
| Cysteine | -21.0 | * | -48.5 |
| Peptide | -73.4 | * | -21.8 |
| PE head group | -12.3 | -286.6 | -286.8[a] |
| | | | -239.1[b] |

PE = phosphatidylethanolamine, * = not done, a = enthalpy for Fig 55 and b = enthalpy for Fig 56.

The computer generated interaction between a small peptide (glycine dimer) and the pyrithiolate anion (Fig 52b) gave similar results to that observed between the pyrithiolate anion and cysteine. An amine interaction was observed by the presence of hydrogen bonding between the N-terminus of the peptide and the oxygen and sulphur atoms of the pyrithiolate anion. Formation of a stable complex was observed with an enthalpy of -73.4 Kcal $mole^{-1}$ (Table 10). This indicates an increased stability for the pyrithiolate/glycine dimer complex when compared to that for the pyrithiolate/cysteine complex, which exhibited a less stable enthalpy of -23.0 Kcal $mole^{-1}$. The interactions between the pyrithiolate anion and the peptide indicate potential neutralisation of NaPT in the presence of amine-containing compounds. However, similar to the interaction with cysteine, there was no observed neutralisation by the amino acid L-alanine in the tube dilution neutraliser studies (Table 7). This may suggest that *in vivo*, the pyrithiolate anion will preferentially bind to cationic agents (eg: metal cations). This would lead to the formation of metal chelates in solution and would subsequently, inhibit the formation of interactions with the amine groups present in the peptide, cysteine or head group residues.

Figure 52c exhibits the formation of a stable complex which possesses a negative enthalpy of -12.3 Kcal $mole^{-1}$ (Table 10) between the phosphatidylethanolamine head group structure and the pyrithiolate anion. Formation of a stable complex between the head group and the pyrithiolate anion would signify potential membrane interactions *in vivo* by the biocide. The phospholipid head group possesses two polar regions, an amine tail and a central orthophosphoric acid grouping which is joined to the lipid tail *via* a methyl group. The complex obtained from the computer generated image exhibited hydrogen bonding between the pyrithiolate and the amine tail on the phospholipid head group. The observed formation of this complex is similar to that seen in complexes formed between the pyrithiolate anion and cysteine (Fig 52a) and the pyrithiolate anion and peptide (Fig 52b) which both exhibited electrostatic amine interactions. The interactions observed between potential reactants and the pyrithiolate anion have exhibited amine interactions between cysteine, a small peptide (glycine dimer) and the phosphatidylethanolamine head group. However, *in vivo* these interactions are disabled as the presence of divalent cations would bind preferentially to the pyrithiolate anion with increased affinity. This may explain why no neutralisation was

observed between cysteine and NaPT and alanine and NaPT in the tube dilution neutraliser studies.

The interaction between the ZnPT dimer and cysteine (Fig 53) indicates hydrogen bond formation between the thiol group of the cysteine molecule and the central zinc atoms of the ZnPT dimer. The reaction between the dimer and cysteine gave a stable negative enthalpy of -48.5 Kcal $mole^{-1}$. A slight change in the geometry of the ZnPT dimer is observable in this interaction. The geometry of an unreacted ZnPT dimer molecule exhibits a purely tetrahedral shape (Fig 31). When this figure is compared with figure 53, a slight change in the tetrahedral formation of the molecule is observed. This is due to the cysteine molecule pulling one of the pyrithiolate groups from the central zinc-oxygen bridges and 'opening up' the molecule as a result of the electrostatic interactions between the two compounds. This reaction may explain the observed neutralisation of the antimicrobial action of ZnPT in the presence of cysteine and the observed change in peak wavelengths in the scanning spectrophotometry studies (Fig 49). It should be noted that the computer generated data in figure 53 shows the interaction of only one cysteine molecule. *In vivo*, another molecule would be able to interact with the ZnPT dimer at the opposite geometrical location. This would further disrupt the dimeric ZnPT configuration.

Figure 54 shows the possible interaction between a ZnPT dimer and a small peptide (glycine dimer) which gives rise to a stable complex (enthalpy = -21.8 Kcal $mole^{-1}$, Table 10). No distinct change in the geometry of the dimer is observable. However, the peptide does appear to be hydrogen bonding at a similar site as cysteine but is not such a stable complex having a higher enthalpy (-21.8 in comparison with -48.5 Kcal $mole^{-1}$ for cysteine). This may be indicative of possible amine interactions by ZnPT. However, no neutralisation of antimicrobial activity was observed with the exposure of ZnPT to the amino acid L-alanine in the tube dilution neutraliser studies. This situation is similar to that observed between the peptide and the pyrithiolate anion and may be explicable by the increase in the presence of divalent cations *in vivo*. As discussed above, the presence of divalent cations would disable complex formation between the amine group and the biocide due to the divalent cations possessing an increased electronegative affinity with the biocide.

**Figure 52:** Computer generated interaction between (a) the pyrithiolate anion (diffused form of NaPT in solution) and a cysteine monomer, (b) the pyrithiolate anion and a small peptide (a glycine dimer) and (c) the pyrithiolate anion and the phosphatidylethanolamine head group.

a)

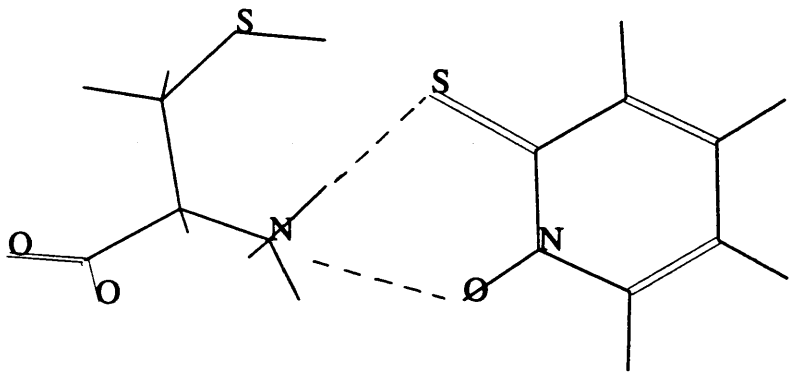


Interaction Between Cysteine and Pyrithiolate Anion

b)

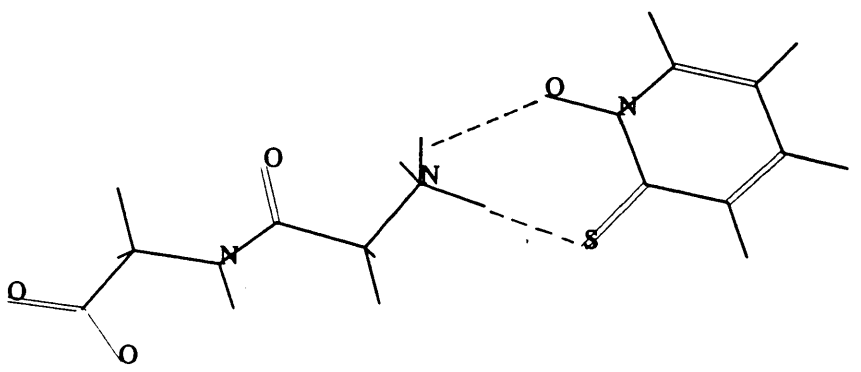


Interaction Between Peptide Dimer and Pyrithiolate

c)

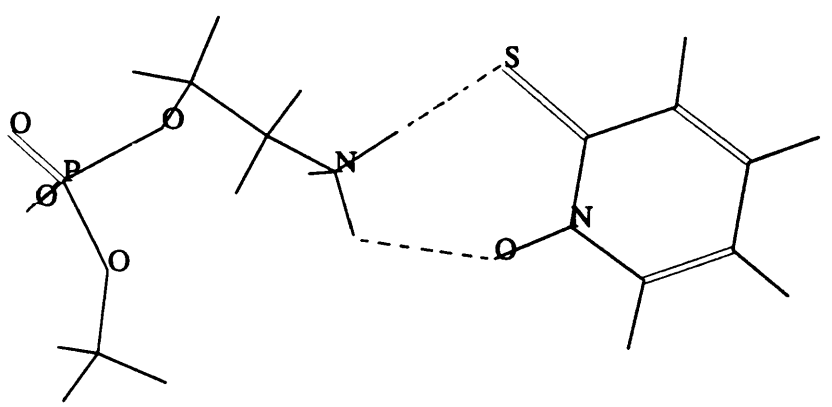


Ethanolamine Phospholipid Head-Group
Interaction with Pyrithiolate

The computer generated complexes between the ZnPT dimer and the phosphatidyl ethanolamine head group produced the formation of two possible complexes (Figs 55 & 56). Both of the reaction products generated possess high negative enthalpies (-286.8 and -239.1 Kcal $mole^{-1}$ for Fig 55 & 56 respectively). Figure 55 exhibits a large amount of geometrical distortion of the ZnPT dimer *via* the interaction of the amine component of the phosphatidyl ethanolamine head group. The interaction has resulted in bond formation between the sulphur atom of one of the dimer's pyrithiolate groups and the oxygen atom of another, with the breakage of one of the intermolecular oxygen-zinc bridges. The enthalpy obtained from this reaction is -239.1 Kcal $mole^{-1}$ and indicates the complex to be highly stable. The ZnPT dimer would also be susceptible to an identical interaction from the amine component of the head group on the opposing geometrical site of the dimer. The action of the amine head group may also open the dimer to further possible interactions with other amine head groups. The capped-stick diagram from figure 55 exhibits elongation of the bonds between the oxygen and the zinc atoms of the dimer. Although these bonds are shown to be intact in the capped-stick diagram, in the filled orbital diagram the same bonds are broken. This was due to the inability of the capped-stick bond visualisation program of SYBIL 6.1 to break bonds no matter how far they were stretched. However, the filled-orbital diagram represents the sizes of atomic orbitals in space and shows the orbitals to be too small to maintain the bonding between the oxygen and zinc atoms of the ZnPT dimer.

Figure 56 shows another possible complex which has been formed between the ZnPT dimer and the phosphoric acid group of the phosphatidyl ethanolamine head group. This also has a highly negative enthalpy (-239.1 Kcal $Mole^{-1}$) and is therefore a stable complex. However, unlike the interaction between the amine group of the phospholipid (Fig 55), this interaction has cleaved all of the intermolecular zinc-oxygen bridges and splits the ZnPT dimer. Subsequently, the dimer is no longer held together with covalent bonds, but is the result of hydrogen bond formation between the sulphur and oxygen of one pyrithiolate group and the hydrogens on the aromatic ring of another.

A similar interaction has also been observed with the ZnPT monomer and the phospholipid head group (Fig 57). This also has a negative enthalpy (-268.6 Kcal mole-1) and is a stable

chemical structure. However, in this interaction both the phosphoric acid and amine groups of the phospholipid are bonding with the ZnPT molecule. This bonding distorts the geometry of the monomer and results in hydrogen bonding between the phosphoric acid group of the phospholipid and the zinc atom of the monomer. Bonding has also occurred between the amine group of the phospholipid and the sulphur and oxygen atoms of one of the pyrithiolate groups.

At a cellular level, the action of dimeric and monomeric ZnPT upon the bacterial membrane would involve interactions with both the phosphoric acid and amine groups of the phosphatidylethanolamine molecules in both the outer and inner Gram-negative bacterial membranes. ZnPT would disturb the structure of the outer membrane by interacting with the phosphatidylethanolamine residues and the LPS. The LPS of the outer membrane contains phosphorylethanolamine (Fig 5), which is the phosphatidylethanolamine head group structure, as part of the core region. Interactions between ZnPT as both monomers and dimers and the phosphorylethanolamine groups of the core region of LPS must be detrimental to LPS structure and function. Interactions at this point would disable metal cation chelation at the distal leaflet of the bacterial outer membrane and would subsequently disable outer membrane structure. This may be indicative of a similar mode of action by the pyrithiones to that of PHMB and other quaternary ammonium compounds (Broxton *et al* 1984). Subsequently, distortion of the hydrophobic inner leaflet of the membrane would occur again *via* ZnPT/phosphatidylethanolamine head group interactions. These interactions would also distort the arrangement of acyl chains in the membrane and disrupt overall membrane configuration.

**Figure 53:** Computer generated interaction between the ZnPT dimer and a cysteine monomer, green = zinc, yellow = sulphur, dark blue = nitrogen, light blue = hydrogen, white = carbon and red = oxygen. Distortion of the tetrahedral shape of the dimer is observable as a result of the hydrogen bonding between the sulphur of the cysteine and the zinc of the ZnPT dimer. Hydrogen bonding is also observable between the amine group of the cysteine molecule and the oxygen on one of the pyrithiolate groups.

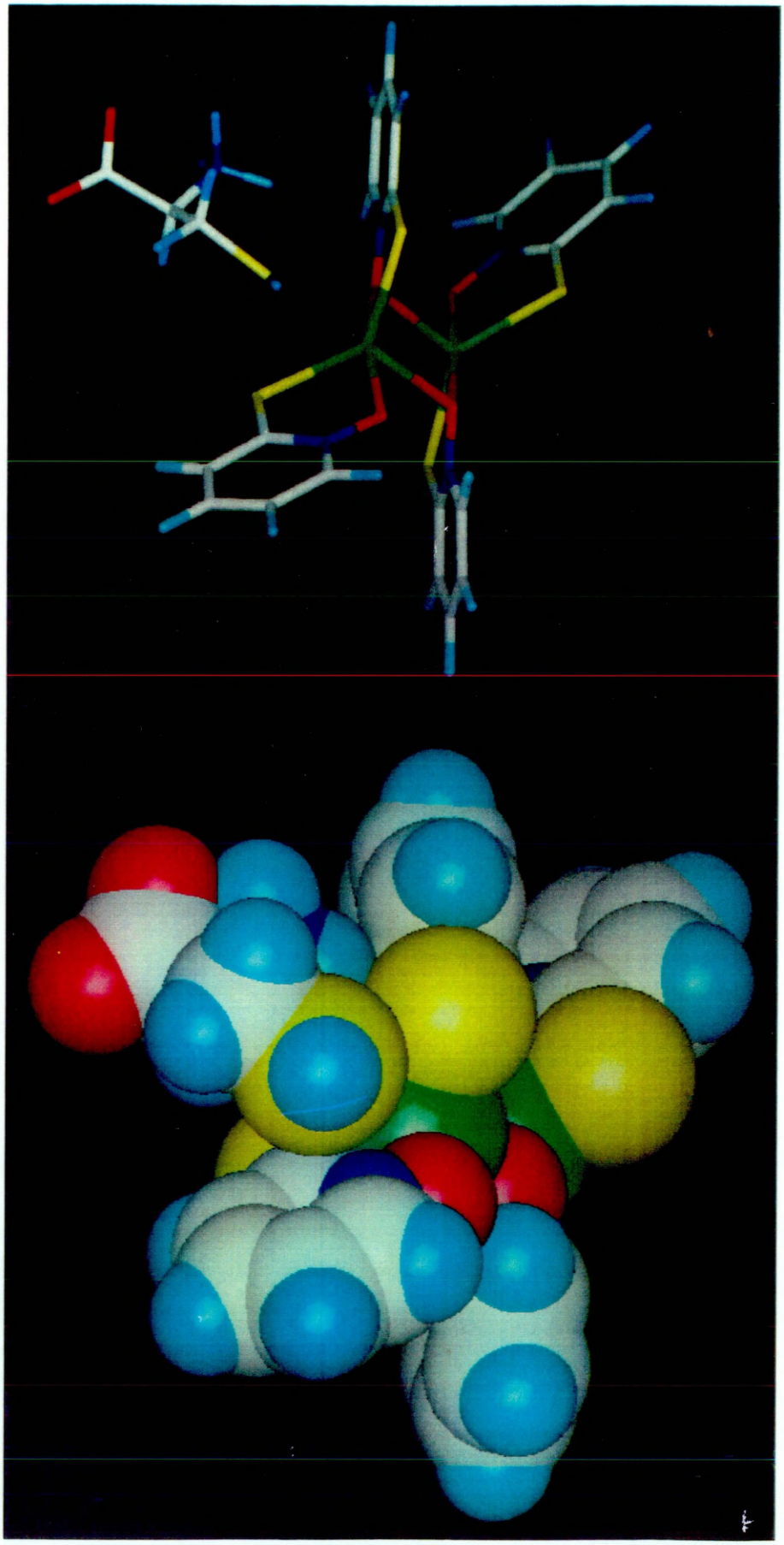

**Figure 54:** Computer generated interaction between a small peptide (a glycine dimer) and the ZnPT dimer. Hydrogen bonding is observable between the amine tail of the peptide and the sulphur and oxygen groups at the central zinc complex of the ZnPT dimer.

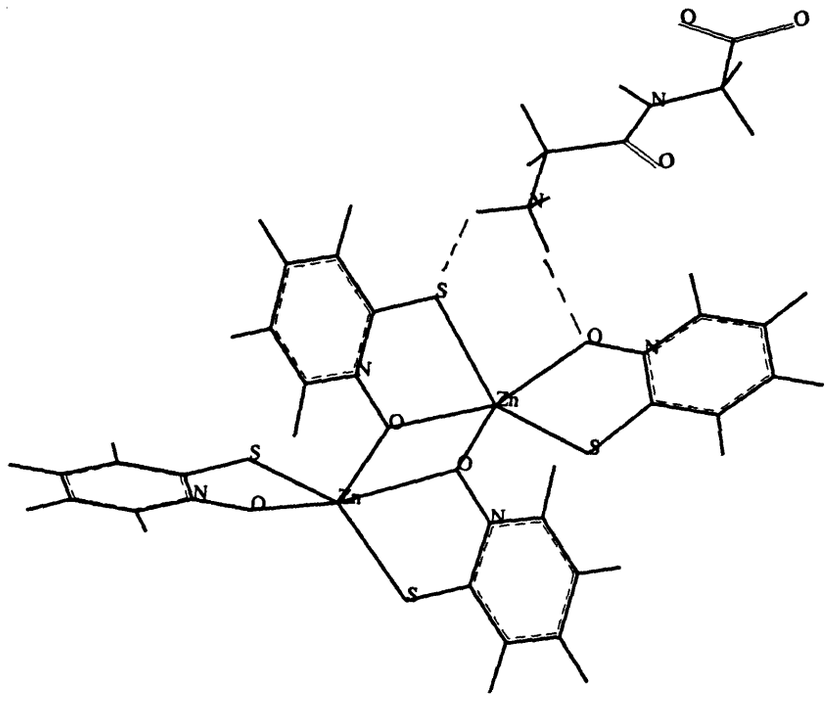


Interaction Between Peptide Dimer and
Zinc Pyrithione Dimer

**Figure 55:** Computer generated interaction between a ZnPT dimer and the phosphatidylethanolamine head group, green = zinc, yellow = sulphur, dark blue = nitrogen, light blue = hydrogen, white = carbon, red = oxygen and purple = phosphorous. The amine tail of the head group structure has hydrogen bonded with the oxygen molecule of one pyrithiolate group and the sulphur atom of another pyrithiolate group. This interaction has grossly disturbed the geometry of the ZnPT dimer and may allow the molecule to interact with another three head group structures.

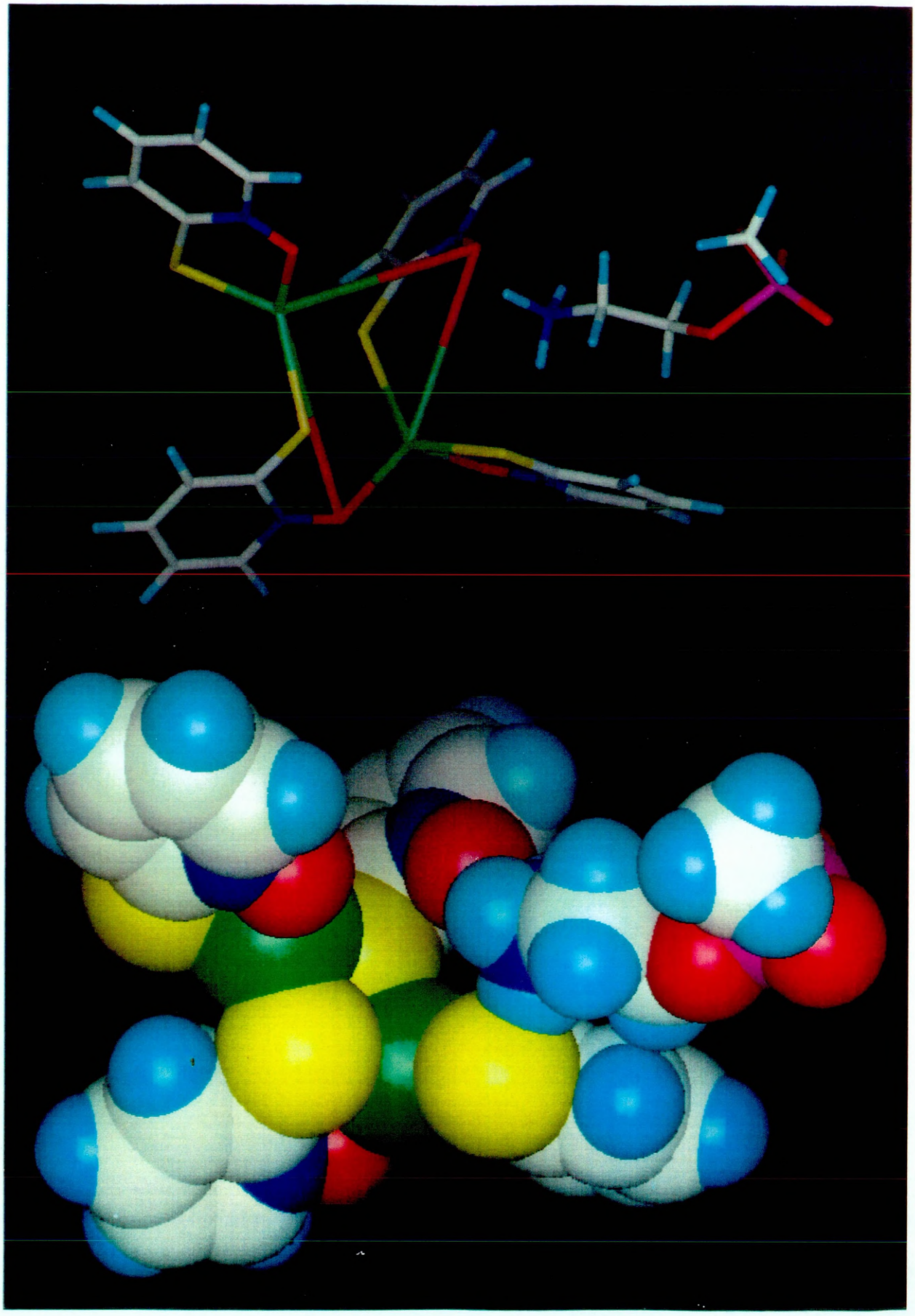

**Figure 56:** Interaction between a ZnPT dimer and the phosphatidylethanolamine head group, green = zinc, yellow = sulphur, dark blue = nitrogen, light blue = hydrogen, white = carbon, red = oxygen and purple = phosphorous. The phosphoric acid grouping of the phosphatidyl ethanolamine tail has bonded with the central zinc atom of one of the ZnPT monomers. Subsequently, the interaction has disrupted the dimer structure and it is only electrostatic forces between the sulphur and oxygen of one monomer and the aromatic ring of the other which holds the two ZnPT compounds together.

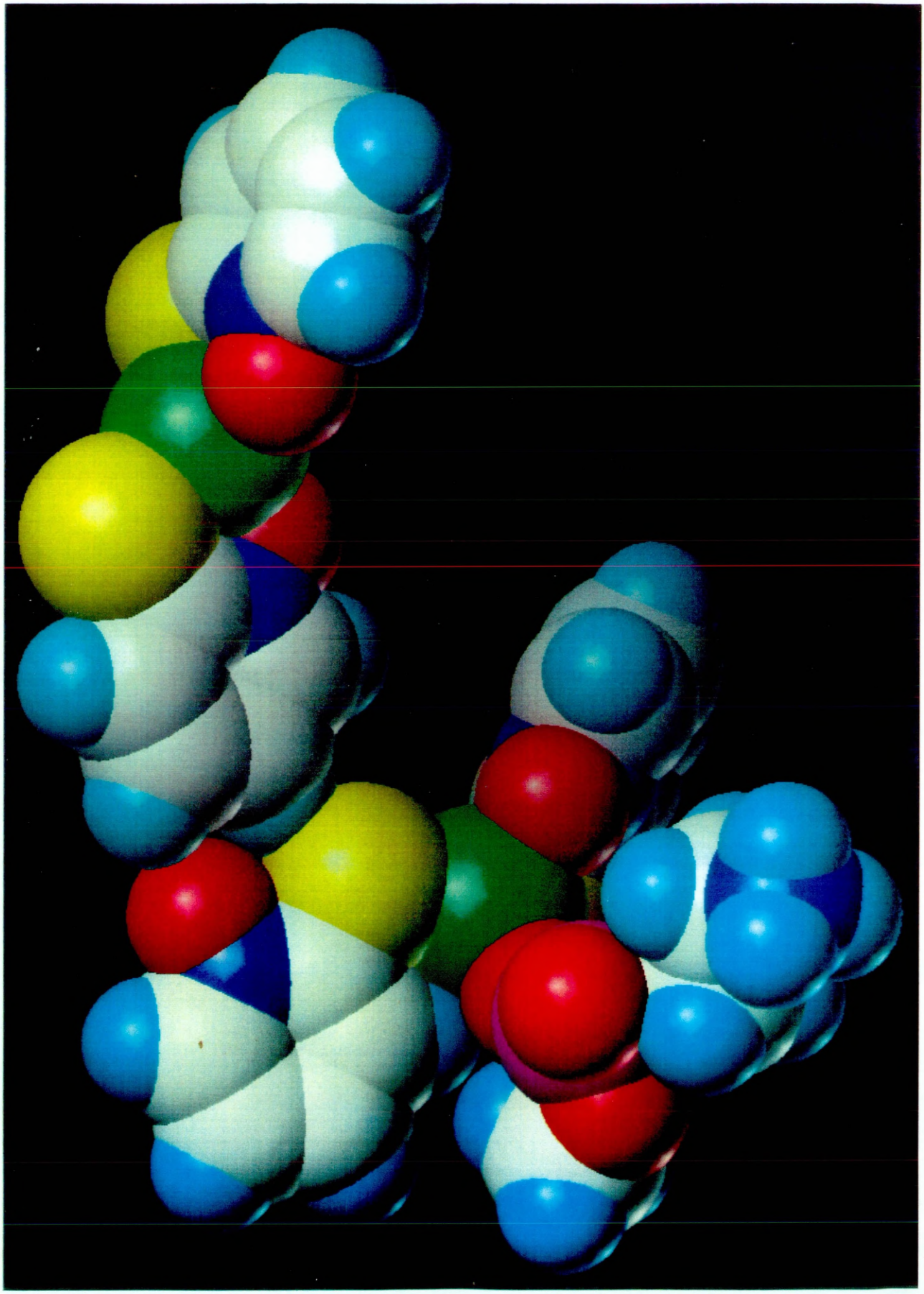

**Figure 57:** Computer generated interaction between a ZnPT monomer and the phosphatidylethanolamine head group, green = zinc, yellow = sulphur, dark blue = nitrogen, light blue = hydrogen, white = carbon, red = oxygen and purple = phosphorous. The phosphoric acid core of the phosphatidyl ethanolamine head group has directly bonded with the central zinc atom of the ZnPT monomer. The amine tail of the head group has also bonded with oxygen and sulphur atoms of one of the pyrithiolate groups. These interactions have distorted the dimer shape and appear to be cleaving the zinc atom from the core of the ZnPT monomer.

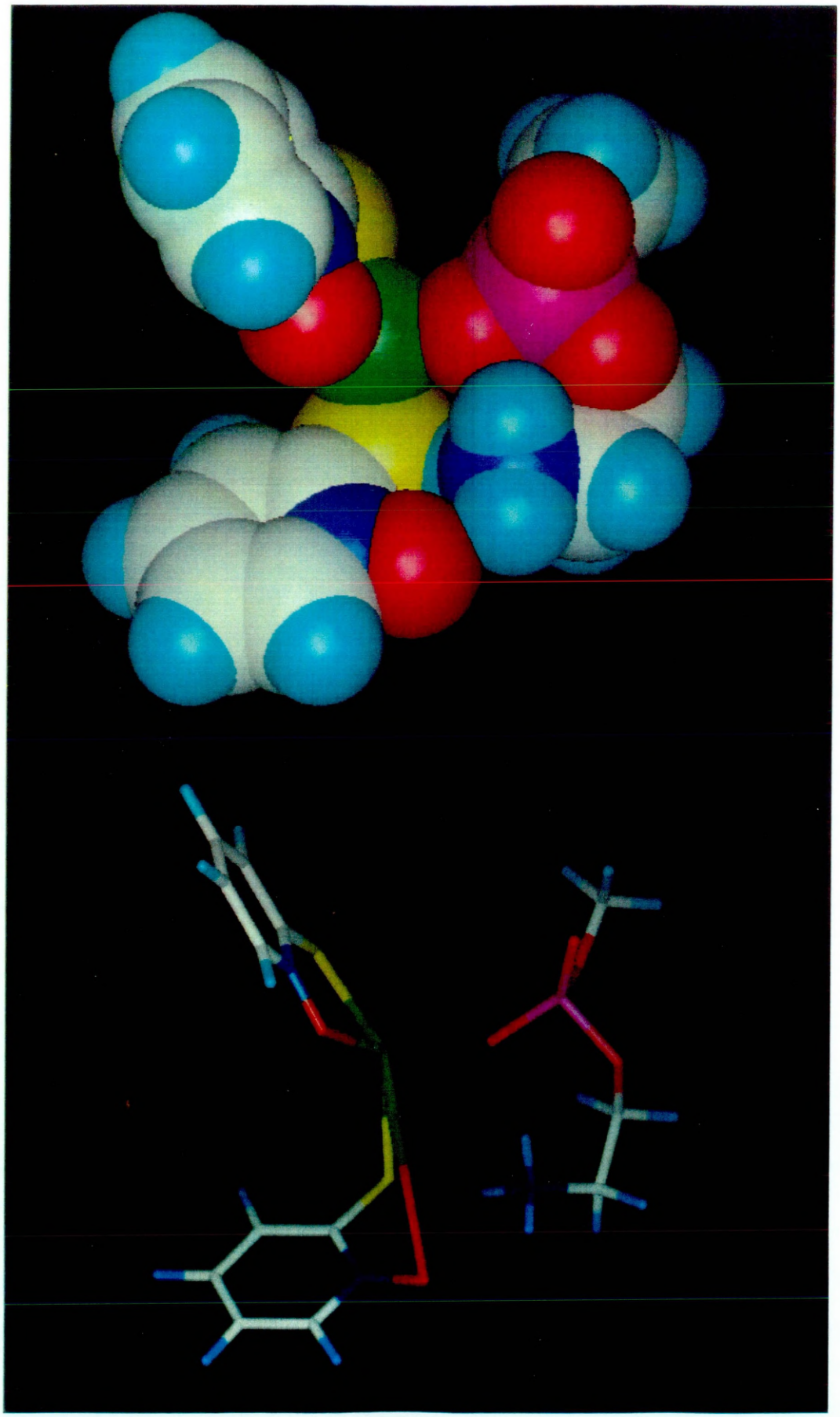

# THE EFFECT OF THE PYRITHIONE BIOCIDES UPON METABOLIC ACTIVITY

## THE EFFECT OF SUB-MIC LEVELS OF PYRITHIONE BIOCIDES UPON SUBSTRATE CATABOLISM OF VARIOUS SUBSTRATES BY *ESCHERICHIA COLI* NCIMB 10000 AND *PSEUDOMONAS AERUGINOSA* PAO1 NCIMB 10548

The rate of metabolism of a substrate by a bacterial population can be monitored by the rate of oxygen consumption by the bacterial cells concerned. Subsequently, the effect of a biocide on the rate of oxygen consumption by a bacterial cell, which is actively metabolising a specific substrate, can be used to identify the target metabolic pathways of an antimicrobial agent. For example, inhibition of the oxygen uptake of an amino acid by the test biocide may indicate that the catabolism of these amino acids serves as a target for the action of these antimicrobial agents. Similarly the inhibition of the metabolism of a carbohydrate would indicate carbohydrate metabolism as being the antimicrobial metabolic target. Such studies may also elucidate the intracellular or extracellular activity of a biocide. Inhibition of the metabolism of a substrate which is transported into the cell by active transport or group translocation may be indicative of membrane disruption by the test antimicrobial agent as well as inhibition of intracellular enzymic pathways.

In this study, the effects of the pyrithione biocides upon the rate of catabolism of six substrates (Table 11) were observed as a function of oxygen consumption using a Clark-type oxygen electrode and metabolic chamber (Rank Brothers, Cambridge, England) (Figure 43). The substrates used enabled observations to be made upon the effects of ZnPT and NaPT on the metabolism of four major metabolic groups, carbohydrate metabolism, protein synthesis, RNA synthesis and DNA synthesis. Glucose, acetate and pyruvate were used as substrates in order to observe the effects of ZnPT and NaPT upon specific catabolism in both *E. coli* and *P. aeruginosa*. Proline was used to investigate the effects of the pyrithiones upon amino acid catabolism. Thymidine and uracil were used to enable the observation of

the effects of the pyrithiones upon catabolism of nucleotides.

Comparisons of the levels of catabolic inhibition of substrates which enter the bacterial cell by diverse processes can be indicative of the physical site of action of the biocide. Disruption of the transmembrane proton motive force (PMF), which drives many of the membrane-bound transport processes, would be reflected in the inhibition of catabolism of substrates which are dependent upon the PMF for their carriage into the cytosol.

Glucose is transported into the cell *via* group translocation and the phosphotransferase system (PTS). This process actively carries glucose across the bacterial membrane whilst catalysing the first step in the breakdown of glucose with the utilisation of ATP (Postma 1987) (Equation 12, where Hk = hexokinase). Observed inhibition of glucose metabolism by the test biocide is indicative of membrane disruption without disturbance of the PMF. This inhibition of glucose metabolism would also suggest biocide inhibition of the intracellular carbohydrate metabolic pathways.

(12)

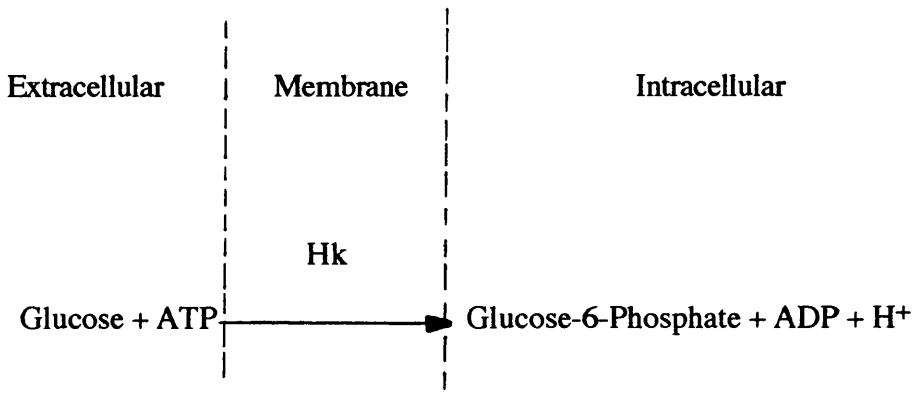


Pyruvate, proline, thymidine and uracil are all actively transported across the bacterial membrane by chemiosmotic coupling (Maloney 1987, Cronan *et al* 1987. Neuhard & Nygaard 1987). This process utilises a chemical gradient to drive the transport of the substrate into the cell with the consequent expenditure of ATP and is reliant upon the PMF (Maloney 1987, Cronan *et al* 1987. Neuhard & Nygaard 1987). Therefore, the inhibition of the rate of catabolism of these compounds would be indicative of PMF inhibition. Acetate, however, enters the bacterial cell *via* passive diffusion and does not require the expenditure of ATP to drive the process.

**Table 11:** Substrates used in the metabolic studies, the biochemical processes in which they are involved and their mode of transport into the bacterial cell.

| Substrate | Biochemical Process | Mode of Transport into the Bacterial Cell |
|---|---|---|
| Glucose | Carbohydrate metabolism | Group translocation (PTS) |
| Pyruvate | Carbohydrate metabolism | Active transport ($H^+$ ATPase) |
| Acetate | Carbohydrate metabolism | Passive diffusion |
| Proline | Protein synthesis | $H^+/Na^+$ Pump |
| Thymidine | DNA Synthesis | $H^+$ ATPase |
| Uracil | RNA Synthesis | $H^+$ ATPase |

Studies which observe the rate of metabolism in a whole cell system are dependent upon intracellular enzymes and the reactions which they catalyse as rate determining steps. Therefore, the utilisation of enzyme kinetic systems, such as Michaelis-Menten kinetics may be applied to whole cell metabolic rate determining systems. In this study, Michaelis-Menten substrate kinetics were applied so the rate of metabolism of the cells could be monitored. The Michaelis constant ($K_m$, Michaelis & Menten 1913) was replaced with the cell saturation constant ($K_S$) (Monod 1949). The $K_S$ is a concentration constant which is equal to half of the concentration at which the maximum rate of metabolism for a particular substrate occurs ($V_{max}$) (Michaelis & Menten 1913). Therefore, application of substrate at concentrations equal to or greater than twice the concentration at which the $K_S$ occurs ensured the saturation of the cellular pathways for that particular substrate.

$K_S$ values for the catabolism of the six substrates in *E. coli* and *P. aeruginosa* were determined by the following protocol. An aliquot (1ml) of washed cell suspension was

prepared from an overnight culture either *E. coli* or *P. aeruginosa* grown in 25ml of nutrient broth (Oxoid CM1) at 37°C in an orbital incubator (200osc/min) and resuspended in 0.067M phosphate buffer at an optical density of 1.36 at $E_{470nm}$. The aliquot was added to a previously calibrated Clark-type oxygen electrode at 37°C (Rank Brothers, Cambridge, England). The cells were allowed to equilibrate to 37°C for 1 minute. The metabolic chamber was closed and the endogenous cellular oxygen consumption was observed from a recorder trace (Servogor 120, BBC Goerz Metrawatt, Austria) of oxygen tension (Fig 58a). Aliquots (10$\mu$l) of substrate were then injected into the metabolic chamber and the rates of substrate catabolism were observed as a decrease in the oxygen tension within the metabolic chamber. The $K_s$ values (Table 12) were calculated from double reciprocal plots (Lineweaver & Burke 1934) of substrate concentration and rates of oxygen consumption.

**Table 12:** $K_s$ values for the rate of catabolism of six substrates by *E. coli* and *P. aeruginosa.*

| Substrate | Ks Value | |
|---|---|---|
| | *P. aeruginosa* | *E. coli* |
| Glucose | 0.75mM | 0.1923mM |
| Acetate | 0.164mM | 2.66mM |
| Pyruvate | 0.113mM | 3.33mM |
| Proline | 0.588mM | 45.45mM |
| Thymidine | 11.9$\mu$M | 1.25mM |
| Uracil | 0.0435$\mu$M | 0.238$\mu$M |

Observation of the effects of NaPT and ZnPT at sub-MIC levels upon the catabolism of the six substrates was carried out by following the same method for $K_s$ determination with the following changes. An aliquot of biocide (10$\mu$l), at sub-MIC levels, was added to the washed cell suspension and allowed to incubate for three minutes prior to monitoring the endogenous rate of oxygen consumption (Fig 58b). The specific concentration ranges of

**Figure 58:** (a) Recorder trace of background oxygen uptake by washed cells of *E. coli* prior to addition of glucose (0.38mM). (b) Recorder trace of oxygen consumption by washed cells of *E. coli* after incubation with NaPT ($70\mu g\ ml^{-1}$) and subsequent addition of glucose (0.38mM).

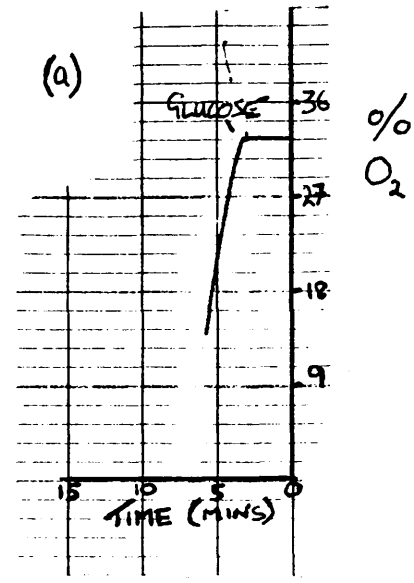
(a)
GLUCOSE
36
27
18
9
%
$O_2$
15
10
5
0
TIME (MINS)

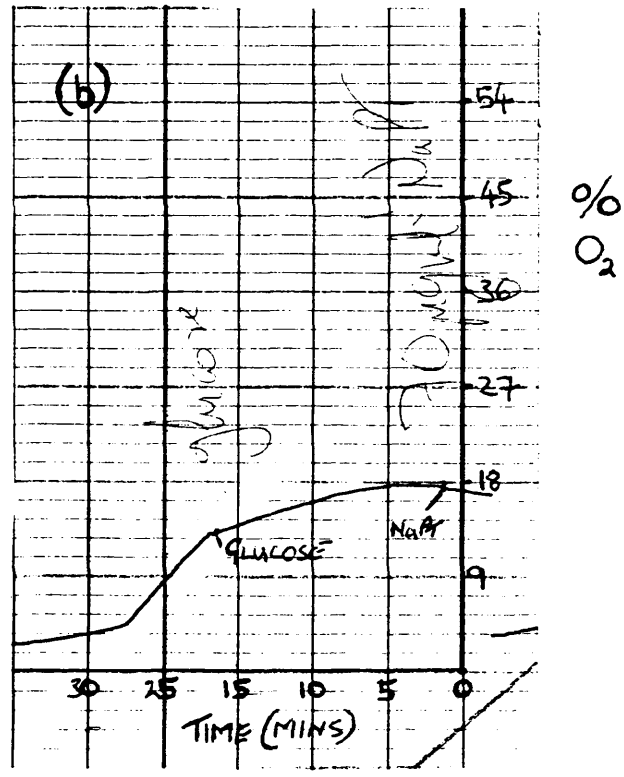
(b)
54
45
36
27
18
9
%
$O_2$
GLUCOSE
NaA
30
25
15
10
5
0
TIME (MINS)

biocide used against the test microorganisms were as follows; for *E. coli*, NaPT was added at concentrations in a range between 0 and 120$\mu$gml$^{-1}$ and ZnPT was added at concentrations from 0 to 5 $\mu$g ml$^{-1}$; for *P. aeruginosa*, NaPT was added at concentrations from 0 to 100 $\mu$g ml$^{-1}$ and ZnPT was added at concentrations from 0 to 13 $\mu$g ml$^{-1}$. The chamber was then closed and the endogenous rate of oxygen consumption was recorded for a further minute. Substrate was added at concentrations equivalent to twice $K_s$ (this ensured substrate saturation of the cellular catabolic processes). The rate of substrate catabolism was monitored *via* the decrease in oxygen tension within the metabolic chamber. The rates of reaction were calculated from the gradients of the oxygen depletion traces obtained from these experiments. All gradients were then calculated as a percentage of the control gradient (0 $\mu$g ml-1 biocide) and they were then plotted against biocide concentration (Figures 59 to 62). $ID_{25\%}$ and $ID_{50\%}$ values (dose of biocide at which 25% and 50% inhibition of a pathway occurs) were determined as the intercept of a line indicating an inhibitive trend in the initial stages of biocide exposure (Tables 13 & 14).

**Table 13:** $ID_{25\%}$ values from the effects of NaPT and ZnPT on the catabolism of various substrates by *E. coli* and *P. aeruginosa*.

| | $ID_{25\%}$ Values ($\mu$g ml$^{-1}$) | | | |
|---|---|---|---|---|
| | *E. coli* | | *P. aeruginosa* | |
| Substrate | NaPT | ZnPT | NaPT | ZnPT |
| Glucose | * | 3.6 | 55.5 | * |
| Acetate | 24.0 | 3.2 | 22.0 | 8.75 |
| Pyruvate | 6.5 | 4.5 | * | 13.0 |
| Proline | 13.5 | 0.95 | 8.0 | * |
| Thymidine | 6.5 | 0.55 | 68.0 | * |
| Uracil | 14.5 | * | * | * |

*= No obtainable value.

**Table 14:** $ID_{50\%}$ values from the effects of NaPT and ZnPT on the catabolism of various substrates by *E. coli* and *P. aeruginosa*.

| | $ID_{50\%}$ Values ($\mu g\ ml^{-1}$) | | | |
|---|---|---|---|---|
| | *E. coli* | | *P. aeruginosa* | |
| Substrate | NaPT | ZnPT | NaPT | ZnPT |
| Glucose | * | 4.125 | * | * |
| Acetate | * | * | * | * |
| Pyruvate | 53.5 | * | * | * |
| Proline | * | * | 18.5 | * |
| Thymidine | 15.0 | * | * | * |
| Uracil | * | * | * | * |

*= No obtainable value.

**Figure 59:** The effect of sub-MIC levels of NaPT upon substrate catabolism in *E. coli*. ID25% values are determined as the concentration of biocide which exhibits 75% of control rate of metabolism. ( ○ ), glucose; ( △ ), acetate; ( □ ), pyruvate; ( ● ), proline; ( ▲ ), thymidine; ( ■ ), uracil. Error bars are calculated from and plotted as the Standard Error of the data set.

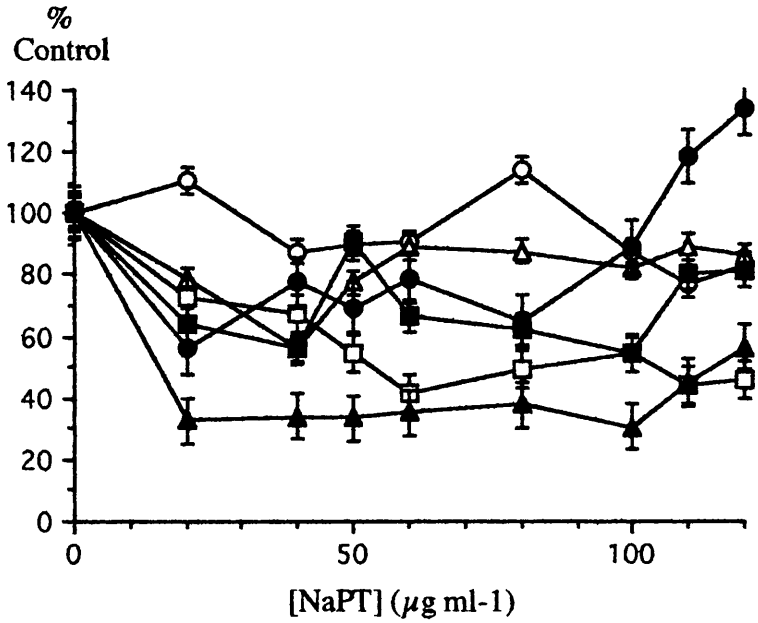
%
Control
140
120
100
80
60
40
20
0
0
50
100
[NaPT] (μg ml-1)

**Figure 60:** The effect of sub-MIC levels of ZnPT upon substrate catabolism in *E. coli*. ID25% values are determined as the concentration of biocide which exhibits 75% of control rate of metabolism. ( ○ ), glucose; ( △ ), acetate; ( □ ), pyruvate; ( ● ), proline; ( ▲ ), thymidine; ( ■ ), uracil. Error bars are calculated from and plotted as the Standard Error of the data set.

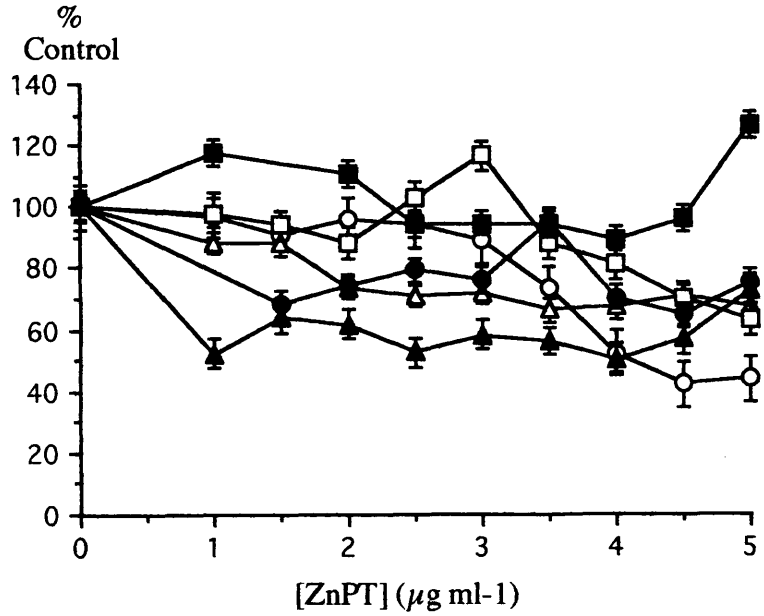
%
Control
140
120
100
80
60
40
20
0
0
1
2
3
4
5
[ZnPT] (μg ml-1)

**Figure 61:** The effect of sub-MIC levels of NaPT upon substrate catabolism in *P. aeruginosa* ID25% values are determined as the concentration of biocide which exhibits 75% of control rate of metabolism. ( ○ ), glucose; ( △ ), acetate; ( □ ), pyruvate; ( ● ), proline; ( ▲ ), thymidine; ( ■ ), uracil. Error bars are calculated from and plotted as the Standard Error of the data set.

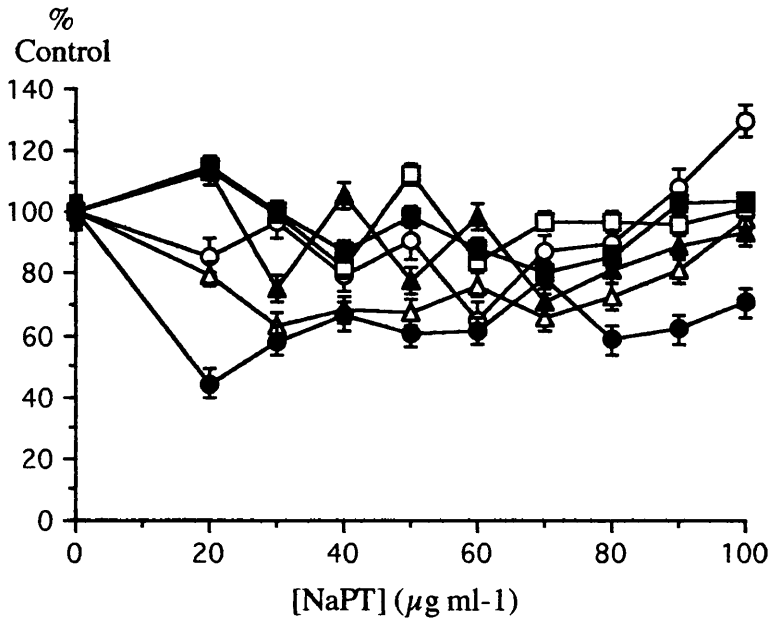
%
Control
140
120
100
80
60
40
20
0
0
20
40
60
80
100
[NaPT] (μg ml-1)

**Figure 62:** The effect of sub-MIC levels of ZnPT upon substrate catabolism in *P. aeruginosa* ID25% values are determined as the concentration of biocide which exhibits 75% of control rate of metabolism. ( ○ ), glucose; ( △ ), acetate; ( □ ), pyruvate; ( ● ), proline; ( ▲ ), thymidine; ( ■ ), uracil. Error bars are calculated from and plotted as the Standard Error of the data set.

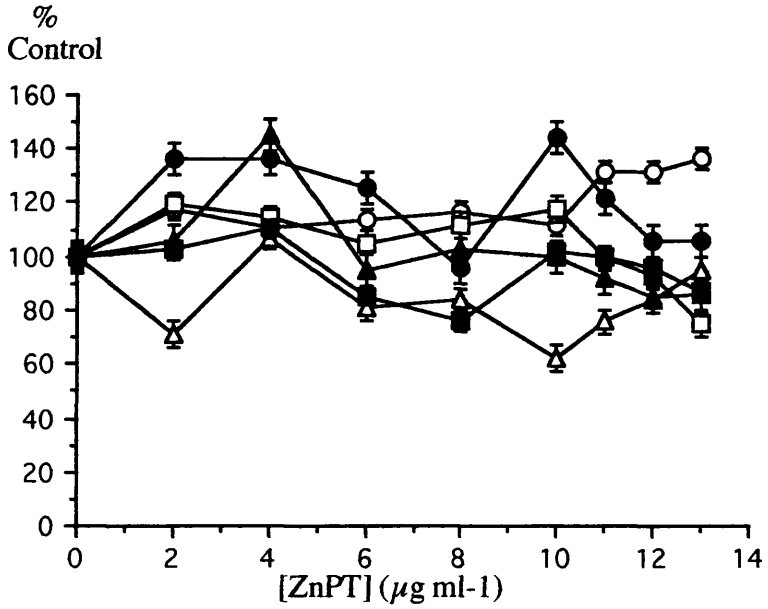
%
Control
160
140
120
100
80
60
40
20
0
0
2
4
6
8
10
12
14
[ZnPT] (μg ml-1)

In studies which investigate the effects of a biocide upon cellular catabolic processes, $ID_{50\%}$ values are normally determined and calculated as a comparison of the effects of a biocide upon the catabolism of more than one substrate. The range of $ID_{50\%}$ values obtainable from the data presented in figures 59 to 62 (Table 14) indicates a poor range of metabolic activity by both NaPT and ZnPT. Therefore, $ID_{25\%}$ values were determined in order to give a comparison of results (Table 13). However, a full range of $ID_{25\%}$ values was still not obtainable for each of the six substrates against both NaPT and ZnPT for the test organisms. This indicates that both NaPT and ZnPT are poor inhibitors of cellular catabolic processes and may also be suggestive of poor inhibition of membrane integrity. These results suggest that the pyrithiones do not target the metabolism of one particular group of substrates or one significant intracellular metabolic process (Table 11). The poor inhibition of metabolic processes and the observation of L-shaped curves of substrate inhibition (Figs 59 to 62) are indicative of some form of saturation effect regarding the activity of NaPT and ZnPT towards intracellular metabolism. This is also exhibited in the $ID_{50\%}$ values and $ID_{25\%}$ values (Tables 13 & 14) indicating that none of the substrates were inhibited by either NaPT or ZnPT to a maximal level which is equal to 0% of the control rate of reaction (100% inhibition).

Table 13 indicates that NaPT possesses a wider range of anti-metabolic activity than ZnPT. This is reflected in the fact that NaPT exhibits nine $ID_{25\%}$ values against the two organisms; eg, in *E. coli* NaPT exhibits $ID_{25\%}$ values against the metabolism of acetate, pyruvate, proline, thymidine and uracil and in *P. aeruginosa* the same biocide exhibits $ID_{25\%}$ values against all of the substrates used except pyruvate and uracil. This is in comparison with seven values for ZnPT against both organisms; eg, ZnPT exhibits $ID_{25\%}$ values against all of the substrates in *E. coli* except uracil and only two $ID_{25\%}$ values against *P. aeruginosa* for acetate and pyruvate. Although a wider metabolic effect is observed with NaPT, the biocide concentrations at which $ID_{25\%}$ values occur for ZnPT are much lower than those for NaPT and exhibit increased inhibitive capacity for ZnPT as a function of concentration. For example, the $ID_{25\%}$ value for NaPT against thymidine metabolism in *E. coli* is 6.5 $\mu g\ ml^{-1}$ which is 1181.8% greater than the $ID_{25\%}$ value observed for ZnPT against the same

substrate. These differences reflect the increased antimicrobial activity of ZnPT over NaPT, which has been observed in previous experiments.

The patterns observed in the data exhibited in figures 59 to 62 may be indicative of the inhibition of membrane bound transport processes such as active transport and group translocation. Disruption of these processes would result in the breakdown of the proton motive force (PMF) and the subsequent inhibition of ATP synthesis. The inhibition of ATP synthesis would disrupt the transport of glucose by membrane bound hexokinase, a process which is ATP dependent. PMF inhibition would also inhibit transport of $H^+/Na^+$ ATPase dependent substrates. However, membrane disruption by the presence of the pyrithiones at concentrations approaching the MIC may allow passive diffusion of substrates, which were previously dependent on the PMF for their transportation, into the cytosol (Table 11). This would still enable the continuation of the catabolism of pyruvate, proline, thymidine and uracil by the action of intracellular enzymes and would explain the stimulation of metabolism of these substrates at biocide concentrations which are approaching MIC.

Although inhibition of substrate catabolism is observed by both biocides against the catabolism of *E. coli* and *P. aeruginosa*, none of the substrates used in the experiment indicate 100% inhibition by the pyrithiones. This is indicative of no direct metabolic action by either NaPT or ZnPT, however, thymidine was effectively inhibited to values of about 30% of the control for NaPT and ZnPT against *E. coli*. This together with the observed stimulation of glucose, proline, thymidine and uracil at concentrations of biocide approaching the MICs (Figs 59 to 62), would suggest that observed catabolic inhibition is brought about as a result of membrane activity. Membrane activity of the biocide would bring about a direct effect upon the PMF, which would be reflected by decreasing intracellular ATP concentrations.

## THE EFFECT OF NaPT AND ZnPT UPON THE INTRACELLULAR ATP LEVELS OF *ESCHERICHIA COLI* NCIMB 10000 AND *PSEUDOMONAS AERUGINOSA* PAO1 NCIMB 10548

The production of ATP *via* oxidative phosphorylation is driven by the proton motive force (PMF) (Harold 1972). The PMF is associated with the bacterial membrane and is driven by a proton gradient upon which membrane bound ATPases are dependent (Harold 1972). Potassium ions are brought into the bacterial cell, due to the action of the PMF and the F1/F0 ATPases, with the exchange of protons or sodium ions to the extracellular environment during ATP production (Harold *et al* 1969, Harold 1972).

As a result of the cellular events related to the production of ATP, the effects of antimicrobial agents upon membrane bound processes may be monitored as a function of the intracellular levels of ATP or the intracellular accumulation of potassium ions. Studies with chlorhexidine have shown that the observation of intracellular potassium ion accumulation may be utilised as a way of elucidating disruption of the proton gradient and membrane bound ATPases by membrane active agents (Harold *et al* 1969). The effect of a biocide upon the activity of membrane-bound enzymes, both in their free state and as vesicle bound proteins, is another method by which the activity of a biocide upon membrane bound metabolic processes may be observed (Chopra *et al* 1987).

The measurement of intracellular ATP levels reflects the activity of the test biocide upon the bacterial membrane and the membrane bound processes which drive ATP production. In this study, the effect of the pyrithiones at sub-MIC levels upon intracellular ATP content was used to investigate their effect upon membrane processes related to membrane bound ATP metabolism in *E. coli* NCIMB 10000 and *P. aeruginosa* PAO1 NCIMB 10548.

Five sterile Ehrlenmeyer flasks containing aliquots (24.5ml) of sterile CDM were inoculated with 0.25ml of overnight bacterial culture which had been grown up in an orbital incubator (200 osc/min at 37°C). The time of inoculation was recorded and at 1, 2, 3, 4, 5 and 6 hours an aliquot of culture (200$\mu$l) was removed and assayed for ATP content using the Luciferin/luciferase methodology (p111). Prior to removal and assay of the second hour

sample, an aliquot (0.25ml) of biocide was added to the flasks to give final biocide concentrations equivalent to 0, 20%, 40%, 60% and 80% of MIC in 25ml. This was repeated for *E. coli* and *P. aeruginosa* using NaPT and ZnPT. Results were calculated as $10^{-12}$mol (pmol) ATP per ml of culture and as $10^{-18}$mol (amol) ATP per cell and were plotted as a function of intracellular ATP levels against time (Figures 63 to 70).

**Figure 63:** Effect of NaPT at various sub MIC concentrations upon ATP metabolism of *E. coli* NCIMB 10000 expressed as ATP content per ml of cells. ( ○ ), 0%MIC; ( △ ), 20%MIC; ( □ ), 40%MIC; ( ● ), 60%MIC; ( ▲ ), 80%MIC. Error bars are calculated from and plotted as the Standard Error of the data set.

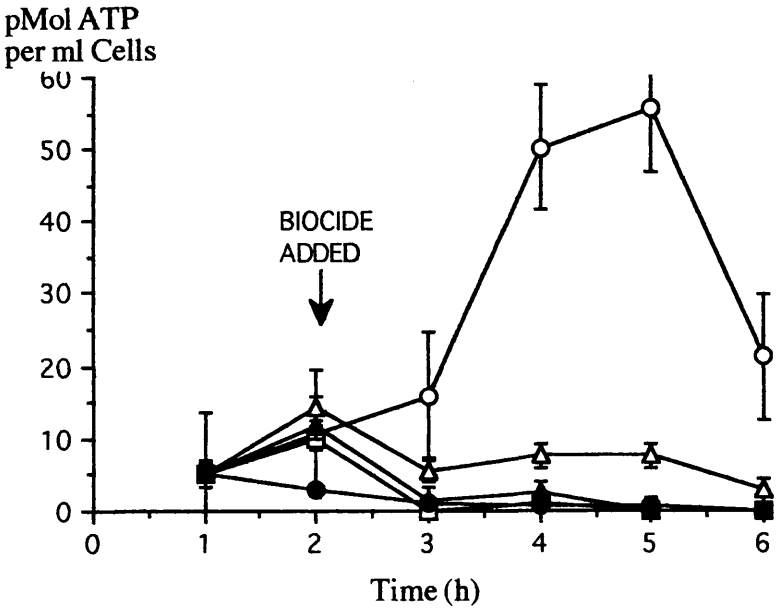
pMol ATP
per ml Cells
60
50
40
30
20
10
0
BIOCIDE
ADDED
0
1
2
3
4
5
6
Time (h)

**Figure 64:** Effect of ZnPT at various sub MIC concentrations upon ATP metabolism of *E. coli* NCIMB 10000 expressed as ATP content per ml of cells. ( ○ ), 0%MIC; ( △ ), 20%MIC; ( □ ), 40%MIC; ( ● ), 60%MIC; ( ▲ ), 80%MIC. Error bars are calculated from and plotted as the Standard Error of the data set.

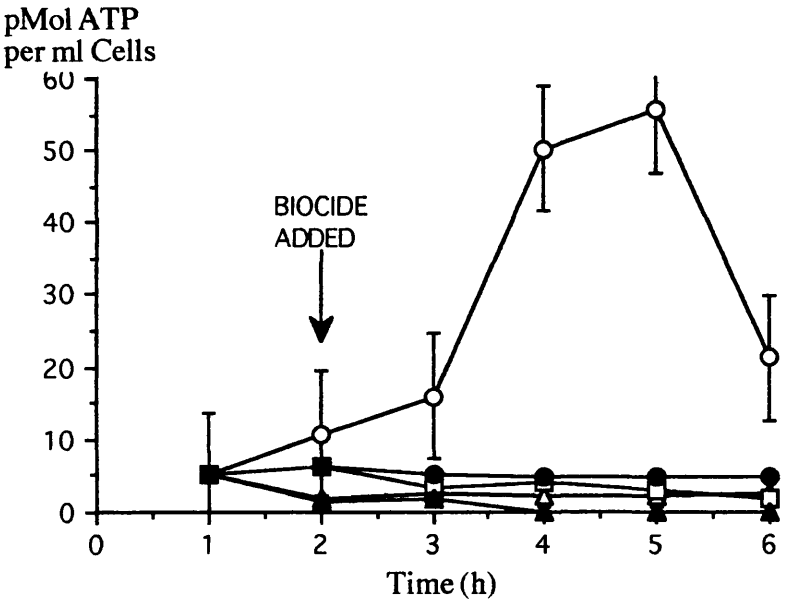
pMol ATP
per ml Cells
60
50
40
30
20
10
0
BIOCIDE
ADDED
0
1
2
3
4
5
6
Time (h)

**Figure 65:** Effect of NaPT at various sub MIC concentrations upon ATP metabolism of *P.aeruginosa* PAO1 NCIMB 10548 expressed as ATP content per ml of cells. ( ○ ), 0%MIC; ( △ ), 20%MIC; ( □ ), 40%MIC; ( ● ), 60%MIC; ( ▲), 80%MIC. Error bars are calculated from and plotted as the Standard Error of the data set.

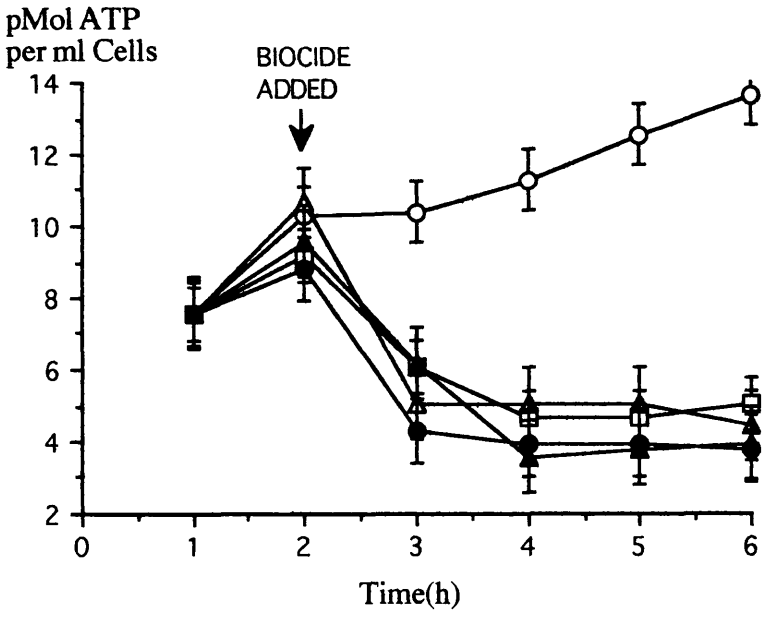
pMol ATP
per ml Cells
BIOCIDE
ADDED
14
12
10
8
6
4
2
0
1
2
3
4
5
6
Time(h)

**Figure 66:** Effect of ZnPT at various sub MIC concentrations upon ATP metabolism of *P. aeruginosa* PAO1 NCIMB 10548 expressed as ATP content per ml of cells. ( ○ ), 0%MIC; ( △ ), 20%MIC; ( □ ), 40%MIC; ( ● ), 60%MIC; ( ▲ ), 80%MIC. Error bars are calculated from and plotted as the Standard Error of the data set.

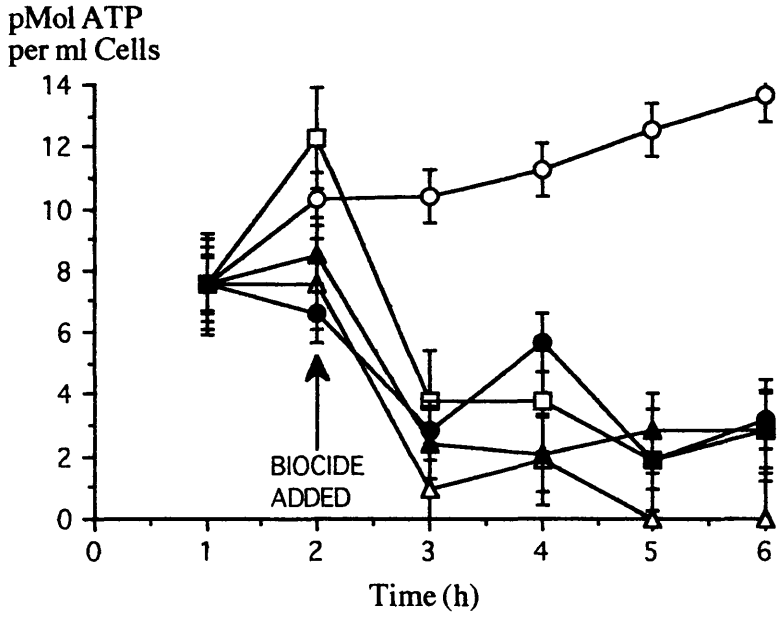
pMol ATP
per ml Cells
14
12
10
8
6
4
2
0
0
1
2
3
4
5
6
BIOCIDE
ADDED
Time (h)

**Figure 67:** Effect of NaPT at various sub MIC concentrations upon ATP metabolism of *E. coli* NCIMB 10000 expressed as ATP content per cell. ( ○ ), 0%MIC; ( △ ), 20%MIC; ( □ ), 40%MIC; ( ● ), 60%MIC; ( ▲ ), 80%MIC. Error bars are calculated from and plotted as the Standard Error of the data set.

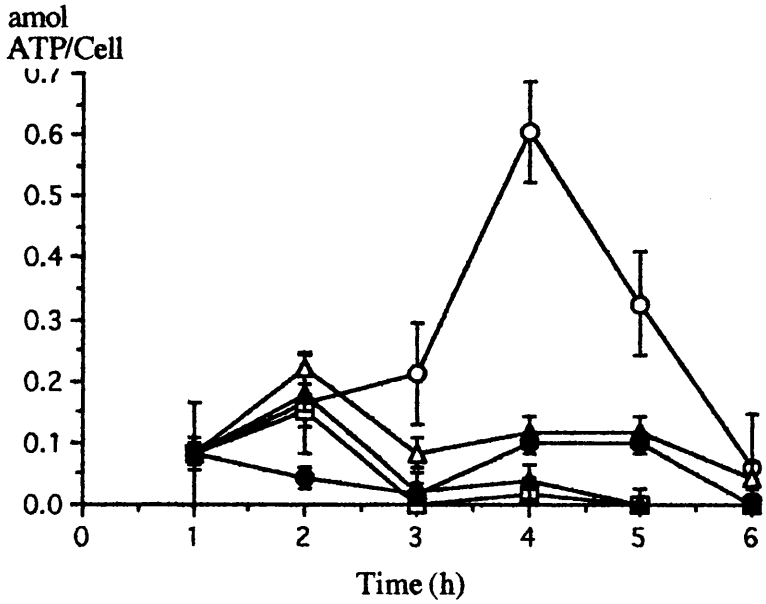
amol
ATP/Cell
0.7
0.6
0.5
0.4
0.3
0.2
0.1
0.0
0
1
2
3
4
5
6
Time (h)

**Figure 68:** Effect of ZnPT at various sub MIC concentrations upon ATP metabolism of *E. coli* NCIMB 10000 expressed as ATP content per cell. ( ○ ), 0%MIC; ( △ ), 20%MIC; ( □ ), 40%MIC; ( ● ), 60%MIC; ( ▲ ), 80%MIC. Error bars are calculated from and plotted as the Standard Error of the data set.

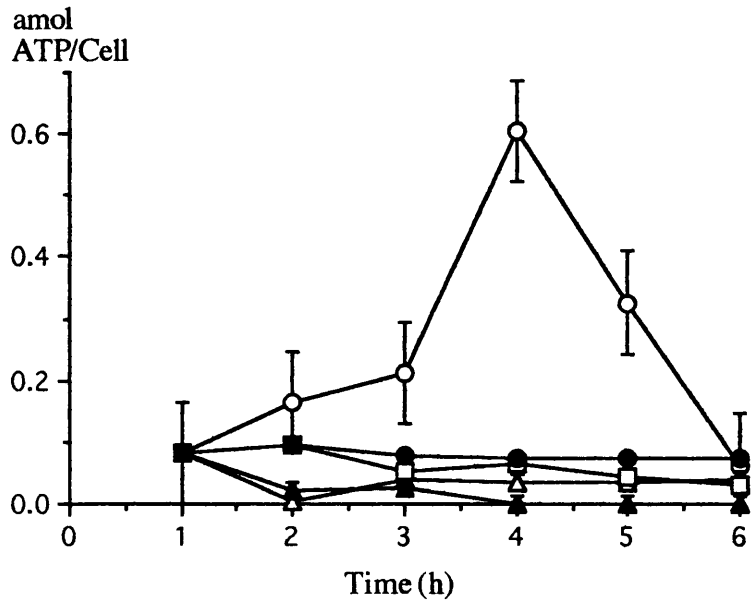
amol
ATP/Cell
0.6
0.4
0.2
0.0
0
1
2
3
4
5
6
Time (h)

**Figure 69:** Effect of NaPT at various sub MIC concentrations upon ATP metabolism of *P. aeruginosa* PAO1 NCIMB 10548 expressed as ATP content per cell. ( ○ ), 0%MIC; ( △ ), 20%MIC; ( □ ), 40%MIC; ( ● ), 60%MIC; ( ▲ ), 80%MIC. Error bars are calculated from and plotted as the Standard Error of the data set.

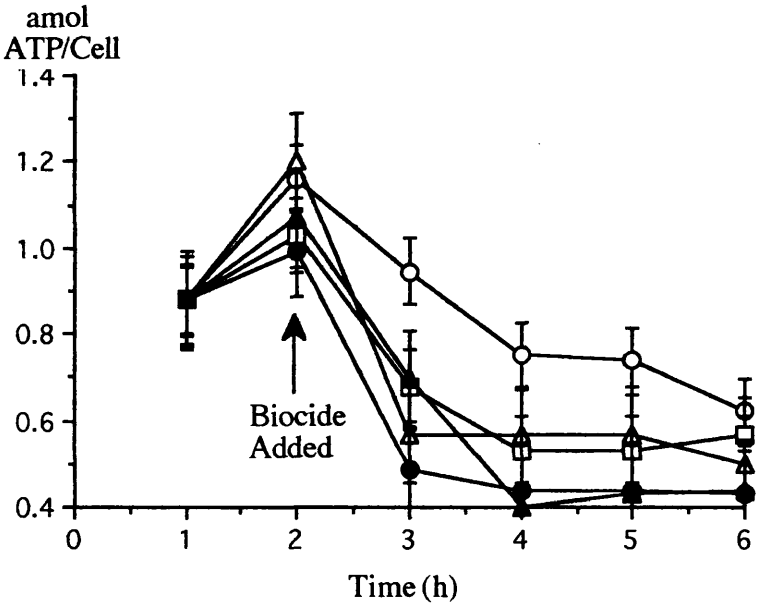
amol
ATP/Cell
1.4
1.2
1.0
0.8
0.6
0.4
0
1
2
3
4
5
6
Biocide
Added
Time (h)

**Figure 70:** Effect of ZnPT at various sub MIC concentrations upon ATP metabolism of *P. aeruginosa* PAO1 NCIMB 10548 expressed as ATP content per cell. ( ○ ), 0%MIC; ( △ ), 20%MIC; ( □ ), 40%MIC; ( ● ), 60%MIC; ( ▲ ), 80%MIC. Error bars are calculated from and plotted as the Standard Error of the data set.

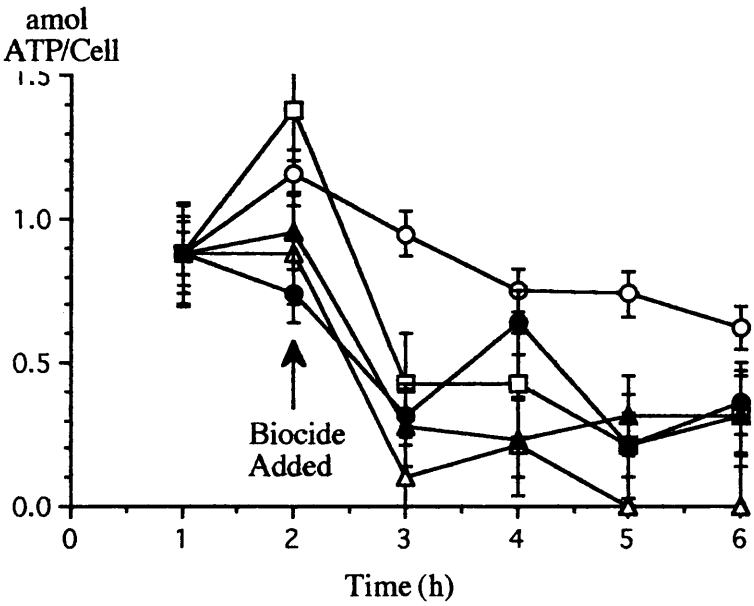
amol
ATP/Cell
1.5
1.0
0.5
0.0
0
1
2
3
4
5
6
Biocide
Added
Time (h)

Figures 63 and 64 exhibit the effects of NaPT and ZnPT, respectively, upon the intracellular ATP levels in *E. coli*. Figures 63 and 64 exhibit a dramatic decrease in the ATP content of *E. coli* (dropping from $1x10^{-11}$mol ATP/ml cells to $5x10^{-12}$mol ATP/ml cells) after the addition of biocide at all four sub-MIC levels of biocide (20, 40, 60 and 80% MIC). This difference between the control group and biocide exposed cells is observable even at the lowest concentration of biocide (20% MIC). However, a difference between the activity of NaPT (Fig 63) and ZnPT (Fig 64) upon the intracellular ATP content of *E. coli* is observed. The effect of NaPT upon ATP content in *E. coli* is not observable until one hour after the addition of the biocide, even at 80% MIC. With ZnPT, the effect of biocide addition is immediately exhibited with a decrease in intracellular ATP levels from $1x10^{-11}$mol/ml cells for the control cultures to $1.5x10^{-12}$mol/ml cells. If the ATP concentrations are expressed as the amount of ATP per cell (Figures 65 & 68), then the same general pattern is observed. From these observations, the addition of ZnPT and NaPT, at sub-MIC levels and at comparative concentrations as a percentage of MIC, suggest that the exposure of *E. coli* to these biocides induces stasis of intracellular ATP levels in the test microorganisms.

Unlike the data for *E. coli* against ZnPT, a direct effect upon the intracellular levels of ATP was not observed upon the addition of this biocide to cells of *P. aeruginosa* (figs 65, 66, 69 & 70). Both biocides exhibited the same effect upon ATP content of *P. aeruginosa*, that is, a decrease in cellular levels of ATP one hour after biocide addition was observed followed by stasis in intracellular ATP/ml of culture (Figs 65 & 66). Regardless of the concentration of biocide used, stasis of intracellular ATP levels was always exhibited. This intracellular ATP content in cells of *P. aeruginosa* exposed to all biocide concentrations was shown to become static at between $2x10^{-12}$ and $5x10^{-12}$mol ATP/ml cells after one hour of biocide addition (Figures 65 & 66). The levels of ATP per cell were not congruent with the amount of ATP per ml of culture. Figures 69 and 70 exhibit the intracellular ATP levels of *P. aeruginosa* to maintain a decrease in ATP expressed as ATP concentration per cell. The decrease in ATP levels was shown to occur even with the control cultures and exhibits a difference in the requirement for ATP by the test microorganisms. *E. coli* is a facultative anaerobe and produces ATP by both fermentative and anaerobic metabolism. *P. aeruginosa* is much slower growing than *E. coli* and therefore, it's immediate requirement for ATP is somewhat

lower than that of *E. coli*. These differences between the organisms may explain the levels of ATP/cell for control figures (Figs 67, 68, 69 &70).

The results of this experiment (Figures 63 to 70) exhibit no significant differences between the effects of NaPT or ZnPT against either *P. aeruginosa* or *E. coli*. However, the pyrithiones are shown here to have a significant effect upon the intracellular levels of ATP, both when ATP concentration is expressed as a function of culture volume and as ATP concentration per cell. The results show the pyrithiones possess an effect upon intracellular ATP levels of exposed cells which decreases intracellular levels of ATP. The observed reduction in ATP does not automatically indicate that NaPT or ZnPT target either substrate-level or oxidative phosphorylation as primary sites of action. However, the reduction in ATP does suggest that the pyrithiones effect and reduce intracellular levels and then maintain these low concentrations. The effects of the pyrithiones upon ATP metabolism may suggest that NaPT and ZnPT are acting at the level of the bacterial membrane and subsequently damage membrane bound ATP metabolism due to disruption of bacterial membrane integrity. Such damage to the membrane would explain the results from the effects of the pyrithiones upon metabolism and may also indicate the effects of the pyrithiones on intracellular ATP content. It is therefore necessary to further investigate the effects of the pyrithiones upon the membrane and to observe if they induce direct damage to the Gram negative bacterial cell envelope.

# DIRECT MEMBRANE DAMAGE TO THE ENVELOPES OF GRAM-NEGATIVE BACTERIA BY NaPT AND ZnPT

There are several methods by which biocide induced damage to the bacterial cell membranes may be monitored. The most favoured method is probably the observation of leakage of intracellular material from biocide exposed cells (Denyer & Hugo 1991b). Upon exposure of a bacterial cell to a membrane active agent, there is a specific order in which the intracellular material leaks from the damaged cell (Salton 1968). Initially, there is an efflux of potassium ions from damaged cells into the bathing solution. This is followed by the leakage of intracellular material which absorbs light at 260nm (mainly purines and pyrimidines), small phosphate containing compounds and small sugars (Rye & Wiseman 1964, Salton 1968, Lambert & Hammond 1973, Denyer & Hugo 1991b). After the appearance of these smaller biochemicals in the bathing solution, the distribution of molecular size and the order of leakage from the cells becomes less defined and the appearance of proteins, ribosomes, RNA and small strands of DNA occurs (Denyer & Hugo 1991b). The order by which the compounds leave the cell has been elucidated using known membrane active agents such as PHMB, chlorhexidine, miconazole and various amines (diamines and aliphatic monoamines) (Harold *et al* 1969, Wiseman 1964, Broxton *et al* 1983a, Beggs 1992, Bernheim 1976).

Despite the known effects of membrane active agents upon bacterial cells and membrane bound metabolism, it has been argued that the killing effect of biocides is not a primary effect of membrane action (Rye & Wiseman 1964, Beggs 1992). Such considerations are due to the differences in concentrations at which membrane active agents (ie, PHMB and chlorhexidine) exhibit membrane damage on exposed cells and the concentrations at which they cause cell death. The concentrations at which such agents induce membrane damage have been shown to be much lower than those concentrations required to bring about bacterial cell death (Beggs 1992). However, it has been shown with the PHMB membrane active agents that the degree of membrane damage is related to cell death and that cell death does not occur as a secondary effect of membrane damage (Broxton *et al* 1983a, 1983b).

In this study, the leakage of two intracellular components (potassium ions and material which absorbs light at $E_{260nm}$) were monitored in order to determine whether or not NaPT and ZnPT were causing direct membrane damage to cells of *E. coli* and *P. aeruginosa.* Transmission electron microscopy studies were also carried out in order to visualise the effect of NaPT upon cells of *P. aeruginosa* exposed to MIC levels of the biocide.

## Leakage of Intracellular Material from *E. coli* NCIMB 10000 and *P. aeruginosa* PAO1 NCIMB 10548 Exposed to NaPT and ZnPT

### Observation of Leakage of Potassium Ions

An aliquot of cells (48ml) grown overnight in an orbital incubator (37°C at 200 osc/min) in nutrient broth (Oxoid CM1) was washed twice with tris-HCl buffer (pH7.0, 0.2M) by centrifugation (3000 rpm for 10 minutes, IEC Centra-4R Centrifuge, International Equipment, Dunstable). The cells were resuspended in a clean 100ml beaker to a volume of 48ml with trisHCl buffer (pH7.0, 0.2M). The washed cell suspension was placed on a magnetic stirrer and a pre-calibrated potassium ion sensitive electrode (Qualiprobe Potassium Ion Selective Electrode (QSE 314), EDT Instruments, Dover, UK) and it's reference electrode (E8092 Double Junction Reference Electrode, EDT Instruments, Dover, UK) connected to a Whatman 220 pH/mV meter (Whatman, Maidstone, Kent), were placed in the suspension. The background potassium ion content of the suspension was monitored for 5 minutes. An aliquot (2ml) of a 3.2 mg $ml^{-1}$ solution of biocide was added to the suspension to yield a final biocide concentration of 128 $\mu$g $ml^{-1}$ and the fluctuation in potassium ion content was recorded in mV at times 0, 20, 40, 60, 90 seconds, 2, 3, 4, 5,10, 15 and 20 minutes. This procedure was carried out for both *E. coli* and *P. aeruginosa* against NaPT and ZnPT. Reference biocides, cetrimide, fentichlor and dichlorophen, which have known membrane activity (Chapman 1987, Hugo & Bloomfield 1971, Paulus 1993), the thiol-interactive agent benzisothiazolone (BIT) (Collier *et al* 1991) and a non antimicrobial potassium chelating agent, 18-crown-6-ether (Gokel & Durst 1976), were used as controls. The readings in mV obtained from the experiments were converted to moles of potassium ions using a previously constructed calibration curve (Figure 36). The concentration of

potassium ions ($Log_{10}$ moles) present in the cell suspension bathing solution were then plotted against time (Figures 71 & 72).

**Observation of Leakage of Material which Absorbs Light at 260nm**

An aliquot (25ml) of cells grown overnight in an orbital incubator (37°C at 200 osc/min) in nutrient broth (Oxoid CM1) were washed twice by centrifugation and resuspended in tris-HCl buffer (pH7.0, 0.2M) to a volume of 23ml. An aliquot (2ml) of a 3.2 mg $ml^{-1}$ biocide solution was added to the suspension to yield a final biocide concentration of 128 $\mu$g $ml^{-1}$. An aliquot (2ml) of biocide exposed cell suspension were removed and centrifuged (13000rpm, 1min, Sanyo MSE Microcentaur, Sanyo UK). Changes in $E_{260nm}$ were then recorded at 0, 5, 10, 15 and 20 minutes after biocide addition. This was carried out using a spectrophotometer (Cecil Series 2 UV/vis spectrophotometer, Cecil Instruments, Cambridge) which had been previously blanked with 128 $\mu$g $ml^{-1}$ test biocide in tris-HCl buffer. This procedure was carried out for both *E. coli* and *P. aeruginosa* against NaPT and ZnPT. Reference biocides, cetrimide, fentichlor and dichlorophen, which have known membrane activity, the thiol interactive agent benzisothiazolone (BIT) and a non antimicrobial potassium chelating agent, 18-crown-6-ether, were used as controls. Fluctuations in $E_{260nm}$ were plotted against time for both organisms against the various antimicrobial agents (Figures 73 & 74).

**Figure 71:** Potassium ion leakage from *E. coli* NCIMB 10000 exposed to 128 $\mu$g ml$^{-1}$ of various biocides. ( ○ ), Cetrimide; ( △ ), NaPT; ( □ ), Dichlorophen; ( ● ), Fentichlor; ( ▲ ), BIT; ( ■ ), ZnPT; ( + ), 18-crown-6-ether. Error bars are calculated from and plotted as the Standard Error of the data set.

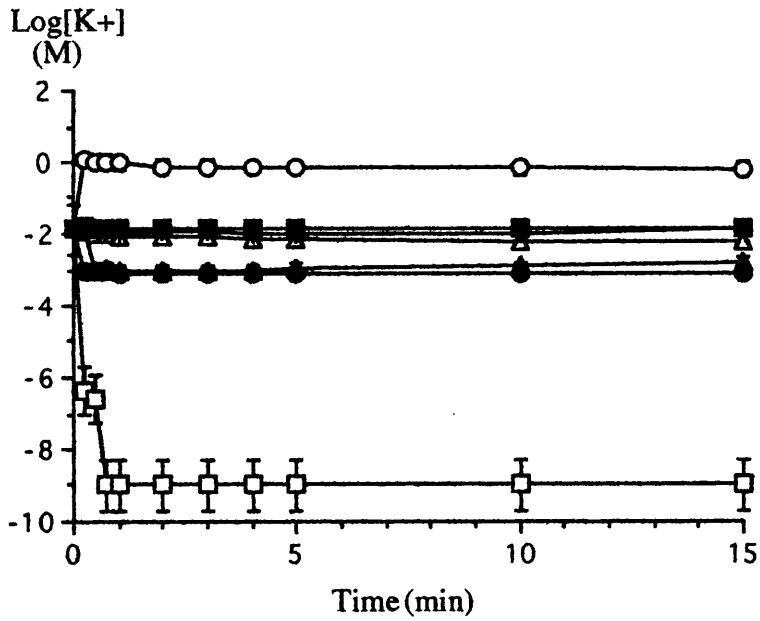
Log[K+]
(M)
2
0
-2
-4
-6
-8
-10
0
5
10
15
Time (min)

**Figure 72:** Potassium ion leakage from *P. aeruginosa* PAO1 NCIMB 10548 exposed to 128 $\mu$g ml$^{-1}$ of various biocides.

(○), Cetrimide; (△), NaPT; (□), Dichlorophen; (●), Fentichlor; (▲), BIT; (■), ZnPT; (+), 18-crown-6-ether. Error bars are calculated from and plotted as the Standard Error of the data set.

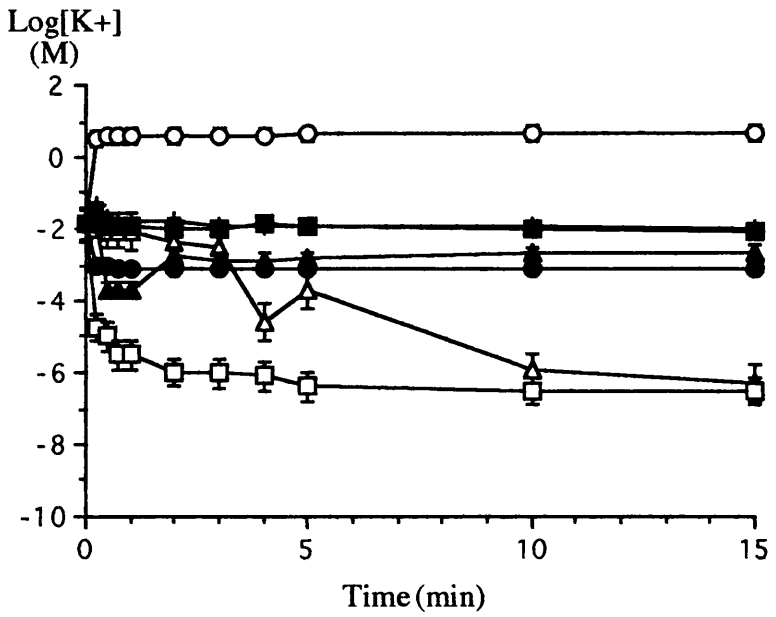
Log[K+]
(M)
2
0
-2
-4
-6
-8
-10
0
5
10
15
Time (min)

**Figure 73:** Leakage of $E_{260nm}$ absorbing material from *E. coli* NCIMB 10000 exposed to 128 $\mu$g ml$^{-1}$ of various biocides.

( ○ ), Cetrimide; ( △ ), NaPT; ( □ ), Dichlorophen; ( ● ), Fentichlor; ( ▲ ), BIT; ( ■ ), ZnPT. Error bars are calculated from and plotted as the Standard Error of the data set.

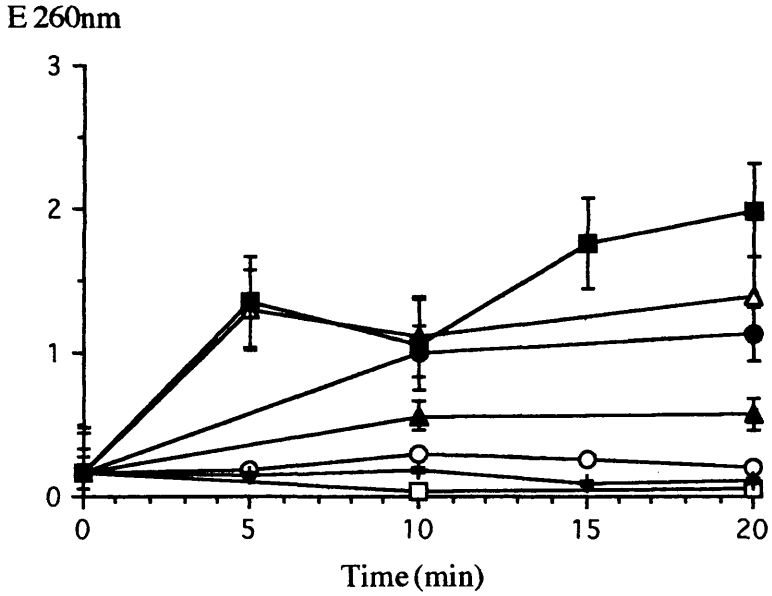
E 260nm
3
2
1
0
0
5
10
15
20
Time (min)

**Figure 74:** Leakage of $E_{260nm}$ absorbing material from *P. aeruginosa* PAO1 NCIMB 10548 exposed to 128 $\mu$g $ml^{-1}$ of various biocides. ( ○ ), Cetrimide; ( △ ), NaPT; ( □ ), Dichlorophen; ( ● ), Fentichlor; ( ▲ ),BIT; ( ■ ), ZnPT. Error bars are calculated from and plotted as the Standard Error of the data set.

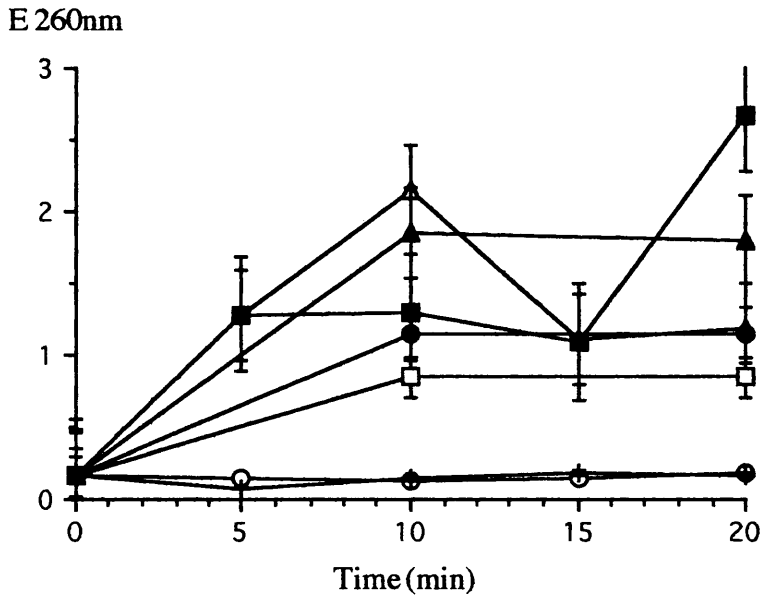
E 260nm
3
2
1
0
0
5
10
15
20
Time (min)

Figures 71 and 72 represent the effects of the various biocides upon the membranes of *E.coli* (Fig 71) and *P. aeruginosa* (Fig 72) as indicated by potassium ion leakage. These figures indicate that cetrimide has observable and marked leakage effects upon both organisms and that the onset of this effect is rapid. The initial potassium ion concentration of the bathing solution for both micro-organisms in all experiments was $1.1x10^{-4}M$. The maximal rate of Cetrimide-induced leakage was achieved within 1 minute for *E. coli* ($1.15x10^{-2}M$) and then the levels of potassium ions appeared to reduce slowly over the rest of the period of observation, finally reaching $6.7x10^{-3}M$ at 15 min. However, for *P. aeruginosa* the onset of leakage appeared to be as rapid as that for *E. coli* , $3.8x10^{-2}M$ at 1 min, but continued to exhibit leakage over the rest of the period of observation, eventually reaching a level of $4.75x10^{-2}M$ at 15 min. This result indicates that the degree of leakage caused by cetrimide is similar for both organisms.

Of the other biocides tested, only BIT gave any observable leakage of potassium ions and this was at a much lower rate than that for cetrimide at the same concentration, 128 $\mu$g $ml^{-1}$. The onset of leakage with BIT only became apparent over the 15 minutes of the experiment and attained levels of only $1.4x10^{-4}M$ against *E. coli* and $2.3x10^{-4}M$ against *P. aeruginosa.*

Fentichlor gave no observable potassium ion leakage for either micro-organism. The closely related compound Dichlorophen, however, gave evidence of potassium ion uptake or chelation. In the case of *E. coli* the concentration of potassium ions in the bathing solution fell from $1.1x10^{-4}M$ to $5.0x10^{-9}M$ and for *P. aeruginosa* the fall was from $1.1x10^{-4}M$ to $3.0x10^{-8}M$. This observation would suggest that Dichlorophen acts as an ion chelating agent in the presence of bacterial cells. This is an unusual result as Dichlorophen is often sited as a membrane active agent (Paulus, 1993).

Sodium Pyrithione exhibited effects similar to those of Dichlorophen in that it apparently chelated potassium ions from the bathing solutions of both *E. coli* and *P. aeruginosa.* In the case of *E. coli* this represented a loss of ions from an initial concentration of $1.1x10^{-4}M$ to $5.22x10^{-5}M$ at 15 min. Such a reduction is equivalent to a halving of available bathing

potassium ions. However, unlike Dichlorophen, the pyrithiones appeared to exhibit species-specific chelation properties. In the case of *P. aeruginosa*, the concentration of potassium ions was reduced from $1.1 \times 10^{-4}$M to $3.2 \times 10^{-8}$M. Such a result indicates that *P. aeruginosa* cells appeared to be more susceptible to loss of potassium ions from their external environment by chelation. Such an implication is, however, unlikely to be the case in reality. It is more likely that this result was the simultaneous observation of two separate, but related events involving the potassium ions. The first of these events would be the straight forward chelation of potassium ions from the bathing medium by the sodium pyrithione. This event should not be species specific and should have exhibited a result similar to that for Dichlorophen. The second event, however, is the simultaneous membrane activity of the biocide upon the bacterial cell. This would result in the leakage of potassium ions from the cell and their subsequent chelation by excess pyrithione. This would result in an apparent differential potassium ion loss between the two species of micro-organism dependent upon the differing sensitivity of the two species towards the biocide. In effect, *P. aeruginosa* would exhibit a much greater level of potassium ion loss from the bathing solution if it were less sensitive to the membrane active effects of the biocide, whereas *E. coli* would exhibit a lower level of potassium ion loss due to its corresponding greater potassium ion leakage. However, this suggestion is not supported by the MIC data. This data shows that the MIC values for *E. coli* and *P. aeruginosa* are very similar at 120 $\mu$g ml$^{-1}$ and 100 $\mu$g ml$^{-1}$ respectively and that, if anything, the *P. aeruginosa* cells should be more susceptible to the effects of this compound. The results for zinc pyrithione against both microorganisms, however, exhibit no obvious signs of either potassium ion leakage or chelation. Such a result indicates that either this compound has no membrane effect upon either microorganism or that its induced potassium leakage is exactly balanced by its potassium ion chelation. In the light of the 260nm material leakage results (Figs 73 & 74) this latter theory is the more probable as these results indicate that both NaPT and ZnPT exhibit marked membrane activity against both *E. coli* and *P. aeruginosa*. Indeed, most of the biocides tested gave higher levels of leakage than the positive control compound, cetrimide. The 18-Crown-6 ether exhibited no apparent potassium ion or 260nm material leakage in either experiment.

These results have shown the pyrithione biocides to maintain membrane action towards *E. coli* and *P. aeruginosa* and indicate *P. aeruginosa* to be less susceptible then *E. coli* to the

membrane action of NaPT.

## Observation of the Effect of NaPT upon *Pseudomonas aeruginosa* NCIMB 10548 using Transmission Electron Microscopy

Transmission electron microscopy (TEM) enables the visual observation of the effects of a biocide upon single bacterial cells. It enables direct comparisons to be made of the membranes of unexposed control cells with those of cells which have been treated with test biocide and subsequently enables the visualisation of microbial membrane damage. Utilisation of TEM technology has facilitated monitoring of filament formation in *E. coli* and irregular cell fusion in *Staphylococcus aureus* by exposing cells to biocides such as 4-(2-hydroxyethoxy) acetanilide, betane and 2-phenoxyethanol (Beveridge *et al* 1991, Lorian & Atkinson 1976, Gilbert *et al* 1980). The processes which lead to the fixation and staining of bacterial cells for electron microscopy involve several steps of dehydration so that the cell may be viewed by transmission electron microscopy under vacuum (Beveridge *et al* 1991). Subsequent to the rigours of the fixation and staining processes, much of the membrane integrity and resolution is lost. The fixation process involves maintaining the physical appearance of the bacterial cell, using gluteraldehyde as a preservative of physical integrity. During the fixation process, the cells are stained using either osmium tetraoxide or uranyl acetate. Once fixation is complete the cells are dehydrated. This involves the passaging of cell samples through various ethanol solutions in increasing concentration (50 to 100%) in order to remove any water present in the biological sample. Once the cells have undergone the dehydration process, they are then embedded into a support matrix which will later be placed in the TEM. This process involves two steps; firstly the cells are infiltrated with a solution of the embedding resin in order to decrease any chemical or osmotic shock by placing the cells into pure resin. Secondly, the cells which have been previously incubated in a weak resin solution are embedded into pure resin which is allowed to polymerise with the addition of catalytic hardeners prior to ultra thin sectioning.

**Fixation of cells for TEM observation**

An overnight culture of *Pseudomonas aeruginosa*, which had been grown in 25.0ml of nutrient broth (Oxoid CM1) in an orbital incubator (37°C, 200 osc/min), was harvested by centrifugation (3000 rpm for 10min, IEC Centra-4R Centrifuge, International Equipment, Dunstable) and resuspended in 25.0ml sterile normal saline. An aliquot (9.0ml) of the cell suspension was removed and NaPT was added to give a final concentration of 100 $\mu$g $ml^{-1}$. The bacteria were then incubated at 37°C for five minutes. After incubation, the cells were harvested by centrifugation (3000rpm for 10min) and were resuspended in 9.0ml of cacodylate buffer (0.1M, pH7.0). 60$\mu$l of gluteraldehyde were then added and the cell suspension was mixed by shaking. The cells were then centrifuged (3000rpm for 10min) and resuspended in gluteraldehyde (9.0ml of 3% v/v gluteraldehyde in 0.1M pH7.0 cacodylate buffer). The gluteraldehyde/cell suspension was incubated for one hour at 4°C. After this incubation step the cells were harvested by centrifugation (3000rpm for 10min) and were resuspended in cacodylate buffer (0.1M, pH7.0), this step was repeated once more with the resuspension of the culture in 9.0ml of osmium tetraoxide solution (1% w/v $OsO_4$ in cacodylate buffer, 0.1M, pH7.0). The cells were then incubated in $OsO_4$ for 2 hours at 4°C. After incubation, the culture was prepared for dehydration. This involved centrifugation of the cells (3000rpm for 10min) and their resuspension in cacodylate buffer (0.1M, pH7.0). The fixing process was repeated using control cells which were not exposed to NaPT.

**Dehydration of cells for TEM visualisation**

Dehydration of the bacterial culture was carried out by centrifuging the cells prior to each dehydration step and resuspending them in an aliquot (9.0ml) of the appropriate concentration of ethanol for the allotted incubation time. Incubation times were as follows; 10minutes in 50% ethanol, 20minutes in 60% ethanol, 10minutes in 70% ethanol, 10 minutes in 80% ethanol and two 15 minute incubation steps in 100% ethanol. Once the dehydration process was completed, the cells were ready for embedding in resin.

**Embedding of cells into resin**

The cells were removed from the final 100% ethanol incubation step and were resuspended in propylene oxide (9.0ml, 100%) for 15minutes at 20°C, after which the cells were

centrifuged (3000rpm for 10min) and resuspended in another 9.0ml aliquot of propylene oxide. The sample was removed from propylene oxide by centrifugation (3000rpm for 10min) and the pellet was carefully placed, so as not to disrupt pellet structure, in propylene oxide:resin mixture at a ratio of 1:1. The resin was previously prepared by mixing together 5.0ml of Araldite (CY 212), 6.0ml of Araldite hardener (HY 964) and 0.4ml of accelerator (2,4,6-dimethylaminomethylphenol). After incubating for 3 hours at 20°C, the pellet of cells was carefully removed from the propylene oxide:resin mixture and was placed into pure resin. This was left to incubate overnight at 20°C. After incubation, the resin was polymerised into the solid state by incubating for 48 hours at 60°C. After polymerisation, the samples were then prepared for viewing under the transmission electron microscope (CBS, Modified TEM, Holland) by ultra thin-sectioning using a microtome (Microm microtome, Mieirom, Heidelberg, Germany).

**Figure 75:** Control transmission electron micrograph of *Pseudomonas aeruginosa* PAO1 NCIMB 10548 cells which were not exposed to NaPT. Extensive blebbing is observable from the outer membranes of the cells as a result of the embedding process. However, the outer and inner membranes are still observable as is the peptidoglycan layer. (72,000 times magnification).

Scales ?

**Figure 76:** Cells of *Pseudomonas aeruginosa* PAO1 NCIMB 10548 which have been exposed to MIC levels of NaPT (100 $\mu$g ml$^{-1}$). The cytosol has lost it's electron dense uniformity and ghost cells are observable at the top left of the picture. (72,000 times magnification).

Figure 75 shows the control set of cells of *P. aeruginosa* which were not exposed to NaPT biocide. However, as a result of the embedding process, some 'blebbing' of the outer membrane is observable. 'Blebbing' is a general term used to describe a variety of outer membrane effects including, bubbling, lifting and sloughing of membranous material. The cytosol of the cells which were not exposed to biocide exhibit some degree of electron dense uniformity where the same degree of shading is noticeable throughout the cytosol (Fig 75). When the cells which have been exposed to NaPT (Fig 76) are compared to the cells in figure 75, then a marked difference in their appearance is observed. Coagulation of the cytosol towards the bacterial cell envelope occurs in cells which have been exposed to NaPT. This apparent 'movement' of the cytosol towards the inner membrane of biocide exposed cells (Fig 76) exhibits a lesser degree of uniform shading of the cytosol which is observed in the control cells (Fig 75). The appearance of ghost cells, the empty cell envelopes observable at the top left of figure 76, is shown to occur with the exposure of NaPT to cells of *P. aeruginosa*. This together with increased cell debris around the central NaPT exposed bacterium in figure 76, may be indicative of NaPT induced membrane disruption in *P. aeruginosa*. The biocide induced cell lysis may occur in a manner which is similar to that exhibited by the PHMB antibacterial agents (Broxton *et al* 1984) (Fig 13). Hyde and Nelson (1984) have suggested that the pyrithione biocides possess a pseudo-quaternary ammonium site (Fig 26) and from this they have suggested that the pyrithione biocides may work in a similar manner to that of quaternary ammonium compounds and biguanides such as cetrimide and PHMB. However, the antimicrobial activity of such bactericidal agents is thought to be dependent upon the chain length of the central acyl chain in the biguanides and the acyl side chain of the monomeric QAC antimicrobial agents (Chawner & Gilbert 1989a, 1989b). The pyrithione antimicrobials do not possess a long organic side chain and as such may not behave in exactly the same manner as PHMB. For example, the chain length of PHMB facilitates the interaction of the active guanide head groups of PHMB with phospholipids in the bacterial membranes (Fig 14). This interaction precludes the breakdown of bacterial membrane ultrastructure which is the basis of the mode of action of PHMB and other QACs. The pyrithione antimicrobials may bind to phospholipid structures in the membranes (as has been shown in previous experiments, Figs 54 to 57). However, the absence of an acyl side chain on the pyrithiones, by which the biocide may physically interact with two chemical sites in the bacterial membrane, disables

the potential antimicrobial effectiveness of these biocides in membrane disruption.

The data from the leakage studies of both potassium ions and material which absorbs light at 260nm (Fig 71 to 74) exhibited strong signs of membrane disruption by the pyrithione biocides. However, from the TEM data (Fig 75 & 76), an intracellular mode of action cannot be excluded in elucidating the effect of NaPT upon the envelope of *P. aeruginosa.* The observed effect of NaPT upon the *P. aeruginosa* cytosol shows that the biocide exhibits an intracellular effect (Fig 76). This effect upon the cytosol may be secondary to the membrane activity of NaPT, in which case the biocide acts at the membrane extracellularly. However, the effect of NaPT upon the membrane and the leakage of intracellular material shown in figures 71 to 74 may have been caused by the intracellular action of the pyrithiones. This would mean that, after entry into the cytosol, the pyrithiones disrupt membrane ultrastructure from intracellular sites of action (the inner leaflet of the inner membrane). This would suggest, that although the pyrithiones are active towards the bacterial membrane, their main site of activity is in the cytosol.

The data from these experiments suggest the pyrithione biocides are active towards the bacterial envelope. However, the observed effect on the cytosol from figure 76, which indicates cytosolic aggregation at the inner face of the bacterial envelope, together with the data from the metabolism studies would suggest that some degree of intracellular activity is possessed by NaPT and ZnPT.

# AN ASSAY FOR THE DETECTION OF PYRITHIONE BIOCIDES AND THEIR DISTRIBUTION IN GRAM-NEGATIVE BACTERIAL CELLS

The effect of an antimicrobial agent upon a target organism is only noticeable once the biocide has bound to the target site in or on the microbial cell (Salt & Wiseman 1991). The observation of the uptake and binding of an antimicrobial cell can also help determine if the action of a biocide is intra- or extracellular. That is, if a biocide is isolated in the bacterial cell envelope, then it is probably active at the envelope, likewise if it is isolated in the cytosol then it is most likely to be active intracellularly. Before the distribution of a biocide can be assessed, an assay for the biocide must be developed. Such assays are dependent upon the chemical properties of the respective biocides involved and the development of such assays is dependent upon the degree of chemical reactivity displayed by the antimicrobial agent. Once an appropriately sensitive assay has been characterised, the fractionation of the test population of bacteria into their general components (cell envelope, cytosol and bacterial bathing solution) may be carried out together with the assaying of subcellular fractions for biocide content. Utilisation of distribution studies does not only indicate where the biocidal agent is active, but also indicates how a biocide affects the barrier properties of the microbial cell provided by the envelope. Biocide entry into a cell may not be due solely to passive diffusion of the biocide across the bacterial membranes, but may result from the effect of the biocide upon the membrane itself. For example, an antimicrobial which elicits an effect towards the bacterial envelope, and is not observable in the envelope subcellular fractions, may have entered the cell as a result of membrane activity.

Biocide uptake into bacteria may also be classified using uptake isotherms which were originally based upon data from solute uptake of inert support material (Giles *et al* 1974a, 1974b). The degree of solute uptake and the classification of uptake isotherms may be exhibited by plotting concentration of solute absorbed by the matrix against concentration of solute applied in solution (the equilibrium concentration). The uptake of solutes by inert supports has been well documented (Giles & Tolia 1964, Giles *et al* 1974a, 1974b) and is

shown to be affected by both the support matrix used and the degree of solute concentration. Although solute uptake isotherms were originally classified using inert support matrixes, they may be applied to bacterial cells as a result of the finite volume and surface area of the bacterial cell. Four major classes of uptake isotherms have been characterised (Giles *et al* 1974a, 1974b) and these may be defined as the S or sigmoidal isotherm, the L or Langmuirian isotherm, the H or high affinity isotherm and the C or constant compartmentalisation isotherm (Fig 77). The S and L isotherms both possess similar characteristics. However, with the S isotherm, the concentration of solute taken up is shown to increase slightly with increasing solute concentration before the onset of saturation (Giles *et al* 1974a, 1974b). The L isotherm exhibits typical Langmuirian saturation kinetics which indicate the reduction of solute uptake as the applied concentration increases and as saturation of the cell surface occurs (Giles *et al* 1974a, 1974b, Salt & Wiseman 1991) (Fig 77). The H type isotherm, a variation of the S or L type isotherms, in which the affinity between the cell surface and applied solute are such that there appears to be an immediate uptake of solute at the initial concentration (Giles *et al* 1974a, 1974b). The C type isotherm exhibits a constant degree of partitioning between the absorbance matrix and the applied solute. This explains the observation of the abrupt plateau onset when the saturation point occurs (Giles *et al* 1974a, 1974b) (Fig 77). The utilisation of uptake isotherms can elucidate much information about the absorbant behaviour of an antibacterial agent. Giles and coworkers (1974a) have divided the four main sets of uptake isotherms into various subsets which are dependent upon the degree of saturation of the utilised adsorption matrix or absorption by bacteria. Diphasic isotherms (Types S4, L4 and H4, Fig 77) exhibiting two saturation kinetic patterns in one isotherm, have been shown for various antimicrobial agents, ie, CTAB and tetradecylbenzyldimethylammonium bromide (Salt & Wiseman 1968, Achaempong & Wiseman 1981). The onset of such plateaux, after saturation has been achieved, indicate two phenomena. Firstly, the adsorption of the antimicrobial to the outside of the bacterial cell and secondly, the absorption of the antimicrobial into the bacterial cytosol. These two events indicate how saturation kinetic patterns may be observed twice in the same bacterial cell. If no plateau is achieved, then saturation has not occurred and if the concentration of absorbed antimicrobial is shown to decrease as the applied concentration increases, then the disruption of the bacterial cell by the antimicrobial agent may account for the decrease in absorbed biocide as it is lost through the ruptured cell envelope.

**Figure 77:** Examples of the patterns obtained for the S, L, H and C uptake isotherms as defined by Giles *et al* (1974a).

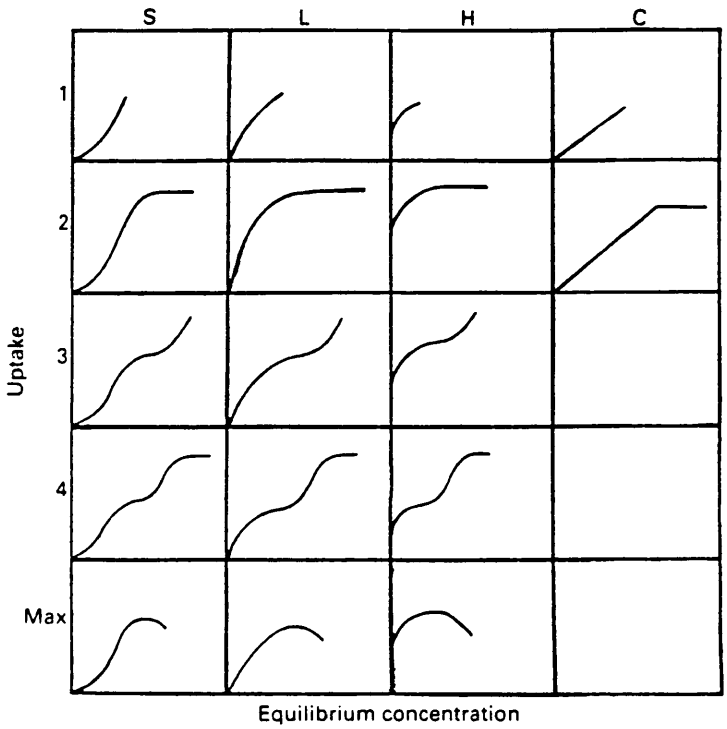
S
L
H
C
1
2
3
4
Max
Uptake
Equilibrium concentration

Distribution studies utilising radiolabelled biocide assays can also be applied to determine the kinetics of the uptake of biocides by bacterial cells as a function of time. Data from the kinetics of biocide uptake against time can be used together with growth inhibition data in order to determine how quickly the effect of a biocide is elicited upon a test organism once it enters a bacterial cell. The preparation of radiolabelled biocide compounds and their application in observation of uptake isotherms and the observation of biocide uptake against time have enabled the onset of extremely sensitive assays which are independent of the chemical activity of the respective biocide. No readily available supply of radiolabelled pyrithiones exists. The cost of commercial preparations of such compounds is prohibitive. As a result it was decided to develop a chemical assay for the presence of pyrithiones, based upon their metal cation chelating properties. In order to observe the distribution of the pyrithiones in *E. coli* and *P. aeruginosa*, an assay was developed using the metal chelating qualities of the pyrithiones. The assay was subsequently used to observe the distribution of the pyrithiones in bacterial cells.

**Assay development and procedure**

It is known that, as a result of their ability to behave as Lewis bases in solution, the pyrithione group of compounds are good metal cation chelating agents (Hyde & Nelson 1984, Davies 1985, Fenn & Alexander 1988, Seymour & Bailey 1981, Nakajima *et al* 1993, Marks *et al* 1985, Imokawa & Okamoto 1982, Hyde & Auerbach 1979). As discussed in the introduction (p85), the metal chelating properties of the pyrithiones have been used to facilitate their isolation and identification using HPLC and TLC techniques (Fenn & Alexander 1988, Imokawa & Okamoto 1982). In this study, a spectrophotometric assay was developed utilising the chelation of copper (II) ions by NaPT and ZnPT.

Scanning spectrophotometry in the range of 250nm to 450nm (Perkin Elmer UV/vis Scanning Spectrophotometer Lambda 2, Uberlingen, Germany) was carried out by reacting an aliquot (1ml) of NaPT and ZnPT (64 $\mu$g ml$^{-1}$) with 5.0ml of copper chloride dihydrate solution (1mM). Traces were obtained and analysed for new reaction peaks. A reaction peak at a wavelength of 318nm was observed in absorption spectra of both copper chloride dihydrate reacted NaPT and copper chloride dihydrate reacted ZnPT. The peak of 318nm was not observable in unreacted NaPT and ZnPT samples or 1mM copper chloride dihydrate

solution and was therefore used as the identification wavelength in a spectrophotometric assay of the pyrithiones in subcellular fractions.

Calibration curves of varying concentration of NaPT and ZnPT at $E_{318nm}$ were obtained (Figs 78 & 79) using the following assay procedure. An aliquot (5ml) of 1mM copper chloride dihydrate was added to 1ml of biocide. For NaPT the concentration range used was from 0 to 100 $\mu g\ ml^{-1}$ in 10 $\mu g\ ml^{-1}$ steps and for ZnPT the concentration range was from 0 to 21 $\mu g\ ml^{-1}$ in 3.0 $\mu g\ ml^{-1}$ steps. $E_{318nm}$ of the samples was recorded and biocide concentration was plotted against absorbance at this wavelength. The assay of subcellular fractions followed the same procedure, replacing the biocide sample with 1ml of cellular fraction. For the determination of the calibration curves, the blank used was 1mM copper chloride dihydrate. When determining the amount of NaPT present in subcellular fractions, the sample was diluted four-fold prior to determination of $E_{318nm}$. This was due to the observation of maximum absorbance at $E_{318nm}$ as a function of concentration in the form of a concentration dependent plateau against absorbance. The onset of the plateau was subsequent to the observation of the Lambert-Beer law which states that absorbance of light is partly dependent upon the sample concentration (Lawrence & Maier 1977, Holum 1986). Therefore, the plateau of the L-shaped curve of NaPT concentration against $E_{318nm}$ prevented the direct observation of greater than 25 $\mu g\ ml^{-1}$ NaPT. The concentration of the diluted sample was then calculated from the curves of pyrithione concentration against $E_{318nm}$ (Figs 78 & 79). The concentration of the dilute cellular fraction was multiplied by the dilution factor and the correct concentrations of NaPT for the subcellular fraction was calculated. A culture containing no biocide was treated in the same way as biocide exposed cells, using each subcellular fraction to blank the spectrophotometer.

**Table 15:** Concentrations of biocide applied to *E. coli* and *P. aeruginosa* during the distribution studies (80%MIC).

| Microorganism | [Biocide] ($\mu g\ ml^{-1}$) | |
|---|---|---|
| | NaPT | ZnPT |
| *E. coli* | 108 | 4.05 |
| *P. aeruginosa* | 90 | 11.7 |

**Distribution studies**

A washed cell suspension was prepared from overnight bacterial cultures grown in 25ml of nutrient broth (Oxoid CM1) in an orbital incubator (200 osc/min, 37°C). The cells were harvested by centrifugation and washed twice in normal saline by centrifuging (3000 rpm for 10min, IEC Centra-4R Centrifuge, International Equipment, Dunstable). The washed cell suspensions were then divided into 10ml aliquots in clean glass boiling tubes. Biocide was added at 80% MIC concentrations (Table 15). After five minutes of incubation of cells with the biocide at room temperature, 2.0ml of of the cell suspension was removed, centrifuged and the supernatant was assayed for biocide content. The cells were resuspended in normal saline (10ml) and were then homogenised (Ultra Turrax T8, S8N-5G, IKA Labortechnik, Staufer, Germany) at the appropriate homogenisation time (Ht, PG). An aliquot (2.0ml) of homogenate was centrifuged at 6500rpm for 1min (Sanyo MSE Microcentaur Microfuge, UK). The supernatant was retained and the pellet (cell debris) was resuspended in normal saline (2.0ml) and assayed for pyrithione content. The retained supernatant was centrifuged for a further 10 minutes at 13000rpm (Sanyo MSE Microcentaur Microfuge, UK). After centrifugation, the supernatant (cytosol) was removed and assayed for pyrithione content. The pellet (cell envelope) was resuspended in normal saline (2.0ml) and was assayed for pyrithione content. This procedure was repeated for ZnPT and NaPT against both *E. coli* and *P. aeruginosa* and results were tabulated (Table 16).

**Table 16:** Distribution of NaPT and ZnPT in subcellular fractions of *E. coli* and *P. aeruginosa.*

| Sample | *E. coli* | | *P. aeruginosa* | |
|---|---|---|---|---|
| | [NaPT] ($\mu g\ ml^{-1}$) | [ZnPT] ($\mu g\ ml^{-1}$) | [NaPT] ($\mu g\ ml^{-1}$) | [ZnPT] ($\mu g\ ml^{-1}$) |
| Supernatant | 89.4 | 1.95 | 87.0 | 10.2 |
| Cell Debris | 0.0 | 0.0 | 0.0 | 0.0 |
| Cytosol | 55.8 | 3.15 | 81.0 | 9.1 |
| Cell Envelope | 0.0 | 0.0 | 0.0 | 4.2 |

**Figure 78:** Calibration curve of the change in absorbance ($E_{318nm}$) against concentration of NaPT ($\mu g\ ml^{-1}$). Error bars are calculated from and plotted as the Standard Error of the data set.

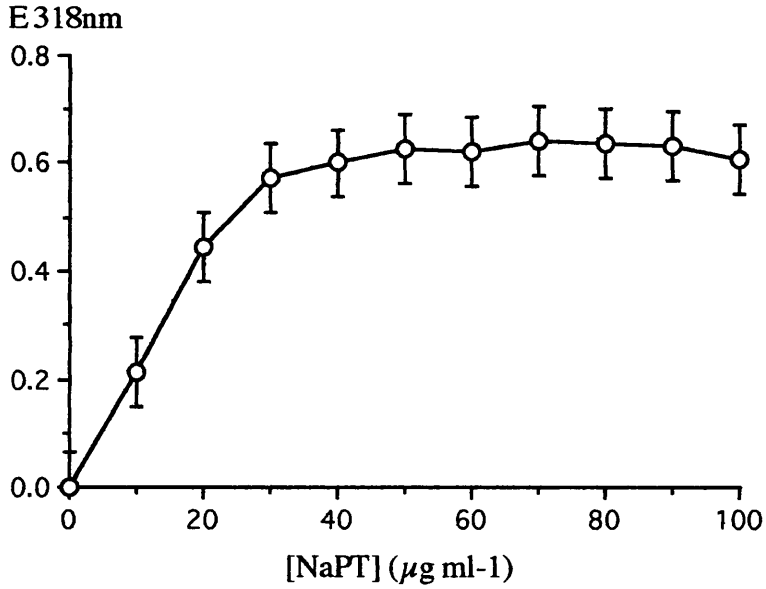
E318nm
0.8
0.6
0.4
0.2
0.0
0
20
40
60
80
100
[NaPT] (μg ml-1)

**Figure 79:** Calibration curve of the change in absorbance ($E_{318nm}$) against concentration of ZnPT ($\mu g\ ml^{-1}$). Error bars are calculated from and plotted as the Standard Error of the data set.

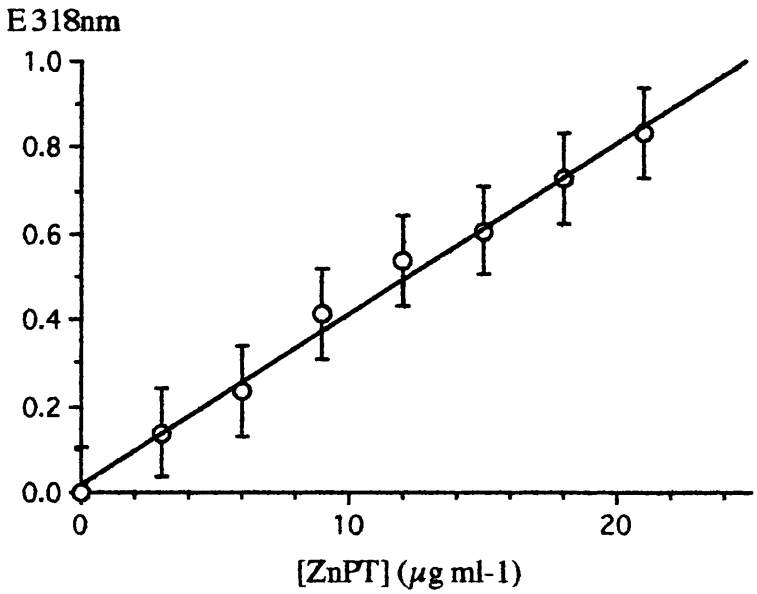
E318nm
1.0
0.8
0.6
0.4
0.2
0.0
0
10
20
[ZnPT] (μg ml-1)

The data from table 16 shows that NaPT and ZnPT enter the cytosol of both *E. coli* and *P. aeruginosa*. The data for *P. aeruginosa* exposed to ZnPT may suggest that a barrier effect is deterring the entry of some of the biocide into the cytosol. This may be due to the thicker exopolysaccharide layer possessed by Pseudomonads, which is rich in metal cations and would therefore lend itself to some chelation of pyrithione compounds. The isolation of ZnPT in the cell envelope of *P. aeruginosa* may help explain the observed *Pseudomonas*-gap between *E. coli* and *P. aeruginosa* which was noticeable in the growth inhibition studies (Table 5).

This colourimetric assay of the pyrithiones based upon copper ion chelation indicates that the biocide enters the bacterial cytosol and the entry of these compounds is not affected by the barrier properties of the bacterial cell envelope. The observation of entry of NaPT and ZnPT into the bacterial cytosol may also be indicative of perhaps part of the mode of action of these biocides. From previous experiments, it is understood that a membrane active effect is elicited by NaPT and ZnPT against the two test microorganisms. However, from the assay, envelope bound biocide is only observed with ZnPT exposed to *P. aeruginosa*, although ZnPT is still observed in the cytosol. This may be indicative that once pyrithione has acted at the level of the bacterial envelope it leaves that site of action and enters the cytosol. This may occur as a result of the chelation of pyrithione by other metal cations which are present in the bacterial envelope, ie, magnesium or calcium. The pyrithiones may chelate these metal ions as a result of membrane disruption and carry them into the cytosol due to an osmotic effect, metal cationic concentration gradient or passive diffusion. The observed entry of these biocides into the cytosol, regardless of how they get there, indicates that these biocides may act at more than one site in the bacterial cell and that they possess an intracellular as well as an extracellular mode of action.

The addition of the numerical concentration values in table 16 indicates that the remaining levels of pyrithione inside the test cells are greater than the applied pyrithione concentrations. This phenomenon may be explained by one or both of two possibilities. Firstly, there may be an experimental anomoly between the values of cellular material assayed. This may have the effect of apparently concentrating the levels of pyrithione observed. Secondly, this phenomenon may be the result of some form of cellular partitioning of the pyrithione

biocides. This suggests that the cells possess some chemical structures that form chelates or complexes with the pyrithiones and facilitates their uptake into the cell.

# DISCUSSION

The pyrithione biocides have been shown to possess antimicrobial and antifungal properties (Albert *et al* 1956, Cooney 1969, Khattar & Salt 1993). They exhibit low toxicological properties and as such have been widely utilised in the cosmetics industry as preservatives, antidandruff and antifungal agents (Nelson & Hyde 1981, Hyde & Nelson 1984). They are metal ion chelating agents and have been used in the mining industry to chelate precious and semiprecious metals from ore samples (Edrissi *et al* 1971). They have also been used in the fuel industry as pipeline preservatives and heating system microbicides (Cooney 1969). The Introduction to this thesis has discussed the work of previous investigators into the mode of antimicrobial action of the pyrithiones, but to date these studies have not been fully conclusive (Albert *et al* 1956, Cooney 1969, Chandler & Segel 1978, Ermolayeva *et al* 1995). The elucidation of their mode of action would increase the commercial application of these antimicrobial agents and would facilitate their environmental targeting as biocidal and preservative agents.

## EVIDENCE OF A DIRECT CELLULAR INTERACTION BY THE PYRITHIONE BIOCIDES

The growth inhibitory and killing effect of the pyrithione biocides is indicative of a detrimental effect by NaPT and ZnPT towards the target Gram-negative bacteria *E. coli* and *P. aeruginosa*. However, although growth inhibition and killing of the target microorganisms has been observed (Figs 39 & 40, Tables 5 & 6), it is not known if the exhibited effect was subsequent to a direct cellular action by these biocides or as a secondary effect of their presence in the bacterial medium.

### Neutralisation of Pyrithione Antimicrobial Activity

The pyrithione group compounds are known chelators of metal cations and as such have been widely used in industry (Edrissi *et al* 1971, Fenn & Alexander 1988, Nakajima *et al* 1993). In this study, the chelating properties of NaPT have been observed as the deposition of particulate iron from solution in a chemically defined medium (p124). The chelating

properties of the pyrithiones proved problematic during the tube dilution neutraliser studies. The presence of EDTA together with NaPT resulted in the chelation and removal of free iron from the chemically defined medium. Subsequently, bacterial growth was inhibited. This was overcome in these experiments by the addition of extra iron to the medium which enabled bacterial growth. This chelating property of the pyrithiones suggests that these biocides may induce stasis of bacterial growth by starving the organisms of vital cationic nutrients, ie, iron, calcium or potassium. The neutralisation of pyrithione action by EDTA (Table 7) reflects published experimental data (Khattar *et al* 1988). The observed neutralisation of these biocides by EDTA suggests that direct chemical effect upon the biocides was elicited by this neutraliser. However, in solution both EDTA and NaPT are anionic. In the case of EDTA this is due to the carboxylic acid groupings on the molecule and for NaPT is as a result of the presence of the oxyanion on the pyrithiolate ring structure (Figs 26 & 30). The presence of such structures indicates that no chemical interaction would occur between EDTA and NaPT, under conditions required for bacterial growth, as a result of the physical repulsion of two negatively charged groups (Holum 1986). Subsequently, the neutralisation effect of EDTA towards NaPT must be occurring at a biochemical level. The neutralisation of the antimicrobial action of ZnPT by EDTA is the result of a chelation effect. EDTA possesses stronger electronegative properties than ZnPT and may form a complex with it *via* the chelation of the central zinc atom. This is explained by the changes in the UV/visible scanning spectra for ZnPT and EDTA when they are present together in solution (Tables 8 and 9, p128).

It is known that EDTA causes removal of lipopolysaccharide (LPS) and phospholipid groups from the outer membrane of Gram-negative bacteria (Franklin & Snow 1991). Subsequently, this compound is classed as a membrane active antibacterial agent and when utilised in high concentrations may induce bacteristasis and even bacterial death (Franklin & Snow 1991). This occurs as a result of the chelation of divalent metal cations (which help to maintain outer membrane structure) from the outer leaflet of the membrane (Hoyle & Beveridge 1983a, 1983b). Removal of these ions causes the breakdown of the Gram-negative outer membrane with the subsequent release of the LPS and phospholipid bilayer. Subsequently, Gram-negative cells treated with EDTA then stain Gram-positive (Franklin & Snow 1991). The removal of metal cations from the bacterial outer membrane by EDTA

would prevent their chelation by pyrithione compounds and stop bacterial membrane breakdown by these biocides. This may also occur in the opposite form, where pyrithione chelation of membrane bound divalent metal cations prevents the action of EDTA at the Gram-negative envelope. The observed neutralisation of NaPT and ZnPT by the presence of EDTA is indicative of a direct cellular interaction by these antimicrobial agents.

The neutralisation of the antimicrobial activity of ZnPT and NaPT by other important biomolecules (phosphatidylethanolamine and cysteine, Table 7) is also indicative of direct interactions between the pyrithione biocides and the bacterial cell. The thiol-containing amino acid cysteine was shown to neutralise the antimicrobial effect of ZnPT (Table 7). From the tube dilution neutraliser studies (Table 7), the scanning spectrophotometry studies (Tables 8 & 9) and computer generated molecular modelling (Fig 53) cysteine was also shown to chemically bind to ZnPT. The bacterial membrane phospholipid phosphatidylethanolamine was shown to neutralise the effects of both NaPT and ZnPT in the tube dilution neutraliser studies and to chemically interact with both biocides in the computer generated molecular modelling data (Table 7, Figs 55, 56 & 57). This information suggests the pyrithiones are chemically interactive with important biomolecules and also suggests that NaPT and ZnPT are capable of direct biochemical interactions with bacterial cells. However, because the molecular modelling studies were virtual experiments (ie, there were no background ionic compounds, pH or concentration gradients in the computerised system) then the results from such experimental data must be treated only as being indicative of a true reaction. Therefore, although the pyrithiones may be able to bind with thiol groups and membrane phospholipid head groups, further experimental work is required to investigate if a direct interaction is occurring between NaPT, ZnPT and the component chemicals of bacterial cells.

**Direct Interaction of Pyrithiones at the Bacterial Cell Envelope**

Studies observing the leakage of cytosolic components (p174, Figs 71 to 74) have shown that NaPT and ZnPT induce the leakage of cytoplasmic constituents (material which absorbs light at 260nm) from cells of *E. coli* and *P. aeruginosa*. The leakage of cytosolic components indicates that membrane disruption has occurred as a result of exposure of the target microorganisms to the test biocides (Salton 1968, Lambert & Hammond 1973, Bernheim 1976, Beggs 1992). This has been exhibited with membrane active agents such as PHMB,

chlorhexidine, alexidine and miconazole which induce the leakage of potassium ions, phosphate molecules and material which absorbs light at 260nm from biocide exposed cells (Hugo & Longworth 1966, Denyer & Hugo 1991b, Gilbert *et al* 1990b, Beggs 1992).

Although the bacterial envelope is the first physical barrier which a biocide must traverse in order to obtain entry to the cytosol, the deterioration of the bacterial cell envelope may be a secondary effect of the intracellular action of the test biocide. For example, a hydrophilic biocide may be taken up into the bacterial cytosol as a result of hydrophilic channelling *via* porins (Hancock & Bell 1988). Subsequently, this may induce intracellular chemical shock (Hancock & Bell 1988). The effect of this chemical shock (as a consequence of intracellular chelation or protein coagulation through thiol and amine interactions) may be the intracellular deterioration of the bacterial envelope, manifesting itself as the leakage of intracellular constituents. However, molecular modelling (Figs 52c, & 55 to 57), neutraliser studies (Table 7) and the assay of pyrithione in subcellular fractions (Table 16) have shown that the pyrithione biocides have the potential to interact with the bacterial membrane.

Computer generated interactions have been exhibited for both NaPT (in the form of the pyrithiolate ion) and ZnPT (both the monomer and dimer forms) with the bacterial membrane phospholipid phosphatidylethanolamine (Figs 52c & 55 to 57). Electrostatic interactions between the phospholipid head group and NaPT were observed (Fig 52c). ZnPT exhibited more reactive qualities with the phospholipid head group than did NaPT, indicating interactions with the orthophosphoric acid group and amine interactions with the phospholipid head group (Figs 55 to 57). Neutralisation of the antimicrobial activity of NaPT and ZnPT in the tube dilution neutraliser studies was elicited with the addition of extracellular phosphatidylethanolamine (Table 7). The MIC values for NaPT against *P. aeruginosa* and for ZnPT against both *E. coli* and *P. aeruginosa* were effectively increased, supporting the suggestion of interactions between NaPT and ZnPT and the membrane phospholipid. The MIC for *P. aeruginosa* exposed to NaPT was increased by 20 $\mu$g ml$^{-1}$ from 100 $\mu$g ml$^{-1}$ to 120 $\mu$g ml$^{-1}$. The MIC for ZnPT against *E. coli* was more than doubled, and changed from 4.5 $\mu$g ml$^{-1}$ to 10 $\mu$g ml$^{-1}$. The MIC for ZnPT against *P. aeruginosa* was shown to have increased from 13 $\mu$g ml$^{-1}$ to 24 $\mu$g ml$^{-1}$. The increases in

these MICs indicate an effect upon NaPT and ZnPT by the presence of extracellular phosphatidylethanolamine. If this is considered together with the molecular modelling data, then there is a strong indication of some direct chemical interaction between the pyrithiones and extracellular phosphatidylethanolamine. The assaying of distributed pyrithione in subcellular fractions exhibited the presence of ZnPT in the cell envelope of *P. aeruginosa* (Table 16). This indicates that, as a result of some chemical interaction, ZnPT has become irreversibly bound to the cell envelope of *P. aeruginosa.*

These results, together with the known chelating properties of the pyrithiones would suggest that, in bacterial cultures, these biocides can bind to the cationic bacterial cell surface and interact with lipid bilayer head groups before being absorbed into the bacterial cell (Edrissi *et al* 1971, Fenn & Alexander 1988, Nakajima *et al* 1993). This suggests that the pyrithione biocides interact with the bacterial cell membrane and that NaPT and ZnPT exhibit direct cellular interactions at the level of the bacterial cell envelope.

**Direct Interactions of Pyrithiones in the Bacterial Cytosol**

Inhibition of substrate catabolism was shown to occur when *E. coli* and *P. aeruginosa* were exposed to both NaPT and ZnPT (Figs 59 to 62). Although the degree of inhibition was in no case greater than 70% of the control metabolism, an intracellular anti-metabolic effect was observed. However, the decrease in levels of substrate catabolism by the pyrithiones may have been an effect secondary to some type of membrane activity. For example, the breakdown of transport processes in the membrane as a result of the biocide-induced disruption of membrane-maintained catabolic control processes, ie, disruption of pH gradients, concentration gradients and transport processes may have resulted in decreased metabolism of specific substrates (Harold 1972, Chandler & Segel 1978, Chopra *et al* 1987, Broxton *et al* 1983a). However, the assay of pyrithione distribution in fractionated cells has shown that both NaPT and ZnPT enter the bacterial cytosol (Table 16). Although, as a result of the assay design, it is not possible to determine the exact concentration of biocide per unit volume of subcellular fraction, the distribution studies exhibit the presence of the pyrithiones in the cytosol, regardless of the concentration. This suggests that once inside the cell, the pyrithiones would elicit antimicrobial action towards the cytosol. Subsequently, this has been reflected in decreased levels of substrate catabolism (Figs 59 to 62) and by decreased

ATP production (Figs 63 to 70).

Coagulation of the cytosol in proximity to the inner leaflet of the cytosolic membrane has been exhibited in cells of *P. aeruginosa* which have been exposed to MIC levels (100 $\mu$g $ml^{-1}$) of NaPT. The chelating properties of the pyrithione biocides may have induced such a phenomenon. The cationic chelating properties of the pyrithione group compounds have been previously discussed (p68), particularly with regards to metal cations (Edrissi *et al* 1971, Hyde & Nelson 1984). Subsequent to this chemical property, when inside the bacterial cell, the pyrithiones may chelate intracellular metalloenzymes and free divalent cations as well as cause the coagulation of proteins *via* positively charged amino acid side groups. This interaction together with electrostatic and covalent interactions between the pyrithiones and amine and/or thiol groups possessed by proteins may be the cause of cytosolic coagulation. In turn, this would be detrimental to cellular substrate catabolism and ATP production, suggesting that the pyrithiones undertake direct chemical interactions in the cytosol.

## METABOLIC ACTIVITY OF THE PYRITHIONE BIOCIDES

### Inhibition of Substrate Metabolism

Low levels of activity were observed when cells of *E. coli* and *P. aeruginosa* were exposed to sub-MIC concentrations of NaPT and ZnPT (Figs 59 to 62). Of the six substrates investigated (glucose, acetate, pyruvate, proline, thymidine and uracil, Table 11) only the catabolism of thymidine exhibited significant inhibition of approximately 70% of the control rate of metabolism in *E. coli* (Figs 59 & 60). This reflects published data which has reported the inhibition of thymidine uptake when bacteria are exposed to NaPT (2.5 $\mu$g $ml^{-1}$) (Friedman 1981, Khattar *et al* 1989, Khattar & Salt 1993). Uracil catabolism was not highly inhibited by the presence of NaPT and ZnPT, even at concentrations approaching the MIC. The lack of inhibition of uracil catabolism is contradictory to the published findings of Khattar & Salt (1993), who reported the inhibition of uracil uptake to be greater than that observed for thymidine uptake in *Klebsiella pneumoniae* and *E. coli*. However, the uptake mechanisms for uracil and thymidine are both the same, being dependent upon the

membrane bound $H^+$/ATPase (the proton motive force) (Maloney 1987, Cronan *etal* 1987. Neuhard & Nygaard 1987). Therefore, it is either an intracellular catabolic effect of NaPT and ZnPT which is inducing the increased inhibition of thymidine catabolism reported here or the cells of *E. coli* and *P. aeruginosa* more readily catabolise thymidine as opposed to uracil as a substrate.

The growth inhibitory activity of NaPT and ZnPT may be reflected in the substrate catabolism data. NaPT exhibited two $LT_{90}$ values and an MIC of 100 $\mu$g ml$^{-1}$ against *P. aeruginosa* in comparison with three $LT_{90}$ values and an MIC of 13.0 $\mu$g ml$^{-1}$ for ZnPT (Tables 5 & 6). *E. coli* exhibited one $LT_{90}$ value and an MIC of 120 $\mu$g ml$^{-1}$ when exposed to NaPT in comparison with three $LT_{90}$ values and an MIC of 4.5 $\mu$g ml$^{-1}$ for ZnPT (Tables 5 & 6). However, in the catabolic inhibition studies (Figs 59 to 62) both biocides were applied to the test organisms at concentrations ranging from 0 $\mu$g ml$^{-1}$ biocide up to their respective MICs (Table 5). This suggests that both NaPT and ZnPT exhibit a similar degree of inhibitory activity towards bacterial substrate catabolism at biocide concentrations which reflect the MICs. The degree of inhibition exhibited by NaPT towards both organisms may reflect the low levels of growth inhibitory activity observed with this biocide (Figs 59 & 61). For ZnPT, the differences between NaPT MIC data and the ZnPT MIC data were not reflected in the substrate catabolic studies. This suggests that, irrespective of the MIC, both biocides are poor inhibitors of cytosolic metabolic processes. This may be reflected in the killing data for both biocides (Table 6) as the difference displayed in the MIC data (Table 5) is not proportionally observed in the killing data. NaPT MICs were 100 $\mu$g ml$^{-1}$ for *E. coli* and 120 $\mu$g ml$^{-1}$ for *P. aeruginosa* (Table 5). ZnPT MIC values were 13.0 $\mu$g ml$^{-1}$ for *P. aeruginosa* and 4.5 $\mu$g ml$^{-1}$ for *E. coli* (Table 5). The difference in these values reflects a marked difference in the growth inhibitory action of the two antimicrobial agents towards the target microorganisms. The killing data, however, did not proportionally reflect this difference and the patterns of biocide-induced bacterial death were similar for NaPT and ZnPT against *E. coli* and *P. aeruginosa* (Figs 43 to 46).

**Stimulation of Substrate Metabolism**

Figures 59 to 62 exhibit stimulation of the rates of metabolism of some substrates as the biocide concentration approaches the MIC. For NaPT against *E. coli*, the metabolism of glucose, proline, thymidine and uracil are stimulated (Fig 59). For *P. aeruginosa* metabolism of the same substrates, together with acetate, was increased by the same biocide. ZnPT stimulated the metabolism of acetate, uracil and thymidine in *E. coli* and acetate and glucose in *P. aeruginosa*. The observed stimulation of metabolism in figures 59 to 62 may be as a result of one or both of two possibilities; (i) the loss of intracellular metabolic control mechanisms induced by target organism exposure to pyrithiones resulting in increased metabolism or (ii) the breakdown of membrane integrity and the membrane associated pH gradients, concentration gradients, ATPases and transportases.

If (i) above is occurring as a result of exposure of *E. coli* and *P. aeruginosa* to pyrithiones, it may reflect the hypothesis that the pyrithione biocides act as a result of their structural analogy to the pyridine nucleotide precursor nicotinic acid (Cooney 1969). Nicotinic acid is a vitamin involved in the electron transport chain and the metabolism and production of $NAD^+$, NADH, NADP and NADPH (Tritz 1987). It is also involved in pyrimidine base metabolism and during times of intracellular pyrimidine precursor shortage, nicotinic acid may be used to supply the pyrimidine pool (Stryer 1988). Subsequently, the entry of a structural analogue of nicotinic acid into the bacterial cytosol may disrupt control mechanisms involved in $NAD^+$ production. Nicotinic acid is actively transported into the cytosol by the action of nicotinate phosphoribosyl transferase and is dependent upon the hydrolysis of ATP (Rowe *et al* 1985, Tritz 1987). This may indicate that the pyrithione biocides are actively transported into the bacterial cytosol by the same mechanistic action of the chemiosmotic coupling theory (Harold 1972, Konings 1977, Maloney 1987, Stryer 1988). However, ZnPT exists in monomeric and dimeric forms which both differ greatly from the molecular structure of nicotinic acid (Figs 31 & 33) and probably would not be transported by such a mechanism. NaPT, however, possesses a greater structural similarity to nicotinic acid than ZnPT and may be susceptible to transportation into the bacterial cytosol by nicotinate phosphoribosyl transferase. $NAD^+$ is the precursor for NADH, NADP and NADPH within the bacterial cytosol and is produced *via* the utilisation of nicotinic acid from

the pyridine nucleotide production cycles (Tritz 1987). This would involve the transmembrane NADH dehydrogenase which is driven by the proton gradient and forms part of the electron transport chain (Ingraham *et al* 1983, Tritz 1987). NADH dehydrogenase converts $NAD^+$ to NADH and the increase in an NADH analogue (intracellular pyrithione) may provoke disruption of metabolic processes which are dependent upon low levels of $NAD^+$ and NADH (ie, steps within the Krebs cycle). This may result in positive feedback which would decrease the inhibition of substrate metabolism at higher concentrations of pyrithione biocides. However, in order for NaPT and ZnPT to be effective towards $NAD^+$ metabolism and therefore the disruption of metabolic control, they must be shown to enter the cytosol regardless of the mode of transport. This has been exhibited during the assay for pyrithione in subcellular fractions (Table 16) and such results support the above hypothesis.

The breakdown of pH gradients, concentration gradients, transportases and membrane integrity would result in the passive diffusion of the substrate into the cytosol where it could be freely catabolised by intracellular enzymes (Konings 1977, Kirstensen 1994). Activation of substrate metabolism was exhibited for glucose, acetate, proline, thymidine and uracil and involves various transport processes. If NaPT or ZnPT targeted one specific membrane transport pathway, then the inhibition of the substrate transport mechanisms for all of the five substrates above would not be observed. However, the possibility of active transport of NaPT *via* the nicotinic acid transport system requires the hydrolysis of ATP with the consequent expenditure of protons (the proton motive force, PMF). This mechanism is also required for the transport of thymidine and uracil into the cytosol (Table 11). It may be that the transport processes which are dependent upon ATP hydrolysis and the PMF are linked together as a result of chemiosmotic coupling (Konings 1977, Kirstensen 1994). This would result in increased NaPT transport together with increased thymidine and uracil transport (reflected by an increase or activation of their rates of metabolism). This is shown in *E. coli* and in *P. aeruginosa* when exposed to NaPT at biocide concentrations approaching the MIC (Figs 59 & 61). Activation of thymidine and uracil metabolism is also exhibited when cells of *E. coli* are exposed to MIC levels of ZnPT. The difference in molecular structure between NaPT and ZnPT, and therefore the dissimilarity between ZnPT and nicotinic acid, suggests that the stimulation of substrate metabolism may not result in the increased uptake of ZnPT

by the nicotinic acid transport system. However, it may be facilitated by another chemiosmotically linked substrate transport system such as thymidine or uracil which are dependent upon the PMF (Table 11).

If the activation of thymidine and uracil metabolism is considered together with the activation of glucose, acetate and proline metabolism, then it would seem more likely that it is the breakdown of membrane potentials, pH gradients, concentration gradients and membrane integrity which is occurring and that the substrates are passively diffusing into the cytosol, subsequently inducing activated substrate metabolism.

**Inhibition of ATP Metabolism by NaPT and ZnPT**

Concentrations of ATP in cells of *E. coli* and *P. aeruginosa* decreased upon exposure to the pyrithione biocides. This indicates ATP metabolism to be sensitive to the presence of the pyrithione biocides. The bacterial levels of ATP proved remarkably sensitive to the presence of the pyrithiones. This was exhibited by almost total loss of intracellular ATP in cells which were exposed to both low (20% MIC) and high levels of biocide (80% MIC) (Figs 63 to 70). This decrease in intracellular ATP levels may be the result of the effect of the pyrithione biocides on substrate metabolism. However, only low levels of metabolic inhibition have been observed (Figs 59 to 62). Another possibility is that the observed decrease in ATP levels may be the result of an increased rate of ATP consumption by biocide exposed cells in order to combat and repair biocide induced cellular damage. This suggests that ATP production within the biocide exposed cells is almost balanced by ATP hydrolysis required to counteract biocide induced stress. Therefore, at any single point, the ATP assay is exhibiting the presence of free ATP within the bacterial cell and only minimal concentrations of ATP are observed. The increased turn over in cellular ATP may also account for the observed activation of substrate metabolism. This may result in a feedback cycle which causes an imbalance in intracellular ATP and cyclic AMP levels (Equation 13).

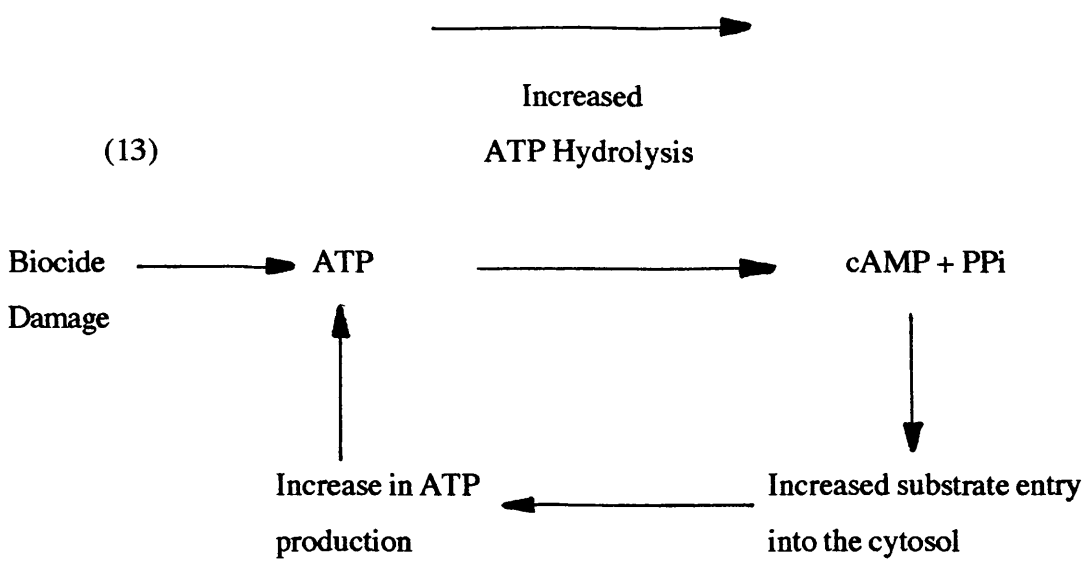


(13)

The biocide exposed cell may increase ATP metabolism in order to maintain the energy required to repair the biocide induced cell damage (Equation 13). This increase may be reflected in the increased substrate metabolism observed in earlier experiments (Figs 59 to 62). The higher levels of ATP present would act as a signal for the cell to produce cyclic AMP (cAMP) (Equation 13) and pyrophosphate (PPi) (Postma 1987, Stauffer 1987). The utilisation of ATP to repair cellular damage and produce cAMP would result in low intracellular ATP levels (exhibited by the luciferin-luciferase assay, Figs 63 to 70). This imbalance in intracellular ATP and intracellular cAMP is the metabolic signal for increased substrate uptake into bacterial cells (Postma 1987, Equation 13). The final outcome of this scheme may therefore be stimulated entry of substrate into biocide exposed cells in order to produce sufficient ATP to combat biocide induced stress. The excess production of ATP would continue until the biocide damage is either alleviated and intracellular ATP levels return to normal, or until the cell dies as a result of biocide exposure.

The isolation of NaPT and ZnPT in the cytosol indicates that these biocides enter the bacterial cell (Table 16). The chelating properties of the pyrithiones together with their potential to carry out thiol and amine interactions may account for the coagulated appearance of the cytosol. The activation of substrate metabolism by the pyrithione biocides may be explained as an intracellular effect upon ATP metabolism and the balance between cellular levels of ATP and cAMP. This information indicates that NaPT and ZnPT possess

intracellular modes of action towards *E. coli* and *P. aeruginosa.*

## Protonophoric Activity of the Pyrithione Biocides

The inhibition of various membrane-bound processes by NaPT and ZnPT such as ATP production and nutrient transport have been discussed (pages 205, 206, 208 and 210). These biochemical processes are dependent upon transmembrane pH and proton gradients and are subsequently driven by these gradients. The metal cationic chelating abilities of the pyrithione compounds have also been discussed (page 68). The chelating abilities of these molecules subsequently allow the pyrithiones to chelate and sequester protons. The membrane depolarisation of *Neurospora crassa* has been shown to occur readily with the exposure to NaPT (Ermolayeva *et al* 1995). Depolarisation of the transmembrane electro-potential is due to the disruption of pH gradients across the membrane. This suggests, therefore, that the sequestration of protons by NaPT disrupts the transmembrane potential. A loss of protons from the cytosol would result in decreased ATP production, which is dependent upon the PMF and therefore the intracellular presence of protons (pages 209 and 210). The chelation of hydrogen ions by NaPT may, therefore, explain the observed decrease of intracellular ATP content when the pyrithiones are added to cells of *P. aeruginosa* and *E. coli* (Figs 63 to 70). This proposed protonophoric action by the pyrithione biocides may also explain the observed inhibition of substrate catabolism of uracil and thymidine by low concentrations of biocide relative to the MIC. The uptake and transport of these substrates are dependent upon the PMF *via* the chemiosmotic coupling hypothesis (Figs 59 to 62, page 206).

# MEMBRANE ACTIVITY OF THE PYRITHIONE BIOCIDES

## Molecular Modelling Studies

### Interactions between Phosphatidylethanolamine and NaPT

Interactions between the phosphatidylethanolamine head group structures (phosphorylethanolamine) and NaPT or ZnPT have been exhibited in the molecular modelling studies (Figs 52c & 55 to 57). NaPT (the pyrithiolate anion) exhibited electrostatic

interactions with the head group structure, hydrogen bonding between the sulphur and oxygen molecules of the pyrithiolate ion and the amine tail of the head group. The occurrence of this interaction at the bacterial outer membrane may result in the disaggregation of the phospholipid head structure at the outer leaflet of the membrane. It may also result in the chelation of phosphoryl ethanolamine head groups from the core structure of the external lipopolysaccharide which may contribute to outer membrane disruption. In addition, chelation of divalent metal cations present on the bacterial envelope would also breakdown bacterial envelope configuration. The presence of such ions ($Mg^{2+}$ and $Ca^{2+}$) on the envelope maintains membrane integrity, the loss of which results in weakened binding of the Gram-negative outer membrane to the peptidoglycan layer *via* Braun's lipoprotein (Hoyle & Beveridge 1983a, 1983b, Beveridge 1989). The disrupted configuration of the bacterial cell envelope would then allow the passage of free pyrithione molecules across the envelope and into the cytosol. This in turn would result in the intracellular action of NaPT molecules and may allow them to interact with phospholipid head groups on the inner leaflet of the cytosolic membrane.

The chelation of metal cations at the bacterial envelope by NaPT in solution and the electrostatic interactions between NaPT and the phosphatidylethanolamine head group may account for the membrane disruption observed in cells of *P. aeruginosa* exposed to NaPT (100 $\mu$g $ml^{-1}$) (Fig 76). The appearance of ghost cells and the leakage of cytoplasmic material from partially disrupted cells may be as a result of the interactions between NaPT and the bacterial cell envelope. The appearance of NaPT in the cytosol of *P. aeruginosa* may be indicative of membrane disruption from both inside the cytosol and from the bacterial exterior.

**Interactions between Phosphatidylethanolamine and ZnPT**

Membrane activity of the pyrithione biocides is further indicated by the interactions between ZnPT and the phosphatidylethanolamine head group. The interaction between phosphatidylethanolamine and the ZnPT and NaPT has been discussed previously with reference to a direct cellular interaction of the biocides (p204) and with reference to the chelative effect of the pyrithiones at the level of the Gram-negative outer membrane (p203).

However, the exact effect of such interactions were not discussed with reference to the specific mode of action of these antimicrobial agents. The ZnPT dimer exhibited two potential interactions with the phospholipid head group (Figs 55 & 56) and one potential interaction was exhibited for the ZnPT monomer and the head group structure (Fig 57). Figure 55 exhibits bonding between the amine tail of the head group and the sulphur and oxygen atoms of the ZnPT dimer. Disruption of the ZnPT dimer's configuration occurs as a result of this interaction. Figure 56 exhibits a potential interaction between the phosphoric acid group of the phospholipid head structure and the central zinc atom of one of the ZnPT monomers within the dimer. This has resulted in the breakdown of the original interaction between the two ZnPT monomers (the zinc-oxygen bridges) and may result in the release of a separate ZnPT monomer which would be capable of reaction with adjacent phospholipid head groups. The interaction between the ZnPT monomer and the phospholipid (Fig 57) is similar to that exhibited by the ZnPT dimer reaction in figure 56. This is suggested by the potential chelation of the zinc atom from the monomer by the phosphoric acid group of the phospholipid head structure (Fig 57). The disruption of the ZnPT monomeric and dimeric configuration by the phospholipid head groups may result in the release of up to four free pyrithiolate ions. The chelation of the zinc atom would result from the interaction of adjacent phospholipids upon a singular ZnPT molecule. This would occur at the Gram-negative outer membrane which may already be disrupted by the interactions of the phosphatidylethanolamine head groups and bound ZnPT molecules. Such interactions would allow the released pyrithiolate ions to diffuse across the disrupted membrane into the bacterial cell. Such a migration would subsequently allow the pyrithiolate anions to act at an intracellular level where they could chelate important cationic molecules (Figure 80). This suggested mode of action for the pyrithione biocides is not dissimilar to that of the quaternary ammonium compounds (QACs) which destabilise the ionic content of the bacterial membrane prior to disruption of the phospholipid bilayer (Broxton *et al* 1984, Woodcock 1988). It has been reported that the pyrithione ring structure is structurally analogous to some of the QAC group members (Hyde & Nelson 1984, Fig 26). However, literature survey has revealed no instances where the suggestion has been made that the pyrithione biocides act as pseudo-QAC antimicrobial agents. The experimental evidence from this study supports the above hypothesis.

Further experimental evidence which indicates confirmation of the interactions of the pyrithiones and the phosphatidylethanolamine head group lies in the neutralisation of ZnPT and NaPT action by this phospholipid (Table 7). As discussed previously (p203), the chemical interactions provided by the computer generated molecular modelling data did not take into account the presence of other cationic molecules and the exact conditions within bacterial growth medium. Therefore, the interactions may only be regarded as being potential interactions which require further experimental evidence. Subsequently, the observed neutralisation of pyrithione activity by phosphatidylethanolamine (Table 7) together with the presence of pyrithione in the cell envelope of *P. aeruginosa* (Table 16) strongly supports the occurrence of such interactions.

## Inhibition of Metabolism as an Indication of Membrane Activity

### Intracellular ATP Levels

The disintegration of membrane integrity and the metabolic controlling factors which are maintained by the membrane (pH gradients, PMF, concentration gradients) results in the decrease of intracellular ATP levels (Harold 1972). This has been shown with various membrane active agents such as fentichlor, PHMB antimicrobial agents, chlorhexidine and alexidine (Bloomfield 1974, Broxton *et al* 1983a, Chopra *et al* 1987, Chawner & Gilbert 1989b). It has also been reported that the pyrithione biocides are agents capable of inducing reduction of intracellular ATP levels and ATP dependent transport processes in fungi as a result of depolarisation of the membrane potential (Chandler & Segel 1978, Ermolayeva *et al* 1995). The effect of NaPT and ZnPT upon intracellular ATP levels in both *E. coli* and *P. aeruginosa* has been discussed in reference to the intracellular activity of the pyrithione biocides (p210). However, the evidence for membrane action by these antimicrobial agents, which indicates disruption of Gram-negative cellular integrity, suggests that NaPT and ZnPT may reduce intracellular ATP levels as a direct result of membrane action (Figs 63 to 70). The disruption of pH gradients and concentration gradients would occur as a result of the disruption of membrane integrity by NaPT and ZnPT. The breakdown of such processes would reduce ATP production by the PMF dependent $F_1/F_0$ membrane-bound ATPase and the chemiosmotic coupling process (Harold 1972, Konings

**Figure 80:** (1) Suggested mode of action for zinc pyrithione at the level of the bacterial membrane. (2) The association of ZnPT with the the phospholipid head groups would result in the disruption of the lipid bilayer. (3) This would result in the chelation of the zinc atom from the ZnPT dimer, releasing pyrithiolate ions (**PT** $^{-}$) which may passively diffuse across the damaged membrane and chelate intracellular cationic structures ($Mn^{2+}$, $Ca^{2+}$, $Mg^{2+}$, $K^{+}$, proteins and metalloenzymes).

(1)

ZnPT +

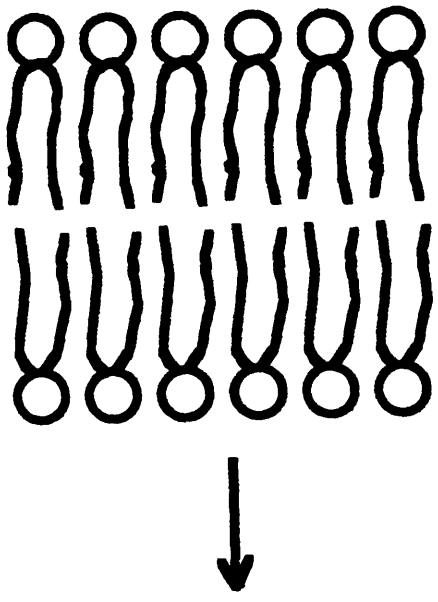


Cytosol

(2)

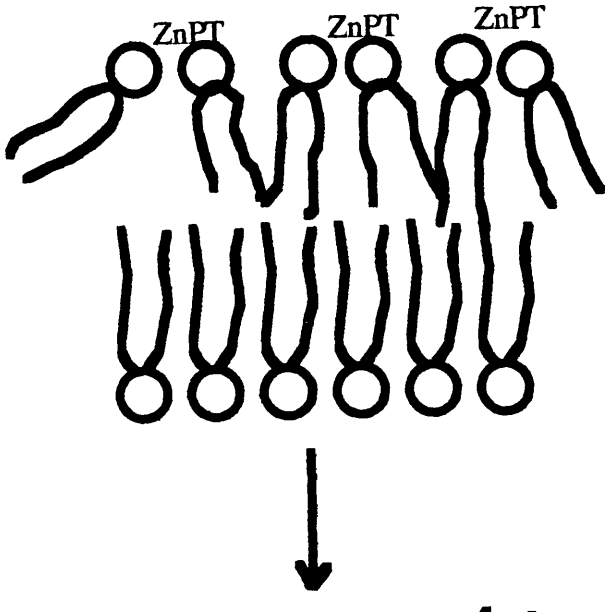


(3)

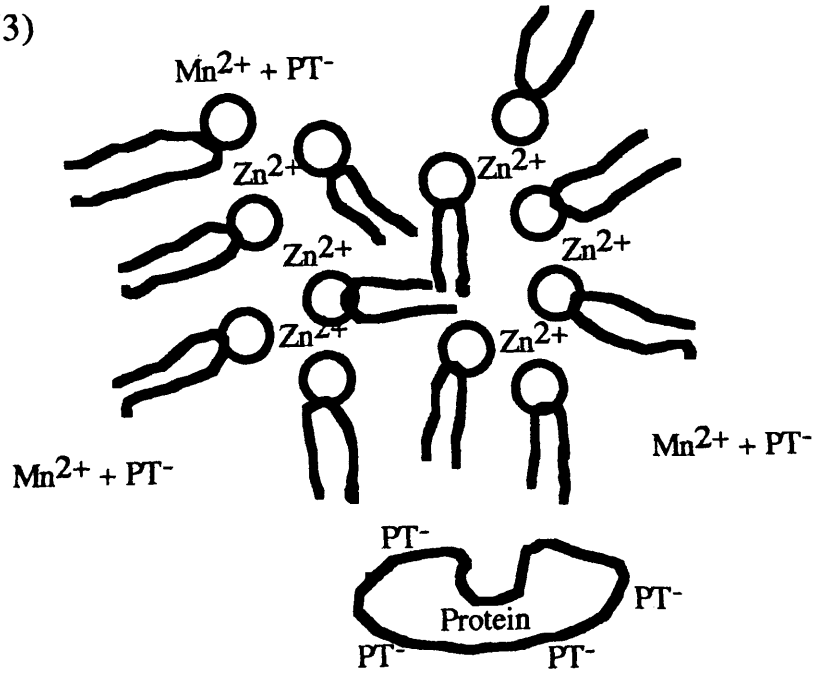

1977, Kirstensen 1994). The $F_1/F_0$ ATPase is also involved in the active transport of solutes into bacterial cells and it's breakdown would decrease the level of substrates being actively transported into the cytosol (Konings 1977). This suggests that the reduced catabolic activity of substrates exhibited in figures 59 to 62 is a function of reduced ATP production by pyrithione exposed cells of *E. coli* and *P. aeruginosa.*

**Activation of Substrate Metabolism**

The stimulation of substrate metabolism at MIC levels of NaPT and ZnPT in *E. coli* and *P. aeruginosa* may be as a result of the membrane activity of these biocides. The disruption of the bacterial envelope and the leakage of cytoplasmic constituents has been observed in cells of *P. aeruginosa* exposed to MIC levels of NaPT (Fig 76). This may suggest that passive diffusion of substrates into the bacterial cytosol may occur at concentrations of pyrithiones which approach the MIC (Figs 59 to 62). If the stimulation of substrate metabolism was dependent or related solely to ATP production, an increase in intracellular ATP levels correlating to the activation of substrate metabolism at biocide concentrations of 80% of MIC would have been observed. However, this was not the case. Therefore stimulation of metabolic activity must be due to a different mechanism. Decreased intracellular ATP levels by NaPT and ZnPT were similar at low levels of biocide (20%) and at higher concentrations (80%). As biocide concentration increases, the degree of membrane disruption may also increase. This would allow the passive diffusion of substrates from the medium into the cytosol where they would be catabolised by cytosolic enzymes. However, ATP levels would still remain low as a result of decreased membrane integrity (Harold 1972, Konings 1977). The effect of such membrane activity would be high levels of substrate metabolism and low levels of ATP production. This hypothesis reflects the results obtained from the metabolic studies. This further suggests that the pyrithione biocides disrupt membrane integrity in *E. coli* and *P. aeruginosa.*

## Leakage of Intracellular Components as Evidence of Membrane Activity by the Pyrithione Biocide

Known membrane active agents such as cetrimide, PHMB, chlorhexidine and alexidine exhibit leakage of intracellular components as an effect of the disruption of membrane integrity (Wiseman 1964, Salton 1968, Chopra *et al* 1987, Denyer & Hugo 1991b). The degree of membrane activity may be monitored in the order which cytoplasmic constituents leak from cells exposed to the membrane active agents (Salton 1968, Denyer & Hugo 1991b, Beggs 1992). The order is normally as follows, leakage of potassium ions followed by purines and pyrimidines (material which absorbs light at 260nm), then phosphate molecules, small strands of DNA and RNA and finally, free ribosomes (Salton 1968, Denyer & Hugo 1991b).

Figures 71 to 74 exhibit the effects of NaPT and ZnPT respectively, upon membrane integrity in *E. coli* and *P. aeruginosa* as a function of the leakage of cytoplasmic material (potassium ions and material which absorbs light at 260nm). NaPT against *E. coli* and ZnPT against *E. coli* and *P. aeruginosa* exhibit very little change in the potassium ion levels of the bathing solution. This would immediately suggest that these antimicrobial agents have no direct effect upon potassium ion leakage from exposed bacterial cells. However, the apparent lack of movement in potassium ion levels may be as a result of a chelation effect exhibited by NaPT and ZnPT (Al-Adham *et al* 1995). Free pyrithiones present in the bacterial bathing solution would chelate free potassium ions which are also present. However, as there is no apparent movement in the potassium ion levels in the bathing solution, the potassium ions must be replenished from another source. The source of potassium ions entering the bathing solution must be from leaking cells of *E. coli* and *P. aeruginosa* which have been exposed to pyrithiones. Such an event would result in no significant increase or decrease in potassium ion levels in the bacterial bathing solution. Furthermore, the observation of leakage of material which absorbs light at 260nm from cells of *E. coli* and *P. aeruginosa* exposed to NaPT and ZnPT indicates that leakage of potassium ions must also be occurring. The leakage of material which absorbs light at 260nm from cells exposed to the pyrithiones was shown to occur at a greater level than that exhibited by the known membrane active agent cetrimide (Al-Adham *et al* 1995) (Figs 73 & 74). Upon exposure of *E. coli* to cetrimide, the

$E_{260nm}$ increased from approximately 0.2 to 0.3. When exposed to NaPT the $E_{260nm}$ increased from 0.2 to 1.4 and upon exposure to ZnPT it increased to 1.9. Similar results were also obtained for *P. aeruginosa* when exposed to cetrimide and the pyrithiones (Figs 73 & 74).

Exposure of cells of *P. aeruginosa* to NaPT resulted only in the chelation of potassium ions in the bathing solution (Fig 72). This was reflected as a decrease in bathing solution potassium ion content. It is known that the exopolysaccharide layer (EPS) and the outer membrane of *Pseudomonas* species possess higher divalent metal ion content than most other bacterial species. This may account for the presence of NaPT in assayed fractions of the cell envelope of *P. aeruginosa* and may be explained by the chelation of metal ions in the EPS and outer membrane of *P. aeruginosa* by NaPT. The NaPT would then be permanently bound to these components of *P. aeruginosa* cells. In turn, this may explain the lack of observed leakage of potassium ions from *P. aeruginosa* cells which were exposed to NaPT (Fig 72). NaPT in these subcellular envelope fractions may chelate some of the potassium ions which are leaking from cells of *P. aeruginosa*. This chelation effect in the cell envelope of *P. aeruginosa* would explain the observed decrease in potassium ion levels in the bathing solution. The observation of leakage of material which absorbs light at 260nm (which by definition is composed of much larger particulate and molecular structures than potassium ions) suggests that the observed result concerning the leakage of potassium ions from *P. aeruginosa* is due to an extracellular chelation effect. The data from the leakage studies and the observation of potential interactions between the pyrithione biocides and membrane phospholipid molecules suggests that NaPT and ZnPT induce the leakage of intracellular material as a result of membrane disruption.

# CONCLUSION

The growth inhibitory data suggests that ZnPT is a more effective bacteristatic agent than NaPT. A *Pseudomonas*-gap was observed between *E. coli* and *P. aeruginosa* when both cells were exposed to ZnPT. This was not shown for NaPT which gave similar MIC values for both antimicrobial agents. The increased growth inhibitory activity of ZnPT over NaPT exhibited no proportionality in the killing data which suggests that both biocides are poor bactericidal agents. The action of both pyrithiones was neutralised by the addition of EDTA to the test cultures. This is indicative of some type of membrane effect by EDTA, which decreased the inhibitory action of both biocides. Thiol interactions between ZnPT and cysteine were shown to occur by the neutralisation of ZnPT activity in the presence of the thiol-containing amino acid. This was further indicated by the occurrence of thiol interactions between cysteine and ZnPT in computer generated molecular modelling data. The antimicrobial activities of both NaPT and ZnPT were neutralised by phosphatidylethanolamine and strong indications of the types of interactions between these compounds were exhibited using computer generated molecular modelling. Both biocides exhibited intracellular activity. This is supported by the exhibition of inhibition towards substrate catabolism. The observation of pyrithione biocides in the cytosol of fractionated cells, using a colourimetric assay, and the coagulation of the cytosol of cells of *P. aeruginosa* exposed to NaPT, exhibited by transmission electron microscopy, also suggests some degree of intracellular activity.

A body of evidence exists which suggests that NaPT and ZnPT are mainly membrane interactive. This is exhibited by the activation of substrate metabolism as biocide concentration increases. The increasing biocide levels were thought to allow passive diffusion of substrate across a partially disrupted bacterial membrane. ATP levels in biocide exposed cells were shown to be sensitive to the pyrithiones. The disruption of transmembrane oxidative phosphorylation processes (ie; the PMF and active transport) were thought to be the mechanism by which the intracellular ATP levels were decreased. The disruption of such processes is also implicated in the decreased rates of substrate catabolism of pyrithione biocide exposed cells. This information, together with the observation of potential interactions between these biocides and phospholipid molecules and the leakage of

intracellular material from pyrithione exposed cells suggests that the pyrithione biocides possess membrane active properties. However, evidence from this study indicates these agents to be mainly membrane active with some potential activity at an intracellular level. Subsequently, this suggests that the pyrithione biocides induce bacterial death as the result of a cumulative inhibitory effect.

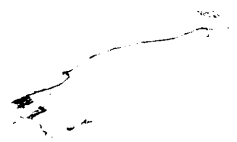

# SUGGESTIONS FOR FUTURE WORK

1) Investigation of the protonophoric activity of the pyrithione antimicrobial agents *via* the use of a pH probe in biocide exposed washed cell suspensions.

2) Development of an assay for the pyrithione biocides which enables the exact concentration of pyrithione in subcellular fractions to be determined. This would enable the elucidation of the uptake isotherm for the pyrithiones in microorganisms and may facilitate determination of the mode of absorption of these biocides into microbial cells.

3) The use of NMR spectroscopy upon pyrithione-phosphatidylethanolamine reaction mixtures. This would allow the observation of a direct interaction between microbial phospholipids and the pyrithione biocides. Such an experiment would help to prove or otherwise, that the suggested interactions obtained from the computer generated molecular modelling data are correct.

4) Observation of the effect of the pyrithiones upon the cell envelope of bacterial cells. This may be observed as changes in hydrophobicity and increased exoantigen production. This would help determine the effect of the pyrithiones upon bacterial resistance and virulence factors.

5) Utilisation of SDS-PAGE to observe the effect of the pyrithiones upon the cell envelope protein profile of bacterial cells. This may elucidate the presence of a specific carrier protein for the pyrithione biocides. The observation of the conditions which induce the production of such a protein may elucidate the observation of phenotypic or genotypic bacterial resistance towards these antimicrobial agents.

6) The use of radio-label techniques to investigate the potential effects of the pyrithione biocides as inhibitors and analogues of the nicotinic acid metabolic pathway.

# REFERENCES


ACHAEMPONG, Y.B. & WISEMAN, D. (1981) The uptake of nonyl and tetradecylbenzyldimethylammonium compounds by *Escherichia coli*. *Journal of Pharmacy and Pharmacology*. **33**, 30P.

AL-ADHAM, I. S. I., DINNING, A. J., EASTWOOD, I. & COLLIER, P. J. (1995) Cell membrane effects of some common biocides. *Submitted to International Biodeterioration and Biodegradation*, August 1995.

ALBERT, A., GIBSON, M. I. & RUBBO, D. (1953) The influence of chemical constitution on antibacterial activity. Part VI: The bactericidal action of 8-hydroxyquinoline (oxine). *British Journal of Experimental Pathology*. **36**, 119-130.

ALBERT, A., REES, C.W. & TOMLINSON, J.H. (1956) The influence of chemical constitution on anti-bacterial activity. Part VIII. 2-Meracptopyridine-N-oxide, and some general observations on metal binding agents. *British Journal of Experimental Pathology*. **37**, 500-511.

ASMUS, S.D. (1990) Sulfur centred free radicals. *Methods in Enzymology*. **186**, 168-180.

BARNETT, B.L., KRETSCHMAR, H.C. & HARTMAN, F.A. (1977) Structural characterization of Bis (N-oxopyridine-2-thionato) zinc(II). *Inorganic Chemistry*, **16** (8), 1834-1838.

BALDRY, M.G.C. & FRASER, J.A.L. (1988)Disinfection with peroxygens. In: *Industrial Biocides*. pp91-116. Payne (Ed), John Wiley and Sons, Chichester, UK.

BEGGS, W. H. (1992) Direct membrane damage and miconazole lethality. *Research Communications in Chemical Pathology and Pharmacology*. **77** (2), 249-252.

BERNHEIM, F. (1976) Effect of sulphydryl reagents on potassium ion efflux from *Pseudomonas aeruginosa* caused by amines. *Microbios Letters*, **3**, 111-115.

BERNSTEIN, J. & LOSEE, K. (1957) Heavy metal derivatives of 1-hydroxy-2-pyridinethiones and method of preparing same. *United States Patent Document* 2 809 971. Olin Matheson Chemical Corporation.

BEVERIDGE, E. G., BOYD, I., DEW, I., HASWELL, M. & LOWE, C. W. G. (1991) Electron and light microscopy of damaged bacteria. In: *Mechanisms of Action of Chemical Biocides their Study and Exploitation.* pp135-154. Denyer & Hugo (Eds). Blackwell Scientific Publications, Oxford, UK.

BEVERIDGE, T.J. (1988) The bacterial cell surface: General considerations towards design and function. *Canadian Journal of Microbiology*, **34**, 362-372.

BEVERIDGE, T.J. (1989) Role of cellular design in bacterial metal accumulation and mineralization. *Annual Reviews in Microbiology.* **43**, 147-171.

BEVERIDGE, T.J. (1993) Current trends and future prospects in prokaryotic envelope research: a microscopists view. *Journal of Applied Bacteriology Symposium Supplement*, **74**, 143S-153S.

BLACK, J.G. & HOWES, D. (1978) Toxicity of pyrithiones. *Clinical Toxicology.* **13** (1), 1-26.

BLOOMFIELD, S.F. (1974) The effect of the phenolic antibacterial agent fentichlor on energy coupling in *Staphylococcus aureus. Journal of Applied Bacteriology*, **37**, 117-131.

BLOOMFIELD, S.F. (1991) Methods for assessing antimicrobial activity. In: *Mechanisms of Action of Chemical Biocides their Study and Exploitation.* pp1-22. Denyer & Hugo (Eds). Blackwell Scientific Publications, Oxford, UK.

BOIVIN, J., CREPON, E. & ZARD, S.Z. (1992) Generation of hydroxyl radicals from 1-hydroxypyridine-2(1H)-thione and their application to organic synthesis. *Bulletin de la Societe du Chimie Francaise.* **129**, 145-150.

BOYCE, J.M., POTTER-BYNOE, G., OPAL, S.M., DZIOBEK, L. & MEDEIROS, A.A. (1990). Tracing the source of a *Staphylococcus epidermis* "outbreak" in a hospital. *Journal of Infectious Diseases*, **161**, 493-499.

BOYD, R.F. *General Microbiology* (2nd ed). 1988 Times Mirror/Mosby College Publishing, Missourri, USA.

BROWN, G.M. & WILLIAMSON, J.M. (1987) Biosynthesis of folic acids, riboflavin, thiamine and pantothenic acid. In: *Escherichia coli and Salmonella typhimurium Cellular and Molecular Biology* pp521-538. Neidhardt *et al* (Eds), ASM Press, Washington DC, USA.

BROXTON, P., WOODCOCK, P.M. & GILBERT, P. (1983a) Action of some polyhexamethylene biguanides upon the respiration of *Escherichia coli* ATCC 8739. *Journal of Pharmacy and Pharmacology Supplement.* **35**, 66.

BROXTON, P., WOODCOCK, P.M. & GILBERT, P. (1983b) A study of the antibacterial activity of some polyhexamethylene biguanides towards *Escherichia coli* ATCC 8739. *Journal of Applied Bacteriology.* **54**, 345-353.

BROXTON, P., WOODCOCK, P.M., HEATLEY, F. & GILBERT, P. (1984) Interaction of some polyhexamethylene biguanides and membrane phospholipids in *Escherichia coli*. *Journal of Applied Bacteriology*, **57**, 115-124.

BRÖZEL, V. S. & CLOETE, T. E. (1994) Resistance of *Pseudomonas aeruginosa* to isothiazolone. *Journal of Applied Bacteriology.* **76**, 576-582.

CHANDLER, C. J. & SEGEL, I. H. (1978) Mechanism of the antibacterial action of pyrithione: Effects on membrane transport, ATP levels and protein synthesis. *Antimicrobial Agents and Chemotherapy.* **14** (1), 60-68.

CHAPMAN, D.G. (1987) Preservatives available for use. In: *Preservatives in the Food, Pharmaceutical and Environmental Industries.* pp177-196. Board *et al* (Eds), Blackwell Scientific Publications, Oxford, UK.

CHAWNER, J.A. & GILBERT, P. (1989a) A comparative study of the bactericidal and growth inhibitory activities of the bisbiguanides alexidine and chlorhexidine. *Journal of Applied Bacteriology*, **66**, 243-252.

CHAWNER, J.A. & GILBERT, P. (1989b) Interaction of the bisbiguanides chlorhexidine and alexidine with phospholipid vesicles: evidence for separate modes of action. *Journal of Applied Bacteriology*, **66**, 253-258.

CHOPRA, I., JOHNSON, S. C. & BENNETT, P. M. (1987) Inhibition of *Providencia stuartii* cell envelope enzymes by chlorhexidine. *Journal of Antimicrobial Chemotherapy*. **19**, 743-751.

COHEN, S.C. (1979) Comparative biochemistry and drug design for infectious disease. *Science*, **205**, 964-970.

COLLIER, P.J., AUSTIN, P. & GILBERT, P. (1990a) Uptake and distribution of some isothiazolone biocides into *Escherichia coli* ATCC 8739 and *Schizosaccharomyces pombe* NCYC 1354. *International Journal of Pharmaceutics*. **66**, 201-206.

COLLIER, P.J., RAMSAY, A.J., AUSTIN, P. & GILBERT, P. (1990b) Growth inhibitory and biocidal activity of some isothiazolone biocides. *Journal of Applied Bacteriology*. **69**, 569-577.

COLLIER, P.J., RAMSAY, A.J., WAIGH, R.D., DOUGLAS,K.T., AUSTIN, P. & GILBERT, P. (1990c) Chemical reactivity of some isothiazolone biocides. *Journal of Applied Bacteriology*. **69**, 578-584.

COLLIER, P.J., AUSTIN, P. & GILBERT, P. (1991) Isothiazolone biocides: Enzyme inhibiting pro-drugs. *International Journal of Pharmaceutics*. **74**, 195-201.

COONEY, J.J. (1969) Effects of polyurethane foams on microbial growth in fuel-water systems. *Applied Microbiology*. **17** (2), 227-231.

COOPER, S. (1991) *Bacterial Growth and Division, Biochemistry and Regulation of Prokaryotic and Eukaryotic Division Cycles*. Academic Press, California, USA.

COTTON, J. E. (1963) *Some Cytological and Biochemical Effects of 2-Pyridinethiol-1-oxide*. PhD Thesis. The University of Texas, USA.

CRONAN, J. E., GENNIS, R. B. & MALOY, S. R. (1987) Cytoplasmic membrane. In: *Escherichia coli and Salmonella typhimurium Cellular and Molecular Biology*. pp31-54. Neidhardt *et al* (Eds), ASM Press, Washington DC, USA.

CROOKS, J. E. (1978) *The Spectrum in Chemistry*. Academic Press, London, UK.

DAVIES, T.W. (1985) Dissolution rate of zinc pyrithione. *International Journal of Cosmetic Science*. **7**, 153-156.

DELAHUNT, C.S., STEBBINS, R.B., ANDERSON, J. & BAILEY, J. (1962) The cause of blindness in dogs given hydroxypyridinethione. *Toxicology and Applied Pharmacology*. **4**, 286-288.

DENYER, S.P. & HUGO, W.B, (1991a) Biocide induced damage to the bacterial cytoplasmic membrane. In: *Mechanisms of Action of Chemical Biocides, Their Study and Exploitation* pp171-188. Denyer & Hugo (Eds) Blackwell Scientific Publications, Oxford, UK.

DENYER, S.P. & HUGO, W.B. (1991b) Preface. In: *Mechanisms of Action of Chemical Biocides Their Study and Exploitation.* ppxiii - xiv. Denyer & Hugo (Eds), Blackwell Scientific Publications.

DEPARTMENT OF HEALTH. *Report of the expert committee on biocides.* 1989. Her Majesty's Stationery Office.

DEWAR, M.J.S., ZOEBISCH, E.G., HEALEY, E.F. & STEWART, J.J.P. (1985) AM1: A new general purpose quantum mechanical molecular model. *Journal of the American Chemical Society.* **107**, 3902-3909.

DONACHIE, W.D. & ROBINSON, A.C. (1987) Cell division: parameter values and the process. In: *Escherichia coli and Salmonella typhimurium Cellular and Molecular Biology.* pp1578-1593. Neidhardt *et al* (Eds), ASM Press, Washington DC, USA.

DRLICA, K. (1987) The Nucleoid. In: *Escherichia coli and Salmonella typhimurium Cellular and Molecular Biology* pp91-103. Neidhardt *et al* (Eds), ASM Press, Washington DC, USA.

EDRISSI, M., MASSOUMI, A. & DALZEIL, J.A.W. (1971) Comparative studies of 1-hydroxy-2-pyridinethione and it's metal derivatives as analytical reagents for metal ions. *Microchemistry Journal.* **16**, 538-547.

ERMOLAYEVA, E. & SANDERS, D. (1995) Mechanism of pyrithione- induced membrane depolarization in *Neurospora crassa.. Applied and Environmental Microbiology*, **61** (9), 3385-3390.

FENN, R.V. & ALEXANDER, M.T. (1988) Determination of zinc pyrithione in hair care products by normal phase liquid chromatography. *Journal of Liquid Chromatography.* **11** (16), 3403-3413.

FENN, R. V. & CSEJKA, D. A. (1982) The stability of 2-pyridinethiol-1-oxide sodium salt

as a function of pH. *Journal of the Society of Cosmetic Chemists.* **33**, 243-248.

FERRIS, F.G. & BEVERIDGE, T.J. (1986a) Physichochemical roles of soluble metal cations in the outer membrane of *Escherichia coli* K12. *Canadian Journal of Microbiology*, **32**, 594-601.

FERRIS, F.G. & BEVERIDGE, T.J. (1986b) Site specificity of metallic ion binding in *Escherichia coli* K-12 lipopolysaccharide. *Canadian Journal of Microbiology*, **32**, 52-55.

FLEMING, A. (1929) On the antibacterial action of a Penicillium with special reference to their use in the isolation of *Bacillus influenzae. British Journal of Experimental Pathology*, **10**, 226-236.

FRANKLIN, T.J. & SNOW, G.A. (1991) *Biochemistry of Antimicrobial Action.* (4th ed), Chapman and Hall, London, UK.

FREDRIKSIN, T. & FEARGEMANN, J. (1983) Double-blind comparison of a zinc pyrithione shampoo and it's shampoo base in the treatment of *Tinea versicolor. Cutis*. **31** (4), 436-437.

FRIEDMAN, S. A. (1981) *Studies on the Mode of Antimicrobial Action of Metal Complexing Thiohydroxamic Acids Against Escherichia coli*. PhD Thesis. University of San Diego, California, USA.

GABRIEL, O. (1987) Biosynthesis of sugar residues for glycogen, peptidoglycan, lipopolysaccharide and related systems. In: *Escherichia coli and Salmonella typhimurium Cellular and Molecular Biology*. pp504-511. Neidhardt *et al* (Eds), ASM Press, Washington DC, USA.

GIBSON, W. T., HARDY, W. S. & GROOM, M. H. (1985) The effect and mode of action of zinc pyrithione on cell growth II. In vivo studies. *Federation of Chemical Toxicology*. **23** (1), 103-110.

GILBERT, P. (1975) PhD Thesis. Sunderland Polytechnic.

GILBERT, P., BEVERIDGE, E.G. & CRONE, P.B. (1980) Effect of 2-phenoxyethanol upon RNA, DNA and protein biosynthesis in Escherichia coli NCTC 5933. *Microbios* **111**, 7-17.

GILBERT, P., COLLIER, P. J. & BROWN, M. R. W. (1990a) Influence of growth rate on susceptibility to antimicrobial agents: Biofilms, cell cycle, dormancy and stringent response. *Antimicrobial Agents and Chemotherapy*. **34** (10), 1865-1868.

GILBERT, P., PEMBERTON, D. & WILKINSON, D. E. (1990b) Barrier properties of the Gram-negative cell envelope towards high molecular weight polyhexamethylene biguanides. *Journal of Applied Bacteriology*. **69**, 585-592.

GILBERT, P., PEMBERTON, D. & WILKINSON, D. E. (1990c) Synergism within polyhexamethylene biguanide biocide formulations. *Journal of Applied Bacteriology*. **69**, 593-599.

GILBERT. P., BARBER, J. & FORD, J. (1991) Interaction of biocides with model membranes and isolated membrane fragments. In: *Mechanisms of Action of Chemical Biocides*. pp155-170. Denyer & Hugo (Eds), Blackwell Scientific Publications, Oxford, UK.

GILES, H., D'SILVA, A. P. & EASTON, I. A. (1974a) A general treatment and classification of the solute adsorption isotherm. Part II. Experimental interpretation. *Journal of Colloid and Interface Science*. **47** (3), 766-778.

GILES, H., SMITH, D. & HUITSON, A. (1974b) A general treatment and classification of the solute adsorption isotherm. Part I. Theoretical. *Journal of Colloid and Interface Science*. **47** (3), 755-765.

GILES, H. & TOLIA, A. H. (1964) Studies in adsorption. XIX. Measurement of external specific surface of fibres by solution adsorption. *Journal of Applied Chemistry*. **14**, 186-195.

GOKEL, G. W. & DURST, H. D. (1976) Crown ether chemistry: Principles and applications. *Aldrichimica Acta.* **9** (1), 3-12.

GRAHAM, L.L., BEVERIDGE, T.J. & NANNINGA, N. (1991) Periplasmic space and the concept of the periplasm. *Trends in Biochemical Sciences*, **16**, 328-329.

HALLIWELL, B. (1993) The chemistry of free radicals. *Toxicology and Industrial Health.* **9** (1 & 2), 1-21.

HANCOCK, R. E. W. & BELL, A. (1988) Antibiotic uptake into Gram-negative bacteria. *European Journal of Clinical Microbiology and Infectious Diseases.* **7** (6), 713-720.

HAROLD, F. M. (1972) Conservation and transformation of energy by bacterial membranes. *Bacteriological Reviews.* **36** (2), 172-230.

HAROLD, F. M., BAARDA, J. R., BARON, C. & ABRAMS, A. (1969) Dio 9 and chlorhexidine: Inhibitors of membrane-bound ATPase and of cation transport in *Streptococcus feacalis. Biochimica et Biophysica Acta.* **183**, 129-136.

HERSHEY, J.W.B. (1987) Protein synthesis. In: *Escherichia coli and Salmonella typhimurium Cellular and Molecular Biology.* pp613-647. Neidhardt *et al* (Eds), ASM Press, Washington DC, USA.

HOEL, P. G. (1971) *Elementary Statistics* (3rd ed). Wiley International, New York, USA.

HOLUM, J. R. (1986) *Fundamentals of General, Organic and Biological Chemistry*. 3rd Ed. J. Wiley & Sons Inc, Canada.

HOWARD, B.M.A., PINNEY, R.J. & SMITH J.T. (1993) Function of the SOS process in the repair of DNA damage induced by modern 4-quinolones. *Journal of Pharmacy and Pharmacology.* **45**, 658-662.

HOWARD, B.M.A., PINNEY, R.J. & SMITH J.T. (1994) Antagonism between bactericidal activities of 4-quinolones and coumarins gives insight into 4-quinolone killing mechanisms. *Microbios.* **77**, 121-131.

HOYLE, B. & BEVERIDGE, T. J. (1983a) Binding of metallic ions to the outer membrane of *Escherichia coli. Applied and Environmental Microbiology.* **46** (3), 749-752.

HOYLE, B. & BEVERIDGE, T. J. (1983b) Metal binding by the peptidoglycan sacculus of *Esherichia coli* K12. *Canadian Journal of Microbiology.* **30**, 204-211.

HUGO, WB & BLOOMFIELD, SF. (1971) Studies on the mode of action of the phenolic antibacterial agent Fentichlor against *Staphylococcus aureus* and *Escherichia coli*: The effects of Fentichlor on the bacterial membrane and the cytoplasmic constituents of the cell. *Journal of Applied Bacteriology.* **34**, 569-578.

HUGO, W.B. & LONGWORTH, A.R. (1964) Some aspects of the mode of action of chlorhexidine. *Journal of Pharmacy and Pharmacology*, **16**, 655-622.

HUGO, W.B. & LONGWORTH, A.R. (1965) Cytological aspects of the mode of action of chlorhexidine diacetate. *Journal of Pharmacy and Pharmacology*, **17**, 28-32.

HUGO, W.B. & LONGWORTH, A.R. (1966) The effect of chlorhexidine on the electrophoretic mobility, cytoplasmic constituents, dehydrogenase activity and cell walls of *Escherichia coli* and *Staphylococcus aureus*. *Journal of Pharmacy and Pharmacology*, **18**, 569-578.

HYDE, G.A. & NELSON, J.D. (1984) Sodium and zinc omadine. In: *Cosmetic and Drug Preservation: Principles and practice.* pp 115-128. Kabara (Ed). Marcel Dekker, New York, USA.

HYDE, G.A. & AUERBACH, H.M. (1979) Formulation techniques for zinc pyrithione

antidandruff shampoos. *Cosmetics and Toiletries.* **94**, 57-59.

IMOKAWA, G. & OKAMOTO, K. (1982) The inhibitory effect of zinc pyrithione on the epidermal proliferation of animal skins. *Acta Dermatovener (Stockholm).* **62**, 471-475.

IMOKAWA, G. & OKAMOTO, K. (1983) The effect of pyrithione on human skin cells *in vitro. Journal of the Society of Cosmetic Chemists.* **34**, 1-11.

IMOKAWA, G., SHIMIZU, H. & OKAMOTO, K. (1982) Antimicrobial effect of zinc pyrithione. *Journal of the Society of Cosmetic Chemists.* **33**, 27-37.

INGRAHAM, J.L., MAALOE, O. & NEIDHARDT, F.C. (1983) *Growth of the Bacterial Cell.* Sinauer Associates Inc. Maryland, USA.

JANN, K., GOLDEMAN, G., WEISBERGER, C., WOLF-ULLISCH, C. & KANEGASAKI, S. (1982) Biosynthesis of the O9 antigen of *Escherichia coli. European Journal of Biochemistry*, **127**, 157-164.

KARSTEN, K. S. & TAYLOR, W. S. (1968) Germicidal detergent compositions. *United States Patent* 3 412 033. R. T. Vanderbilt Co.

KARSTEN, K. S., TAYLOR, W. S. & PARRAN, J. J. (1966) Methods of combatting dandruff with pyridinethione metal salts detergent compositions. *United States Patent* 3 236 733. R. T. Vanderbilt Co and The Proctor and Gamble Co.

KAY, W.W. & TRUST, T.J. (1991) Form and functions of the regular surface array (S-layer) of *Aeromonas salmonicida. Experientia*, **47**, 412-414.

KHATTAR, M.M. & SALT, W.G. (1993) Aspects of the mode of action of pyrithione against *Klebsiella pneumoniae. Journal of Chromatography.* **5** (S1), 175-177.

KHATTAR, M.M., SALT, W.G. & STRETTON, J.R. (1988) The influence of pyrithione on

the growth of microorganisms. *Journal of Applied Bacteriology.* **64**, 265-272.

KHATTAR, M.M., SALT, W.G. & STRETTON, J.R. (1989) Growth and survival of *Klebsialla pneumoniae* in the presence of pyrithione. *Journal of Chromatography.* **1** (S4), 224-226.

KIRSTENSEN, S. R. (1994) Importance of various types of metabolic inhibition for cell damage caused by direct membrane damage. *Molecular and Cellular Biochemistry.* **140** (1), 81-84.

KONINGS, W. N. (1977) Active transport of solutes in bacteria. *Advances in Microbiological Physics.* **15**, 171-251.

KROLL, R.G. & PATCHETT, R.A. (1991) Biocide-induced perturbations of aspects of cell homeostasis: Intracellular pH, membrane potential and solute transport. In: *Mechanisms of Action of Chemical Biocides.* pp189-202. Denyer & Hugo (Eds), Blackwell Scientific Publications, Oxford, UK.

LAMBERT, P. A. & HAMMOND, S. M. (1973) Potassium fluxes, first indications of membrane damage in microorganisms. *Biochemistry and Biophysics Research Communications.* **54**, 796-799.

LAWRENCE, J. V. & MAIER, S. (1977) Correction for the inherent error in optical density readings. *Applied and Environmental Microbiology.* **33** (2), 482-484.

LEYDEN, M. D. & KLIGMAN, A. M. (1979) Dandruff-cause and treatment. *Cosmetics and Toiletries.* **94**, 23-28.

LEYDEN, M. D., MCGINLEY, K. J. & KLIGMAN, A. M. (1976) Role of microorganisms in dandruff. *Archives of Dermatology.* **112**, 333-338.

LORIAN, V. & ATKINSON, B. (1976) Effects of subinhibitory concentrations of antibiotics

on cross walls of cocci. *Antimicrobial Agents and Chemotherapy*, **9**, 1043-1053.

MCMACKEN, R., SILVER, L. & GEORGOPOULOS, C. (1987) DNA replication. In: *Escherichia coli and Salmonella typhimurium Cellular and Molecular Biology*. pp564-612. Neidhardt *et al* (Eds), ASM Press, Washington DC, USA.

MALONEY, P. C. (1987) Coupling to an energized membrane: Role of ion motive gradients in the transduction of metabolic energy. In: *Escherichia coli and Salmonella typhimurium Cellular and Molecular Biology*. pp222-243. Neidhardt *et al* (Eds), ASM Press, Washington DC, USA.

MARKS, R., PEARSE, A.D. & WALKER, A.P. (1985) The effects of a shampoo containing zinc pyrithione on the control of dandruff. *British Journal of Dermatology*. **112**, 415-422.

MARTIN, N.L. & BEVERIDGE, T.J. (1986) Gentamicin interaction with *Pseudomonas aeruginosa* cell envelope. *Antimicrobial Agents and Chemotherapy*. **29** (6), 1079-1087.

MICHAELIS, L. & MENTEN, M.L. (1913) Die kinetik der invertinwirkung. Biochemistrie Zeitschrift. **49**, 333-369.

MOE, R., KIRPAN, J. & LINEGAR, C.R. (1960) Toxicology of hydroxypyridinethione. *Toxicology and Applied Pharmacology*. **2**, 156-170.

MONOD, J. (1949) The growth of bacterial cultures. *Annual Reviews in Microbiology*, **3**, 371-394.

MOORE, K.E. & STRETTON, R.V. (1981) The effect of pH, temperature and certain media constituents on the stability and activity of the preservative Bronopol. *Journal of Applied Bacteriology*. **51**, 483-494.

MOPAC 93, QCPE Program 455, Dept of Chemistry, Indiana University, Bloomington,

Indiana, USA.

MORRIS, C.E. & WELCH, C.M. (1983) Antimicrobial finishing of cotton with zinc pyrithione. *Textiles Research Journal.* **53** (12), 725-728.

NAKAJIMA, K., OHTA, M., YAZAKI, H. & NAKAZAWA, H. (1993) High performance liquid chromatographic determination of zinc pyrithione in antidandruf shampoos using on-line copper chelate formation. *Journal of Liquid Chroimatography.* **16** (2), 487-496.

NATIONAL COLLECTION OF INDUSTRIAL AND MARINE BACTERIA (1994) *Strains catalogue.* Media number 149, *Pseudomonas* media.

NEIHOF, R.A., BAILEY, C.A., PTOUILLET, C. & HANNAN, P.J. (1979) Photodegradation of mercaptopyridine-N-oxide biocides. *Archives of Environmental Contamination and Toxicology.* **8**, 355-368.

NELSON, J. D. (1990) Chitosan pyrithione as an antimicrobial agent useful in personal care products.*United States Patent Document* 4 957 908.

NELSON, J.D. & HYDE, G.A. (1981) Sodium and zinc omadine antimicrobials as cosmetic preservatives. *Cosmetics and Toiletries.* **96**, 87-90.

NEU, H.C. (1993) Oral Beta-lactam antibiotics from 1960-1993. *Infectious Diseases and ClinicalPractice*, **2** (6), 394-404.

NEUHARD, J. & NYGAARD, P. (1987) Purines and Pyrimidines. In: *Escherichia coli and Salmonella typhimurium Cellular and Molecular Biology. pp445-473.* Neidhardt *et al* (Eds), ASM Press, Washington DC, USA.

NIKAIDO, H. & VAARA, M. (1987) Outer Membrane. In: *Escherichia coli and Salmonella typhimurium Cellular and Molecular Biology* p13-15. Neidhardt *et al* (Eds), ASM Press

Washington DC, USA.

OLIVER, D, B. (1987) Periplasm and protein secretion. In: *Escherichia coli and Salmonella typhimurium Cellular and Molecular Biology* p56-69. Neidhardt *et al* (Eds), ASM Press Washington DC, USA.

OSBORN, M.J. (1969) Structure and biosynthesis of the bacterial cell wall. *Annual Reviews in Biochemistry*, **38**, 501-538.

PANSY, F.E., STANDER, H., KOENBERGER, W.L. & DONOVICK, R. (1953) *In vitro* studies with 1-hydroxy-2(1H)-pyridinethione. (20041). *Proceedings for the Society of Experimental Biology (New York).* **82**, 122-124.

PARK, J.T. (1987) Murein synthesis. In: *Escherichia coli and Salmonella typhimurium Cellular and Molecular Biology*. pp663-671. Neidhardt *et al* (Eds), ASM Press, Washington DC, USA.

PAULUS, W. (1993) *Microbicides for the protection of materials: a handbook.* Chapman and Hall, London, UK.

PEARSE, A. D., WALKER, A. P. & MARKS, R. (1985) Effect of zinc pyrithione on mitotic activity in normal human skin. *Archives of Dermatological Research.* **277** (2), 118-120.

POSTMA, P. W. (1987) Phosphotransferase system for glucose and other sugars. In: *Escherichia coli and Salmonella typhimurium Cellular and Molecular Biology.* pp127-141. Neidhardt *et al* (Eds), ASM Press, Washington DC, USA.

POXTON, I.R. (1993) Prokaryotic envelope diversity. *Journal of Applied Bacteriology Symposium Supplement*, **74**, 1S -11S.

PRIESTLY, G. C. & BROWN, J. C. (1980) Acute toxicity of zinc pyrithione to human skin cells in vivo. *Acta Dermatovener (Stockholm).* **60**, 145-148.

PRIESTLY, G.C. & SAVIN, J.A. (1976) Microbiology of dandruff. *British Journal of Dermatology.* **94**, 469-471.

RICK, P.D. (1987) Lipid biosynthesis. In: *Escherichia coli and Salmonella typhimurium Cellular and Molecular Biology*. pp648-662. Neidhardt *et al* (Eds), ASM Press, Washington DC, USA.

ROWE, J. J., LEMMON, R. D. & TRITZ, G. J. (1985) Nicotinic acid transport in *Escherichia coli. Microbios.* **44**, 169-184.

RUBBO, S. D., ALBERT, A. & GIBSON, M. I. (1950) The influence of chemical constitution on antimicrobial activity part V: The antibacterial action of 8-hydroxyquinoline (oxine). *British Journal of Experimental Pathology.* **31**, 425-441.

RUSSELL, A.D. & CHOPRA, I. (1990) *Understanding Antibacterial Action and Resistance.*, Ellis Horwood, Chichester, UK.

RYE, R.M. & WISEMAN, D. (1964) Release of P-32 containing compounds from *Micrococcus lysodeikticus* treated with chlorhexidine. *Journal of Pharmacy and Pharmacology*, **16**, 516-521.

SALT, S. G. & WISEMAN, D. (1991) Biocide uptake by bacteria. In: *Mechanisms of Action of Chemical Biocides their Study and Exploitation.* pp65-86. Denyer & Hugo (Eds). Blackwell Scientific Publications, Oxford, UK.

SALT, S. G. & WISEMAN, D. (1968) The uptake of cetyltrimethylammonium bromide by *Escherichia coli. Journal of Pharmacy and Pharmacology.* **20**, 14S-17S.

SALTON, M. R. J. (1968) Lytic agents, cell penetrability and monolayer penetrability. *Journal of General Physiology.* **52**, 227S-252S.

SALYERS, A.A. & WHITT, D.D. (1994) *Bacterial Pathogenesis a Molecular Approach.*, ASM Press, Washington DC, USA.

SARA, M., PUM, D. & SLEYTR, U.B. (1992) Permeability and charge-dependent adsorption properties of the S-layer lattice from *Bacillus coagulans* E38-66. *Journal of Bacteriology*, **174**, 3487-3493.

SCHLEGEL, H.G. (1988) *General Microbiology* (6th ed)., Cambridge University Press.

SEYMOUR, M.D. & BAILEY, D.L. (1981) TLC of pyrithiones. *Journal of chromatography.* **206**, 301-310.

SHAW, E. (1949) Analogs of aspergillic acid I. The tautomerism of the hydroxypyridine-N-oxides. *Journal of the American Chemistry Society.* **71**, 67-70.

SHAW, E. N. & BERNSTEIN, J. (1954) N-Hydroxy-2-pyridinethiones. *United States Patent Document* 2 686 786. Mathieson Chemical Company.

SHAW, E., BERNSTEIN, J., LOSEE, K. & LOTT, W.A. (1950) Analogs of aspergillic acid IV. Substituted 2-bromopyridine-N-oxides and their conversion to cyclyc thiohydroxamic acids. *Journal of the American Chemistry Society.* **72**, 4362-4364.

SHEPHERD, J.A. (1987) *The antimicrobial action of gem-bromo-nitro containing antimicrobial agents.* PhD Thesis. Manchester University.

SHISHIDO, T. (1981) Glutathione-S-transferases from *E. coli. Agricultural and Biological Chemistry.* **45**, 2951-2953.

SIEWART, G. & STROMINGER, J.J. (1967) Bacitracin: an inhibitor of the dephosphorylation of lipid pyrophosphate, an intermediate in biosynthesis of the peptidoglycan of cell walls. *Proceedings of the National Academy of Sciences of the USA*, **57**, 767-773.

SKALIY, P., THOMPSON, T.A., GORMAN, G.W., MORRIS, G.K., MCEARCHEN, M.V. & MACKEL, D.C. (1980) Laboratory studies of disinfectants against *Legionella pneumophila. Applied and Environmental Microbiology.* **40** (4), 697-700.

SKOULIS, N.P., BARBEE, S.V., JACOBSON-KRAM, D., PUTMAN, D.L. & SAN, R.H.C. (1993) Evaluation of the genotoxic potential of zinc pyrithione in the *Salmonella* mutagenicity (Ames) assay. *Journal of Applied Toxicology.* **13** (4), 283-289.

SLEYTR, U.B. & MESSNER, P. (1988) Crystalline surface layers in procaryotes. *Journal of Bacteriology*, **170**, (7), 2891-2897.

SLEYTR, U.B., MESSNER, P., PUM, D. & SARA, M. (1993) Crystalline bacterial cell surface layers: General principles and application potential. *Journal of Applied Bacteriology Symposium Supplement*, **74**, 21S-32S.

SLEYTR, U.B., SARA, M. MESSNER, P. & PUM, D. (1994a) Application potential of 2D protein crystals (S-Layers). *Annals of the New York Academy of Sciences*, **745**, 261-269.

SLEYTR, U.B., SARA, M. MESSNER, P. & PUM, D. (1994b) Two-dimensional protein crystals (S-Layers): fundamentals and applications. *Journal of Cellular Biochemistry*, **56** (2), 171-176.

SNYDER, F.H., BUEHLER, E.V. & WINEK, C.L. (1965) Safety evaluation of zinc 2-pyridinethiol-1-oxide in a shampoo formulation. *Toxicology and Applied Pharmacology.* **7**, 425-429.

SNYDER, D.R., GRALLIA, E.J. & COLEMAN, G.L. (1977) Preliminary neurological evaluation of generalised weakness in zinc pyrithione treated rats. *Federation of Cosmetic Toxicology.* **15**, 43-47.

STAUFFER, G. V. (1987) Biosynthesis of serine and glycine. In: *Escherichia coli and Salmonella typhimurium Cellular and Molecular Biology.* pp412-418. Neidhardt *et al* (Eds), ASM Press, Washington DC, USA.

STREHLER, B. J. (1974) Adenosine-5'-triphosphate and creatine phosphate. Determination with luciferase. In; *Methods of Enzymic Analysis.* pp2112-2116. Bergmeyer (Ed). Academic Press, New York, USA.

STRYER, L. (1988) *Biochemistry.* (3rd ed), W. H. Freeman and Company, New York, USA.

SYBYL 6.1, Tripos Associates Inc, St Louis, Missouri, USA.

TOMSIKOVA, A., STERBA, J., PROKOPIC, J. & NOVACKOVA, D. (1982) Antifungal activity of pyrithione against *Emmonsia crescens in vitro and in vivo. FoliaParasitologia* (PRAHA). **29**, 271-278.

TRITZ, G. J. (1987) NAD biosynthesis and recycling. In: *Escherichia coli and Salmonella typhimurium Cellular and Molecular Biology.* pp557-563. Neidhardt *et al* (Eds), ASM Press, Washington DC, USA.

VANCUTSEM, J. VANGERVEN, F., FRANSEN, J., SCHROOTEN, P. & JANSSEN, P.A. (1990) The in vitro antifungal activity of ketoconazole, zinc pyrithione and selenium sulfide against *Pityrosporum* and their efficacy as a shampoo in the treatment of experimental pityrosporosis in guinea pigs. *Journal of the American Academy of Dermatology.* **6** (1), 993-998.

VANDER, A. J., SHERMAN, J. H. & LUCIANO, D. S. (1986) *Human Physiology: The Mechanisms of Body Function.* International Edition. McGraw-Hill, London, UK.

WAIGH, R.D. & GILBERT, P. (1991) Mechanisms of chemical reactions with biomolecules. In: *Mechanisms of Action of Chemical Biocides*. pp251-262. Denyer & Hugo (Eds), Blackwell Scientific Publications, Oxford, UK.

WAINWRIGHT, M. (1988) Structure and biology of bacteria relevant to the action of disinfectants. In: *Industrial Biocides*. pp1-18. Payne (Ed), John Wiley & Sons, Chichester, UK.

WALKER, C.J. (1987) The SOS response of *Escherichia coli*. In: *Escherichia coli and Salmonella typhimurium Cellular and Molecular Biology*. pp1346-1357. Neidhardt *et al* (Eds), ASM Press, Washington DC, USA.

WILLIAMS, D. H. & FLEMING, I. (1980) *Spectroscopic Methods in Organic Chemistry*. 3rd Ed. McGraw-Hill, Maidenhead, UK.

WISEMAN, D. (1964) The effect of chlorhexidine on the permeability and succinoxidase activity of *Micrococcus lysodeikticus*. *Journal of Pharmacy and Pharmacology*, **16**, 56T-57T.

WISHART, J. G. (1984) Effects of lipid peroxide formation in fowl semen on sperm motility, ATP content and fertilizing ability. *Journal of Reproduction and Fertility*. **71**, 113-118.

WOESE, C. R. (1987) Bacterial Evolution. *Microbiological Reviews*. **51** (2), 221-271.

WOODCOCK, P.M. (1988) Biguanides as industrial biocides. In: *Industrial Biocides*. pp19-36. Payne (Ed), John Wiley and Sons, Chichester, UK.

# APPENDIX

# CELL MEMBRANE EFFECTS OF SOME COMMON BIOCIDES

**Ibrahim S.I. AL-Adham[1], Anthony J. Dinning[3], Ian Eastwood[2] & Phillip J. Collier[3]***

[1]Faculty of Pharmacy, University of Jordan, Amman, (Jordan), [2]Zeneca plc, Manchester, M9 3DA, (U.K.) and [3]Department of Molecular and Life Sciences, University of Abertay Dundee, Dundee, DD1 1HG, (U.K.)

*Corresponding Author

Key Words: Cytoplasmic membrane; Biocides; Potassium leakage; *Escherichia coli*; *Pseudomonas aeruginosa*; *Pseudomonas*-gap

**Abstract**

Many antimicrobial compounds exhibit bacterial cell membrane activity as either potassium ion leakage and or leakage of 260nm material from the cell. In this experiment a potassium ion selective electrode and spectrophotometric observation of 260nm leakage were used in order to examine cell membrane effects in a selection of common biocides upon both *Escherichia coli* NCIMB 10000 and *Pseudomonas aeruginosa* NCIMB 10548. The observation of potassium ion leakage for the pyrithione biocides yielded results which were initially difficult to interpret, but are thought to suggest a species dependent combination of potassium ion leakage from affected membranes and chelation of those leaked ions in the bathing suspension. Such a result is not, however, supported by the 260nm material leakage results, which indicate very similar levels of membrane active effects for both species of bacteria.

**Introduction**

The bacterial cytoplasmic membrane is a very delicate organelle and is highly active metabolically. It acts mainly as a selective permeability barrier between the cytosol and the cells external environment. Any membrane active agent can induce damage to the membrane by action upon either the membrane potentials, bound enzymes or permeability.

Kuhn & Bielgi (1940) suggested that the cationic surface active agents might act on the bacterial membrane by dissociating conjugated proteins in a manner analogous to haemolysis. It was also shown by Hotchkiss (1944) that nitrogen and phosphorous containing compounds leaked from staphylococci treated with quaternary ammonium compounds or polypeptide antibiotics. Chlorhexidine causes leakage of intracellular material from *Escherichia coli* and *Staphylococcus aureus* during which a diphasic leakage / concentration pattern is observed. The first part of the curve represents increasing leakage with increasing concentration of the biocide, but at high concentration the protoplasmic contents and / or cytoplasmic membrane become gradually coagulated so that the leakage progressively declines (Hugo & Longworth, 1965). The interaction between the cytoplasmic membrane and Chlorhexidine was found to be through interaction with the acidic lipid components of the membrane (Broxton *et al*, 1983a, 1984). This leads to changes in membrane permeability which result in the loss of intracellular potassium (Elferink & Booij, 1974), 260nm absorbing materials (Hugo & Longworth, 1964) and phosphates (Rye & Wiseman, 1964; Hugo & Longworth, 1965, 1966). This action causes

concomitant alterations in the function of certain membrane associated enzymes (Hugo & Longworth, 1966; Broxton *et al*, 1983b) and transport systems (Harold *et al*, 1969; Hugo & Daltrey, 1974). Although not fully elucidated, it was suggested that Chlorhexidine interacts with protein moieties of the membrane and perturbs the function of the electron transport chain (Wiseman, 1964; Hugo & Daltrey, 1974).

Cetrimide, which is employed extensively in urology and gynaecology as an antiseptic in the form of aqueous and alcoholic solution is also one of the membrane active biocides. In this respect Lambert & Hammond (1973) concluded that cetrimide (0.2mM) causes the release of cell constituents from *E. coli* in the following order; $K^+$, $PO_4^{3+}$ followed by material absorbing at 260nm. The release of $K^+$ ions was completed in 30 minutes. Using *Staphylococcus aureus*, Denyer & Hugo (1977) found that cetrimide (18$\mu$g/ml or $5.3 \times 10^{-5}$M) causes the discharge of pH components of $\Delta p$. This concentration is the bacteriostatic concentration and the concentration which caused the maximum leakage of material absorbing at 260nm.

Fentichlor, which has both antibacterial and antifungal activity, has an application in the treatment of dermatophytic conditions. However, its application as a preservative in cosmetics might be limited by virtue of its photosensitization. Although little work had been done on the mode of action of Fentichlor, Hugo & Bloomfield (1971) found that it causes leakage of material absorbing at 260nm in both *E. coli* and *S. aureus*.

Pyrithione is an effective preservative for cosmetics and toiletry products. The membrane effect of Pyrithione is due to the disruption of proton gradient across the cell membrane and thus inhibition of the transport of solutes through membrane barrier (Ermolayeva *et al*, Personal Communication). Dichlorophen is a preservative for toiletries, textiles and cutting fluids and prevents the growth of bacteria in water cooling systems and humidifying plants. Due to its low toxicity, however, it is used in the treatment of tapeworm in man and domestic animals and for the treatment of athletes foot.

Isothiazolone biocides such as Benzisothiazolone (BIT) are widely used as industrial biocides (Singer, 1976; Andrykovitch & Neihof, 1987). BIT (Proxel; Zeneca plc, Manchester, UK) isothiazolones react mainly with intracellular thiol groups (Fuller *et al*, 1985; Collier *et al*, 1990a, b, c; 1991). Initial reaction between thiol and BIT leads to the formation of a disulphide conjugate. Further reaction of this conjugate with excess thiol leads to the formation of thiol

dimers and ring-opened forms of the biocides, which can themselves serve as a further source of interactive thiols to give dimerised biocide (Fuller *et al*, 1985; Collier *et al*, 1990a, b, c; 1991).

This paper aims to compare and contrast the membrane active nature of these common biocides and the observation of their ability to cause leakage of both $K^+$ ions and 260nm material.

## Materials and Methods

*Organisms and Chemicals*

*Escherichia coli* NCIMB 10000 and *Pseudomonas aeruginosa* NCIMB 10548 (PA01) were obtained from the NCIMB and were maintained on Nutrient agar (Oxoid CM3) slopes at room temperature in a darkened cupboard. Both cultures were incubated throughout this study at 37°C.

Benzisothiazolone (BIT), Fentichlor and Dichlorophen were the kind gift of Nipa Laboratories Ltd. (Pontypridd, U.K.). Cetrimide was the kind gift of Rhone-Poulenc, (Stockport, U.K.). Zinc pyrithione was the kind gift of Zeneca plc (Manchester, U.K.). Sodium pyrithione and all other reagents were purchased from Sigma, (Poole, U.K.).

*Growth Inhibitory Activity*

The minimal inhibitory concentrations (MIC) of Fentichlor, Dichlorophen, BIT, Pyrithione and Cetrimide were determined by the serial dilution (tube dilution) method as described by Bloomfield (1991). Both *E.coli* and *P. aeruginosa* were grown in Nutrient broth (Oxoid CM1) for this test.

*Preparation of Washed Cell Suspensions*

Overnight, liquid cultures of *E. coli* and *P. aeruginosa* were prepared in Nutrient broth (50ml in 100ml Erlenmayer flasks; Oxoid CM1). These were incubated in a shaking incubator (180 oscillations/min) at 37°C. Cells were harvested, in late exponential phase of growth, by centrifugation (4000xg, 10min) at room temperature, washed twice and resuspended in sterile Tris/HCl buffer (pH 7.2) at an absorbance ($OD_{470nm}$) of 1.5.

*Determination of Potassium Ion Leakage*

50ml of harvested and washed cells ($OD_{470nm}$ = 1.5) were placed in a clean 100ml beaker which was magnetically stirred. 5ml of ionic strength adjustment buffer (ISAB; 18.37g of tetraethylammonium chloride dissolved in deionised water and made up to 100ml, volumetrically) was added to the beaker. This ensured that the background ionic strength of all solutions was kept constant. The potassium-ion sensing electrode (Qualiprobe QSE 314, EDT Instruments, Dover, U.K.) and its reference electrode (Qualiprobe double junction reference electrode E8092, EDT Instruments, Dover, U.K.) were placed into the cell suspension. The potential difference (mV) derived by the electrodes was measured using a Whatman PHA 220 pH/mV meter (Whatman, Maidstone, U.K.). An aliquot (1ml) of the biocide, at a pre-determined concentration (6.4mg $ml^{-1}$, in DMSO) was added to the cell suspension to give a final reaction concentration of 128$\mu$g $ml^{-1}$. The potassium efflux from the cells in suspension was measured at time intervals over 20 minutes as a potential difference in mV. These values were converted to concentrations of $K^+$ ions (M) by reference to a conversion graph which had been constructed earlier using KCl standard solutions. The concentration of $K^+$ ions released was plotted against time and is given in figures 1 and 2.

*Determination of the Leakage of 260nm Absorbing Material*

50ml of harvested and washed cells ($OD_{470nm}$ = 1.5) were placed in a clean 100ml beaker and maintained at room temperature whilst stirred. At time t=0 min, an aliquot (1ml) of biocide (6.4mg $ml^{-1}$, in DMSO) was added to the cell suspension to give a final concentration of 128$\mu$g $ml^{-1}$. Aliquots (2 x 1ml) of the treated cell suspension were removed at regular intervals, placed in Eppendorf tubes and centrifuged at 12000xg for 2 min in a MSE Microfuge. The supernatant was then decanted from the Eppendorf tubes and pooled into a plastic UV cuvette (1cm path length). The absorbance of the cuvette was read against a buffer control at 260nm and plotted against time in figures 3 and 4.

*18-Crown-6 Ether*

18-Crown-6 ether is a compound with known $K^+$ ion chelation properties. This compound was used to repeat both experiments in an attempt to demonstrate the effects of a $K^+$

ion chelating compound upon the operation of a $K^+$ ion selective electrode.

**Results and Discussion**

Determination of the minimal inhibitory concentration of the various biocides used indicated an observable *Pseudomonas*-gap for four of the six biocides (Table 1). This is expressed as a higher MIC value for the inhibition of *P. aeruginosa* as opposed to that for *E. coli*. Cetrimide exhibited the largest gap where approximately 8 times the MIC for *E. coli* was required to inhibit *P. aeruginosa*. This was followed by BIT and Fentichlor, both requiring between two and four times the *E. coli* MIC to inhibit *P. aeruginosa*. Dichlorophens observable *Pseudomonas*-gap was only an increase of about 50% in MIC and both Zinc and Sodium Pyrithiones actually proved more effective against *P. aeruginosa* than *E. coli*. The *Pseudomonas*-gap has been observed elsewhere (Russell & Chopra, 1990; Paulus, 1993) and may be the result of one or more physiological factors expressed by cells of *Pseudomonas* spp. This resistance to both biocides and antibiotics by the Pseudomonads is thought to be intrinsic and related to the nature of the cell envelope, in particular the structure and composition of the Gram-negative outer membrane. The cation content of the *Pseudomonas* spp outer membrane is significantly higher than that of other Gram-negative organisms. In particular, the concentration of $Mg^{2+}$ is thought to help maintain the integrity of the outer membrane by ensuring strong Lipopolysaccharide-Lipopolysaccharide linkage and subsequent resistance to membrane active antimicrobials such as the quaternary ammonium compounds (Russell & Chopra, 1990).

**Table 1:** Minimal inhibitory concentrations of various biocides against *Escherichia coli* NCIMB 10000 and *Pseudomonas aeruginosa* NCIMB 10548.

| Organism | Minimal Inhibitory Concentration ($\mu g$ $ml^{-1}$) | | | | | |
|---|---|---|---|---|---|---|
| | NaPT | ZnPT | Fen | Dic | BIT | Cet |
| *Escherichia coli* NCIMB 10000 | 120 | 13 | 30 | 25 | 20 | 16 |
| *Pseudomonas aeruginosa* NCIMB 10548 | 100 | 4.5 | 80 | 35 | 80 | 128 |

Where; NaPT = Sodium Pyrithione, ZnPT = Zinc Pyrithione, Fen = Fentichlor, Dic = Dichlorophen, BIT = Benzisothiazolone and Cet = Cetrimide.

Figures 1 and 2 represent the effects of the various biocides upon the membranes of *E.coli* (Fig 1) and *P. aeruginosa* (Fig 2) as indicated by potassium ($K^+$) leakage. These figures indicate that cetrimide has observable and marked leakage effects upon both organisms and that the onset of this effect is rapid. The initial $K^+$ ion concentration of the bathing solution for both micro-organisms in all experiments was $1.1x10^{-4}M$. The maximal rate of Cetrimide-induced leakage was achieved within 1 minute for *E. coli* ($1.15x10^{-2}M$) and then the levels of K+ ions appeared to reduce slowly over the rest of the period of observation, finally reaching $6.7x10^{-3}M$ at 15 min. However, for *P. aeruginosa* the onset of leakage appeared to be as rapid as that for *E. coli* , $3.8x10^{-2}M$ at 1 min, but continued to exhibit leakage over the rest of the period of observation, eventually reaching a level of $4.75x10^{-2}M$ at 15 min. This result indicates that whilst the MIC for cetrimide against *P. aeruginosa* is considerably higher than that for cetrimide against *E. coli*, the subsequent leakage it causes at the same concentration is similar for both organisms.

Of the other biocides tested, only BIT gave any observable leakage of $K^+$ ions and this was at a much lower rate than that for cetrimide at the same concentration, $128\mu g\ ml^{-1}$. The onset of leakage with BIT only became apparent over the 15 minutes of the experiment and

attained levels of only $1.4x10^{-4}M$ against *E. coli* and $2.3x10^{-4}M$ against *P. aeruginosa.*

Fentichlor gave no observable rate of $K^+$ ion leakage for either micro-organism. The closely related compound Dichlorophen, however, gave evidence of $K^+$ ion uptake or chelation. In the case of *E. coli* the concentration of $K^+$ ions in the bathing solution fell from $1.1x10^{-4}M$ to $5.0x10^{-9}M$ and for *P. aeruginosa* the fall was from $1.1x10^{-4}M$ to $3.0x10^{-8}M$. This observation would suggest that Dichlorophen acts as an ion chelating agent in the presence of bacterial cells. This is an unusual result as Dichlorophen is often sited as a membrane active agent (Paulus, 1993).

Sodium Pyrithione exhibited effects similar to those of Dichlorophen in that it apparently chelated $K^+$ ions from the bathing solutions of both *E. coli* and *P. aeruginosa.* In the case of *E. coli* this represented a loss of ions from an initial concentration of $1.1x10^{-4}M$ to $5.22x10^{-5}M$ at 15 min. Such a reduction is equivalent to a halving of available bathing $K^+$ ions. However, unlike Dichlorophen, the pyrithiones appeared to exhibit species-specific chelation properties. In the case of *P. aeruginosa*, the concentration of $K^+$ ions was reduced from $1.1x10^{-4}M$ to $3.2x10^{-8}M$. Such a result indicates that *P. aeruginosa* cells appeared to be more susceptible to loss of $K^+$ ions from their external environment by chelation. Such an implication is, however, unlikely to be the case in reality. It is more likely that this result was the simultaneous observation of two separate, but related events involving the $K^+$ ions. The first of these events would be the straight forward chelation of $K^+$ ions from the bathing medium by the sodium pyrithione. This event should not be species specific and should have exhibited a result similar to that for Dichlorophen. The second event, however, is the simultaneous membrane activity of the biocide upon the bacterial cell. This would result in the leakage of $K^+$ ions from the cell and their subsequent chelation by excess pyrithione. This would result in an apparent differential $K^+$ ion loss between the two species of micro-organism dependent upon the differing sensitivity of the two species towards the biocide. In effect, *P. aeruginosa* would exhibit a much greater level of $K^+$ ion loss from the bathing solution if it were less sensitive to the membrane active effects of the biocide, whereas *E. coli* would exhibit a lower level of $K^+$ ion loss due to its corresponding greater $K^+$ ion leakage. However, this

suggestion is not supported by the MIC data. This data shows that the MIC values for *E. coli* and *P. aeruginosa* are very similar at 120$\mu$g ml-1 and 100$\mu$g ml-1 respectively and that, if anything, the *P. aeruginosa* cells should be more susceptible to the effects of this compound. The results for Zinc pyrithione against both microorganisms, however, exhibit no obvious signs of either K+ ion leakage or chelation. Such a result indicates that either this compound has no membrane effect upon either microorganism or that its induced potassium leakage is exactly balanced by its K+ ion chelation. In the light of the 260nm material leakage results this latter theory is the more probable as these results indicate that both NaPT and ZnPT exhibit marked membrane activity against both *E. coli* and *P. aeruginosa*. Indeed most of the biocides tested gave higher levels of leakage than the positive control compound, cetrimide. The 18-Crown-6 ether exhibited no apparent $K^+$ ion or 260nm material leakage in either experiment.

## Conclusions

The results of these studies indicate that the pyrithione biocides are able to disrupt membrane function of Gram-negative bacteria. In addition to and simultaneously with this disruption, these compounds can also chelate $K^+$ ions from the bathing medium. A combination of these two events may explain some of the inhibitory effects of these compounds upon bacterial cells.

## Acknowledgements

We wish to thank Miss Nancy Hakooz, Mr A. AL-Mowaswess, Mr S. AL-Najjar, Mr F. Abu Hiyyeh, Mr G. Molloy, Ms D. Franklin, Mr D. Flynn and Mr M. Dorward for all their help in both technical and academic areas of this research.

## References

Andrykovitch, G & Neihof, RA (1987) Fuel soluble biocides for control of *Cladosporium resinae* in hydrocarbon fuels. *Journal of Industrial Microbiology*, **2**, 35-40.

Bloomfield, S (1991) Methods of assessing antimicrobial activity. *In* SP Denyer & WB Hugo

(Eds), *Mechanisms of action of chemical biocides; Their study and exploitation*, Blackwell Scientific, Oxford, U.K.

Broxton, P, Woodcock, PM & Gilbert, P (1983a) A study of the antibacterial activity of some polyhexamethylene biguanides towards *Escherichia coli* ATCC 8739. *Journal of Applied Bacteriology*, **54**, 345-353.

Broxton, P, Woodcock, PM & Gilbert, P (1983b) Action of some polyhexamethylene biguanides upon respiration of *Escherichia coli* ATCC 8739. *Journal of Pharmacy and Pharmacology, Supplement*, **35**, 67P.

Broxton, P, Woodcock, PM & Gilbert, P (1984) Interaction of some polyhexamethylene biguanides and membrane phosphate in *Escherichia coli* ATCC 8739. *Journal of Applied Bacteriology*, **57**, 115-124.

Collier, PJ, Ramsey, AJ, Austin, P & Gilbert, P (1990a) Growth inhibitory and biocidal activity of some isothiazolone biocides. *Journal of Applied Bacteriology*, **69**, 569-577.

Collier, PJ, Ramsey, A, Waigh, RD, Douglas, KT, Austin, P & Gilbert, P (1990b) Chemical reactivity of some isothiazolone biocides. *Journal of Applied Bacteriology*, **69**, 578-584.

Collier, PJ, Austin, P & Gilbert, P (1990c) Uptake and distribution of some isothiazolone biocides into *Escherichia coli* ATCC 8739 and *Schizosaccharomyces pombe* NCYC 1354. *International Journal of Pharmaceutics*, **66**, 201-206.

Collier, PJ, Austin, P & Gilbert, P (1991) Isothiazolone biocides: enzyme inhibiting pro-drugs. *International Journal of Pharmaceutics*, **74**, 195-201.

Denyer, SP & Hugo, WB (1977) The mode of action of cetyltrimethylammonium bromide (CTAB) on *Staphylococcus aureus*. *Journal of Pharmacy and Pharmacology*, **29**, 669.

Elferink, JGR & Booij, HL (1974) Interaction of chlorhexidine with yeast cells. *Biochemical Pharmacology*, **23**, 1413-1419.

Ermolayeva, E, Eastwood, I & Sanders, D. Mechanism of pyrithione-induced membrane depolarization in *Neurospora crassa*. Personal Communication.

Fuller, SJ, Denyer, SP, Hugo, WB, Pemberton, D, Woodcock, PM & Buckley, AJ (1985) The mode of action of 1,2-benzisothiazolin-3-one on *Staphylococcus aureus*. *Letters in Applied Microbiology*, **1**, 13-15.

Harold, FM, Baarda, JR & Abrams, A (1969) Dio 9 and chlorhexidine: Inhibitors of membrane bound ATPase and cation transport in *Streptococcus faecalis*. *Biochemica et Biophysica Acta*, 183, 129-136.

Hotchkiss, RD (1944) Gramicidin, tyrocidin and Lyrothricin. *Advances in Enzymology*, **4**, 153-199.

Hugo, WB & Bloomfield, SF (1971) Studies on the mode of action of the phenolic antibacterial agent Fentichlor against *Staphylococcus aureus* and *Escherichia coli*: The effects of Fentichlor on the bacterial membrane and the cytoplasmic constituents of the cell. *Journal of Applied Bacteriology*, **34**, 569-578.

Hugo, WB & Daltrey, DC (1971) Studies on the mode of action of the antibacterial agent chlorhexidine on *Clostridium perfringens*. 2 Effect of chlorhexidine on metabolism and cell membrane. *Microbios*, **11**, 131-146.

Hugo, WB & Longworth, AR (1964) Some aspects of mode of action of chlorhexidine. *Journal of Pharmacy and Pharmacology*, **16**, 655-662.

Hugo, WB & Longworth, AR (1965) Cytological aspects of mode of action of chlorhexidine. *Journal of Pharmacy and Pharmacology*, **17**, 28-32.

Hugo, WB & Longworth, AR (1966) The effect of chlorhexidine on the electrophoretic mobility, cytoplasmic membrane constituents, dehydrogenase activity and cell walls of *Escherichia coli* and *Staphylococcus aureus*. *Journal of Pharmacy and Pharmacology*, **18**, 569-578.

Kuhn, R & Bielgi, HJ (1940) Ubes Invertseifen. I Die Einwerkung von Invertseifen auf Eiweiss-Stoffe. *Berichte der Deutschen Chemischen Gesellschaft*, **73**, 1080-1091.

Lambert, PA & Hammond, SM (1973) Potassium fluxes, first indications of membrane damage in microorganisms. *Biochemica et Biophysica Acta*, **54**, 796-799.

Paulus, W (1993) *Microbicides for the protection of materials: a handbook.* Chapman and Hall, London.

Russell, AD & Chopra, I (1990) *Understanding antibacterial action and resistance.* Ellis Horwood, London.

Rye, RM & Wiseman, D (1964) Release of Phosphorous-32 containing compounds from *Micrococcus lysodeikticus* treated with chlorhexidine. *Journal of Pharmacy and Pharmacology*, **20**, 145-178.

Singer, M (1976) Laboratory procedures for assessing the potential of antimicrobial agents as industrial biocides. *Process Biochemistry*, **11**, 30-35.

Wiseman, D (1964) The effect of chlorhexidine on the permeability and succinooxidase activity of *Micrococcus lysodeikticus*. *Journal of Pharmacy and Pharmacology*, **16**, 56T-57T.

Fig. 1. Potassium fluxes associated with suspensions of *Escherichia coli* NCIMB 10000 exposed to 128$\mu$g ml$^{-1}$ of (○) cetrimide, (△) sodium pyrithione, (□) dichlorophen, (●) fentichlor, (▲) benzisothiazolone, (■) zinc pyrithione and (+) 18-crown-6 ether.

Fig. 2. Potassium fluxes associated with suspensions of *Pseudomonas aeruginosa* NCIMB 10548 exposed to 128$\mu$g ml$^{-1}$ of (○) cetrimide, (△) sodium pyrithione, (□) dichlorophen, (●) fentichlor, (▲) benzisothiazolone, (■) zinc pyrithione and (+) 18-crown-6 ether.

Fig. 3. Leakage of 260nm material from cell suspensions of *Escherichia coli* NCIMB 10000 exposed to 128$\mu$g ml$^{-1}$ of (○) cetrimide, (△) sodium pyrithione, (□) dichlorophen, (●) fentichlor, (▲) benzisothiazolone, (■) zinc pyrithione and (+) 18-crown-6 ether.

Fig. 4. Leakage of 260nm material from cell suspensions of *Pseudomonas aeruginosa* NCIMB 10548 exposed to 128$\mu$g ml$^{-1}$ of (○) cetrimide, (△) sodium pyrithione, (□) dichlorophen, (●) fentichlor, (▲) benzisothiazolone, (■) zinc pyrithione and (+) 18-crown-6 ether.

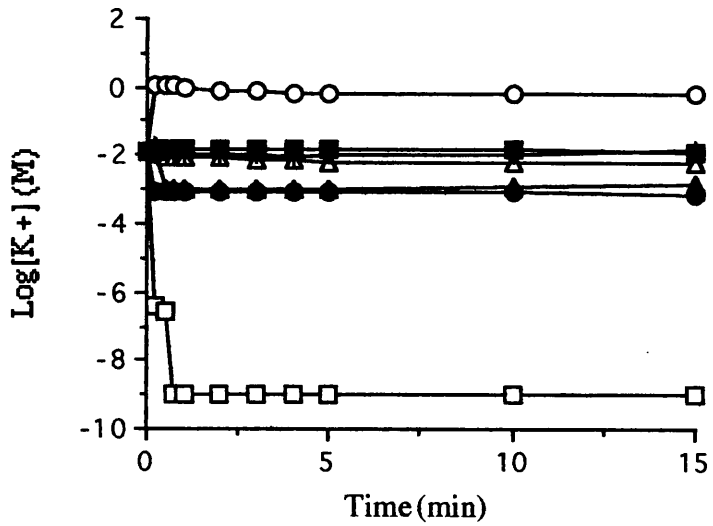
2
0
-2
-4
-6
-8
-10
Log[K+] (M)
0
5
10
15
Time (min)

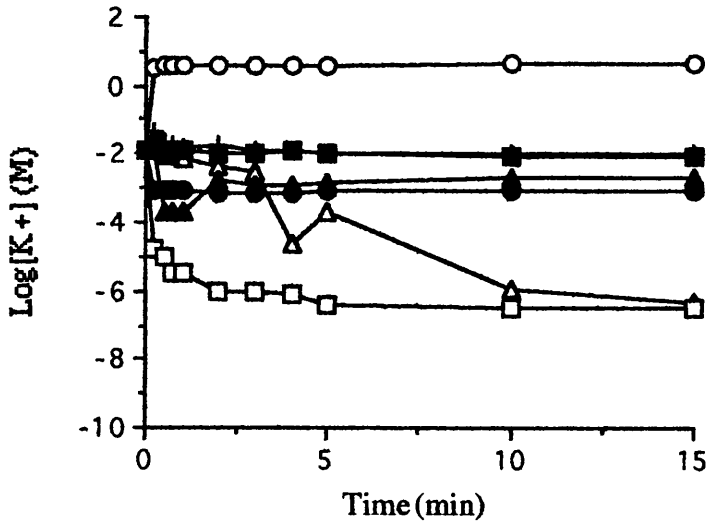
2
0
-2
-4
-6
-8
-10
Log[K+] (M)
0
5
10
15
Time (min)

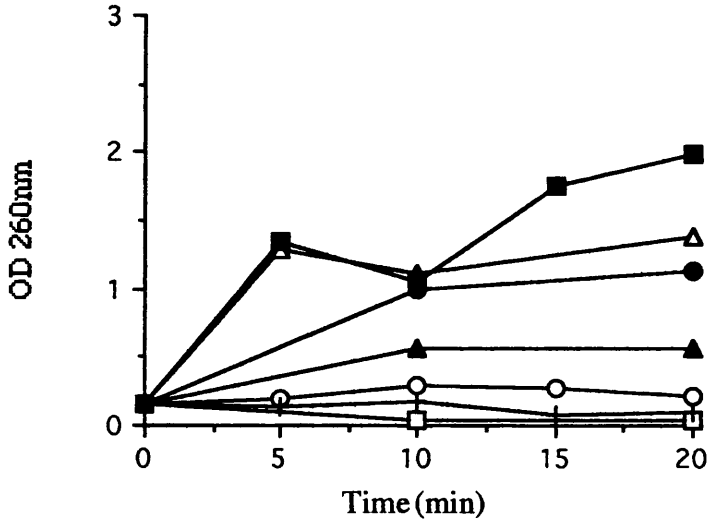
OD 260nm
3
2
1
0
0
5
10
15
20
Time (min)

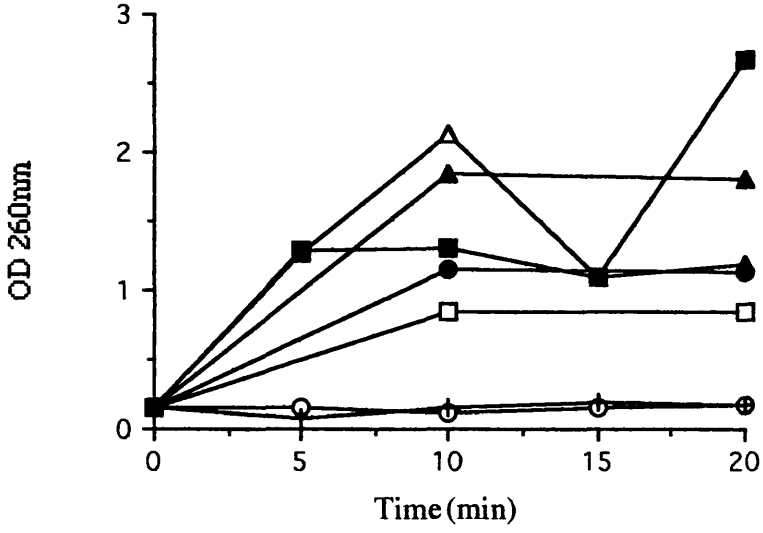
OD 260nm
3
2
1
0
0
5
10
15
20
Time (min)